Analysis of the roles of CDK1 and PP1 in the regulation of chromosome segregation



Iona Manley

The Queen's College

University of Oxford

A thesis submitted for the degree of

Doctor of Philosophy

Michaelmas 2022

Acknowledgments

I would like to take this opportunity to thank the many people who have supported and encouraged me over the last four years and to acknowledge the funding which supported my research.

I am indebted to the Wellcome Trust and their programme director Prof. Matthew Whitby for offering me a place on their research programme and providing generous funding to support my research. This work would also not have been possible without the funding awarded to the Gruneberg Lab by Cancer Research UK. I also acknowledge that this work would not have been possible without the HeLa cell line, which was developed from Henrietta Lacks' cells taken without compensation or informed consent.

I am privileged to have worked in the Gruneberg Lab, in which I have benefitted from the expertise of many great scientists. I am particularly grateful to the unlimited guidance and support of my supervisor, Prof. Ulrike Gruneberg. Thank you for keeping me on track and for your invaluable patience and feedback over the past four years. Also, thank you to all the members of the Gruneberg Lab, past and present, in particular Dr. Daniel Hayward, Zoe Geraghty, Emile Roberts, Dr. James Bancroft and Izzy Leitch. You have been an amazing source of support and laughter throughout my DPhil. For all your scientific advice, wisdom and friendship, I am very grateful.

I would also like to thank Prof. Jordan Raff and Prof. Rob Klose for their supervision during two rotation projects at the beginning of my DPhil. Further thanks go to Prof. Fumiko Esashi and Prof. Lars Jansen for their insightful comments and suggestions as my Transfer and Confirmation of Status examiners. The review and assessment of my thesis was undertaken by Prof. Jonathon Pines and Dr. Fanni Gergely and I am most grateful for their valuable feedback and input.

I am incredibly grateful to my friends and family who have supported and encouraged me throughout my DPhil. In particular, thank you to Alice Jones for taking on the mammoth task of proof-reading this thesis as non-scientist. I would like to express my deepest thanks to my parents and to my husband, Colin, for their unwavering support and belief in me during the highs and lows of this DPhil. Finally, I would like to thank God. He is my ultimate source of strength and without His grace and blessing this thesis would not have been possible.

"Trust in the LORD with all your heart and lean not on your own understanding; in all your ways acknowledge him, and he will make your paths straight."

Proverbs 3:5-6

The work described in this thesis is the candidate’s own, except where stated to the contrary.

Abstract

Accurate chromosome segregation in mitosis is essential for the faithful inheritance of genetic material. The Spindle Assembly Checkpoint (SAC) ensures genomic stability is maintained by monitoring the attachment of chromosomes to the mitotic spindle and preventing erroneous chromosome segregation. Checkpoint regulation is coordinated by the opposing activities of kinases and phosphatases. CDK1 is the major mitotic kinase required for mitotic entry and activation of the SAC. In particular, CDK1 regulates recruitment of the principal checkpoint kinase MPS1 to kinetochores, a critical event for downstream checkpoint signalling. However, this thesis demonstrates that circumventing this particular requirement for CDK1 is insufficient for SAC signalling when CDK1 is inhibited, therefore revealing a crucial, unknown role of CDK1 in SAC signalling. Using high-resolution live and fixed cell imaging combined with biochemical assays, this study confirms that outer-kinetochore assembly is CDK1 dependent and that the disassembly of outer-kinetochore proteins is differentially regulated by the CDK1-opposing phosphatases PP1 and PP2A-B55. Critically, this work uncovers that the outer-kinetochore protein and checkpoint scaffold KNL1 is rapidly lost at the metaphase-to-anaphase transition, before other outer-kinetochore proteins. This occurs through a hitherto unrecognised CDK1-mediated interaction between the MIS12 complex and KNL1 that is critical for regulating checkpoint function. Therefore, specific phosphatase-mediated disassembly of the outer-kinetochore supports complete SAC shutdown through KNL1 loss while leaving microtubule-kinetochore attachments intact through maintenance of the NDC80 complex. This safeguards the integrity of the

metaphase-to-anaphase transition and ensures accurate chromosome segregation.

This study also highlights the key role of PP1 as a CDK1-opposing phosphatase at the metaphase-to-anaphase transition and sheds light on its previously poorly understood role in mammalian cells. CRISPR editing methodologies and high-resolution live cell imaging are used to develop novel tools for the investigation of the role of PP1 in human tissue culture cells. In particular, the generation of endogenously tagged PP1-GFP isoforms and constitutive PP1 isoform knock-outs now allows the observation of endogenous PP1 and the effect of isoform-specific loss respectively for the first time.

Table of Contents

CHAPTER 1: INTRODUCTION 1

1.1 CELL CYCLE REGULATION IS GOVERNED BY THE BALANCE BETWEEN KINASE AND PHOSPHATASE ACTIVITY 1

1.1.1 The mammalian cell cycle 1

1.1.3 Mitosis 6

1.1.4 Mitotic entry is driven by CDK1 8

1.1.5 Mitotic exit is triggered by phosphoprotein phosphatases 12

1.2 THE KINETOCHORE IS AN ESSENTIAL MACROMOLECULAR STRUCTURE FOR MITOSIS 18

1.2.1 The kinetochore is composed of the inner- and outer-kinetochore .. 18

1.2.2 Regulation of outer-kinetochore assembly 26

1.3 THE SPINDLE ASSEMBLY CHECKPOINT PREVENTS UNTIMELY MITOTIC EXIT 29

1.3.1 The importance of the Spindle Assembly Checkpoint 29

1.3.2 Recognising and signalling unattached kinetochores 33

1.3.3 Recognising and correcting incorrect attachments 37

1.3.4 Silencing the SAC leads to mitotic exit 39

1.3.5 The metaphase-to-anaphase transition relies on a precise balance between kinase and phosphatase activity 41

1.4 THESIS AIMS 51

CHAPTER 2: IDENTIFYING A CRITICAL, UNKNOWN ROLE OF CDK1 IN SAC SIGNALLING BEYOND MPS1 KINETOCHORE RECRUITMENT 53

2.1 TETHERING MPS1 TO KINETOCHORES IS INSUFFICIENT FOR INITIATING SPINDLE ASSEMBLY CHECKPOINT SIGNALLING 53

2.2 OBSERVING THE DIFFERENCE BETWEEN SAC PROTEIN MAINTENANCE AT AND RECRUITMENT TO KINETOCHORES 56

2.3 INVESTIGATING THE ROLE OF CDK1 IN REGULATING MPS1 KINASE ACTIVITY .. 58

2.4 DISCUSSION 63

CHAPTER 3: INVESTIGATING THE ROLE OF CDK1 IN REGULATING OUTER-KINETOCHORE ASSEMBLY AND DISASSEMBLY 68

3.1 OUTER-KINETOCHORE PROTEIN LOCALISATION IS DIFFERENTIALLY REGULATED BY CDK1 68

3.2 OUTER-KINETOCHORE PROTEIN DYNAMICS IN MITOSIS 72

3.3 IDENTIFYING A NOVEL LEVEL OF CDK1 REGULATION BETWEEN THE MIS12 COMPLEX AND KNL1 75

3.4 INVESTIGATING THE EFFECT OF LOSS OF CDK1 REGULATION OF OUTER-KINETOCHORE ASSEMBLY ON CHECKPOINT SIGNALLING AND CELL CYCLE REGULATION 84

3.5 DISCUSSION 87

CHAPTER 4: IDENTIFYING DIFFERENTIAL PHOSPHATASE REGULATION OF OUTER-KINETOCHORE PROTEIN LOCALISATION 96

4.1 IDENTIFYING THE PHOSPHATASES OPPOSING OUTER-KINETOCHORE ASSEMBLY IN MITOSIS 96

4.2 RESTORING CHECKPOINT SIGNALLING THROUGH SPECIFIC PHOSPHATASE DEPLETION 99

4.3 DISCUSSION 102

CHAPTER 5: FURTHER INVESTIGATING THE KEY ROLE OF PP1 IN THE METAPHASE-TO-ANAPHASE TRANSITION 110

5.1 INVESTIGATING THE LOCALISATION OF ENDOGENOUS PP1 ISOFORMS 110

5.2 EXPLORING REGULATION OF PP1 LOCALISATION 117

5.3 OBSERVING THE EFFECT OF PP1 ISOFORM-SPECIFIC LOSS 119

5.4 DISCUSSION 122

CHAPTER 6: CONCLUSIONS 127

CHAPTER 7: MATERIALS AND METHODS 132

7.1 REAGENTS AND ANTIBODIES 132

7.2 SDS-PAGE AND WESTERN BLOTTING 135

7.3 MOLECULAR BIOLOGY 136

7.4 CELL CULTURE 138

7.4.1 Tissue culture *138*

7.4.2 Production of Flp-In stable cell lines *138*

7.4.3 Production of stable cell lines using CRISPR editing *139*

7.5 TRANSFECTION AND RESCUE EXPERIMENTS 142

7.5.1 Transient transfection for protein expression *142*

7.5.2 RNAi *143*

7.5.3 RNAi rescue assays *144*

7.6 IMAGING TECHNIQUES 144

7.6.1 Immunofluorescence staining *144*

7.6.2 Immunofluorescence microscopy *145*

7.6.3 SoRa Confocal Microscopy *146*

7.6.4 Spindle Assembly Checkpoint assays *146*

7.6.5 Live cell imaging assays *147*

7.7 IMAGE PROCESSING AND ANALYSIS 148

7.8 BIOCHEMICAL ASSAYS 151

7.8.1 λ-phosphatase treatment *151*

7.8.2 Immunoprecipitation *151*

7.8.3 In vitro kinase assays *153*

7.8.4 Mass spectrometry *153*

CHAPTER 8: BIBLIOGRAPHY 155

List of Figures

FIGURE 1.1 THE CELL CYCLE IS A SERIES OF STAGES GOVERNED BY CDK:CYCLIN COMPLEXES..... 3

FIGURE 1.2 REGULATION OF CDK1 ACTIVITY.....10

FIGURE 1.3 PHOSPHOPROTEIN PHOSPHATASES IN MITOTIC REGULATION..... 13

FIGURE 1.4 THE STRUCTURE OF THE MAMMALIAN KINETOCHORE..... 20

FIGURE 1.5 PHOSPHO-REGULATION OF OUTER-KINETOCHORE ASSEMBLY..... 26

FIGURE 1.6 THE SPINDLE ASSEMBLY CHECKPOINT..... 31

FIGURE 1.7 POTENTIAL GEOMETRIES OF KINETOCHORE-MICROTUBULE ATTACHMENTS..... 38

FIGURE 1.8 THE METAPHASE-TO-ANAPHASE TRANSITION RELIES ON A PRECISE BALANCE BETWEEN KINASE AND PHOSPHATASE ACTIVITY..... 43

FIGURE 2.1 TETHERING MPS1 TO KINETOCHORES IS INSUFFICIENT FOR INITIATING SAC SIGNALLING..... 54

FIGURE 2.2 OBSERVING THE DIFFERENCE BETWEEN SAC PROTEIN MAINTENANCE AT AND RECRUITMENT TO KINETOCHORES..... 57

FIGURE 2.3 CDK1 IS NOT REQUIRED FOR MPS1 KINASE ACTIVITY *IN VIVO*..... 60

FIGURE 2.4 CDK1 IS NOT REQUIRED FOR MPS1 KINASE ACTIVITY *IN VITRO*..... 62

FIGURE 3.1 OUTER-KINETOCHORE PROTEIN LOCALISATION IS

DIFFERENTIALLY REGULATED BY CDK1..... 70
FIGURE 3.2 OUTER-KINETOCHORE PROTEIN DYNAMICS IN MITOSIS..... 73
FIGURE 3.3 NSL1 IS CRITICAL FOR LOCALISING KNL1 TO KINETOCHORES..... 77
FIGURE 3.4 NSL1 IS MITOTICALLY PHOSPHORYLATED AT T242..... 79
FIGURE 3.5 PHOSPHO-REGULATION OF T242 IS REQUIRED FOR KNL1 KINETOCHORE LOCALISATION..... 82
FIGURE 3.6 CDK1 REGULATION OF OUTER-KINETOCHORE ASSEMBLY IS CRITICAL FOR SAC SIGNALLING AND CELL CYCLE REGULATION. 86
FIGURE 4.1 IDENTIFYING THE PHOSPHATASES OPPOSING OUTER-KINETOCHORE ASSEMBLY IN MITOSIS..... 97
FIGURE 4.2 DEPLETION OF PP1 RESTORES CHECKPOINT SIGNALLING IN THE ABSENCE OF CDK1..... 101
FIGURE 4.3 A NOVEL MECHANISM OF SPINDLE ASSEMBLY CHECKPOINT REGULATION..... 103
FIGURE 5.1 VISUALISING ENDOGENOUS PP1 IN HELA CELLS USING CRISPR/CAS9 FLUORESCENT TAGGING..... 111
FIGURE 5.2 VISUALISING ENDOGENOUS PP1 IN HCT116 CELLS USING CRISPR/CAS9 FLUORESCENT TAGGING..... 113
FIGURE 5.3 OPTIMISING IMAGING METHODOLOGY FOR VISUALISING ENDOGENOUS PP1-GFP..... 114
FIGURE 5.4 PPP1CA AND PPP1CC SHOW DISTINCT CELLULAR LOCALISATIONS THROUGH MITOSIS..... 116
FIGURE 5.5 AURORA B NEGATIVELY REGULATES PPP1CC KINETOCHORE LOCALISATION..... 118

FIGURE 5.6 GENERATING AND OBSERVING THE EFFECTS OF CONSTITUTIVE PP1 ISOFORM KNOCK-OUTS..... 120

List of Tables

TABLE 7.1 LIST OF DRUGS AND INHIBITORS..... 132

TABLE 7.2 PRIMARY ANTIBODY DETAILS..... 134

TABLE 7.3 MUTAGENESIS PRIMERS..... 137

TABLE 7.4 CRISPR/CAS9 GUIDE RNAS..... 139

TABLE 7.5 CRISPR/CAS12 PCR TAGGING PRIMERS..... 140

TABLE 7.6 LENTIVIRAL CRISPR/CAS9 KO GUIDE RNAS..... 142

TABLE 7.7 SIRNA OLIGOS..... 143

List of Abbreviations

ANKRD	Ankyrin repeat domain-containing submit
APC/C	Anaphase-promoting complex/cyclosome
ATP	Adenosine triphosphate
AurBi	Aurora B inhibitor
BUB	Budding uninhibited by benzimidazoles
BUBR1	Budding uninhibited by benzimidazoles related 1
CAK	CDK-activating kinase
CCAN	Constitutive centromere-associated network
Cdc2	Cell division control protein 2
CDC20	Cell division control protein 20
CDC25	Cell division control protein 25
CDK	Cyclin-dependent kinase
CDKi	CDK inhibitor
CENP	Centromere protein
C-MAD2	Closed MAD2
CPC	Chromosomal passenger complex
CRISPR	Clustered regularly interspaced short palindromic repeats
DMEM	Dulbecco’s modified eagle media
DMSO	Dimethyl sulfoxide
DNA	Deoxyribonucleic acid
Dox	Doxycycline
DTT	Dithiothreitol
EDTA	Ethylenediaminetetraacetic acid

EGTA	Ethyleneglycol tetraacetic acid
ENSA	Endosulfine-α
G1	Gap 1
G2	Gap 2
GFP	Green fluorescent protein
HEC1	Highly expressed in cancer 1
HRP	Horseradish peroxidase
INCENP	Inner centromere protein
KD	Kinase dead
KIF18A	Chromosome-associated kinesin 18A
KMN	KNL1-MIS12-NDC80 complex
KNL1	Kinetochore null protein 1
KO	Knock-out
MAD	Mitotic arrest deficient
MASTL	Microtubule-associated serine/threonine protein kinase-like
MCC	Mitotic checkpoint complex
MELT	Methionine-Glutamic acid-leucine-threonine
MIS12	Minichromosome instability 12
MPF	M-phase promoting factor
MPS1	Monopolar spindle 1
NEBD	Nuclear envelope breakdown
NUF2	Nuclear filament-containing protein 2
O-MAD2	Open MAD2
ORF	Open reading frame
PAGE	Polyacrylamide gel electrophoresis

PBS	Phosphate-buffered saline
PCR	Polymerase chain reaction
PIP	PP1-interacting protein
PLK1	Polo-like kinase 1
PLK1i	Polo-like kinase 1 inhibitor
PP1	Phosphoprotein phosphatase 1
PP2A	Phosphoprotein phosphatase 2A
PP6	Phosphoprotein phosphatase 6
PPP	Phosphoprotein phosphatase
PSTP	Protein serine/threonine phosphatase
PTP	Protein tyrosine phosphatase
RNAi	Ribonucleic acid interference
RZZ	ROD-Zwilch-ZW10
SAC	Spindle Assembly Checkpoint
SAPS	SIT4 phosphatase-associated protein
SD	Standard deviation
SDS	Sodium dodecyl sulphate
SEM	Standard error of the mean
siRNA	Small interfering ribonucleic acid
SPC24	Spindle pole body component 24
SPC25	Spindle pole body component 25
TRIP13	Thyroid hormone receptor interacting protein 13
UTR	Untranslated region
WT	Wild type
ZW10	Zest white 10

Chapter 1: Introduction

1.1 Cell cycle regulation is governed by the balance between kinase and phosphatase activity

1.1.1 The mammalian cell cycle

The mammalian cell cycle is the series of events that ensures the faithful inheritance of genetic material from a parent cell into two daughter cells. The importance of this process cannot be understated. In 1855, Rudolf Virchow published his famous aphorism “omnis cellula e cellula” meaning “every cell comes from another cell”. The cell cycle is the process by which a fertilised egg can give rise to a whole organism, and how tissues and organs regenerate after injury. Therefore, accurate and timely cell cycle progression and cell division are essential.

The mammalian cell cycle is split into four stages: gap 1 (G1), synthesis (S), gap 2 (G2) and mitosis (M). The first three stages are collectively referred to as interphase. In G1, the cell grows and prepares for the synthesis stage during which the cell’s DNA is replicated. In G2, further cell growth and protein synthesis occurs, as well as correction of any DNA replication errors. Finally, in mitosis, the replicated DNA is segregated into two new daughter cells. In organisms such as bacteria, DNA replication and mitosis occur simultaneously (Reyes-Lamothe et al., 2008). In mammalian cells, these stages have traditionally been considered as discrete, sequential steps. However, more recent thinking would suggest the stages are not as discrete as once thought, with S and G2 phase, in particular,

no longer being considered as discrete stages. The cell cycle stages are governed by a series of cyclin dependent kinases (CDKs) and their associated activating cyclin subunits (Figure 1.1A). These serine/threonine kinases drive cell cycle directionality by their oscillating behaviour, dictated by the periodic expression of the cyclin subunits which provide their substrate specificity.

Discovery of the key role of CDKs began with work investigating a cytoplasmic factor found to induce meiotic entry in Xenopus oocytes - the M-phase promoting factor (MPF) (Masui and Markert, 1971; Smith and Ecker, 1971). However, the active, M-phase-promoting component of this factor remained unknown. Genetic screens in yeast mutants with cell cycle defects identified the original member of the CDK family, cdc2 (Russell and Nurse, 1986). This protein was found to be essential for cell cycle progression in yeast. The mammalian homolog of cdc2, CDK1, was identified in human cells shortly after (Draetta et al., 1987; Lee and Nurse, 1987) as well as other members of the CDK family such as CDK2 (Elledge and Spottswood, 1991; Paris et al., 1991). Hanks (1987) independently cloned the CDK1 gene using probes were to screen a HeLa cDNA library for genes homologous to known serine/threonine kinases. A third independent study in sea urchin eggs identified a series of proteins that were synthesised and destroyed with each cell cycle, these were termed cyclins (Evans et al., 1983). Cyclins were subsequently clones from fertilized clam and sea urchin embryos and shown to promote meiosis in Xenopus oocytes (Hunt, 1989). These landmark studies converged in 1990 when an interaction was identified between CDK1 and cyclins A and B in clam oocytes, starfish and Xenopus oocytes (Nurse, 1990). From this it was concluded that MPF consists of two key interacting subunits. First, CDK1,

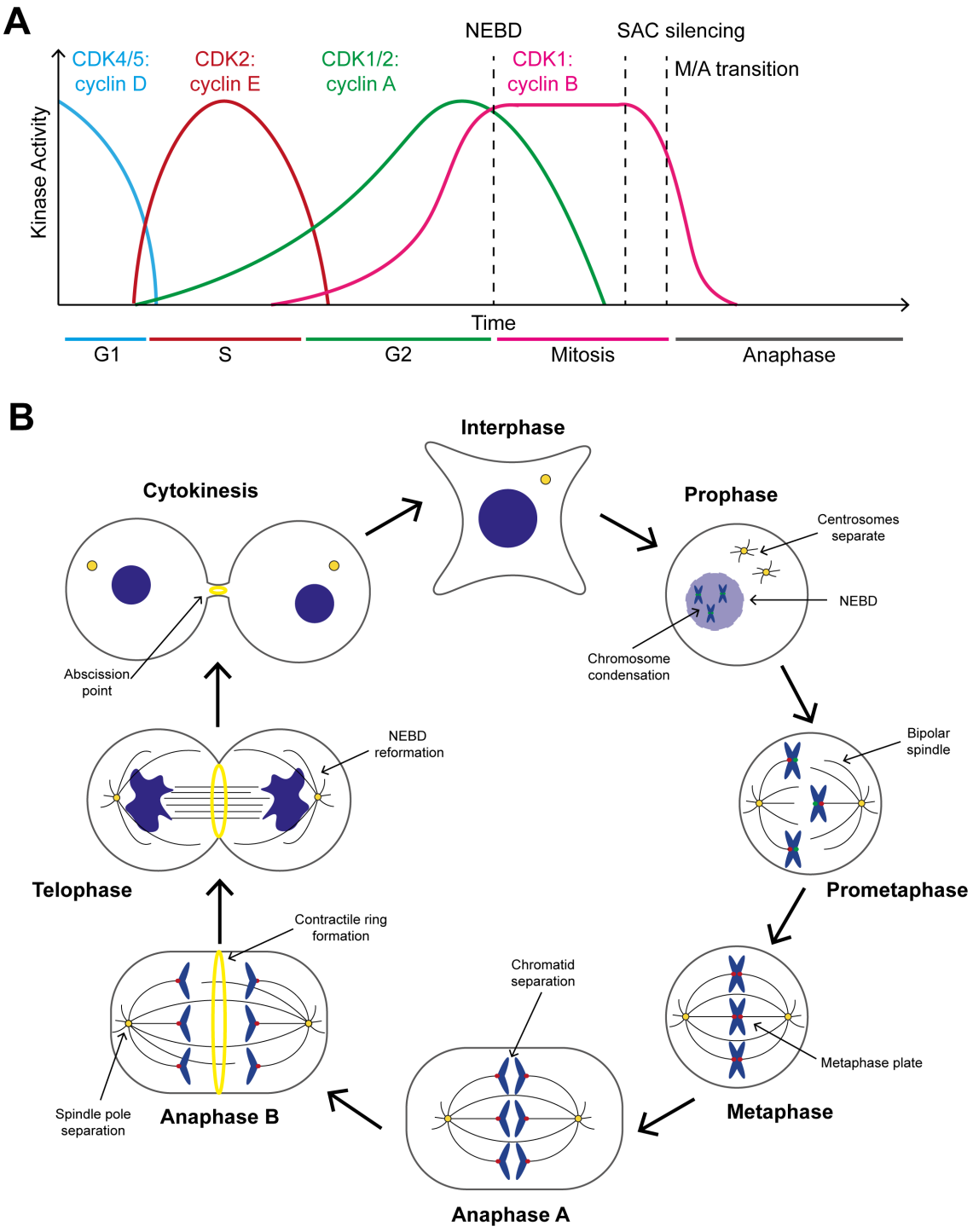


Figure 1.1 The cell cycle is a series of stages governed by CDK:cyclin complexes

(A) Levels of cyclins oscillate throughout the cell cycle, and bind to and activate cyclin dependent kinases (CDKs). The specific CDK:cyclin complexes and their activity associated with each cell cycle stage are shown and colour coded. (B) Mitosis is subdivided into a number of stages that are associated with specific morphological and structural changes within the cell. Diagram shows cell morphology and key

structural features associated with each mitotic stage.

a kinase that phosphorylates proteins during mitosis. Second, cyclins, which bound to and activated CDK1 during mitosis. Furthermore, these studies established the importance of CDKs in promoting transitions through the cell cycle. Subsequent work furthered this understanding by uncovering the distinctions between the A and B-type cyclins (Lehner and O'Farrell, 1990; Pines and Hunt, 1987; Pines and Hunter, 1989) and highlighted the importance of their specific periodic expression during the cell cycle to provide CDK substrate specificity (Minshull et al., 1990).

It is now understood that each cell cycle stage is defined and regulated by a specific CDK:cyclin complex (Figure 1.1A). CDK4/6 coupled with cyclin D drives cell cycle entry in response to external stimuli. CDK2:cyclin E is then responsible for driving cell entry into S phase. Subsequently, CDK1 in complex with cyclin A and B controls mitotic entry and progression. In particular, CDK1:cyclin B is the central driver and maintainer of the mitotic state. Ultimately, it is then the degradation of cyclin B and the subsequent reduction in CDK1 activity that results in mitotic exit (Nigg, 2001, 1995).

Pioneering work from Hartwell and Weinert observed that budding yeast cells arrest their cell cycle following faulty DNA replication. This arrest could be overcome by specific mutations termed "relief of inhibition mutants" (Hartwell and Weinert, 1989; Weinert and Hartwell, 1988). This led to the idea that cell cycle progression is surveyed by a series of checkpoints which halt cell cycle progression until all necessary processes have been completed and any errors

corrected. Checkpoints are now understood to monitor three points of the cell cycle: entry into the cell cycle, success of DNA replication and correct chromosome segregation. The first checkpoint, known as the “restriction point” or “G1 checkpoint” in mammals, controls commitment to the cell cycle in G1 in response to external stimuli. Once progression through the restriction point has occurred, the cell is committed to progressing into S phase, regardless of external stimuli (Pardee, 1987, 1989). The second checkpoint, the “DNA damage checkpoint” or “G2/M checkpoint”, acts during G2 to detect any DNA damage that has occurred during DNA replication. This checkpoint will halt progression into mitosis until any replication errors have been repaired (Wang et al., 2015). The final checkpoint is the “Spindle Assembly Checkpoint” (SAC) or “Metaphase checkpoint”. The SAC monitors the correct attachment of chromosomes to the mitotic spindle during early mitosis and prevents the onset of anaphase until all chromosomes are correctly attached. The SAC will be covered in detail in Chapter 1.3.

1.1.2 Outcome of cell cycle mis-regulation

Disruption of the precise order of the cell cycle and/or failure of a cell cycle checkpoint can be catastrophic for cell viability. A failure of the restriction point can result in cells continually and inappropriately entering the cell cycle, irrespective of external stimuli, a phenotype very commonly seen in cancer (Hanahan and Weinberg, 2011). Furthermore, cells that fail to repair DNA damage before mitotic entry often undergo cell death through “mitotic catastrophe” (Yoo et al., 2004; Wang et al., 2015). Errors in mitosis, either accumulated from previous cell cycle stages or in mitosis itself, can cause major

issues with cell ploidy. A failure of the cell to divide following DNA replication can result in tetraploidy, where the resulting cell has double the number of chromosomes. Alternatively, mis-segregation of chromosomes can result in aneuploidy, where have cells lost or gained whole chromosomes (Levine and Holland, 2018). Changes in chromosome number have significant consequences for the cell due to resultant changes in gene copy number and protein levels. Aneuploidy is a both hallmark and a driving force of many cancers and other pathologies (Cimini and Degrassi, 2005; Weaver and Cleveland, 2006; Weaver et al., 2007). More than 90% of solid tumours are aneuploid (Weaver and Cleveland, 2006) and, in meiosis, it is associated with many developmental disorders such as Down Syndrome (Hwang et al., 2021).

1.1.3 Mitosis

The final stage of the mammalian cell cycle is mitosis, the division of the parent cell into two daughter cells. It can be further subdivided into the following stages: prophase, prometaphase, metaphase, anaphase and telophase. Each stage is associated with specific morphological and structural changes within the cell (Figure 1.1B). As the cell enters mitosis its DNA is in the form of loosely packed chromatin. During prophase, the sister chromatids undergo condensation to form discrete chromosomes, with sister chromatids attached at the centromeric region through remaining centromeric cohesion (Waizenegger et al., 2000). The cell also begins to undergo extensive cytoskeleton remodelling. The duplicated microtubule organising centres (centrosomes) separate to opposite poles in preparation for mitotic spindle formation and begin to create microtubule asters.

At the end of prophase, the nuclear envelope breaks down (NEBD), allowing the mixing of the nucleoplasm and cytoplasm.

As the cell enters prometaphase, the bipolar mitotic spindle forms. This is a microtubule structure originating from the centrosomes at either pole of the cell that attaches to sister chromatids via proteinaceous structures called kinetochores. Once sister chromatids are attached to spindle microtubules from opposite poles, the two centrosomes begin pulling the chromosomes to opposite ends of the cell. This tension aligns the chromosomes along the cell equator to form the metaphase plate. The SAC acts throughout prometaphase to prevent further mitotic progression until all sister chromatids are correctly attached to opposite spindle poles and are aligned along the metaphase plate. It does this by producing a diffusible signal that inhibits the activity of the E3 ubiquitin ligase anaphase-promoting complex/cyclosome (APC/C) specifically towards the mitotic exit inhibitors, securin and cyclin B (Li and Murray, 1991; Hoyt et al., 1991; Musacchio, 2015; Lara-Gonzalez et al., 2012).

Entry into anaphase occurs following the satisfaction of the SAC and the re-activation of the APC/C. This results in the degradation of mitotic exit inhibitors, securin and cyclin B, the subsequent activation of separase and the destruction of the cohesin rings holding sister chromatids together (Sivakumar and Gorbsky, 2015). The tensile forces created by microtubules pulling on sister chromatids are now able to separate the sister chromatids to opposite poles. Anaphase can be separated into two main stages: A; the separation of the sister chromatids,

and B; the separation of spindle poles and elongation of the cell to complete DNA segregation.

In telophase, the nuclear envelope is reformed around the separated sister chromatids and the DNA within these new nuclei decondenses. The final stage of mitosis is the physical separation of the two daughter cells: cytokinesis. This occurs through the concerted action of microtubules at the midbody of the cell, the actin-myosin cytoskeleton, and membrane trafficking machinery (Barr and Gruneberg, 2007). This forms a cleavage furrow which pinches off the separated nuclei to form two daughter cells.

1.1.4 Mitotic entry is driven by CDK1

Entry into mitosis is driven by a global increase in the phosphorylation status of the cell (Dephoure et al., 2008). This is primarily carried out by the kinase CDK1 in complex with cyclin B. Indeed, mouse knockout experiments have shown that only CDK1 can initiate the onset of mitosis (Santamaría et al., 2007). However, other kinases such as those of the Aurora and Polo-like kinase families also play key roles at specific stages of mitosis (Barr and Gergely, 2007; Combes et al., 2017; Lampson et al., 2004). CDK1 phosphorylates a wide variety of substrates during mitosis to trigger whole-cell changes and specific mitotic processes including NEBD, chromosome condensation, inhibition of anaphase, mitotic spindle assembly and SAC licensing (Hayward et al., 2019b; Vassilev et al., 2006; Nigg, 1995; Nigg et al., 1996).

Like all CDKs, CDK1 is a serine/threonine protein kinase, with a preference for the consensus sequence S/T-P-X-K, due to a hydrophobic pocket near its catalytic site that accommodates the proline residue (Higashi et al., 1995; Alexander et al., 2011). In addition to this consensus motifs, the cyclin subunit of CDK:cyclin complexes binds specific short linear motifs (SliMs) on substrates via a hydrophobic binding pocket, which facilitates cell cycle-stage-specific phosphorylation (Örd et al., 2019b; a; Loog and Morgan, 2005; Bhaduri and Pryciak, 2011). For cyclin B, this specific SLiM is LxF (Örd et al., 2019b).

To achieve timely and controlled mitotic entry, the activity of CDK1 is tightly regulated (Figure 1.2). Synthesis of the main mitotic cyclin, cyclin B, begins in late S/early G2 and peaks at late G2 phase (Minshull et al., 1990; Pines and Hunter, 1989; Dynlacht et al., 1994). Synthesis is restricted to this cell cycle stage because it is driven by CDK2:cyclin A, which only accumulates from late G1. CDK2:cyclin A activates the transcription factors B-Myb, NF-Y and FoxM1 which subsequently induce the transcription of cyclin B (Chae et al., 2004; Laoukili et al., 2008; Major et al., 2004; Saville and Watson, 1998). Once synthesised, cyclin B is able to bind to CDK1. However, the binding of cyclin B alone is insufficient for CDK1 activation. Concomitantly to cyclin B binding, CDK1 is also phosphorylated on its T loop (T161) by CDK-activating kinases (CAKs) (Russo et al., 1996; Desai et al., 1995). CAK activity is consistent throughout the cell cycle, but the binding of cyclin B positions the T loop of CDK1 in a more favourable conformation for phosphorylation by CAKs (Desai et al., 1995). As is the case for many kinases, phosphorylation of the T loop promotes kinase activity

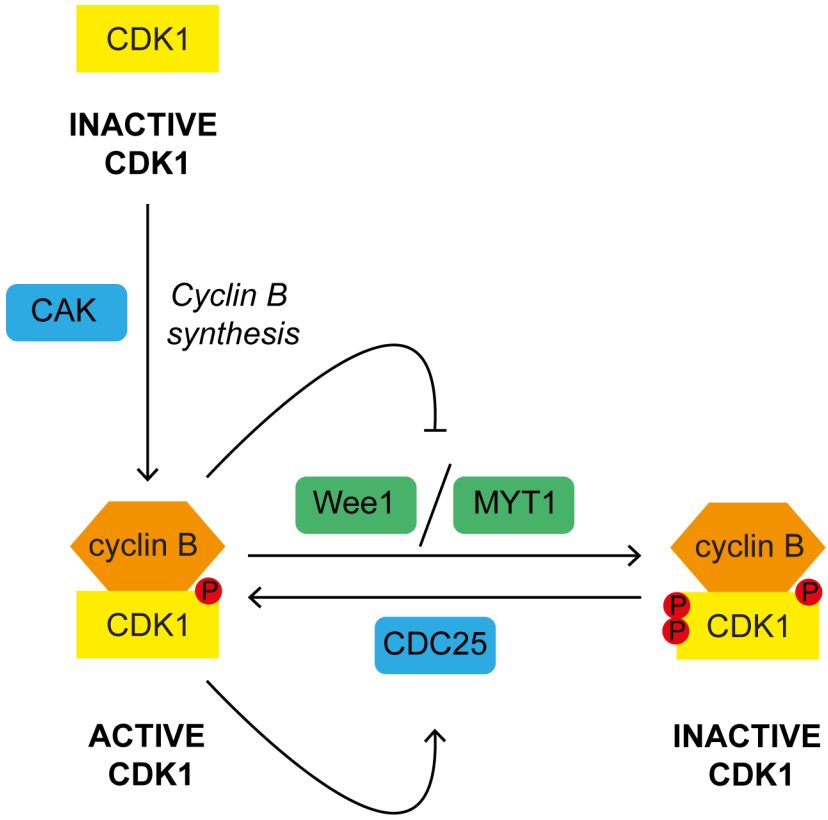


Figure 1.2 Regulation of CDK1 activity

Activity of the major mitotic kinase CDK1 is tightly regulated. CDK1 is bound by cyclin B that is synthesised in G2. It is simultaneously phosphorylated on its T loop by CAKs to promote kinase activity. CDK1:cyclin B complexes are kept inactive during G2 due to phosphorylations by Wee1 and Myt1 kinases. These phosphorylations are opposed by CDC25 phosphatase. CDK1:cyclin B activates CDC25 and inhibits Wee1/Myt1 through phosphorylation. This creates a feedback loop promoting the activation of more CDK1:cyclin B. This ensures the G2/M transition is switch-like and irreversible.

(Kang et al., 2007; Mattison et al., 2007; Jelluma et al., 2008b; Dodson et al., 2013).

However, CDK1 remains inactive due to a final level of regulation that acts at the G2/M transition (Figure 1.2). During G2, CDK1 is kept inactive by inhibitory phosphorylations carried out by the kinases Wee1 and Myt1 at T14 and Y15 (Gould and Nurse, 1989; Kellogg, 2003; Morla et al., 1989). The critical event for

mitotic entry is the removal of these inhibitory phosphorylations on CDK1 by the dual specificity phosphatase CDC25A/B/C (Hoffmann et al., 1993). At the same time, the inhibitory activities of the kinases Wee1/Myt1 are supressed. The mechanisms that activate CDC25 activity are not well understood. However, it is known that CDKs are able to activate CDC25 and inhibit Wee1/Myt1 (Gabrielli et al., 1997; Lammer et al., 1998; Hoffmann et al., 1993; Harvey et al., 2005). It is possible that S-CDKs result in partial activation of CDC25 and thus activation of a subpopulation of CDK1 complexes. This subpopulation then phosphorylates CDC25 and Wee1 promoting the further activation of CDK1. Therefore, CDK1 generates a self-amplifying positive feedback loop. In addition, once CDK1 activity reaches a certain level, it inhibits the activity of its opposing phosphatase PP2A-B55 (see Chapter 1.1.5). This phosphatase maintains Wee1, Myt1 and CDC25 in a dephosphorylated state during interphase. Its inhibition ensures that Wee1 and Myt1 remain inactive and CDC25 is active at the G2/M transition, thereby promoting further CDK1 activation (Mochida et al., 2010; Gharbi-Ayachi et al., 2010). Overall, this creates a bi-stable switch-like transition from low- to high-level CDK1 activity at the G2/M transition. Once this activity reaches a certain threshold level, transition into mitosis in inevitable and irreversible (Mochida et al., 2016; Novak and Tyson, 1993; Pomerening et al., 2003).

CDK1 activity remains high during mitosis in order to maintain the mitotic state. However, following chromosome alignment, satisfaction of the SAC and the subsequent activation of the APC/C, CDK1 activity rapidly drops due to the degradation of cyclin B (Novak et al., 2007; Sivakumar and Gorbsky, 2015; King et al., 1995; Sudakin et al., 1995; Clute and Pines, 1999). This change in CDK1

activity triggers the transition into mitotic exit described in Chapter 1.1.5. It also results in the reactivation of Wee1/Myt1 and the inhibition of CDC25 through dephosphorylation by PP2A-B55. This keeps CDK1 in an inhibited state until the subsequent mitosis.

1.1.5 Mitotic exit is triggered by phosphoprotein phosphatases

In contrast to mitotic entry, mitotic exit is characterised by a global decrease in the phosphorylation status of the cell due to the timely removal of CDK1 phosphorylations following cyclin B degradation. Protein phosphorylation is a highly dynamic modification and its removal requires specific phosphatases that oppose CDK1 and the other mitotic kinases (Barr et al., 2011).

Phosphatases fall into two main categories: protein tyrosine phosphatases (PTPs) and protein serine/threonine phosphatases (PSTPs). PTPs are not heavily involved in cell cycle regulation. The only exceptions are several dual specificity phosphatases like Cdc14 in yeast (Stegmeier and Amon, 2004) and CDC25 in humans (Hoffmann et al., 1993). Instead, it is the latter group, PSTPs, that are key to regulating the cell cycle. PSTPs can be further subdivide into metallo-dependent phosphatases and phosphoprotein phosphatases (PPPs), and it is the PPPs that are responsible for the decrease in phosphorylation seen at mitotic exit (Barr et al., 2011; Shi, 2009). This was discovered by treating cells with the algal toxin okadaic acid that specifically inhibits PPPs. This triggered many mitotic-like changes such as chromatin condensation (Yamashita et al., 1990; Lucocq et al., 1991), indicating that regulation of PPPs, particularly their

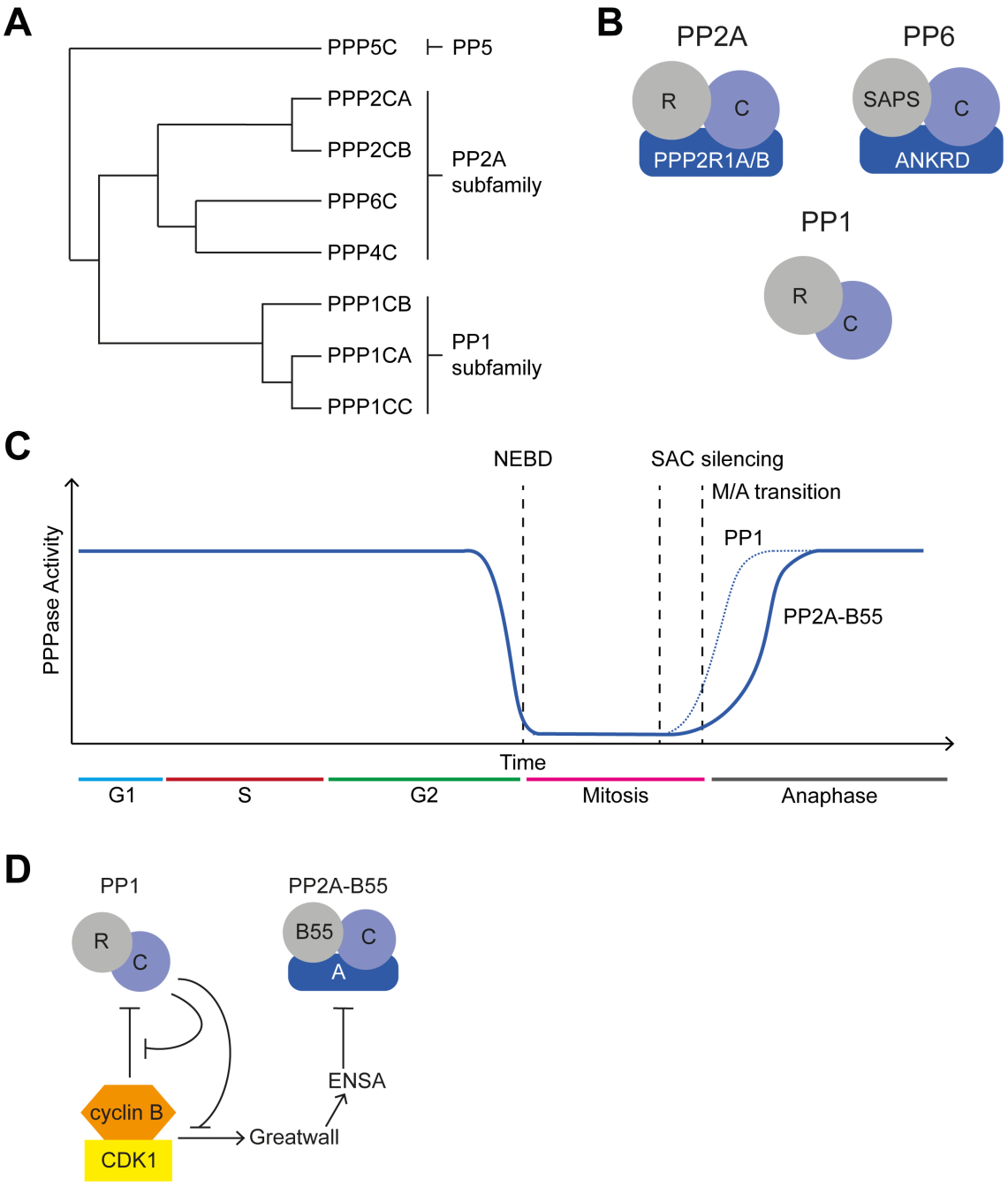


Figure 1.3 Phosphoprotein phosphatases in mitotic regulation

(A) Schematic representing the phosphoprotein phosphatase (PPP) sub-families. (B) Schematic showing PPP subunit composition. PP2A is a heterotrimer formed of catalytic (C), regulatory (R) and scaffold (PPP2R1A/B) subunits. PP6 is a heterotrimer formed of C, SIT4 phosphatase associated protein domain (SAPS) and ankyrin repeat domain-containing (ANKRD) subunits. PP1 is a heterodimer formed of C and R subunits. (C) PP1 and PP2A-B55 are inactive during mitosis and only become active at the metaphase-to-anaphase transition due to CDK1 inhibition. Their relative activities associated with each cell cycle stage are shown. (D) PP1 and PP2A-B55

are inhibited by CDK1:cyclin B during mitosis. PP1 is directly inhibited by CDK1 through phosphorylation. PP2A-B55 is indirectly inhibited by CDK1 through the Greatwall pathway. CDK1 activates the kinase Greatwall which phosphorylates ENSA. Phosphorylated ENSA binds to and inhibits PP2A-B55.

inhibition, was necessary for mitotic progression. Within the PPP family there are three sub-families (Figure 1.3A): PP5, PP2A including PPP2CA, PPP2CB, PPP6C and PPP4C, and PP1 including PPP1CA, PPP1CB and PPP1CC (Barr et al., 2011).

The PSTP family all use two metal ions for catalysis, Mn^{2+} and Fe^{2+}, coordinated by a conserved set of amino acids (Shi, 2009). Within the PPP family, the catalytic subunits are so similar that they can all be inhibited by the potent algal toxins microcystin-LR and okadaic acid. However, they can be distinguished to some extent by their sensitivities to these toxins. For example, PP2A is 100 times more sensitive to okadaic acid than PP1 (Xing et al., 2006). Despite this, there is no observable difference in substrate specificity between the different catalytic subunits. Therefore, phosphatase specificity is determined by regulatory subunits that interact with the catalytic subunits. The three mammalian catalytic isoforms of PP1 form heterodimers with a regulatory subunit (R) or PP1-interacting protein (PIP) (Bollen et al., 2010; Barr et al., 2011) (Figure 1.3B). It has been proposed that PP1 has 100-200 regulatory subunits. In contrast, PP2A phosphatases form a trimeric complex with catalytic, scaffold (PPP2R1A/B) and regulatory subunits (Figure 1.3B). The PP2A holoenzymes contain one of four possible regulatory subunits: B/B55, B'/B56, B'' and B''' which alter the substrate specificity based on their interaction mechanism with the catalytic subunit (Janssens and Goris,

2001; Barr et al., 2011; Xu et al., 2006; Xing et al., 2006). PP6, like PP2A, forms a trimeric complex with a catalytic subunit, an ankyrin repeat domain-containing subunit (ANKRD) and a SIT4 phosphatase associated protein domain (SAPS) (Barr et al., 2011) (Figure 1.3B).

For the timely and accurate removal of phosphorylations at mitotic exit, the PPPs must be regulated in a cell cycle-specific manner. The PPPs show differential regulation in accordance with the functions that they carry out. PP1 and PP2A-B55 are the main phosphatases opposing CDK1 at mitotic exit, as well as other mitotic kinases such as Aurora B. Both PP1 and PP2A-B55 are inhibited by CDK1 during early mitosis, and so only become active once cyclin B levels (and hence CDK1 activity) decrease (Dohadwala et al., 1994; Yamano et al., 1994; Mochida et al., 2010; Blake-Hodek et al., 2012; Vigneron et al., 2011) (Figure 1.3C-D). This prevents premature substrate dephosphorylation in early mitosis but ensures the rapid removal of the phosphorylations following SAC satisfaction and the maintenance of low CDK1 phosphorylation during interphase.

PP1 activity is subject to direct regulation by CDK1 through an inhibitory phosphorylation at a C-terminal threonine residue (Dohadwala et al., 1994; Yamano et al., 1994; Grallert et al., 2015) (Figure 1.3D). To become active at the metaphase-to-anaphase transition, *in vivo* evidence suggests that PP1 auto-dephosphorylates, however this has not been shown conclusively in humans (Dohadwala et al., 1994; Wu et al., 2009; Yamano et al., 1994). It is also not yet clear whether the consequences of CDK1 regulation are the same for all PP1 catalytic isoforms.

PP2A-B55 activity is indirectly regulated by CDK1 via the Greatwall pathway (Cundell et al., 2013; Álvarez-Fernández et al., 2013; Burgess et al., 2010; Vigneron et al., 2009; Castilho et al., 2009) (Figure 1.3D). In this pathway, CDK1 phosphorylates and activates the kinase Greatwall/MASTL (Yu et al., 2004; Blake-Hodek et al., 2012; Vigneron et al., 2011). Greatwall/MASTL subsequently phosphorylates the small proteins ENSA and Arpp19. In their phosphorylated forms, these proteins bind with high affinity to PP2A-B55 and inhibit it (Gharbi-Ayachi et al., 2010; Mochida et al., 2010). Following the decrease in CDK1 activity at mitotic exit, ENSA and Arpp19 become dephosphorylated, thus leading to the activation of PP2A-B55 (Blake-Hodek et al., 2012; Gharbi-Ayachi et al., 2010; Mochida et al., 2010; Williams et al., 2014; Castro and Lorca, 2018). However, the dephosphorylation kinetics of ENSA and Arpp19 are very slow, resulting in a delay in the activation of PP2A-B55 (Williams et al., 2014; Cundell et al., 2013). It has also been proposed that PP1 is the phosphatase that dephosphorylates and inactivates Greatwall/MASTL, suggesting that PP2A-B55 cannot become active until PP1 is active (Heim et al., 2015; Ma et al., 2016). Therefore, at mitotic exit, PP1 becomes active almost immediately after CDK1 levels begin to decrease whereas PP2A-B55 activation is delayed (Figure 1.3C). This difference in regulation and activation timings provides a mechanism for carrying out dephosphorylations and mitotic exit activities with different timings, if acted on by different phosphatases.

Contrastingly, PP2A-B56 is not inhibited by CDK1 because its activity is required throughout mitosis to oppose the activities of the mitotic kinases MPS1 and

Aurora B at the kinetochore (Foley et al., 2011; Kruse et al., 2013; Espert et al., 2014). Instead, PP2A-B56 activity is regulated spatially through the targeting of the holoenzyme to specific binding partners through a short binding motif, LxxIxE (Hertz et al., 2016). These binding partners can either be PP2A-B56 substrates such as Repo-Man (Qian et al., 2013), or direct PP2A-B56 to a specific location in the cell, such as to the kinetochore through BUBR1 (budding uninhibited by benzimidazole related 1) (Kruse et al., 2013; Suijkerbuijk et al., 2012). The targeting of PP2A-B56 to the kinetochore is actually positively regulated by CDK1 through phosphorylation of BUBR1 (Kruse et al., 2013). Furthermore, there is evidence that phosphorylation of the LxxIxE binding motif in binding partners may act to regulate interaction with PP2A-B56 (Hertz et al., 2016). Therefore, while CDK1 prevents PP1 and PP2A-B55 activity, it promotes the recruitment and hence the activity of PP2A-B56 during mitosis.

PP1 is also spatially regulated through short motifs in its binding partners. PIPs contain short motifs recognised by the PP1 catalytic subunit, the most common being the RVxF motif (Bollen et al., 2010; Cohen, 2002; Egloff et al., 1997). Studies have identified numerous RVxF-containing PIPs that precisely determine the localisation and substrate specificity of the PP1 catalytic subunit (Cohen, 2002; Bollen et al., 2010; Egloff et al., 1997; Hendrickx et al., 2009). In mammalian cells, the three PP1 catalytic isoforms show distinct localisations (Trinkle-Mulcahy et al., 2006). For example, in metaphase, PPP1CC and PPP1CA are localised to the outer-kinetochore through a number of RVxF-containing binding partners including KNL1 (Nijenhuis et al., 2014; Rosenberg et al., 2011; Shepperd et al., 2012; Liu et al., 2010; Espeut et al., 2012), KIF18A

(De Wever et al., 2014; Häfner et al., 2014; Meadows et al., 2011), CENP-E (Kim et al., 2010) and Astrin (Conti et al., 2019). Studies suggest that Aurora B phosphorylation of the KNL1 RVxF motif negatively regulates PP1 recruitment to kinetochores, providing yet another mechanism to regulate the localisation and activity of PP1 (Cohen, 2002; Liu et al., 2010; Welburn et al., 2010; Nasa et al., 2019). Additionally, PPP1CB co-localises with the mitotic kinase PLK1 at kinetochores through the RVxF-containing binding partner MYPT1 (Terrak et al., 2004; Yamashiro et al., 2008). Contrastingly, in anaphase, PPP1CC is localised to the chromatin via interaction with Repo-Man (Trinkle-Mulcahy et al., 2006). Interestingly, there is also evidence of RVxF motifs in PP2A-B56 and PP2A-B55 (Grallert et al., 2015). This is suggested to recruit PP1 to these phosphatases to aid in their activation during mitosis through a CDK1-mediated relay.

An additional PP1 binding motif found in seven of the known PIPs is the SILK motif. It is always found N-terminal to the RVxF motif and is thought to carry out an anchoring function to aid in the efficient docking of PP1 to the PIP (Hendrickx et al., 2009).

1.2 The kinetochore is an essential macromolecular structure for mitosis

1.2.1 The kinetochore is composed of the inner- and outer-kinetochore

The accurate segregation of chromosomes in mitosis critically depends on chromosomes interacting appropriately with microtubules of the mitotic spindle. This is mediated by a structure called the kinetochore, a highly dynamic macromolecular structure that assembles at the centromeric region of each chromosome (Cheeseman, 2014; Hinshaw and Harrison, 2019). The kinetochore

carries out two distinct functions. First, it is the point of physical attachment between the chromosome and microtubules of the mitotic spindle. Second, it acts as the sensor of kinetochore-microtubule attachment status by providing the signalling platform for the SAC and error-correction pathways.

The kinetochore is a layered structure of more than 90 proteins. Traditional electron microscopy revealed that it has a dense inner-kinetochore that contacts the centromere and an outer-kinetochore that connects with microtubules (Brinkley and Stubblefield, 1966; Jokelainen, 1967; Roos, 1976) (Figure 1.4). While the inner-kinetochore is present throughout the cell cycle, the outer-kinetochore only assembles in late G2/early mitosis and is subsequently disassembled at mitotic exit (Gascoigne and Cheeseman, 2013). Additionally, unbound kinetochores were observed to have a fibrous corona that extends away from the main kinetochore and disappears upon microtubule attachment (Cassimeris et al., 1990).

The location of the centromere is defined epigenetically by a histone variant of Histone 3, CENP-A, which forms nucleosomes exclusively at centromeric DNA (Palmer et al., 1991, 1987; De Rop et al., 2012). This region of DNA is typically formed of tandem 171-bp repetitive sequences known as α-satellite domains (Musacchio and Desai, 2017). Following its deposition in G1, CENP-A is stably associated with centromeres (Jansen et al., 2007).

Although CENP-A is sufficient to drive outer-kinetochore assembly in *Drosophila* (Heun et al., 2006), it is not sufficient for complete kinetochore assembly in

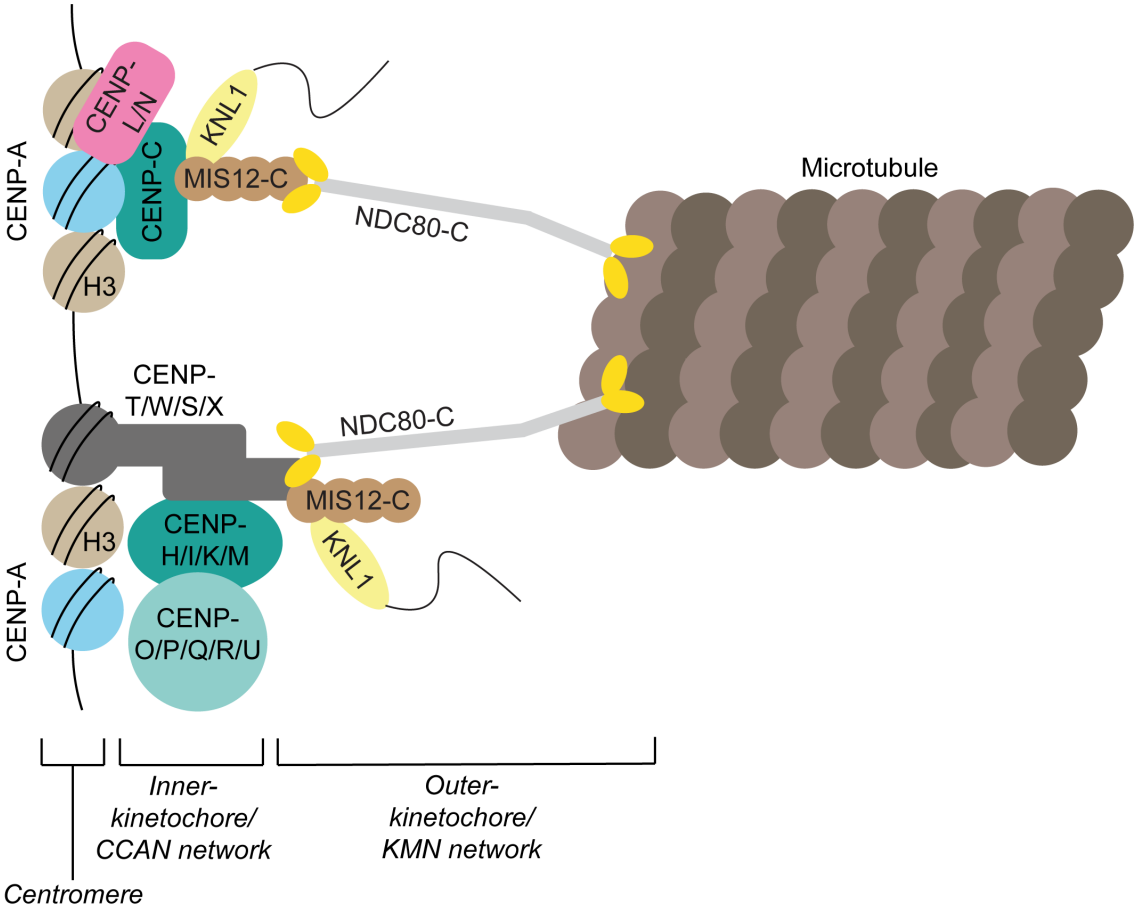


Figure 1.4 The structure of the mammalian kinetochore

The kinetochore is assembled on the centromere, defined by the specialised nucleosome CENP-A. The kinetochore is formed of the inner- and outer-kinetochore. The inner-kinetochore is a collection of 16 proteins called the CCAN network that resides at the kinetochore throughout the cell cycle. The CCAN is formed of four subcomplexes; CENP-CHIKM, CENP-TWSX, CENP-OPQRU and CENP-LN. The outer-kinetochore or KMN network is assembled in mitosis and is formed of KNL1, the MIS12-C and the NDC80-C. The KMN network is assembled through two pathways via CENP-C and CENP-T. Microtubule attachments predominantly occur through interaction with the NDC80-C.

mammalian cells (Van Hooser et al., 2001). Therefore, a collection of 16 proteins known as the constitutive centromere-associated network (CCAN) resides at the centromere throughout the cell cycle to form the inner-kinetochore (Foltz et al., 2006; Amaro et al., 2010; Hori et al., 2008) (Figure 1.4). Functional analyses have shown that these proteins predominantly play a structural role in forming the

platform for outer-kinetochore assembly as well forming the correct environment for further CENP-A assembly (Foltz et al., 2006; Okada et al., 2006; Liu et al., 2006; Okada et al., 2009). However, recent evidence suggests that the CCAN may also directly participate in controlling microtubule dynamics through binding microtubules (Pesenti et al., 2018). Therefore, the inner- and outer-kinetochore may not be as distinct as once thought. The CCAN is formed of four subcomplexes; CENP-CHIKM, CENP-TWSX, CENP-OPQRU and CENP-LN (Hori et al., 2008; Carroll et al., 2009, 2010; Klare et al., 2015; Perpelescu and Fukagawa, 2011; Okada et al., 2006; Foltz et al., 2006; Izuta et al., 2006). Components of the CCAN assemble either via interaction with CENP-A or via direct interaction with centromeric DNA. CENP-C and CENP-N interact with CENP-A and show a tenfold preference for CENP-A over canonical H3 nucleosomes (Weir et al., 2016; Kato et al., 2013; Carroll et al., 2009, 2010). Contrastingly, the CENP-TWSX complex directly binds to DNA to form a specialised nucleosome-like structure (Hori et al., 2008; Gascoigne et al., 2011; Nishino et al., 2012). Two cryo-EM structures have been recently been published, confirming and further revealing the exact structure of the inner-kinetochore components on the centromere and the mechanisms by which the CENP-A nucleosome is recognised by the CCAN (Yatskevich et al., 2022; Pesenti et al., 2022). However, the precise connectively of the inner-kinetochore components is still the focus of much ongoing research. Super-resolution imaging and FRET studies are being employed to map the relative localisations of the kinetochore proteins (Hellwig et al., 2009; Wan et al., 2009). Ultimately the inner-kinetochore results in the formation of two branches of kinetochore assembly, one via CENP-

C and the other via CENP-T (Gascoigne et al., 2011; Hori et al., 2008; Nishino et al., 2013; Hori et al., 2013; Guse et al., 2011) (Figure 1.4).

The outer-kinetochore or KMN network assembles onto the inner-kinetochore in late G2/early mitosis. It is both the point of attachment between chromosomes and microtubules (Ciferri et al., 2008; Varma and Salmon, 2012), and the signalling platform for the SAC to monitor microtubule binding (Yamagishi et al., 2012; Shepperd et al., 2012; London et al., 2012). Early studies using sedimentation assays revealed the direct role of the KMN network in microtubule binding, in particular the cooperative and synergistic nature of the KMN network in microtubule binding (Cheeseman et al., 2006). The KMN network is a nine-subunit network formed of three key complexes: KNL1, the MIS12 complex (MIS12-C) comprising MIS12, NNF1, NSL1 and DSN1, and the NDC80 complex (NDC80-C) comprising NDC80/HEC1, NUF2, SPC24 and SPC25 (Cheeseman et al., 2006; Foley and Kapoor, 2013; DeLuca and Musacchio, 2012) (Figure 1.4). Depletion of any of these components is detrimental to cell viability and mitotic progression. The loss of the NDC80-C results in attachment defects and extensive chromosome mis-segregation (DeLuca et al., 2002; Desai et al., 2003) and in severe cases a complete failure of chromosome segregation (Wigge and Kilmartin, 2001; Wigge et al., 1998). Loss of the MIS12-C or KNL1 results in only a partial chromosome alignment phenotype and SAC failure (Cheeseman and Desai, 2008; Kline et al., 2006; Pagliuca et al., 2009). In all cases, the loss of one KMN component significantly affects the assembly of the other components. Additional kinetochore-associated factors such as the Ska complex, Astrin/Kinastrin, EB proteins and CENP-E also contribute to the microtubule

binding interface and kinetochore signalling network (Foley and Kapoor, 2013), but these will not be covered here. Instead, the following section will focus on the key KMN network components; KNL1, the NDC80-C and the MIS12-C.

KNL1 (Kinetochore null-1) is the largest outer-kinetochore component in humans (2316 residues) (Desai et al., 2003). It is a highly disordered protein and has therefore proven impossible to crystalise in its entirety. However, the largely ordered C-terminus of the protein is known to interact with the MIS12-C via a RWD domain and with Zwint-1 via a coiled-coil domain (Petrovic et al., 2014, 2010). Although the N-terminus of KNL1 has been shown to have microtubule binding ability (Espeut et al., 2012), the main function of KNL1 is as a scaffold protein, coordinating different activities at the outer-kinetochore through numerous protein-protein interactions. In particular, KNL1 contains multiple motifs for the recruitment of the BUB (budding uninhibited by benzimidazole) proteins, which are components of the SAC. It contains two KI motifs (KI1 and KI2) which interact with BUB1 and BUBR1 respectively (Bolanos-Garcia and Blundell, 2011; Krenn et al., 2012). However, these motifs are insufficient for high affinity binding. KNL1 also contains 19 methionine-glutamic acid-leucine-threonine (MELT) motifs which become phosphorylated during SAC signalling and form the major binding sites for BUB checkpoint proteins (Yamagishi et al., 2012; London et al., 2012; Shepperd et al., 2012; Primorac et al., 2013). Furthermore, KNL1 contains an additional SHT motif that can be phosphorylated downstream of MELT motif phosphorylation. This motif is hypothesised to aid BUB protein recruitment (Vleugel et al., 2015). This places KNL1 in the critical role as the scaffold for SAC signalling. Additionally, KNL1 contains RVxF and

SILK motifs in its N-terminus for the recruitment of a key mitotic phosphatase, PP1 (Liu et al., 2010).

The NDC80-C is the primary site of microtubule attachment to kinetochores (Figure 1.4). It is a heterotetrametic complex formed of NDC80 (HEC1 in humans), NUF2, SPC24 and SPC25 (McCleland et al., 2004; DeLuca et al., 2006). The individual monomers interact via coiled-coil domains to form an extended dumbbell-shaped structure. Within this, the SPC24:SPC25 globular heads form the interaction with the rest of the kinetochore. At the other end, the HEC1:NUF2 globular heads form the attachments to microtubules (Ciferri et al., 2008). Cyro-EM studies have observed direct binding of HEC1:NUF2 to microtubules. A tight arrangement of two calponin homology domains in HEC1 and NUF2 combined with the positively charged disordered N-terminal tail of HEC1 form the microtubule binding interface (Alushin et al., 2010, 2012; DeLuca et al., 2006; Ciferri et al., 2008; Wei et al., 2007). As will be discussed in detail in Chapter 1.3, the binding of microtubules to the NDC80-C is tightly regulated. However, critically, Aurora B phosphorylation of the N-terminal tail of the NDC80-C disrupts the ability to form electrostatic interactions and therefore prevents the attachment of microtubules to kinetochores (Welburn et al., 2010; Ciferri et al., 2008; DeLuca et al., 2011).

The MIS12-C is the only KMN network component that does not directly bind to microtubules. Instead, it is a scaffold protein connecting the different components of the KMN network and the inner-kinetochore proteins (Petrovic et al., 2016; Cheeseman et al., 2006). The MIS12-C is formed of four largely helical subunits

that form two dimers: NSL1:DSN1 and MIS12:NNF1. These dimers combine to form the tetrameric rod-shaped MIS12-C (Petrovic et al., 2010, 2016). The N-terminal head domain is able to interact with both CENP-C and CENP-T (Petrovic et al., 2010, 2016; Rago et al., 2015; Huis in 't Veld et al., 2016; Kim and Yu, 2015). This is contrast to the C-terminus, which connects with KNL1 via NSL1 and with SPC24 and SPC25 of the NDC80-C via NSL1 and DSN1 (Petrovic et al., 2010, 2016; Dimitrova et al., 2016). A critical observation is that NSL1 is the key MIS12-C component that supports the interactions with the NDC80-C and KNL1, thus linking the KMN network together (Petrovic et al., 2010).

The KMN network assembles via two branches with distinct conformations, one via CENP-C and the other via CENP-T (Figure 1.4 and 1.5). Studies have shown that the artificial targeting of CENP-C or CENP-T to ectopic sites on chromosome arms can result in the assembly of kinetochore-like structures (Gascoigne et al., 2011; Hori et al., 2008; Nishino et al., 2013; Hori et al., 2013; Guse et al., 2011). The CENP-C pathway recruits the NDC80-C through interaction with MIS12-C:KNL1 which assemble onto the kinetochore together via a direct interaction between MIS12 and CENP-C. In contrast, the CENP-T pathway initially recruits the NDC80-C via interaction with CENP-T. This then promotes the recruitment of MIS12-C:KNL1 through a separate region of CENP-T (Rago et al., 2015). Despite these models, understanding of the exact mechanisms of KMN network assembly is still significantly lacking. In particular, questions remain as to whether the two branches of assembly are distinct, or if there is an overlap between them. For example, it is possible that a single MIS12-C:KNL1 could create a bridge between a CENP-T and a CENP-C pathway, linking them together. These

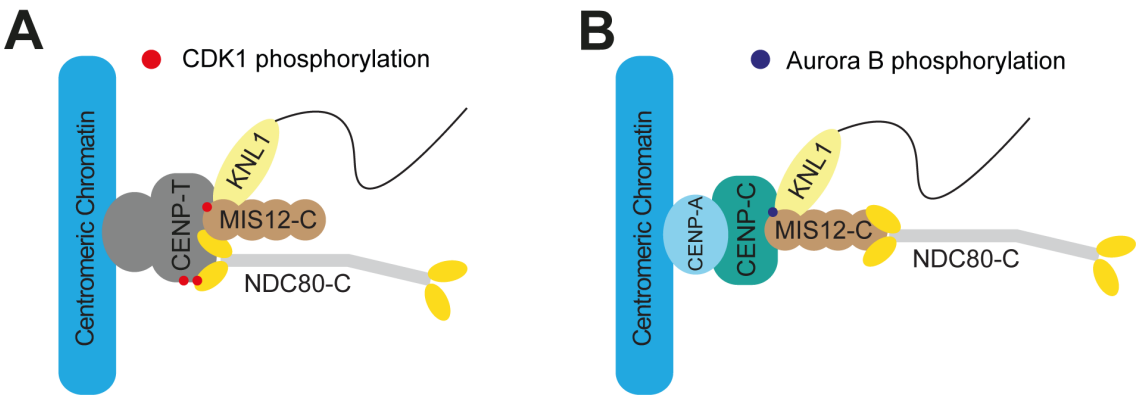


Figure 1.5 Phospho-regulation of outer-kinetochore assembly

Mammalian outer-kinetochore assembly is regulated by CDK1 and Aurora B. (A) Assembly via CENP-T requires three CDK1 phosphorylations on CENP-T, two for the NDC80-C localisation and one for MIS12-C:KNL1 localisation. (B) Assembly via CENP-C requires phosphorylation of DSN1 by Aurora B to regulate the interaction between the MIS12-C and CENP-C.

questions offer a basis for interesting future research into outer-kinetochore assembly.

1.2.2 Regulation of outer-kinetochore assembly

Although past research has provided a detailed knowledge of the structure of the kinetochore, surprisingly little is understood about how outer-kinetochore assembly is regulated to ensure timely assembly/disassembly in mitosis. As the cell enters mitosis, the outer-kinetochore proteins are rapidly assembled onto the inner-kinetochore within a time frame of approximately 20 min (Gascoigne and Cheeseman, 2013). These proteins are equally rapidly disassembled from the kinetochore at mitotic exit, with complete disassembly occurring before cytokinesis (Gascoigne and Cheeseman, 2013). It is a major challenge to the cell for this to occur in a controlled and organised manner. There are two key

mechanisms currently known to regulate outer-kinetochore assembly: protein sub-cellular localisation and phosphorylation.

During interphase, many proteins are excluded from the nucleus by the nuclear envelope. At NEBD, the loss of the nuclear envelope and mixing of the nucleoplasm and cytoplasm allows such proteins access to components such as the kinetochore. This provides a simple mechanism to restrict protein assembly onto the kinetochore until after NEBD has occurred. The NDC80-C is one protein regulated in this manner. It is found in the cytoplasm during interphase and is excluded from the nucleus until NEBD (Gascoigne and Cheeseman, 2013). Studies where a nuclear localisation signal was added to HEC1 revealed that this resulted in premature loading of the NDC80-C onto kinetochores in G2 (Gascoigne and Cheeseman, 2013). This highlights the importance of controlling subcellular localisation of the NDC80-C to regulate timely outer-kinetochore assembly. However, a subset of kinetochore proteins, including the MIS12-C and KNL1, are present in the nucleus prior to NEBD and do not localise to the kinetochore until mitosis (Gascoigne and Cheeseman, 2013; Cheeseman et al., 2008), indicating that this cannot be the only mechanism of regulation.

Phosphorylation of the outer-kinetochore has been implicated in the regulation of outer-kinetochore assembly. Early studies in yeast and Xenopus revealed a critical role of Aurora B in regulating outer-kinetochore assembly (Emanuele et al., 2008). However, the nature of phospho-regulation in mammalian cells appears to be more complex and the relative contribution of kinases remains to be determined. Studies from the Cheeseman and Musacchio labs have revealed

that mammalian outer-kinetochore assembly is regulated by both CDK1 and Aurora B (Gascoigne and Cheeseman, 2013; Rago et al., 2015; Huis in 't Veld et al., 2016) (Figure 1.5A-B). In particular, distinct phosphorylations regulate the two branches of outer-kinetochore assembly (Rago et al., 2015). The CENP-T assembly pathway involves three CDK1 phosphorylations on CENP-T (Figure 1.5A). Two of these are required for the NDC80-C localisation (T11 and T85) and the third for MIS12-C:KNL1 localisation (T195). Contrastingly, assembly via CENP-C is controlled by Aurora B phosphorylation of DSN1 at S100 and S109 which regulates the interaction between CENP-C and MIS12 (Kim and Yu, 2015; Rago et al., 2015; Welburn et al., 2010; Yang et al., 2008) (Figure 1.5B). Interestingly, the latter regulatory pathway is the one also observed in yeast and Xenopus. It appears that the CDK1 pathway of control is an additional level of regulation evolved for mammalian kinetochores. Furthermore, the CDK1 pathway of control appears to be the dominant pathway of outer-kinetochore assembly in mammals with the relative contribution of Aurora B regulation being much smaller (Gascoigne and Cheeseman, 2013). This agrees with the major, overarching role of CDK1 in mammalian mitosis and links outer-kinetochore assembly with global mitosis regulation. Therefore, this provides a mechanism to restrict outer-kinetochore assembly to within mitosis when CDK1 levels are high.

The fact that outer-kinetochore assembly in mammals critically depends on CDK1 suggests that the removal of these phosphorylations by counteracting phosphatases is necessary for timely outer-kinetochore disassembly, and therefore for accurate chromosome segregation. Supporting this, studies have shown that PP2A-B55 opposes CDK1 regulation of the NDC80-C at the

kinetochore (Gascoigne and Cheeseman, 2013). Although the exact phosphatases have not been identified for all outer-kinetochore components, work using diverse phosphatase inhibitors revealed differing effects on the outer-kinetochore components (Gascoigne and Cheeseman, 2013). This suggests differential phosphatase regulation of outer-kinetochore components or multiple pathways of disassembly regulation.

1.3 The Spindle Assembly Checkpoint prevents untimely mitotic exit

1.3.1 The importance of the Spindle Assembly Checkpoint

The cell faces a major challenge in the accurate segregation of its chromosomes in mitosis. Duplicated chromosomes must be separated so that each daughter cell receives one copy of each chromosome. To ensure accurate segregation, chromosomes must be attached to microtubules of the mitotic spindle from opposite spindle poles before they are separated in anaphase. The Spindle Assembly Checkpoint (SAC) is a cell cycle checkpoint and surveillance system that monitors the attachment of chromosomes to the mitotic spindle and prevents anaphase onset until all chromosomes are correctly attached (Musacchio and Salmon, 2007; Lara-Gonzalez et al., 2012). This occurs through the specific inhibition of the E3 ubiquitin ligase, APC/C, towards the mitotic exit inhibitors, securin and cyclin B, preventing their degradation during prometaphase (Fang et al., 1998; Sudakin et al., 2001; Fang, 2002; Wassmann and Benezra, 1998) (Figure 1.6A). Securin is an inhibitor of the protease separase. Separase is required to cleave the cohesin holding the sister chromatids together, an essential step of anaphase (Hornig et al., 2002; Peters, 2004). As previously described, cyclin B is the coactivator of the mitotic kinase CDK1. Its degradation

is required to reduce the cell's global phosphorylation state and induce mitotic exit (Peters, 2004). The SAC is only satisfied when all kinetochores are stably bound to microtubules (Figure 1.6A). At this point, anaphase inhibition is relieved and the cell cycle can proceed (Lara-Gonzalez et al., 2012; Musacchio and Salmon, 2007). Failure of the SAC can result in chromosome mis-segregation, DNA damage and aneuploidy in daughter cells, which are hallmarks of many cancers (Kops et al., 2005; Weaver and Cleveland, 2006; Dobles et al., 2000). Therefore, understanding the exact mechanisms of SAC signalling may prove useful for future cancer and disease therapy.

Early observations of the SAC revealed that if a chromosome is delayed arriving at the metaphase plate, chromosome segregation is postponed until a short time after alignment (Zirkle, 1970). Furthermore, treatment of yeast cells with the microtubule depolymerising drugs nocodazole or methyl benzimidazole carbamate caused a cell cycle arrest prior to chromosome segregation (Jacobs et al., 1988). This arrest prevented the predicted outcome of aneuploidy and cell death in the absence of microtubules. Subsequent yeast genetic screens from the Hoyt and Murray labs identified yeast mutants that were able to progress through cell division in the presence of microtubule depolymerising agents instead of arresting in mitosis (Hoyt et al., 1991; Li and Murray, 1991). These screens identified the founding members of the SAC: three BUB (budding uninhibited by benzimidazole) proteins and three MAD (mitotic arrest deficient) proteins. Following this, other SAC components such as the principal checkpoint kinase MPS1 were identified (Weiss and Winey, 1996). It is now understood that

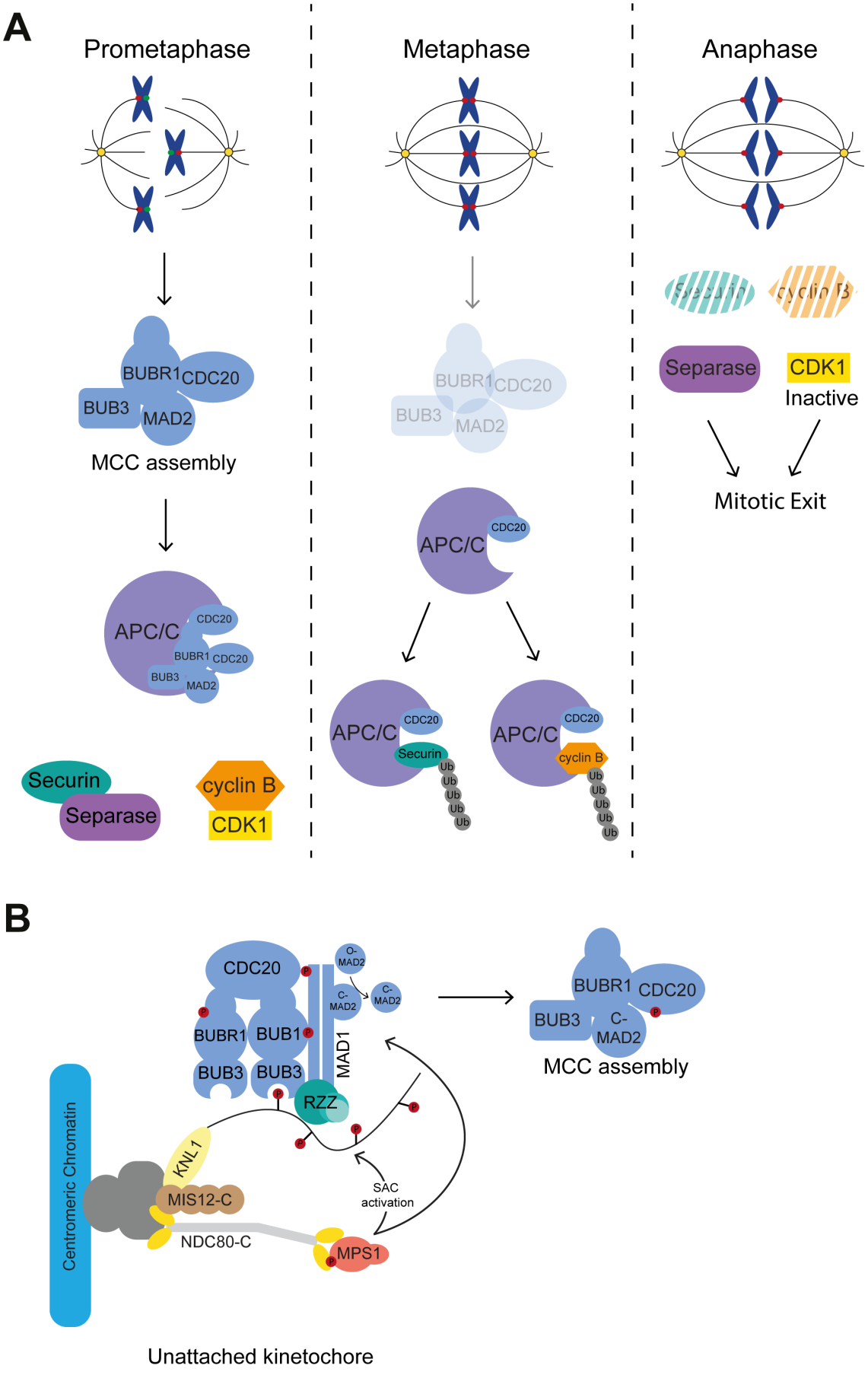

A
Prometaphase
Metaphase
Anaphase
BUBR1
CDC20
BUB3
MAD2
MCC assembly
APC/C
CDC20
Securin
Separase
cyclin B
CDK1
Inactive
Mitotic Exit
B
BUB1
MAD1
RZZ
KNL1
MIS12-C
NDC80-C
MPS1
SAC
activation
Centromeric Chromatin
Unattached kinetochore

Figure 1.6 The Spindle Assembly Checkpoint

The Spindle Assembly Checkpoint is a surveillance mechanism that prevents anaphase onset until all chromosomes are correctly attached to the mitotic spindle. (A) Unattached kinetochores signal MCC formation. The MCC inhibits the APC/C-CDC20 complex, preventing securin and cyclin B degradation. Once all kinetochores are attached, MCC production stops. The APC/C becomes active and targets securin and cyclin B for degradation. This results in separase activation, relief of sister chromatid cohesion and chromosome segregation. (B) Principal checkpoint kinase MPS1 is recruited to unattached kinetochores and phosphorylates checkpoint scaffold KNL1 to localise BUB proteins to kinetochores. MPS1 initiates a phosphorylation cascade, which leads to checkpoint protein accumulation and MCC formation.

MPS1 is critical for the recruitment of all the downstream SAC proteins and catalyses formation of the mitotic checkpoint complex (MCC) (Pachis and Kops, 2018). Furthermore, yeast MAD3 was found to be very similar to BUB1 in humans so was renamed BUBR1 (budding uninhibited by benzimidazole related 1) (D P Cahill et al., 1998; Taylor et al., 1998). The core SAC components are largely conserved from yeast to humans (Kalitsis et al., 2000; Dobles et al., 2000; Lara-Gonzalez et al., 2012; Musacchio, 2015). However, while the SAC is not essential in yeast, research has shown that the SAC is essential for normal mitotic timings in mammals (Kalitsis et al., 2000; Perera et al., 2007; Dobles et al., 2000; May and Hardwick, 2006; Meraldi et al., 2004). In addition, several additional SAC proteins have been identified in metazoa including the RZZ (ROD, Zwilch, ZW10) complex (Basto et al., 2000; Buffin et al., 2005; Zhang et al., 2019).

Following the discovery of the SAC, it was not initially clear what it was detecting to produce a mitotic arrest. Subsequent micromanipulation and laser ablation experiments revealed that unattached kinetochores were generating the “wait

anaphase" signal (Li and Nicklas, 1995; Rieder et al., 1995). Taken together with knowledge of the SAC components, it is now widely accepted that the SAC signal is generated by events at unattached kinetochores.

1.3.2 Recognising and signalling unattached kinetochores

A single unattached kinetochore is sufficient to prevent progression into anaphase (Rieder et al., 1995; Li and Nicklas, 1995). The presence of an unattached kinetochore triggers the generation of a SAC signal and catalyses the formation of a diffusible cell cycle inhibitor: the mitotic checkpoint complex (MCC) (Figure 1.6A-B).

The key organiser of the SAC is the kinase Monopolar spindle 1 (MPS1). It is the principal checkpoint kinase that initiates and maintains the SAC signalling cascade (Abrieu et al., 2001; Liu and Winey, 2012; Stucke et al., 2002; Pachis and Kops, 2018) (Figure 1.6B). MPS1-dependent SAC signalling is initiated at unattached kinetochores. MPS1 is recruited to unattached kinetochores via the calponin homology domains of HEC1 and NUF2 (Hiruma et al., 2015; Ji et al., 2015). This is promoted by both CDK1 and Aurora B phosphorylations (Hayward et al., 2019a; Saurin et al., 2011; Zhu et al., 2013; Nijenhuis et al., 2013; Santaguida et al., 2010). Interestingly, MPS1 negatively regulates its kinetochore localisation via autophosphorylation (Hewitt et al., 2010; Jelluma et al., 2010; Santaguida et al., 2010; Thebault et al., 2012; Wang et al., 2014b). It has been suggested that MPS1 localisation is coupled to microtubule occupancy through direct competition with microtubules for binding sites at the kinetochore (Hiruma et al., 2015; Ji et al., 2015). However, other studies have observed MPS1

localised to microtubule-bound kinetochores (Aravamudhan et al., 2015; Hayward et al., 2022). The actual mechanism of MPS1 kinetochore localisation in response to microtubule occupancy is therefore suggested to involve changes in the balance between Aurora B and PP2A-B56 in response to microtubule binding rather than simply through competition (Hayward et al., 2019a, 2022; Nijenhuis et al., 2013). However, the exact targets of Aurora B at the kinetochore are currently unknown. Upon kinetochore recruitment, MPS1 dimerises, allowing it to trans-autophosphorylate its T loop and activate its kinase activity (Jelluma et al., 2010; Kang et al., 2007; Mattison et al., 2007; Wang et al., 2009; Hayward et al., 2019c).

MPS1 initiates a multi-target phosphorylation cascade at unattached kinetochores (Figure 1.6B). Initially, MPS1 phosphorylates the threonine residue of the MELT motifs in KNL1 (Shepperd et al., 2012; London et al., 2012; Yamagishi et al., 2012; Vleugel et al., 2013). KNL1 then acts as the scaffold for the generation of the SAC signal. MELT motif phosphorylation generates docking sites for recruiting BUB1-BUB3 and BUBR1-BUB3 complexes (Overlack et al., 2015; Primorac et al., 2013; Yamagishi et al., 2012; Shepperd et al., 2012; London et al., 2012). In addition to MELT motifs, KNL1 contains an SHT motif that can be phosphorylated by MPS1 downstream of MELT motif phosphorylation and the KI motifs that are both thought to aid BUB protein recruitment (Vleugel et al., 2015; Bolanos-Garcia and Blundell, 2011; Krenn et al., 2012). MPS1 then phosphorylates BUB1 to recruit MAD1-MAD2 via its CM1 domain (Ji et al., 2017; Zhang et al., 2017; Qian et al., 2017). BUB1 (and potentially BUBR1) also recruits CDC20 to the kinetochore via a separate ABBA motif (Di Fiore et al., 2015; Diaz-

Martinez et al., 2015). As well as this, MPS1 phosphorylation of the C-terminus of MAD1 further aids CDC20 recruitment (Ji et al., 2017). This brings MAD2 and CDC20 into close proximity to promote the formation of the MAD2-CDC20 complex and ultimately the assembly of the MCC, formed of BUBR1-BUB3, MAD2 and CDC20 (Sudakin et al., 2001) (Figure 1.6B).

The formation of the MAD2-CDC20 complex at kinetochores is the rate-limiting step of the SAC (Faesen et al., 2017; Kulukian et al., 2009). The formation of this complex is promoted by the MAD1-MAD2 complex (De Antoni et al., 2005). MAD2 adopts two distinct conformations: open (O-MAD2) and closed (C-MAD2) (Luo and Yu, 2008). Cytosolic, unbound MAD2 is found as O-MAD2 (Luo et al., 2004; Musacchio and Salmon, 2007). During mitosis, O-MAD2 is converted to C-MAD2 at MAD1-C-MAD2 complexes bound to unattached kinetochores via the MPS1 signalling pathway (Kulukian et al., 2009; De Antoni et al., 2005) (Figure 1.6B). In particular, phosphorylation of MAD1-MAD2 by MPS1 triggers it to act as a template for MAD2 conversion (Faesen et al., 2017). The catalytic conversion of O-MAD2 to C-MAD2 is the point of checkpoint signal amplification (DeAntoni et al., 2005; Musacchio and Salmon, 2007). The newly formed C-MAD2 is now able to interact with CDC20 to form the MAD2-CDC20 complex which is incorporated into a new MCC molecule via interaction with BUBR1-BUB3 (Sironi et al., 2002). Many MCC molecules can be generated from a single signalling kinetochore, amplifying the initial checkpoint signal. This ensures that a single unattached kinetochore generates sufficient MCC to maintain a cell cycle arrest.

In mammals, the maintenance of MAD1-MAD2 at kinetochores also requires the RZZ complex (Basto et al., 2000; Buffin et al., 2005; Zhang et al., 2019; Rodriguez-Rodriguez et al., 2018; Silió et al., 2015). Therefore, once SAC signalling is initiated, MPS1 is not required to maintain MAD1-C-MAD2 at kinetochores. Instead, the kinetochore forms a fibrous corona, a kinetochore expansion mainly formed by the proteins of the RZZ complex, which is thought to aid microtubule capture and SAC signalling, in part by recruiting MAD1 and MAD2 (Caldas et al., 2015; Vleugel et al., 2015; Cassimeris et al., 1990; Kops and Gassmann, 2020; Rodriguez-Rodriguez et al., 2018).

The MCC is the diffusible checkpoint effector that prevents anaphase onset. It does this by inhibiting the APC/C and hence preventing cyclin B and securin degradation through two different mechanisms. First, it sequesters CDC20. CDC20 is a unique member of the MCC in that it is also a co-activator of the APC/C (Visintin et al., 1997). By sequestering CDC20 as part of the MCC (Sudakin et al., 2001), there is less CDC20 available to bind and activate the APC/C. Second, the MCC directly binds to and inhibits the APC/C. The MCC is capable of binding two molecules of CDC20 via two separate domains on BUBR1 (Alfieri et al., 2016; Di Fiore et al., 2016). One of these CDC20 molecules can already be bound to the APC/C. Therefore, the MCC can bind to active APC/C acting as a pseudo substrate and preventing other substrates from gaining access (Izawa and Pines, 2015). Additionally, the binding of the MCC alters the conformation of the APC/C meaning it is less able to associate with the E2 enzyme UBE2C/UBCH10 and hence is unable to ubiquitinate substrates (Alfieri et al., 2016; Yamaguchi et al., 2016).

1.3.3 Recognising and correcting incorrect attachments

While the SAC is able to detect unattached kinetochores, it is unable to sense attachment geometry and therefore unable to detect certain types of incorrect attachments. A correct, amphitelic attachment is defined as one in which kinetochores of sister chromatids are attached to microtubules from opposite poles (bioriented) (Figure 1.7). Incorrect attachments such as merotelic attachments (which are bioriented but where one sister kinetochore is attached to microtubules from opposite poles) cannot be detected by the SAC (Cimini et al., 2001, 2002, 2003) (Figure 1.7). During prometaphase incorrect attachments are frequently generated (Santaguida and Musacchio, 2009; Ye et al., 2017). If left uncorrected into anaphase, these attachments can result in lagging chromatids, DNA damage, chromosome mis-segregation and ultimately aneuploidy (Cimini and Degrassi, 2005).

Therefore, the cell employs a mechanism to destabilise and rectify incorrect attachments while preserving correct attachments: the error correction pathway. This pathway depends on the establishment of tension between sister chromatids upon the formation of correct attachments (Liu and Lampson, 2009). Incorrect attachments do not produce this tension and so trigger the error correction pathway (Tanaka et al., 2002; Lampson et al., 2004; Pinsky et al., 2009). The Aurora B kinase is the key mediator of the error correction pathway and its inhibition results in the stabilisation of syntelic and merotelic attachments into anaphase (Shannon and Salmon, 2002; Lampson et al., 2004; Tanaka et al., 2002). Aurora B is recruited to the centromere as a component of the

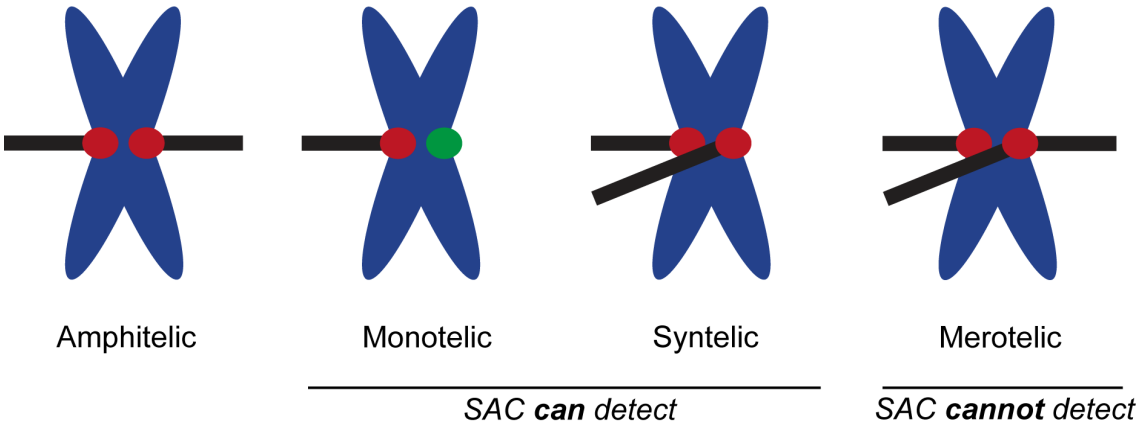


Figure 1.7 Potential geometries of kinetochore-microtubule attachments
Microtubules can form four types of attachments with kinetochores. An amphitelic attachment is defined as kinetochores of sister chromatids attached to microtubules from opposite poles. A monotelic attachment is when only one kinetochore of a sister chromatid pair is attached to a microtubule. A syntelic attachment is defined as both sister kinetochores attached to microtubules from a single pole. A merotelic attachments is defined as bioriented but one sister kinetochore is attached to microtubules from opposite poles. Merotelic attachments cannot be detected by the SAC.

chromosomal passenger complex (CPC) which is composed of Borealin, INCENP, Survivin and Aurora B (Ruchaud et al., 2007). The canonical model for error correction suggests that at the centromere, Aurora B is able to phosphorylate a number of targets at the outer-kinetochore including DSN1, KNL1 and HEC1, reducing their affinity for microtubules and generating an unattached kinetochore that can form a new attachment (Cheeseman et al., 2006; DeLuca et al., 2006; Wei et al., 2007; Welburn et al., 2010). The acquisition of tension is observed as a physical increase in distance between the centromere and Aurora B's targets at the outer-kinetochore (Wan et al., 2009; Maresca and Salmon, 2009; Liu et al., 2009). This would prevent Aurora B from phosphorylating its targets and therefore lead to stabilisation of correct attachments (Liu et al., 2009).

There is also substantial evidence for the requirement of MPS1 for error correction (Santaguida et al., 2010; Hewitt et al., 2010; Maure et al., 2007; Maciejowski et al., 2017; Jelluma et al., 2008a; Hayward et al., 2022). MPS1 has been observed to localise to laterally and end-on attached kinetochores and to promote microtubule release (Maciejowski et al., 2017; Hayward et al., 2022). Proposed substrates for MPS1 in this mechanism include SKA3 and HEC1 (Maciejowski et al., 2017; Sarangapani et al., 2021). However, how MPS1's error correction role coordinates with that of Aurora B has not yet been clarified.

1.3.4 Silencing the SAC leads to mitotic exit

Once all kinetochores are bioriented and under tension, the checkpoint is silenced, APC/C is activated, and cells progress in to anaphase (Figure 1.6A). There are several mechanisms that contribute to this transition: phosphatase counterbalance of the SAC-activating kinases, "stripping" of checkpoint proteins from kinetochores and disassembly of existing MCC (Jelluma et al., 2010; Howell et al., 2001; Gassmann et al., 2010; Mapelli et al., 2006; Xia et al., 2004; Reddy et al., 2007). The phosphatase counterbalance of SAC-activating kinases to prevent further checkpoint signalling will be covered in Chapter 1.3.5.

Kinetochore-localised SAC proteins must be removed from the kinetochore upon microtubule attachment to prevent further MCC formation. Although the mechanism is not fully understood, the principal checkpoint kinase MPS1 is lost from kinetochores in response to microtubule attachment (Hayward et al., 2022; Hiruma et al., 2015; Ji et al., 2015). This prevents further checkpoint signal initiation. Downstream components of the SAC, in particular MAD1, MAD2 and

the RZZ complex, are removed from the kinetochore and redistributed to the poles along microtubules by a process called “stripping” (Maiato et al., 2004). The process is mediated by the minus end-directed microtubule motor dynein and prevents the formation of new MCC complexes (Howell et al., 2001; Wojcik et al., 2001; Gassmann et al., 2010).

In addition to preventing the formation of new MCC, existing MCC complexes must be disassembled to activate the APC/C. The main mechanism by which this is thought to occur involves the thyroid hormone receptor interacting protein 13 (TRIP13), an AAA ATPase, and its interaction partner $p31^{Comet}$. $p31^{Comet}$ is a MAD2-binding protein and *in vitro* competes with O-MAD2 for binding to C-MAD2 (Vink et al., 2006; Habu et al., 2002; Xia et al., 2004). This inhibits the assembly of new MCC by preventing the formation of the C-MAD2-O-MAD2 interaction (Mapelli et al., 2006; Westhorpe et al., 2011). Additionally, following the interaction of $p31^{Comet}$ with C-MAD2, TRIP13 is able to catalyse a change in C-MAD2 conformation, promoting the transition back to O-MAD2 (Teichner et al., 2011; Alfieri et al., 2018; Wang et al., 2014a; Ye et al., 2015). This conformational change of MAD2 results in MCC disassembly by promoting the dissociation of CDC20 from BUBR1 (Westhorpe et al., 2011; Teichner et al., 2011).

Ubiquitination of CDC20 by the small APC/C subunit APC15 has also been proposed as a key mechanism required to promote SAC silencing. Non-degradative ubiquitination of CDC20 in the MCC has been suggested to promote MCC disassembly by accelerating the dissociation of C-MAD2-CDC20 (Reddy et al., 2007; Foster and Morgan, 2012; Uzunova et al., 2012). However, an

alternative hypothesis suggests that CDC20 ubiquitination is not required for MCC disassembly but instead to target CDC20 for degradation to maintain the checkpoint arrest (Nilsson et al., 2008). Indeed, a non-ubiquitinatable form of CDC20 has been shown to overcome the checkpoint (Nilsson et al., 2008). Instead, it has been proposed that CDC20 ubiquitination mediates CDC20 and MCC turnover to allow the SAC to respond to kinetochore attachment state (Mansfeld et al., 2011). Therefore, the roles and contributions of degradative and non-degradative ubiquitination of CDC20 are not yet fully clear.

The exact contributions of the different MCC disassembly mechanisms to APC/C activation is unclear. It is likely that they work together to achieve rapid and complete MCC disassembly and APC/C activation at the appropriate time.

1.3.5 The metaphase-to-anaphase transition relies on a precise balance between kinase and phosphatase activity

Reversible protein phosphorylation is a key SAC regulatory mechanism (Nilsson, 2019). Phosphorylations are carried out by kinases including CDK1, Aurora B, PLK1 and MPS1, and removed by protein phosphatases. Indeed, it is the balance between kinase and phosphatase activity that coordinates the SAC and therefore the metaphase-to-anaphase transition.

CDK1:cyclin B is the major mitotic kinase required for mitotic entry and in particular for activating the SAC (Olsen et al., 2010; D'Angiolella et al., 2003; Alfonso-Pérez et al., 2019; Hayward et al., 2019a) (Figure 1.8A). Early studies demonstrated that sustained CDK:cyclin activity is required to maintain the

mitotic state (Murray et al., 1989) and that inhibition of CDK resulted in MCC disassembly and mitotic exit (D'Angiolella et al., 2003). Subsequent work observed that CDK1 was required for both the initiation and maintenance of the SAC signal (Rattani et al., 2014; Vázquez-Novelle et al., 2014).

The inhibition of CDK1 affects the recruitment of all core SAC components, highlighting its overarching role and indicating that upstream components of the SAC are CDK1 regulated (Vázquez-Novelle et al., 2014). Indeed, CDK1 regulates the kinetochore localisation of the principal checkpoint kinase, MPS1. Phosphorylation of S281 in MPS1's N-terminal domain by CDK1 promotes its recruitment to kinetochores and therefore the initiation of the SAC signal (Ji et al., 2015; Hayward et al., 2019a) (Figure 1.8B). Interestingly, cyclin B itself behaves like a SAC protein: localising to unattached kinetochores and being lost upon microtubule attachment (Alfonso-Pérez et al., 2019; Chen et al., 2008; Bentley et al., 2007; Jackman et al., 2020; Allan et al., 2020). It localises to kinetochores via MAD1, whose localisation is MPS1-dependent (Pagliuca et al., 2011; Alfonso-Pérez et al., 2019; Jackman et al., 2020). This creates a positive feedback loop in which the localisation of CDK1:cyclin B to MAD1 results in an increase in the localisation of MPS1 at unattached kinetochores through CDK1 phosphorylation. This subsequently results in the recruitment of further MAD1 via the MPS1 phosphorylation cascade. This ensures the cell rapidly establishes a SAC signal at unattached kinetochores (Alfonso-Pérez et al., 2019). Furthermore, this interaction between MAD1 and cyclin B is proposed to coordinate nuclear pore complex (NPC) disassembly with initiation of a checkpoint response at the kinetochore. The binding of Cyclin B to MAD1 at the

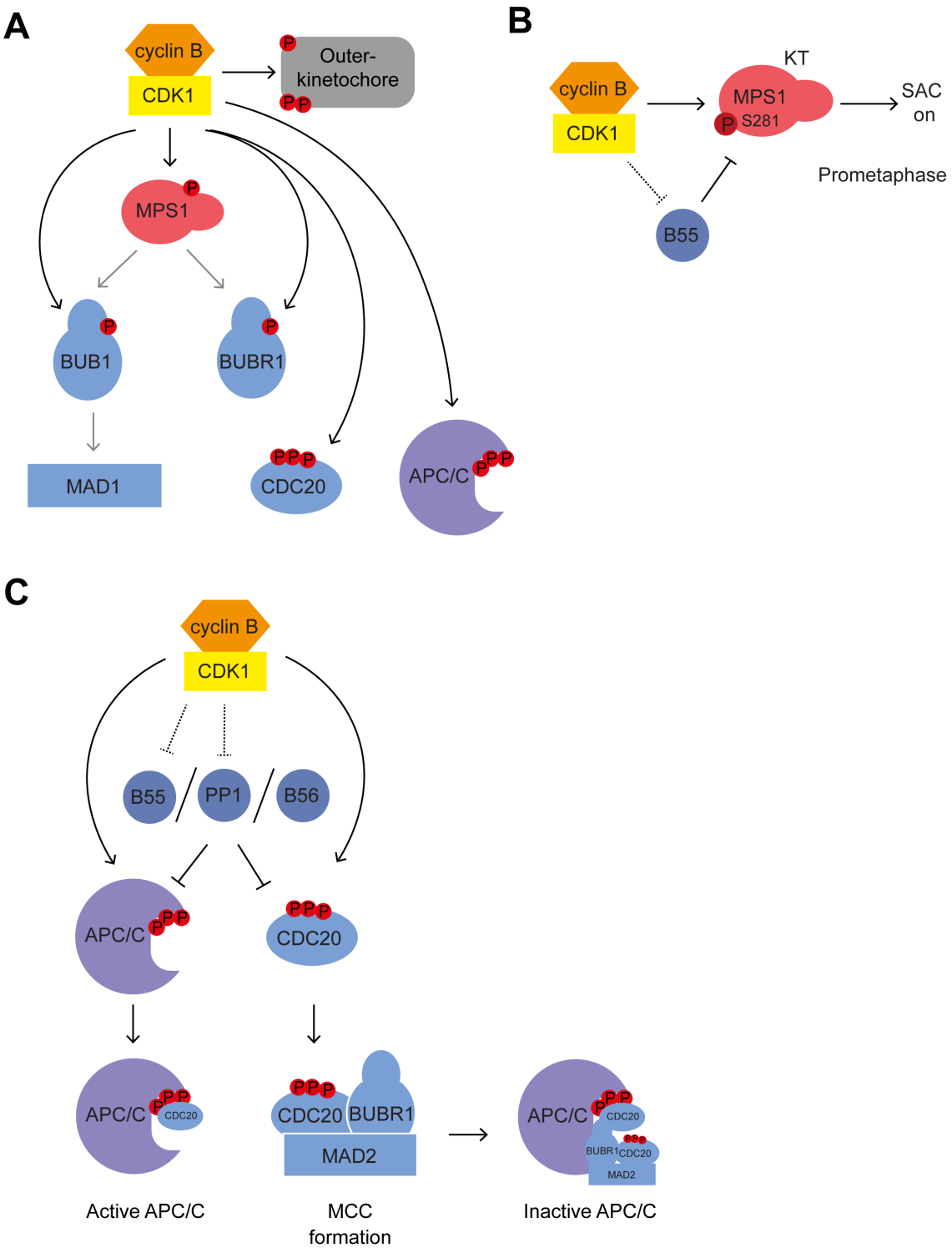


Figure 1.8 The metaphase-to-anaphase transition relies on a precise balance between kinase and phosphatase activity

(A) The major mitotic kinase CDK1:cyclin B is important for activating the SAC. The schematic summarises known roles of CDK1 in the SAC signalling pathway. (B) CDK1 regulates the kinetochore localisation of the principal checkpoint kinase MPS1 through phosphorylation of S281 in MPS1. This phosphorylation site is opposed by

PP2A-B55, after which MPS1 is lost from kinetochores. Therefore, the phosphorylation state of S281 defines the checkpoint permissive period. (C) CDK1 phosphorylates both CDC20 and APC/C to influence their interaction. Phosphorylated CDC20 is incorporated into the MCC, whereas unphosphorylated CDC20 binds the APC/C. CDK1 phosphorylates APC/C to relieve auto-inhibition and enable CDC20 to bind. These phosphorylations are opposed by PPPs. The differential dephosphorylation of CDC20 and APC/C creates a precise time window in which CDC20 and APC/C can interact.

NPC is required for the release of MAD1 from TPR at the nuclear pore before NEBD so it can be recruited to the kinetochore for SAC signalling (Jackman et al., 2020).

In addition to regulating MPS1 localisation, CDK1 has been proposed to regulate MPS1 kinase activity. There is compelling evidence of this occurring at S283 in Xenopus (Morin et al., 2012). However, the equivalent residue in human cells regulates MPS1 localisation rather than activity (Hayward et al., 2019a). Therefore, in mammals, a phosphorylation regulating kinase activity has been suggested to occur at a C-terminal S821 residue (Diril et al., 2016). However, experimental evidence for this is currently incomplete.

Downstream of MPS1, there are several characterised roles of CDK1 in the SAC. This is not an exhaustive review and many more targets of CDK1 are likely to found in the coming years. A critical role of CDK1 is in the phosphorylation of BUB1 to promote the initial kinetochore recruitment of MAD1 (Qian et al., 2017; Zhang et al., 2017; Ji et al., 2017). CDK1 phosphorylation of S459 in BUB1 creates a pseudo-MELT motif that can subsequently be phosphorylated by MPS1

at S461. This creates the binding site for MAD1 and hence recruits it to the kinetochore (Zhang et al., 2017; Ji et al., 2017).

It is thought that the mechanism of one kinase priming the site for another kinase may be used regularly in cell cycle regulation. Another example of this is in the recruitment of the serine/threonine kinase PLK1, which is recruited to PLK1 docking sites by the sequence S-S/T-P in which the S/T residue is phosphorylated – often by CDK1 (Elia et al., 2003a; b). In particular, CDK1 phosphorylation of BUBR1 at T620 creates a docking site for PLK1 to be recruited to the kinetochore (Elowe et al., 2007). At the kinetochore, PLK1 then plays a number of key roles in the checkpoint including enhancing the SAC signal (Espeut et al., 2015; Ikeda and Tanaka, 2017; von Schubert et al., 2015; Cordeiro et al., 2020). PLK1 also aids the formation of efficient microtubule-kinetochore attachments (Dunsch et al., 2011; Geraghty et al., 2021) and recruits the SAC silencing phosphatase PP2A-B56 (Suijkerbuijk et al., 2012).

In addition to PLK1, CDK1 also regulates the localisation of Aurora B as part of the CPC during mitosis (Hümmer and Mayer, 2009; Tsukahara et al., 2010). CDK1's role in regulating both Aurora B and PLK1 highlights the overarching role of CDK1 in the metaphase-to-anaphase transition. Aurora B is a serine/threonine kinase and the catalytic subunit of the CPC which is located at centromeres in early mitosis (Carmena et al., 2012). CDK1 phosphorylates the CPC component INCENP to prevent its interaction with the mitotic kinesin MKLP2 (Hümmer and Mayer, 2009; Tsukahara et al., 2010). This maintains the CPC at the centromere until CDK1 levels decrease, at which point it is transported to the central spindle

by MKLP2 for its role in anaphase (Cooke et al., 1987; Serena et al., 2020; Gruneberg et al., 2004). CDK1 also directly phosphorylates MKLP2 to prevent this movement (Kitagawa et al., 2014).

Centromeric Aurora B plays a critical role in error correction to resolve incorrect microtubule-kinetochore attachments. This has been described in detail in Chapter 1.3.3. In addition, Aurora B also plays a role in the recruitment of MPS1 to kinetochores. This is thought to be a direct role of Aurora B and not simply a downstream effect of generating unattached kinetochores in error correction. Indeed, Aurora B activity is required for MPS1 recruitment even when kinetochores are unattached (Hayward et al., 2019a; Saurin et al., 2011; Zhu et al., 2013; Nijenhuis et al., 2013; Santaguida et al., 2011; Hayward et al., 2019c). It has also been suggested that Aurora B phosphorylation of the N-terminus of HEC1 increases the affinity between the NDC80-C and MPS1 (Ji et al., 2015; Zhu et al., 2013; Saurin et al., 2011), although the information on this is not conclusive (Nijenhuis et al., 2013; Hayward et al., 2022). Interestingly, as Aurora B localisation is CDK1-regulated, this means that MPS1 localisation is both directly and indirectly regulated by CDK1.

CDK1 has also been implicated in the phosphorylation of CDC20 (Figure 1.8C). As CDC20 is both a key member of the MCC and a co-activator of the APC/C, it is a unique SAC protein that must be strictly regulated. N-terminal phosphorylation of CDC20 by CDK1 influences the fate of CDC20. Phosphorylated CDC20 is more readily incorporated into the MCC, whereas unphosphorylated CDC20 preferentially binds the APC/C (D'Angiolella et al.,

2003; Yudkovsky et al., 2000; Hein et al., 2017; Labit et al., 2012). Interestingly, CDK1 also phosphorylates APC/C to relieve auto-inhibition and enable CDC20 to bind (Qiao et al., 2016; Fujimitsu et al., 2016; Zhang et al., 2016) (Figure 1.8C). It is thought that the differential dephosphorylations of CDC20 and APC/C create a precise time window in which CDC20 and APC/C can interact (Hein et al., 2017).

So far, this section has considered the key kinases involved in the metaphase-to-anaphase transition, particularly the major mitotic kinase CDK1. However, to fully understand the precise balance of dynamic phosphorylation, attention must now turn to the phosphatases that counteract these kinases.

Principally, PP2A-B55 is required to terminate the SAC permissive period (Hayward et al., 2019a) (Figure 1.8B). CDK1 regulation of MPS1 kinetochore recruitment allows the SAC to be reactivated after silencing provided that CDK1 levels are sufficiently high. As PP2A-B55 is inhibited by CDK1 (Mochida et al., 2010; Blake-Hodek et al., 2012; Vigneron et al., 2011; Cundell et al., 2013), it is unable to act on the CDK1 phosphorylation while CDK1 levels are still high. Upon the decrease of CDK1 activity at the metaphase-to-anaphase transition and the subsequent activation of PP2A-B55, the phosphatase removes the S281 CDK1 phosphorylation on MPS1. After this point, MPS1 can no longer be recruited to the kinetochore and the SAC permissive period is terminated (Hayward et al., 2019a). Therefore, it has been proposed that the SAC permissive period can be defined by the phosphorylation status of S281. This provides directionality to the metaphase-to-anaphase transition by preventing SAC reactivation after cyclin B

degradation has commenced. In addition to opposing MPS1 kinetochore recruitment, PP2A-B55 has been implicated in the removal of the CDK1 phosphorylation required for MPS1 kinase activity (Diril et al., 2016).

Furthermore, PP2A-B55 indirectly opposes MPS1 kinetochore localisation through the regulation of CPC, and hence Aurora B, localisation. PP2A-B55 has been reported to remove CDK1 phosphorylations on INCENP and MKLP2, which results in the re-localisation of the CPC to the anaphase central spindle (Hein et al., 2017). This also stimulates anaphase processes at the central spindle through Aurora B activity.

PP2A-B55 is also proposed to be the main phosphatase opposing phosphorylations on CDC20 and APC/C (Hein et al., 2017) (Figure 1.8C). As previously described, differential dephosphorylation of CDC20 and APC/C is critical to create a precise time window when they can interact. PP2A-B55 shows a preference for dephosphorylating threonine over serine (Pinna et al., 1976; Cundell et al., 2016), and the majority of phosphorylation sites are threonine in CDC20, but serine in APC/C. It is therefore predicted that during the metaphase-to-anaphase transition, PP2A-B55 would preferentially dephosphorylate CDC20 first and APC/C second, thus creating the time window for interaction. However, clear data for this hypothesis is lacking and there is contradictory evidence for other phosphatases contributing to the dephosphorylation of CDC20, including PP1 (Kim et al., 2017; Visconti et al., 2012; Cundell et al., 2013; Bancroft et al., 2020) and PP2A-B56 (Fujimitsu and Yamano, 2020).

PP1, like PP2A-B55, is inactive during mitosis when CDK1 levels are high (Dohadwala et al., 1994; Yamano et al., 1994). PP1 plays a critical role in yeast SAC silencing (Pinsky et al., 2009; Vanoosthuyse and Hardwick, 2009; Rosenberg et al., 2011; Meadows et al., 2011), and in mammals, the disruption of PP1 causes a metaphase arrest (Liu et al., 2010). However, the role of mammalian PP1 in the metaphase-to-anaphase transition is poorly understood and is likely to differ from yeast. The exact contributions of the three PP1 isoforms to mitotic regulation is currently unclear. Current evidence suggests that PPP1CA and PPP1CC are the major isoforms involved in mitotic regulation and have some level of functional redundancy (Trinkle-Mulcahy et al., 2006; Liu et al., 2010). PPP1CB:MYPT1 has been shown to play a distinct role to PPP1CC and PPP1CA (Yamashiro et al., 2008; Kiss et al., 2019). It has a well characterised role outside of mitosis as a regulator of smooth muscle contractility (Takaki et al., 2017). However, there is more recent evidence that PPP1CB:MYPT1 is involved in mitotic regulation by for example antagonising PLK1 activity (Yamashiro et al., 2008; Kiss et al., 2019). Despite this, due to its distinct role to other PP1 isoforms it will not be considered in detail in this thesis.

PPP1CA and PPP1CC, accumulate at kinetochores during mitosis via RVxF-containing PIPs including KNL1 (Nijenhuis et al., 2014; Rosenberg et al., 2011; Shepperd et al., 2012; Liu et al., 2010; Espeut et al., 2012), KIF18A (De Wever et al., 2014; Häfner et al., 2014; Meadows et al., 2011), CENP-E (Kim et al., 2010) and Astrin (Conti et al., 2019). Genetic and cell biological evidence suggests that kinetochore-localised PP1 acts antagonistically with Aurora B (Liu et al., 2010; Francisco et al., 1994; Emanuele et al., 2008), MPS1 (Nijenhuis et

al., 2014; Moura et al., 2017) and CDK1 (Bancroft et al., 2020; Barr et al., 2011; Nilsson, 2019; Shi, 2009). Conflicting reports propose that PP1 may play a role in SAC silencing and/or APC/C activation and the metaphase-to-anaphase transition. In SAC silencing, proposed PP1 substrates include the CDK1 site on BUB1 required for MAD1 recruitment (Holder et al., 2020), the KNL1 MELT motifs (Nijenhuis et al., 2014) and the MPS1 T loop (Moura et al., 2017). However, the latter two targets are also reported PP2A-B56 sites (Qian et al., 2017; Espert et al., 2014; Hayward et al., 2019c) and require dynamic regulation during mitosis (see below). Therefore, the exact contribution of PP1 to dephosphorylating these sites remains unknown. Additionally, PP1 has been proposed as an alternative phosphatase to PP2A-B55 for the dephosphorylation of CDK1-phosphorylated CDC20 (Bancroft et al., 2020) (Figure 1.8C). This suggests that PP1 promotes the metaphase-to-anaphase transition through APC/C activation and therefore the destruction of cyclin B. Uncovering the exact roles of PP1 in the SAC and the metaphase-to-anaphase transition will be an exciting avenue of future research.

CDK1 and PP2A-B55 have been proposed to define the checkpoint permissive period. However, there are phosphorylations within this period that must be dynamically regulated, in particular those carried out by MPS1 and Aurora B. These phosphorylations cannot be removed by PP2A-B55 or PP1 as these phosphatases are inactive for the majority of this period. PP2A-B56 is active throughout mitosis and is therefore is able to modulate the SAC and error correction during the SAC permissive period (Nilsson, 2019). Kinetochore-localised PP2A-B56 has been reported to dephosphorylate the MELT motifs on KNL1 (Espert et al., 2014), the MAD1 docking motif on BUB1 (Qian et al., 2017),

and the MPS1 activating T-loop (Hayward et al., 2019c). Additionally, PP2A-B56 has been reported to be main phosphatase opposing Aurora B in error correction to ensure that potential new kinetochore-microtubule attachments are promptly stabilised (Xu et al., 2013; Suijkerbuijk et al., 2012; Kruse et al., 2013)

1.4 Thesis aims

From decades of extensive research is it clear that dynamic phosphorylation is critical for the accurate segregation of chromosomes through regulation of the SAC and the metaphase-to-anaphase transition. However, uncovering new levels of phospho-regulation in mitosis is a major focus of ongoing research in the field. In particular, despite knowing the importance of the overarching mitotic kinase CDK1 in the SAC, the exact targets of CDK1 are only more recently being elucidated. In particular, the upstream, initiatory roles of CDK1 in the SAC have, to a large extent, remained a mystery. Significant progress is required to reveal the full role of CDK1 and identify the phosphatases that critically oppose its specific functions. With this in mind, this thesis aims to make a significant contribution to these questions by achieving the following:

- Circumvent the requirement of CDK1 for MPS1 kinetochore recruitment to observe any further requirement for CDK1 in SAC signalling.
- Characterise the dependence of outer-kinetochore protein localisation on CDK1 and determine the impact of this on SAC regulation.
- Identify the phosphatases opposing CDK1 in outer-kinetochore assembly in mitosis.

- Investigate the role of CDK1-opposing phosphatase PP1 in the metaphase-to-anaphase transition through the generation of new *in vivo* tools.

Chapter 2: Identifying a critical, unknown role of CDK1 in SAC signalling beyond MPS1 kinetochore recruitment

2.1 Tethering MPS1 to kinetochores is insufficient for initiating Spindle Assembly Checkpoint signalling

CDK1 is the major mitotic kinase required for mitotic entry and in particular for activating the SAC (Olsen et al., 2010; D'Angiolella et al., 2003; Alfonso-Pérez et al., 2019; Hayward et al., 2019a). However, the exact targets of CDK1 in SAC signalling have been poorly defined. Therefore, it is of critical importance to uncover the targets of CDK1 and understand exactly how CDK1 drives SAC signalling. Substantial progress was made by Hayward et al. (2019a) who revealed that CDK1 is required to recruit the principal checkpoint kinase MPS1 to kinetochores and therefore initiate downstream checkpoint signalling. However, the loss of downstream SAC components following CDK inhibition may not be solely due to CDK1-dependent MPS1 kinetochore recruitment. Rather, it may reflect a requirement for CDK1 phosphorylation beyond MPS1 recruitment.

To investigate the roles of CDK1 in SAC signalling beyond MPS1 kinetochore recruitment, the requirement of CDK1 for MPS1 localisation had to circumvented. This was achieved by utilising the HeLa Flp-In T-REx cell line system (Tighe et al., 2004) to stably express kinetochore-tethered MPS1 through fusion with the kinetochore protein MIS12 (Jelluma et al., 2010) and GFP (Hayward et al., 2019a) (Figure 2.1A). Endogenous MPS1 was depleted using RNAi (Hayward et al., 2019a) and kinetochore-tethered MPS1 was expressed through induction

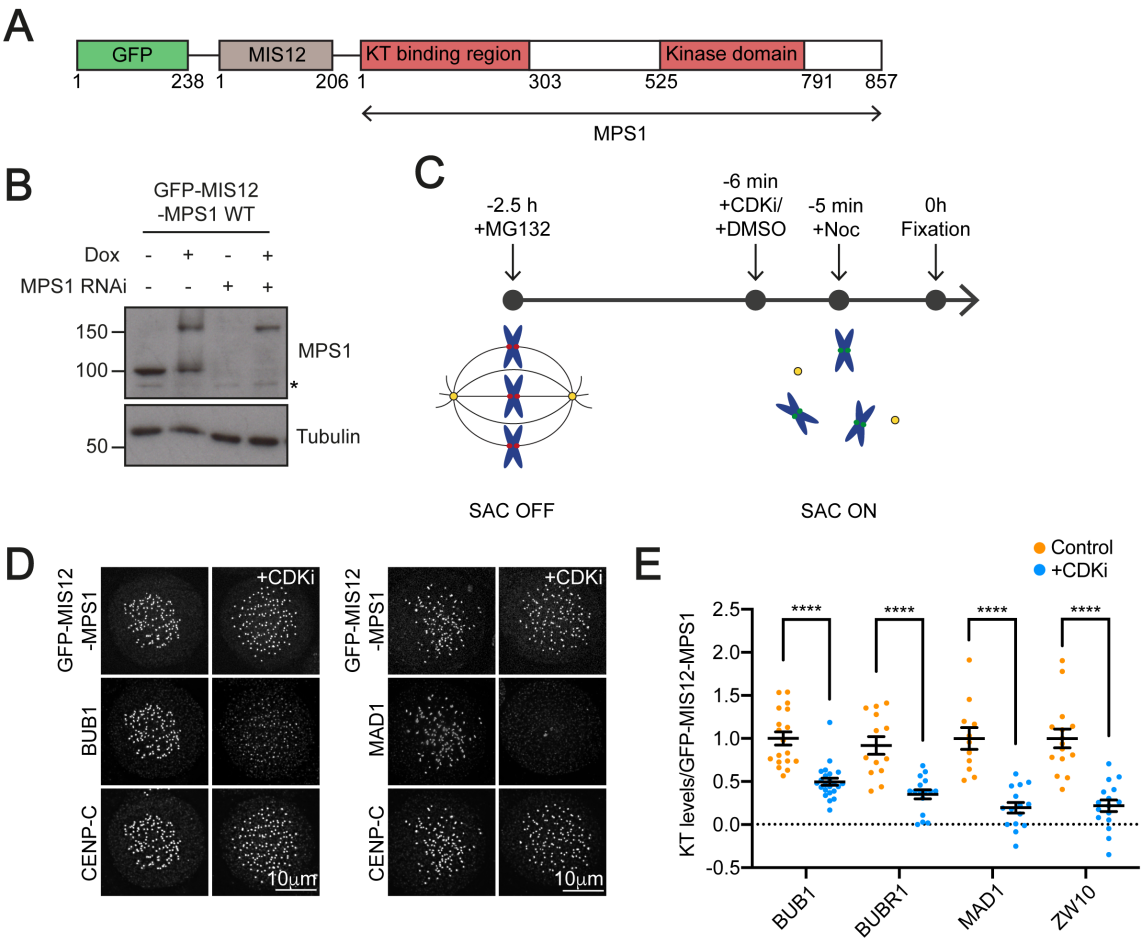


Figure 2.1 Tethering MPS1 to kinetochores is insufficient for initiating SAC signalling

(A) Schematic of the domain organization of GFP-MIS12-MPS1 fusion protein. (B) Western blot confirming successful RNAi rescue with GFP-MIS12-MPS1 fusion protein. HeLa Flp-In/T-REx GFP-MIS12-MPS1 cells were depleted of endogenous MPS1 and GFP-MIS12-MPS1 transgenes were induced by addition of doxycycline as indicated. * indicates non-specific band. (C) Schematic of the “checkpoint reactivation assay”. (D) HeLa Flp-In/T-REx GFP-MIS12-MPS1 cells were depleted of endogenous MPS1. GFP-MIS12-MPS1 transgenes were induced by addition of doxycycline. After 48 h, cells were arrested for 2.5 h with 20 µM MG132, treated with 3 µM nocodazole for the final 5 min, fixed with PTEMF, and immunostained as indicated. If CDK1 was inhibited, 5 µM flavopiridol was added 1 min before nocodazole treatment (+CDKi). (E) Graph shows mean levels of BUB1, BUBR1, MAD1 and ZW10 at kinetochores relative to GFP-MIS12-MPS1 levels. Bars indicate the SEM (each point represents a single cell average intensity of 20 kinetochores, ≥ 11 cells per condition from 3 independent experiments).

by doxycycline (dox) to a similar level as the endogenous protein to rescue the loss of endogenous MPS1 (Figure 2.1B). It has been proposed that the N-terminus of MPS1 may play a role in the regulation of its kinase activity (Combes et al., 2018). However, published characterisation of this cell line showed that tethering MPS1 via its N-terminus resulted in no significant alteration in MPS1's ability to generate a checkpoint signal (Hayward et al., 2019a). Therefore, this is an effective method to circumvent the requirement of CDK1 for MPS1 localisation and subsequently look at checkpoint signalling.

The contribution of CDK1 to the initiation vs the maintenance of the SAC signal was not clear. Therefore, both roles of CDK1 were investigated in turn. To be able to test involvement of CDK1 in initiating the SAC in a synchronised cell population, a "checkpoint reactivation assay" was used, as described in Vleugel et al. (2015) (Figure 2.1C). Cells were initially arrested in metaphase, with all kinetochores correctly attached and therefore with a silenced SAC, using the proteasome inhibitor MG132 (Hayward et al., 2019a). The SAC was then rapidly activated by the depolymerisation of microtubules using nocodazole. For the inhibition of CDK1, the well characterised, broad spectrum CDK inhibitor (CDKi) flavopiridol (Losiewicz et al., 1994) was added 1 min prior to nocodazole treatment (Hayward et al., 2019a). Importantly, flavopiridol has no reported inhibitory activity towards MPS1. Cells were then fixed and stained for imaging. This assay was designed to observe synchronised cells to specifically manipulate CDK1 in SAC signalling and not affect other roles of CDK1 in mitosis. Although the system does not "initiate" checkpoint signalling *per se*, it creates an artificial system to rapidly re-activate the checkpoint following synchronisation and

therefore to observe the mechanisms of checkpoint initiation. Observation of cells following the "checkpoint reactivation assay" revealed that the kinetochore localisations of core upstream SAC components, BUB1 and BUBR1 were significantly reduced following CDK inhibition compared to the DMSO control (Figure 2.1D-E), indicating that the cells were unable to generate a checkpoint signal in the absence of CDK1. Furthermore, kinetochore localisations of downstream checkpoint components, MAD1 and RZZ component ZW10, were also significantly reduced following CDK inhibition (Figure 2.1D-E). Therefore, tethering MPS1 to kinetochores was insufficient for initiating downstream SAC signalling. This revealed the presence of an unknown, critical CDK1 phosphorylation event required for initiating SAC signalling. Indeed, as all checkpoint proteins, including the upstream checkpoint proteins BUB1 and BUBR1, were significantly reduced, this suggested that an upstream, fundamental aspect of the checkpoint is CDK1 regulated.

2.2 Observing the difference between SAC protein maintenance at and recruitment to kinetochores

An alternative assay, here referred to as the "checkpoint maintenance assay" (Figure 2.2A), was subsequently employed to observe the role of CDK1 in SAC protein maintenance and turnover at kinetochores during continued SAC signalling. In this assay, cells were arrested in a prometaphase state by the addition of nocodazole to depolymerise microtubules, thus synchronising cells in a condition where their checkpoint is constantly active. At this stage, kinetochores would have formed the fibrous corona, which is thought to aid SAC signalling, in part by recruiting MAD1 and MAD2 (Kops and Gassmann, 2020). Proteasome

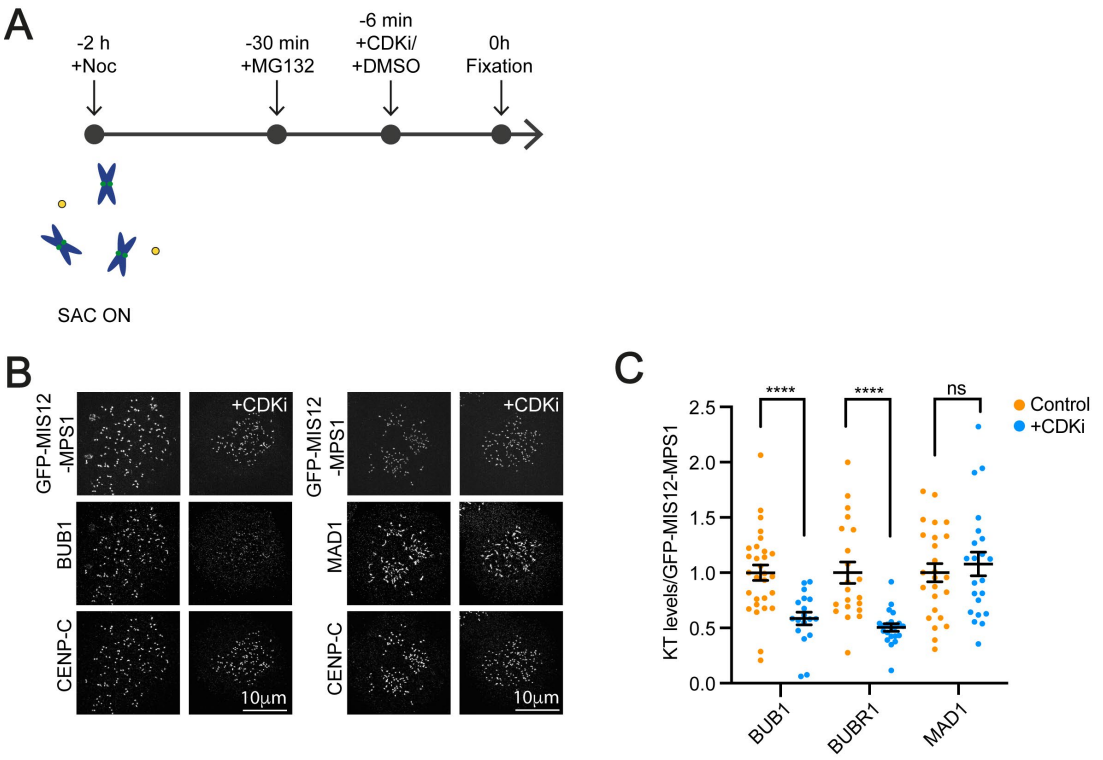


Figure 2.2 Observing the difference between SAC protein maintenance at and recruitment to kinetochores

(A) Schematic of the "checkpoint maintenance assay". (B) HeLa Flp-In/T-REx GFP-MIS12-MPS1 cells were depleted of endogenous MPS1. GFP-MIS12-MPS1 transgenes were induced by addition of doxycycline. After 48 h, cells were arrested for 2 h with 0.3 µM nocodazole, then treated with 20 µM MG132 for the final 30 min, fixed with PTEMF, and immunostained as indicated. If CDK1 was inhibited, 5 µM flavopiridol was added 6 min before fixing (+CDKi). (E) Graph shows mean levels of BUB1, BUBR1 and MAD1 at kinetochores relative to GFP-MIS12-MPS1 levels. Bars indicate the SEM (each point represents a single cell average intensity of 20 kinetochores, ≥ 18 cells per condition from 3 independent experiments).

inhibitor MG132 was added prior to CDK1 inhibition to prevent mitotic exit by maintaining sister chromatid cohesion, and the cells were fixed and stained for imaging. As in the "checkpoint reactivation assay", the kinetochore localisations of core upstream SAC components, BUB1 and BUBR1 were significantly reduced following CDK inhibition using the "checkpoint maintenance assay" in the GFP-MIS12-MPS1 cell lines (Figure 2.2B-C). However, localisation of

downstream checkpoint component MAD1 was not affected following CDK inhibition (Figure 2.2B-C). Therefore, maintenance of the downstream checkpoint signal through MAD1 did not require continued CDK1 activity. The most likely reason for this difference is the differential kinetochore binding of MAD1 under two different regimes – mainly through CDK1 and MPS1-phosphorylated BUB1 in the "checkpoint reactivation assay" whereas through the RZZ complex in the "checkpoint maintenance assay" (Rodriguez-Rodriguez et al., 2018). Therefore, the two assays highlight a crucial difference in CDK1-dependence for the initial generation of a checkpoint signal and its maintenance during prometaphase, particularly for downstream checkpoint components like MAD1.

In subsequent experiments, the "checkpoint reactivation assay" was used following the observation that initiation of the checkpoint was entirely dependent on CDK1 (Figure 2.1D-E). Therefore, it was of interest to investigate the unknown upstream roles of CDK1 in initiating the checkpoint signal. However, the role of CDK1 in the maintenance of checkpoint signalling is an interesting topic for future study.

2.3 Investigating the role of CDK1 in regulating MPS1 kinase activity

Based on previous data, the most compelling hypothesis for the unknown CDK1 phosphorylation event required for promoting SAC signalling was the regulation of MPS1 kinase activity. There is strong evidence for this in Xenopus (Morin et al., 2012), however experimental evidence in mammalian cells is incomplete (Diril et al., 2016). In addition to the CDK1 site required for kinetochore localisation (S281), there are three further CDK1 sites on MPS1 (S436, T453, S821) (Dou et

al., 2011) whose functions have not yet been conclusively identified (Figure 2.3A). In mammals, it has been proposed that CDK1 regulates MPS1 kinase activity through phosphorylation of the C-terminal residue S821 (Diril et al., 2016).

To investigate whether S821 is important for regulating MPS1 kinase activity in mammalian cells, stable cell lines were generated expressing kinetochore-tethered MPS1 with S821 mutated to alanine (S821A) or aspartic acid (S821D), generating phospho-null or phospho-mimetic mutants respectively. For each cell line, multiple clones were successfully generated and characterised before selecting one for in-depth analysis. Endogenous MPS1 was depleted using RNAi and kinetochore-tethered MPS1 was expressed to rescue this loss through induction by doxycycline (Figure 2.3B). The “checkpoint reactivation assay” was carried out with these cell lines using CDK inhibition and cells were fixed and stained for imaging. Interestingly, neither S821 phospho-null or phospho-mimetic mutations showed any significant difference to wild type (WT) MPS1 in their ability to recruit BUB1 to kinetochores and all cell lines showed a significant decrease in BUB1 recruitment following CDK inhibition (Figure 2.3C-D). Therefore, phosphorylation of S821 is not required for BUB1 recruitment and thus, by extension, for MPS1 kinase activity at kinetochores, in contrast to what has been previously reported (Diril et al., 2016).

However, CDK1 regulation of MPS1 activity may occur through a different or a combination of CDK1 phosphorylation sites. To observe the role of any known CDK1 sites in MPS1 activation, stable cell lines were generated expressing kinetochore-tethered MPS1 with all known CDK1 sites mutated to alanine (4A)

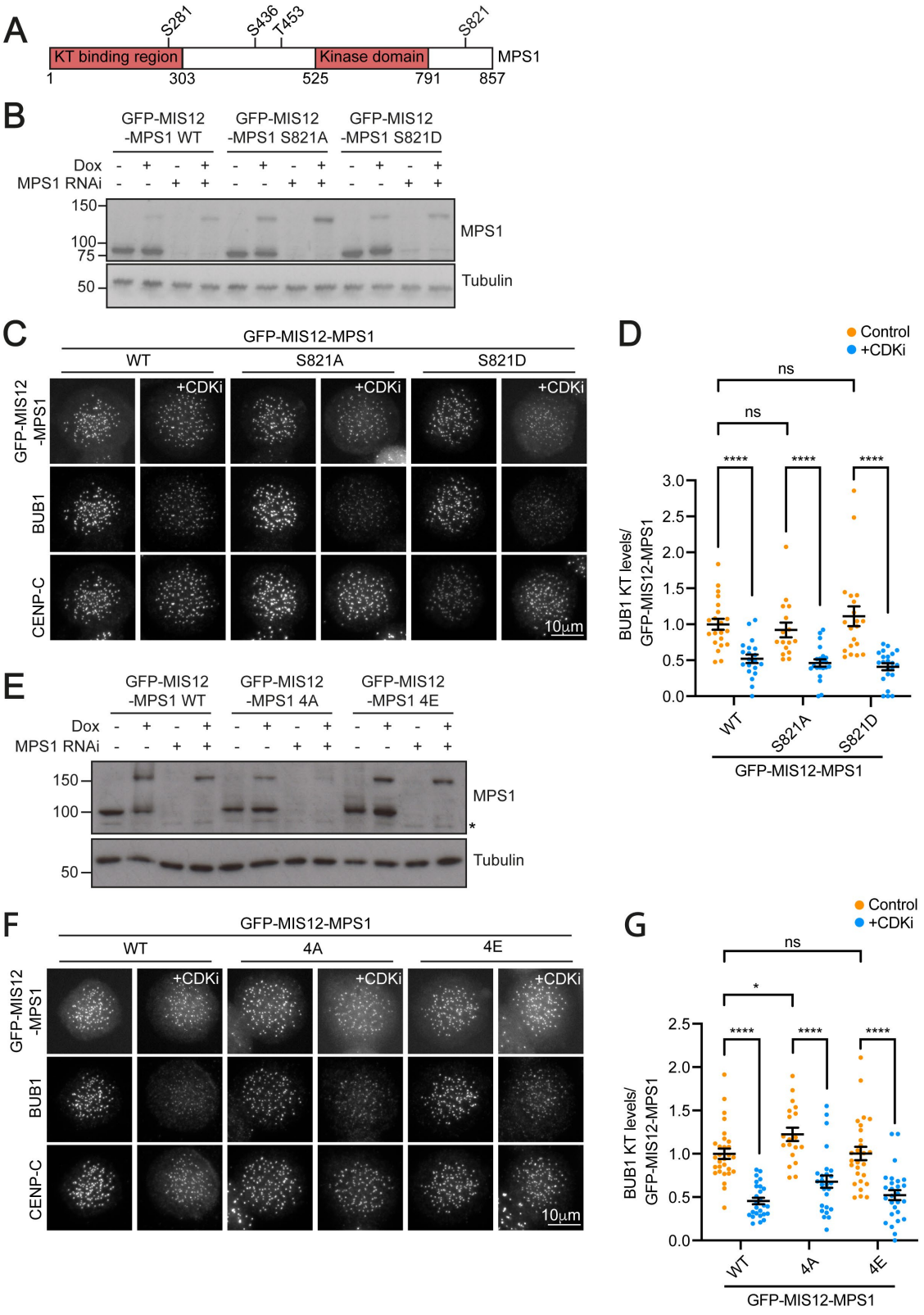


Figure 2.3 CDK1 is not required for MPS1 kinase activity *in vivo*

(A) Schematic of domain organization and reported CDK1 sites of MPS1. (B) Western blot confirming successful RNAi rescue with GFP-MIS12-MPS1 fusion protein with S821A/S821D mutations. HeLa Flp-In/T-REx GFP-MIS12-MPS1 cells were depleted

of endogenous MPS1 and GFP-MIS12-MPS1 transgenes were induced by addition of doxycycline as indicated. (C) HeLa Flp-In/T-REx GFP-MIS12-MPS1 cells were depleted of endogenous MPS1. GFP-MIS12-MPS1 transgenes were induced by addition of doxycycline. After 48 h, cells were arrested for 2.5 h with 20 μM MG132, then treated with 3 μM nocodazole for the final 5 min, fixed with PTEMF, and immunostained as indicated. If CDK1 was inhibited, 5 μM flavopiridol was added 1 min before nocodazole treatment (+CDKi). (D) Graph shows mean level of BUB1 at kinetochores relative to GFP-MIS12-MPS1 levels. Bars indicate the SEM (each point represents a single cell average intensity of 20 kinetochores, ≥ 16 cells per condition from 3 independent experiments). (E) Western blot confirming successful RNAi rescue with GFP-MIS12-MPS1 fusion protein with 4A/4E mutations. HeLa Flp-In/T-REx GFP-MIS12-MPS1 cells were depleted of endogenous MPS1 and GFP-MIS12-MPS1 transgenes were induced by addition of doxycycline as indicated. * indicates non-specific band. (F) HeLa Flp-In/T-REx GFP-MIS12-MPS1 cells were depleted of endogenous MPS1. GFP-MIS12-MPS1 transgenes were induced by addition of doxycycline. After 48 h, cells were arrested for 2.5 h with 20 μM MG132, then treated with 3 μM nocodazole for the final 5 min, fixed with PTEMF, and immunostained as indicated. If CDK1 was inhibited, 5 μM flavopiridol was added 1 min before nocodazole treatment (+CDKi). (G) Graph shows mean level of BUB1 at kinetochores relative to GFP-MIS12-MPS1 levels. Bars indicate the SEM (each point represents a single cell average intensity of 20 kinetochores, ≥ 19 cells per condition from 3 independent experiments).

or glutamic acid (4E), generating phospho-null or phospho-mimetic mutants respectively (Figure 2.3E). For each cell line multiple clones were successfully generated and characterised before selecting one for in-depth analysis. Again, minimal or no effect was seen on BUB1 localisation at kinetochores in the “checkpoint reactivation assay” with either the phospho-null or phospho-mimetic mutant cell lines (Figure 2.3F-G). Cells were able to generate a checkpoint signal even in the presence of the phospho-null mutations. Also, all mutants still showed a significant reduction in BUB1 localisation following CDK inhibition (Figure 2.3F-G). Therefore, none of the known CDK1 phosphorylation sites on MPS1 affected

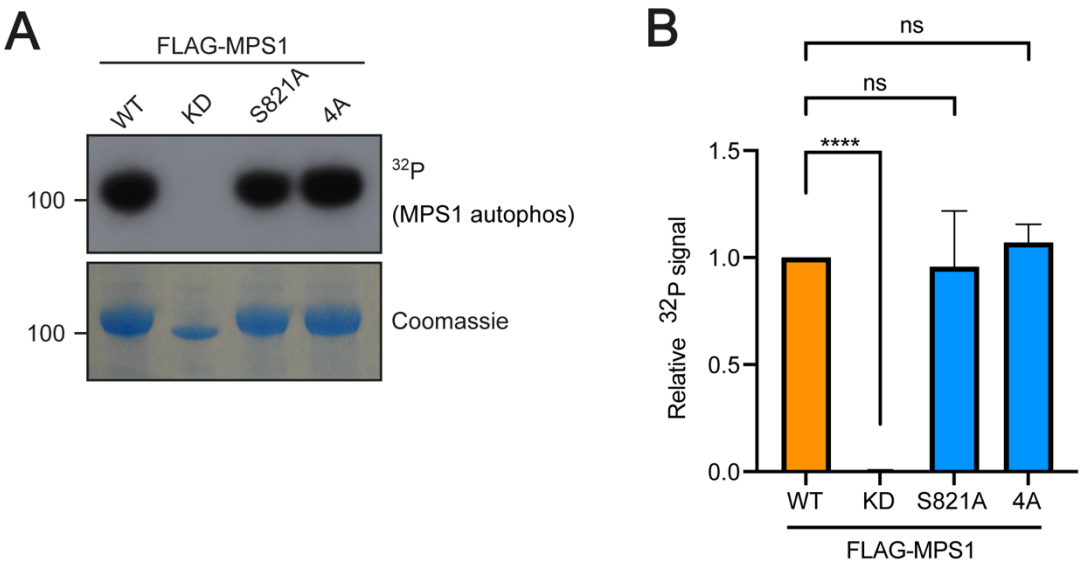


Figure 2.4 CDK1 is not required for MPS1 kinase activity *in vitro*

(A) Coomassie and western blot analysis of a 10 min *in vitro* radioactive kinase assay using purified FLAG-MPS1 and [^{32}P]gamma-ATP. Wild type (WT), Kinase dead (KD). (B) Graph shows mean ^{32}P signal relative to amount of FLAG-MPS1. Bars indicate the SEM from 3 independent experiments.

the cell's ability to generate a checkpoint signal and therefore presumably did not affect MPS1's kinase activity.

To conclusively exclude a role of CDK1 in MPS1 kinase activity regulation, *in vitro* radioactive kinase assays were carried out. FLAG-tagged MPS1 WT, S821A, 4A or D664A/kinase dead (KD) were purified by immunoprecipitation from HEK293T cells and subjected to a 10 min kinase assay using [^{32}P]gamma-ATP (Figure 2.4A). MPS1 itself was used as the substrate as it is heavily autophosphorylated. Western blot analysis of the kinase assay samples showed that there was a significant decrease in MPS1 autophosphorylation with FLAG-MPS1 KD, as expected (Figure 2.4A-B). A similar observation was not seen for the CDK1 site mutations. Both FLAG-MPS1 S281A and 4A showed a comparable level of autophosphorylation to FLAG-MPS1 WT (Figure 2.4A-B).

Therefore, CDK1 phosphorylation of MPS1 does not appear to regulate its kinase activity.

2.4 Discussion

As the major mitotic kinase, CDK1 plays numerous roles in SAC signalling. In particular, CDK1 is required for recruiting the principal checkpoint kinase MPS1 to kinetochores through phosphorylation of its S281 residue (Hayward et al., 2019a). This has been proposed to essential for initiating downstream checkpoint signalling and for defining the checkpoint permissive period. However, this chapter has revealed that tethering MPS1 to the kinetochore is insufficient to overcome the dependency of SAC signalling initiation on CDK1 activity. Interestingly, all components of checkpoint signalling were affected following CDK inhibition in the MPS1-tethered scenario, suggesting the presence of an additional upstream, SAC initiating role of CDK1. There are numerous published roles of CDK1 downstream of MPS1, including MAD1 kinetochore recruitment and the regulation of CDC20 fate (Qian et al., 2017; Zhang et al., 2017; Ji et al., 2017; D'Angiolella et al., 2003; Yudkovsky et al., 2000; Hein et al., 2017; Labit et al., 2012). However, no known roles of CDK1 explain the loss of all SAC components from the kinetochore and the complete absence of a SAC signal observed here. Therefore, CDK1 plays a hitherto unknown, critical upstream role in checkpoint signalling.

Based on previous studies, the primary hypothesis of this thesis was that CDK1 regulates MPS1 kinase activity in addition to kinetochore localisation. In Xenopus, a S283 residue in MPS1 is proposed to regulate MPS1 activity (Morin

et al., 2012). However, the equivalent residue in human cells (S281) is required to regulate MPS1 kinetochore localisation (Hayward et al., 2019a). In mammals, a phosphorylation regulating kinase activity has been suggested to occur at a C-terminal S821 residue in MPS1 (Diril et al., 2016). However, mutagenesis studies of both S821, and all known CDK1 sites in MPS1, using imaging and *in vitro* kinase assays showed that CDK1 is unlikely to regulate MPS1 kinase activity in human cells. This highlights a subtle difference in the regulation of SAC signalling between amphibians and mammals. In particular, this data would indicate that while amphibians regulate MPS1 through its kinase activity using CDK1, mammals do not do this but instead only use CDK1 to regulate MPS1's kinetochore localisation.

Focus must, therefore, turn away from MPS1 to look at other components of the SAC signalling pathway to identify the unknown role of CDK1. There are a number of alternative hypotheses for the role of CDK1 in initiating SAC signalling, of which multiple may be applicable and therefore require thorough future investigation.

Looking upstream of MPS1, work from the Cheeseman and Mussachio labs revealed a requirement of CDK1 for outer-kinetochore assembly (Gascoigne and Cheeseman, 2013; Rago et al., 2015; Huis in 't Veld et al., 2016). Phosphorylation of the kinetochore protein CENP-T by CDK1 leads to the localisation of the KMN network (KNL1, the MIS12-C and the NDC80-C) in mitosis (Gascoigne and Cheeseman, 2013; Rago et al., 2015). As the platform for both microtubule attachment and the SAC signalling machinery, regulation of

outer-kinetochore composition is of the utmost importance to the checkpoint. However, the temporal and functional effects of this process in the metaphase-to-anaphase transition are not well understood. Key outstanding questions surround the regulation of the timings of outer-kinetochore protein assembly and disassembly, in particular the regulation of KMN network protein loss from the kinetochore at mitotic exit. Furthermore, current data suggest that KNL1 and the MIS12-C assemble onto the kinetochore together through a single CDK1 phosphorylation on CENP-T (Rago et al., 2015), but it remains to be discovered whether additional levels of regulation occur between these two KMN components. As KNL1 is the checkpoint scaffold for BUB protein assembly, additional levels of CDK1 regulation for KNL1 localisation is a compelling hypothesis for how checkpoint signalling is regulated. The role of CDK1 in the regulation of outer-kinetochore assembly will be the main focus of subsequent chapters in this thesis.

An alternative strategy is to look downstream of MPS1 to the phosphorylation cascade leading the checkpoint protein recruitment. MPS1 phosphorylation of MELT motifs on KNL1 leads to BUB protein recruitment (Yamagishi et al., 2012; Shepperd et al., 2012; London et al., 2012). Hypothetically, CDK1 could also regulate BUB protein recruitment through KNL1 phosphorylation. Relatedly, CDK1 could regulate BUB protein recruitment through direct BUB protein phosphorylation. As no requirement for CDK1 for direct BUB protein recruitment has yet been reported, it is important to either confirm or exclude such hypotheses in future research.

A key point for discussion and future work is the difference in CDK1 dependency for checkpoint protein initial recruitment versus for checkpoint protein maintenance at the kinetochore. Through observation of the effect of CDK inhibition in two contrasting assays, this work uncovered that, while CDK1 was required for both recruitment and maintenance of BUB proteins at kinetochores, it was only required for the initial recruitment of downstream SAC component MAD1. The maintenance of MAD1 at kinetochores during prolonged SAC signalling was independent of CDK1 activity. As described previously, MAD1 localisation to kinetochores occurs through two separate pathways, one via BUB1 and the other via the RZZ complex (Basto et al., 2000; Buffin et al., 2005; Zhang et al., 2019; Ji et al., 2017; Zhang et al., 2017; Qian et al., 2017; Faesen et al., 2017; Rodriguez-Rodriguez et al., 2018). Extensive work has defined the role of CDK1 and MPS1 in MAD1 kinetochore recruitment through phosphorylation of the MAD1 binding partner BUB1 (Ji et al., 2017; Zhang et al., 2017; Qian et al., 2017). Additionally, the interaction of MAD1 with cyclin B of CDK1:cyclin B is required for the release of MAD1 from TPR at the nuclear pores so that it can be recruited to the kinetochore (Jackman et al., 2020). Once SAC signalling is initiated, MPS1 is not required to maintain MAD1 at kinetochores, MAD1 is instead recruited and maintained via the RZZ complex pathway (Rodriguez-Rodriguez et al., 2018). The role of BUB1 in MAD1 recruitment is catalytic and once RZZ recruitment has occurred, continued MAD1 recruitment is through the latter pathway. During prolonged checkpoint signalling, the RZZ complex polymerises to generate the fibrous corona at the kinetochore, which continues to recruit checkpoint proteins such as MAD1 and generate a checkpoint signal (Kops and Gassmann, 2020; Rodriguez-Rodriguez et al.,

2018). Indeed, in the absence of BUB1, the RZZ complex will localise and generate a fibrous corona that can recruit MAD1, if given sufficient time (Caldas et al., 2015; Vleugel et al., 2015). The work in this thesis suggests that the maintenance of MAD1 at kinetochores is not dependent on CDK1. As the MPS1 pathway of MAD1 recruitment is critically dependent on CDK1, this supports the idea that maintenance of MAD1 during checkpoint signalling is more dependent on the RZZ-localising pool of MAD1. Due to their presence only in mammals, regulation of the RZZ components and thus regulation of fibrous corona formation has not been well investigated. Data here provides an initial insight into RZZ regulation and fibrous corona formation by indicating that it's not regulated by CDK1. Therefore, understanding how this structure is regulated, if not through CDK1 and how exactly this transition from CDK1-dependency to CDK1-independency occurs will be an exciting avenue for future research. Furthermore, this will undoubtedly have consequences for understanding how a prolonged checkpoint signal is silenced, if no longer dependent on CDK1 and therefore the proposed CDK1-determined checkpoint permissive period (Hayward et al., 2019a).

Chapter 3: Investigating the role of CDK1 in regulating outer-kinetochore assembly and disassembly

3.1 Outer-kinetochore protein localisation is differentially regulated by CDK1

Previous studies have identified a dependence of outer-kinetochore assembly on CDK1 phosphorylation (Gascoigne and Cheeseman, 2013; Rago et al., 2015; Huis in 't Veld et al., 2016). However, current research has not investigated the functional impact of phospho-regulation of the KMN network on the metaphase-to-anaphase transition. In particular, although the CDK1 phosphorylations on CENP-T required for assembling the KMN network are well described, neither the timings of these phosphorylations nor the relationship of this to the timings of outer-kinetochore protein localisation are well understood. KNL1 plays a critical role in establishing a checkpoint signal as the checkpoint scaffold protein (Yamagishi et al., 2012; London et al., 2012; Shepperd et al., 2012; Primorac et al., 2013). Therefore, understanding the timing and regulation of its localisation to the kinetochore in comparison to microtubule interactor the NDC80-C, will be key to understanding how the cell regulates the checkpoint in comparison to microtubule attachment.

To begin investigating the role of CDK1 regulation of outer-kinetochore assembly in regulating checkpoint function, the Flp-In T-REx cell line system stably expressing kinetochore-tethered MPS1 was used to observe the localisation of outer-kinetochore components under the same conditions of the "checkpoint

reactivation assay" and CDK inhibition described in Chapter 2.1. In light of previous studies and the prior observation that MIS12 kinetochore localisation is unaffected under these conditions as part of the tethered system, it was expected that all outer-kinetochore proteins would behave similarly and be unaffected by the short CDKi treatment. Indeed, localisation of one NDC80-C component, HEC1, at kinetochores was minimally affected under these conditions (Figure 3.1A-B). Unexpectedly, however, the localisation of KNL1 was significantly reduced at kinetochores following CDK inhibition (Figure 3.1A-B). KNL1 kinetochore localisation had a higher sensitivity to the CDKi than other outer-kinetochore components. This indicated that the outer-kinetochore components are differentially regulated by CDK1 and that there is an additional KNL1-specific role of CDK1, which affects and regulates its kinetochore localisation separately from other outer-kinetochore components.

Due to variations in antibody sensitivity and dynamics, it was critical to corroborate this finding by observing endogenously tagged outer-kinetochore proteins. C-terminus GFP-tagged cell lines for KNL1, MIS12 and HEC1 were generated using a recently developed Cas12a-assisted PCR tagging method (Fueller et al., 2020). This system used a one-step PCR to generate a cassette containing the homology arms, GFP tag, and crRNA. This cassette was transfected into HeLa cells along with a Cas12a helper plasmid. Following cleavage, the tag was integrated into the gene of interest by homologous recombination. This method had the advantage over traditional CRISPR/Cas9 methodologies of being able to rapidly but accurately generate cell lines. Western blot screening confirmed that for each outer-kinetochore protein, multiple

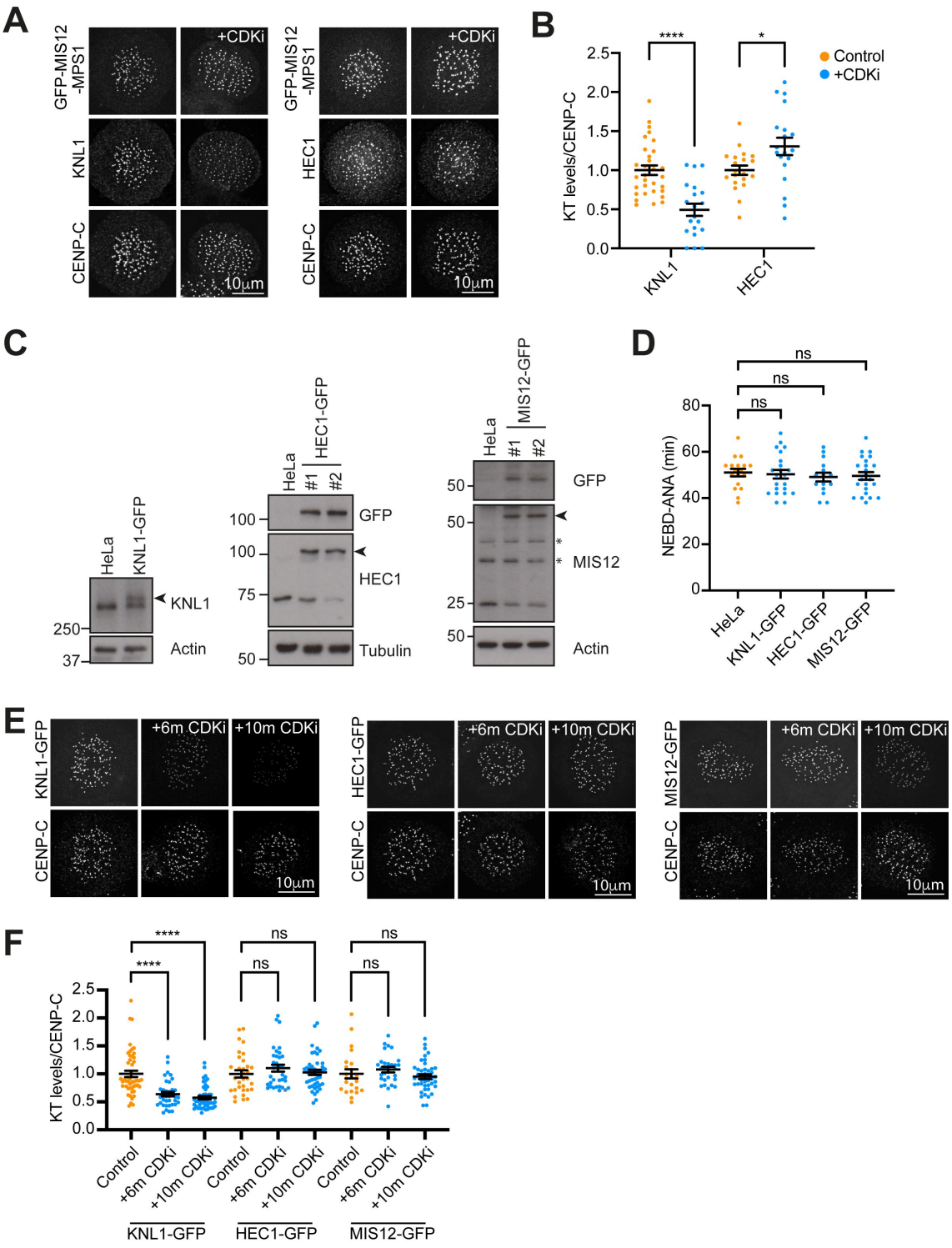


Figure 3.1 Outer-kinetochore protein localisation is differentially regulated by CDK1

(A) HeLa Flp-In/T-REx GFP-MIS12-MPS1 cells were depleted of endogenous MPS1. GFP-MIS12-MPS1 transgenes were induced by addition of doxycycline. After 48 h, cells were arrested for 2.5 h with 20 μM MG132, then treated with 3 μM nocodazole for the final 5 min, fixed with PTEMF, and immunostained as indicated. If CDK1 was

inhibited, 5 μM flavopiridol was added 1 min before nocodazole treatment (+CDKi). (B) Graph shows mean levels of KNL1 and HEC1 at kinetochores relative to CENP-C levels. Bars indicate the SEM (each point represents a single cell average intensity of 20 kinetochores, ≥ 19 cells per condition from 3 independent experiments). (C) Western blot screen confirms heterozygous clones of KNL1-GFP, MIS12-GFP and HEC1-GFP. Arrows indicate GFP-tagged proteins. * indicates non-specific bands. (D) Graph shows mean time from NEBD to anaphase (ANA) (min). Bars indicate the SEM, ≥ 15 cells per condition. (E) HeLa cells expressing KNL1-GFP, HEC1-GFP or MIS12-GFP cells were arrested for 2.5 h with 20 μM MG132, then treated with 3 μM nocodazole for the final 5 min, fixed with PTEMF, and immunostained as indicated. If CDK1 is inhibited, 5 μM flavopiridol was added 1 or 5 min before nocodazole treatment (+6m CDKi and +10m CDKi respectively). (B) Graph shows mean levels of KNL1-GFP, HEC1-GFP or MIS12-GFP at kinetochores relative to CENP-C levels. Bars indicate the SEM (each point represents a single cell average intensity of 20 kinetochores, ≥ 23 cells per condition from 3 independent experiments).

heterozygous clones were generated (Figure 3.1C). As the main function of these cell lines was to observe protein localisation, heterozygous clones were suitable for subsequent experiments. Successfully tagged clones were further screened for any mitotic issues arising from the addition of a GFP tag to the proteins. The progression of the clones through mitosis was observed using live cell imaging and the time from nuclear envelope breakdown (NEBD) to anaphase was measured (Figure 3.1D). All tagged cell lines showed no significant difference to parental HeLa cell lines in mitotic timings, demonstrating that they were unaffected by the addition of the GFP tag. One clone for each cell line was selected for subsequent in-depth analysis.

The “checkpoint reactivation assay” was then carried out on the GFP-tagged outer-kinetochore cell lines, with a CDK inhibition of either 6 min or 10 min to observe the differential effect that inhibition had on endogenous outer-

kinetochore protein levels. Confirming the observations in Figure 3.1A-B, the outer-kinetochore proteins responded differently to addition of CDKi (Figure 3.1E-F). KNL1 localisation at the kinetochore was much more sensitive to the CDKi than both HEC1 and MIS12. The short CDK inhibition times used here resulted in a significant decrease in KNL1 at the kinetochore but had no effect on HEC1 and MIS12 levels at the kinetochore (Figure 3.1E-F). It was particularly interesting that KNL1 localisation was affected but MIS12 localisation was unaffected under these conditions, as current data suggests that KNL1 and the MIS12-C come onto the kinetochore together as a complex through a single CDK1 phosphorylation on CENP-T (Gascoigne and Cheeseman, 2013; Rago et al., 2015; Huis in 't Veld et al., 2016; Petrovic et al., 2010). Therefore, this further pointed towards a novel KNL1-specific level of CDK1 regulation that regulates KNL1 localisation separately to the MIS12-C and the rest of the outer-kinetochore.

3.2 Outer-kinetochore protein dynamics in mitosis

Differential sensitivity to the CDKi may be indicative of different timings of outer-kinetochore protein localisation to the kinetochore in normal cycling cells. This could be in response to factors such as cyclin B levels, CDK1 phosphorylation site availability or opposing phosphatase activity. Initially, immunofluorescence (IF) was carried out on asynchronous HeLa cells with endogenously tagged outer-kinetochore proteins (Figure 3.2A). The levels of the KMN complex components at the kinetochore at different stages of the cell cycle (based on DNA morphology) were quantified (Figure 3.2B). This low-resolution analysis revealed

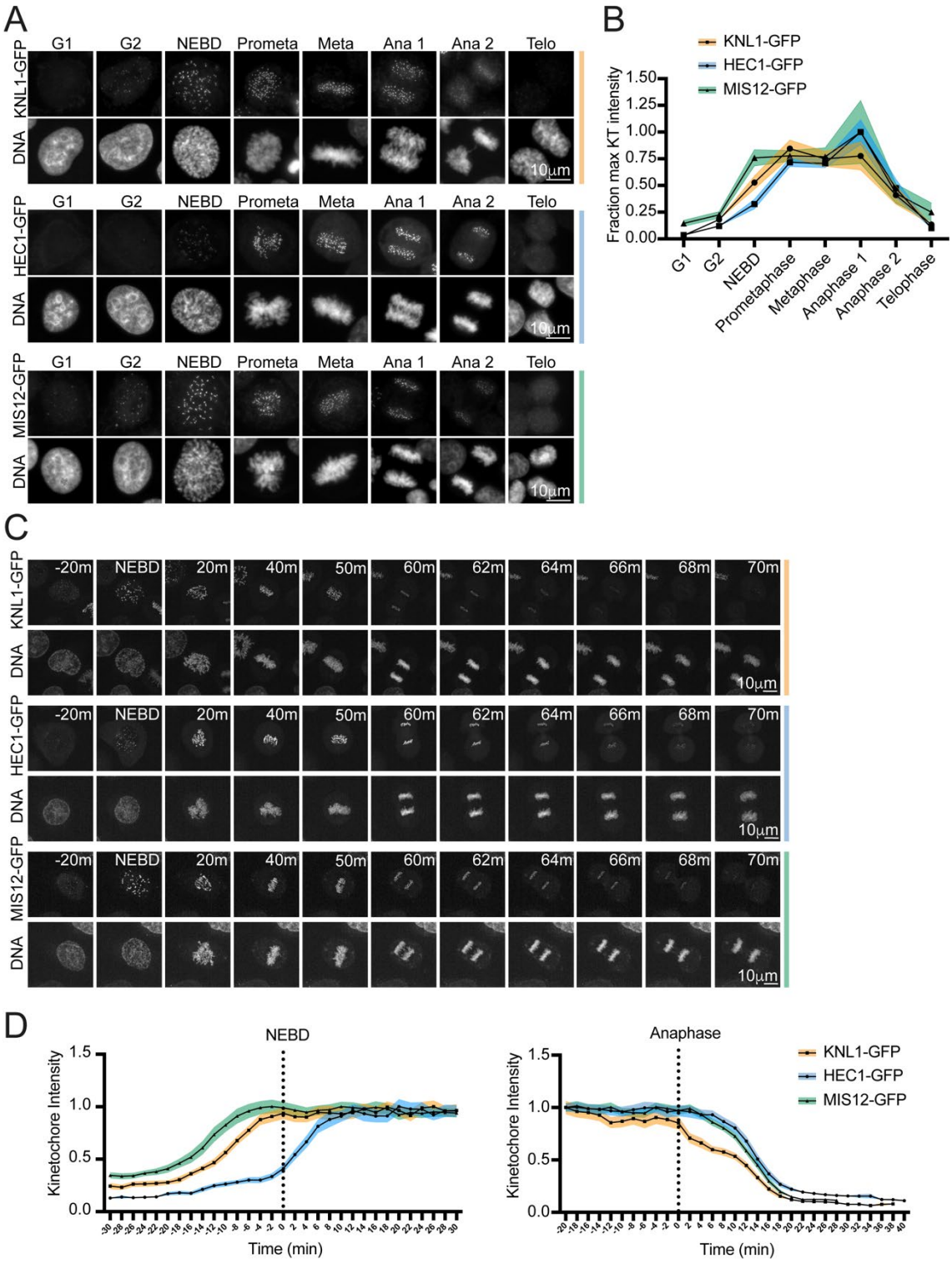


Figure 3.2 Outer-kinetochore protein dynamics in mitosis

(A) Asynchronous HeLa cells expressing KNL1-GFP, HEC1-GFP or MIS12-GFP cells were fixed with PTEMF, and immunostained as indicated. (B) Graph shows level of KNL1-GFP, HEC1-GFP or MIS12-GFP kinetochore signal relative to CENP-C levels as a fraction of the maximum intensity. Shaded regions indicate the SEM (each point represents a single cell average intensity of 10 kinetochores, ≥ 3 cells per condition

from 3 independent experiments). (C) Movie stills of HeLa cells expressing KNL1-GFP, MIS12-GFP or HEC1-GFP and incubated with 100 nM SiR-DNA. Cells were synchronised for 18 h using 2 mM thymidine. Cells were imaged 9 h after thymidine release. (D) Graphs show mean kinetochore intensities of KNL1-GFP, HEC1-GFP or MIS12-GFP at 2 min intervals of cells shown in (C) as a fraction of the maximum intensity. Shaded regions indicate the SEM (≥ 15 cells per condition from 3 independent experiments).

a difference in the timings of assembly and disassembly of the KMN network proteins. Analysis showed that KNL1 and MIS12 began localising to the kinetochore earlier than HEC1 (Figure 3.2B). Of particular interest was the observation that KNL1 levels at the kinetochore appeared to decrease earlier in mitotic exit than the other outer-kinetochore proteins (Figure 3.2B). However, the timing precision of this fixed analysis was limited and the analysis was subjective in the assignment of cell cycle stages.

To obtain more precise timings of outer-kinetochore protein assembly and disassembly, high-resolution live cell imaging was carried out on a SoRa spinning disc confocal microscope using HeLa cells lines with endogenously tagged outer-kinetochore proteins. Cells were imaged at 2 min intervals through mitosis (Figure 3.2C), and the kinetochore intensity of each KMN protein was measured (Figure 3.2D). See Chapter 7.6.5 for further details of imaging conditions. In agreement with the low-resolution fixed analysis, live imaging revealed that KNL1 and MIS12 assembled onto the kinetochore prior to NEBD and reached their maximum kinetochore intensity by NEBD. Interestingly, MIS12 localised slightly prior to KNL1 in the experiment. However, HEC1 did not significantly increase at the kinetochore until NEBD, only reaching its maximum kinetochore level approximately 12 min after NEBD (Figure 3.2D). Strikingly, KNL1 was rapidly lost

from the kinetochore at the metaphase-to-anaphase transition following chromosome alignment. Indeed, KNL1 kinetochore intensity began to decrease prior to anaphase onset (Figure 3.2D). However, both HEC1 and MIS12 did not leave the kinetochore until several minutes after cells had entered anaphase, with MIS12 being lost marginally earlier than HEC1 (Figure 3.2D).

Combining this data with the preceding CDK inhibition data, the rapid loss of KNL1 from the kinetochore and its separate regulation to other KMN network proteins points towards a novel SAC regulatory mechanism. The rapid loss of KNL1 from the kinetochore shuts down the checkpoint following chromosome alignment, but microtubule-kinetochore attachments are maintained through the retention of the NDC80-C until later in anaphase. Subsequent research in this thesis will focus on identifying and characterising the exact nature and importance of this mechanism.

3.3 Identifying a novel level of CDK1 regulation between the MIS12 complex and KNL1

Previous studies have shown that KNL1 and the MIS12-C localise at the kinetochore as a complex. Structural data has detailed that this interaction occurs through the MIS12-C component NSL1 (Petrovic et al., 2010, 2014). Therefore, the additional level of CDK1 regulation that specifically regulates KNL1 localisation may act at the interaction between NSL1 and KNL1.

Initially, the importance of NSL1 for KMN network structure and SAC response was analysed by depleting NSL1 from cells using RNAi. HeLa cells were treated

with a siNSL1 oligo (or a control siRNA) for 48 h and efficient depletion of NSL1 was confirmed by western blotting (Figure 3.3A). Two different siNSL1 oligos were tested and showed similar efficiency at depleting NSL1. One oligo was then taken forward for the in-depth analysis. The effect of NSL1 depletion was observed using IF following a 48h treatment with the siNSL1 oligo (Figure 3.3B). In agreement with phenotypes seen for a MIS12-C depletion, the depletion of NSL1 resulted in a prometaphase arrest in cells and an inability to correctly align chromosomes (Cheeseman and Desai, 2008; Kline et al., 2006; Pagliuca et al., 2009). Looking specifically at protein kinetochore localisation, a significant reduction was observed in the recruitment of checkpoint proteins BUB1 and MAD1, and KMN protein KNL1 to kinetochores (Figure 3.3B-C). Additionally, the kinetochore localisation of HEC1 was reduced (Figure 3.3B-C). However, HEC1 localisation was reduced to a lesser extent than for KNL1 (Figure 3.3C), in keeping with the understanding of two pathways of outer-kinetochore assembly. KNL1 always requires the MIS12-C for its localisation, while HEC1 only requires the MIS12-C for the CENP-C pathway of assembly and so HEC1 is still able to localise to some extent via the CENP-T pathway. These results confirmed that NSL1 is critical for the localisation of KNL1 to kinetochores and for generating a checkpoint signal.

Subsequently, the interaction between KNL1 and NSL1 was analysed by immunoprecipitation using cell lines of the Flp-In T-REx system stably expressing GFP-NSL1. Multiple GFP-NSL1 clones were successfully generated and characterised before selecting one for in-depth analysis. Overexpressed GFP-NSL1 was pulled down using an anti-GFP immunoprecipitation, and the resulting

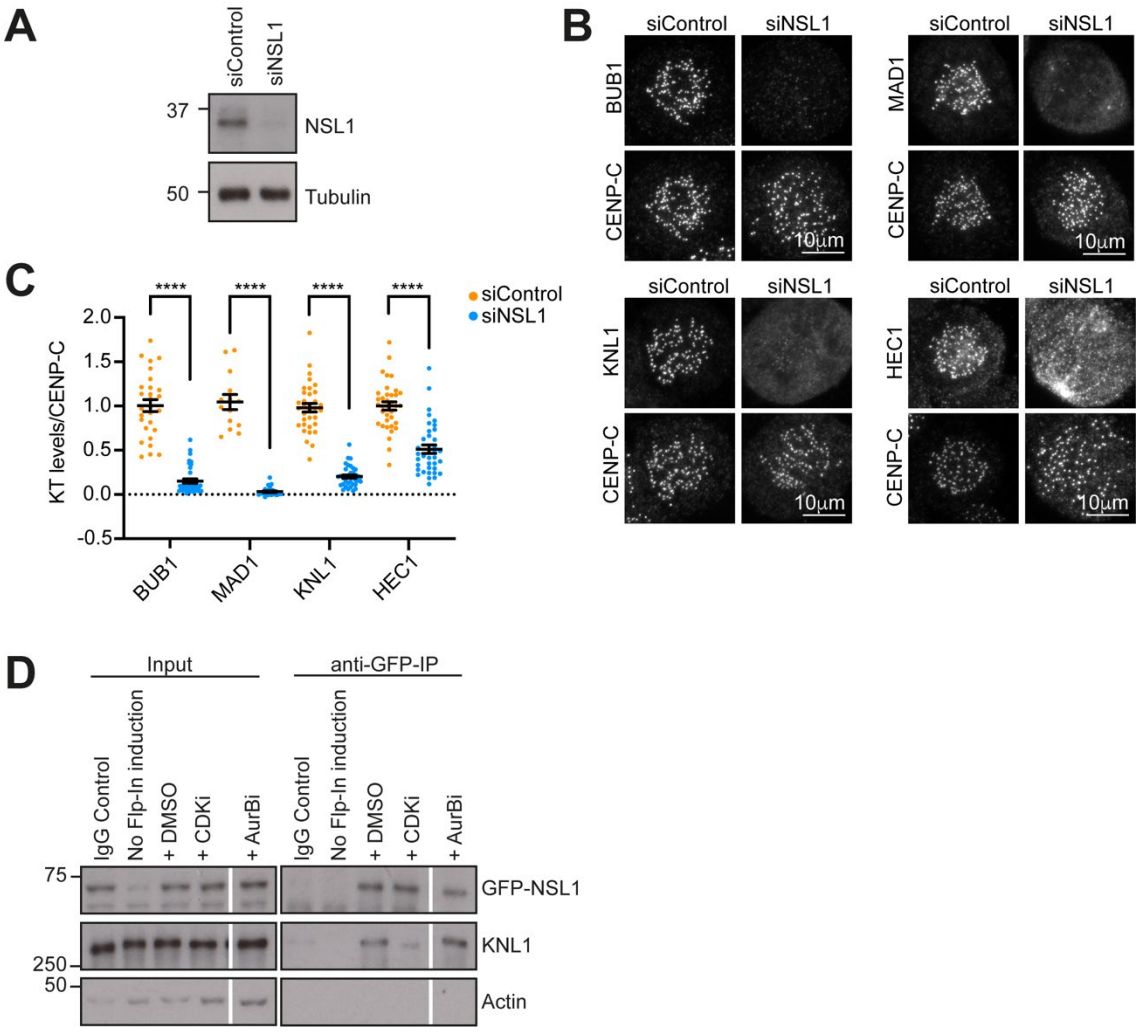


Figure 3.3 NSL1 is critical for localising KNL1 to kinetochores

(A) Western blot showing depletion of NSL1 following a 48 h RNAi in HeLa cells. GL2 was used as a control RNAi. (B) HeLa cells were depleted of endogenous NSL1 (or GL2 as a control). After 48 h, cells were fixed with PTEMF and immunostained as indicated. (C) Graph shows mean levels of BUB1, MAD1, KNL1 or HEC1 at kinetochores relative to CENP-C levels. Bars indicate the SEM (each point represents a single cell average intensity of 20 kinetochores, ≥ 14 cells per condition from 3 independent experiments). (D) HeLa Flp-In/T-Rex GFP-NSL1 cells were induced by addition of doxycycline for 48 h (except where indicated). After 18 h 0.3 µM nocodazole treatment, cells were collected following a 10 min kinase inhibition with DMSO used as a control. GFP-NSL1 was immunoprecipitated (IP) with an anti-GFP antibody. Anti-mCherry was used an IgG control. Immunoprecipitated protein complexes were analysed by western blotting. 0.5% of Input and 10% of IP was loaded on gels.

binding partners pulled down with NSL1 were analysed by western blotting (Figure 3.3D). KNL1 was pulled down with GFP-NSL1 in the control condition (+DMSO), thus confirming an interaction between the two proteins. Additionally, the effect of inhibiting key mitotic kinases on this interaction was tested. Specifically, CDK inhibition reduced the amount of KNL1 pulled down with GFP-NSL1, whereas Aurora B inhibition had no effect (Figure 3.3D). This confirmed the hypothesis that CDK1 regulates the interaction between NSL1 and KNL1.

Due to the nature of this interaction, it was hypothesised that CDK1 is specifically phosphorylating NSL1 to regulate this interaction. Therefore, it was important to confirm that NSL1 is indeed phosphorylated during mitosis when CDK1 would be active. HeLa cells that were either asynchronous or arrested in mitosis using nocodazole were harvested and lysed. A portion of the mitotic samples were subsequently treated with λ-phosphatase to remove any phosphorylations in the lysate. Samples were analysed by western blotting using either standard SDS-PAGE or Phos-tag SDS-PAGE, the latter of which allows proteins to be separated based on their phosphorylation status in addition to their size (Figure 3.4A). Analysis of NSL1 by Phos-tag SDS-PAGE showed an upshifted band in mitotic samples which was very weak in asynchronous samples and lost in the samples treated with λ-phosphatase (Figure 3.4A). Therefore, NSL1 is phosphorylated during mitosis.

To identify the exact site on NSL1 that is phosphorylated by CDK1, the amino acid sequence of NSL1 was analysed. *In vitro* studies using short peptides have previously identified a Y270 residue within the KNL1 interaction region of NSL1

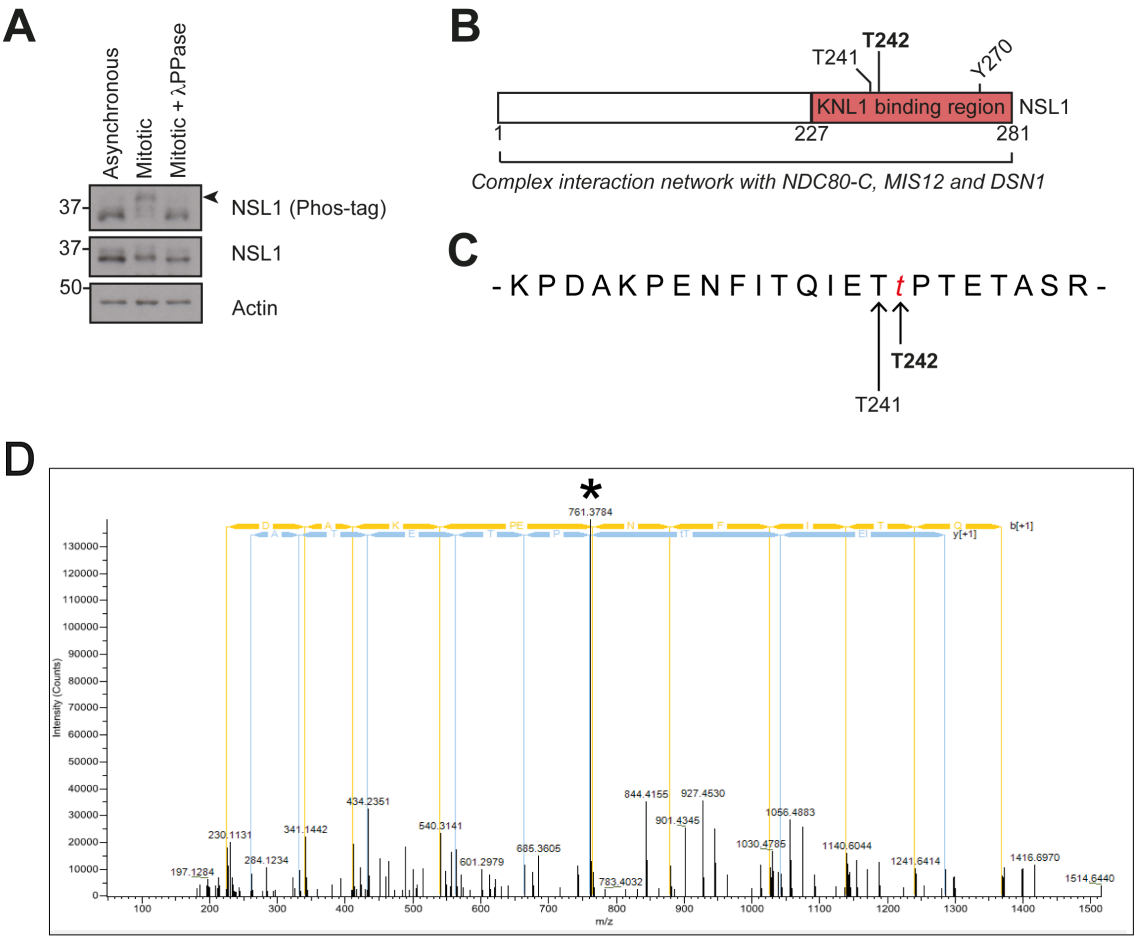


Figure 3.4 NSL1 is mitotically phosphorylated at T242

(A) Western blot of asynchronous and mitotic HeLa cell lysates. Mitotic lysates were treated with λ-phosphatase where indicated. Samples were run on either standard or Phos-tag SDS-PAGE gels as indicated. Arrow indicates phosphorylated NSL1. (B) Schematic of domain organization of NSL1. Essential residue Y270 and proposed CDK1 phosphorylation sites required for KNL1 interaction are indicated. CDK1 consensus site (T242) is shown in bold. (C) Peptide used in phospho-proteomic analysis of T242. Proposed CDK1 phosphorylation sites required for KNL1 interaction are indicated. CDK1 consensus site analysed in the phospho-proteomic study is shown in red. (D) Graph shows m/z data from mass spectrometry analysis of T242 phosphorylation using the peptide in (C). GFP-NSL1 was immunoprecipitated (IP) with an anti-GFP antibody and samples were prepared for mass spectrometry. * indicates phosphorylation peak corresponding to T242.

that is essential for the interaction (Huis in 't Veld et al., 2016). Combining data from online databases (Hornbeck et al., 2015), there are 10 proposed

phosphorylation sites on NSL1, only three of which are CDK1 consensus sites (S4, T31, T242). Of these three, only one, T242, falls within the KNL1 interaction region (NSL1 198-281) (Petrovic et al., 2010) (Figure 3.4B). T242 is preceded by another threonine (T241); both of these threonines are potential CDK1 phosphorylation sites.

Mass spectrometry was used (in collaboration with the Oxford Advanced Proteomics Facility) to investigate whether residue T242 in NSL1 is phosphorylated in mitosis. HEK293T cells were transiently transfected with GFP-NSL1, arrested in mitosis and harvested for immunoprecipitation. Immunoprecipitation was carried out using the GFP tag on the overexpressed NSL1 and samples were prepared for mass spectrometry. All major KMN components were detected in the NSL1 pull-down analysis. Phospho-proteomic analysis of the peptide shown in Figure 3.4C revealed significant phosphorylation of T242 in mitotic cells, seen as a strong peak (*) in the m/z graph (Figure 3.4D). Given the time limitations of this project, it was not possible to carry out further mass spectrometry analysis. However, future mass spectrometry experiments will be used to observe the effect of kinase inhibitions and point mutations on the detection of T242 phosphorylation and NSL1 interaction partners, particularly KNL1.

To investigate the role of T242 *in vivo*, the Flp-In T-REx cell line system was employed to stably express GFP-NSL1 with various mutations. In addition to wild type NSL1, cell lines were generated with the previously identified Y270 residue (Huis in 't Veld et al., 2016) mutated to alanine (Y270A) as a negative control and

the T242 residue under investigation along with the preceding residue T241 mutated to either phospho-null (2TA) or phospho-mimetic (2TD). Both T241 and T242 were mutated as a single aspartic acid mutation is often insufficient to generate a phospho-mimetic effect, as well as the possibility that both residues are phosphorylated by CDK1. For each cell line, multiple clones were successfully generated and characterised before selecting one for in-depth analysis. Endogenous NSL1 was depleted using RNAi as previously optimised, and GFP-NSL1 expression was induced by doxycycline to rescue this loss. Efficient NSL1 depletion and rescue for each cell line was confirmed by western blotting (Figure 3.5A).

Initially, the effect of the mutations was investigated by immunoprecipitation of GFP-NSL1 from the mutant Flp-In T-REx cell lines. NSL1 was pulled down using an anti-GFP immunoprecipitation, and the resulting binding partners pulled down with NSL1 were analysed by western blotting (Figure 3.5B). Compared to GFP-NSL1 WT, there was a significant reduction in the amount of both KNL1 and HEC1 pulled down by GFP-NSL1 Y270A. This points towards a more general role of the Y270 residue in outer-kinetochore assembly. Interestingly, there was a significant reduction in the amount of KNL1 pulled down with GFP-NSL1 2TA which was restored to WT level with GFP-NSL1 2TD (Figure 3.5B). The same change was not observed in the amount of HEC1 pulled down with GFP-NSL1, which was unchanged from WT in both 2T mutants (Figure 3.5B). Therefore, mutation of T241 and T242 specifically affected KNL1's interaction with NSL1.

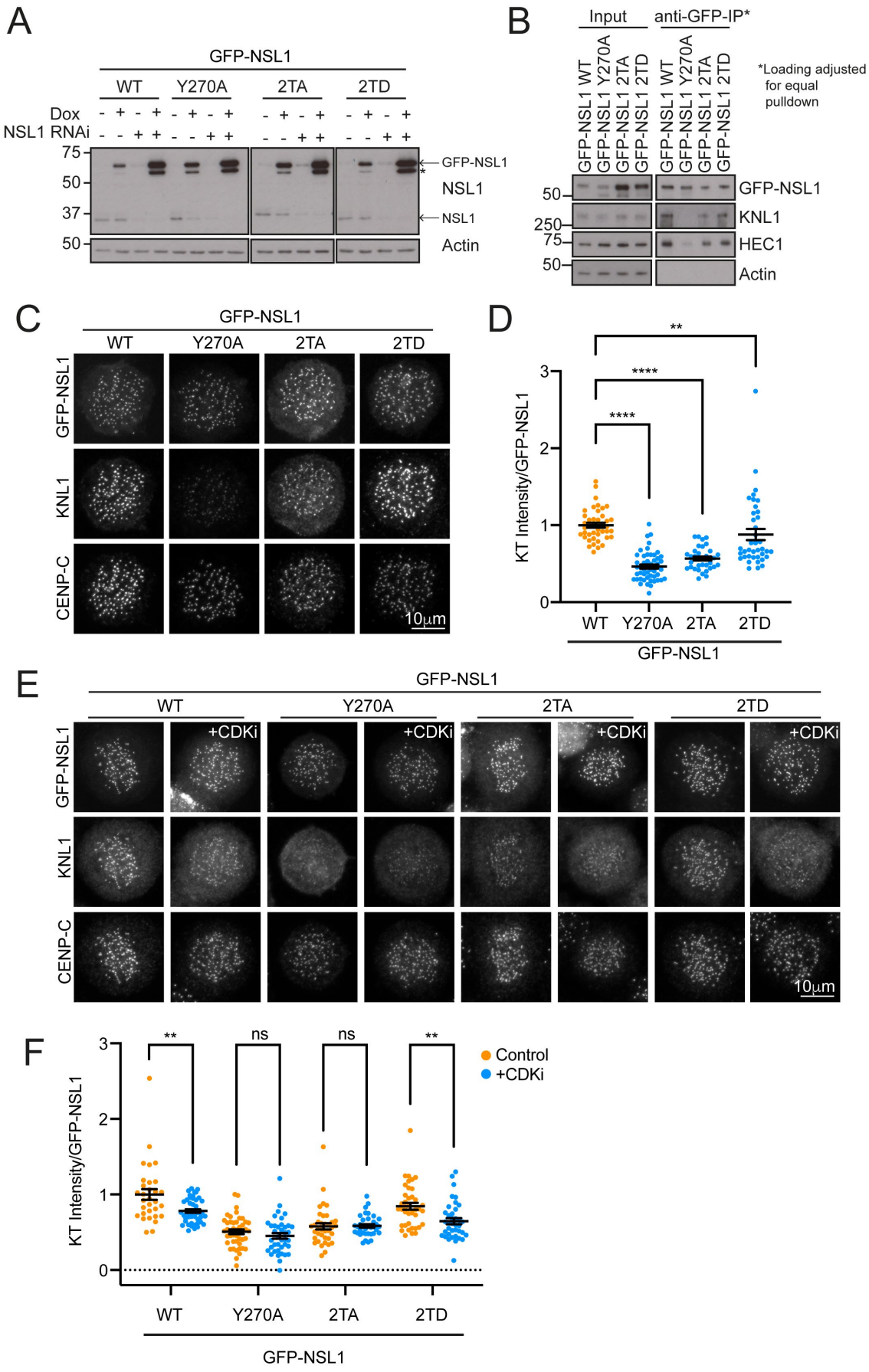

A
GFP-NSL1
WT
Y270A
2TA
2TD
Dox
NSL1 RNAi
75
50
37
50
GFP-NSL1
NSL1
NSL1
Actin
B
Input
anti-GFP-IP*
GFP-NSL1 WT
GFP-NSL1 Y270A
GFP-NSL1 2TA
GFP-NSL1 2TD
*Loading adjusted for equal pulldown
50
250
75
50
GFP-NSL1
KNL1
HEC1
Actin
C
GFP-NSL1
WT
Y270A
2TA
2TD
GFP-NSL1
KNL1
CENP-C
10μm
D
KT Intensity/GFP-NSL1
**
****
****
3
2
1
0
WT
Y270A
2TA
2TD
GFP-NSL1
E
GFP-NSL1
WT
Y270A
2TA
2TD
+CDKi
GFP-NSL1
KNL1
CENP-C
10μm
F
KT Intensity/GFP-NSL1
**
ns
ns
**
Control
+CDKi
3
2
1
0
WT
Y270A
2TA
2TD
GFP-NSL1

Figure 3.5 Phospho-regulation of T242 is required for KNL1 kinetochore localisation

(A) Western blot confirming successful RNAi rescue with GFP-NSL1 mutants. HeLa Flp-In/T-REx GFP-NSL1 cells were depleted of endogenous NSL1 and GFP-NSL1 transgenes were induced by addition of doxycycline as indicated. * indicates GFP-NSL1 transgene splice variant or degradation product. (B) HeLa Flp-In/T-Rex GFP-NSL1 cells were induced by addition of doxycycline for 48 h. After 18 h 0.3 μM nocodazole treatment, cells were collected and lysed. GFP-NSL1 was immunoprecipitated (IP) with an anti-GFP antibody. Immunoprecipitated protein complexes were analysed by western blotting. 0.5% of Input was loaded on gels, IP loading was adjusted for equal NSL1 pulldown. (C) HeLa Flp-In/T-REx GFP-NSL1 cells were depleted of endogenous NSL1. GFP-NSL1 transgenes were induced by addition of doxycycline. After 48 h, the asynchronous populations were fixed with PTEMF, and immunostained as indicated. (D) Graph shows mean levels of KNL1 at kinetochores relative to GFP-NSL1 levels. Bars indicate the SEM (each point represents a single cell average intensity of 20 kinetochores, ≥ 35 cells per condition from 3 independent experiments). (E) HeLa Flp-In/T-REx GFP-NSL1 cells were depleted of endogenous NSL1. GFP-NSL1 transgenes were induced by addition of doxycycline. After 48 h, cells were arrested for 2.5 h with 20 μM MG132, then treated with 3 μM nocodazole for the final 5 min, fixed with PTEMF, and immunostained as indicated. If CDK1 was inhibited, 5 μM flavopiridol was added 1 min before nocodazole treatment (+CDKi). (F) Graph shows mean levels of KNL1 at kinetochores relative to GFP-NSL1 levels. Bars indicate the SEM (each point represents a single cell average intensity of 20 kinetochores, ≥ 31 cells per condition from 3 independent experiments).

To support these observations, the mutant Flp-In T-REx cell lines were fixed and stained as an asynchronous population to observe the effect of the mutations on KNL1 kinetochore localisation (Figure 3.5C). As expected from previous studies, the Y270A mutation resulted in a significant decrease in KNL1 kinetochore localisation compared to GFP-NSL1 WT (Figure 3.5C-D). In agreement with the biochemical data, GFP-NSL1 2TA cells showed a significant decrease in KNL1 localisation at the kinetochore (Figure 3.5C-D). This loss was partially restored in

the 2TD mutation, which showed only a very minor reduction in KNL1 kinetochore localisation compared to GFP-NSL1 WT (Figure 3.5C-D).

Subsequently, the Flp-In T-REx GFP-NSL1 cell lines were subjected to the "checkpoint reactivation assay" to observe the effect of CDK inhibition on KNL1 localisation with the different NSL1 mutations. As previously observed, KNL1 localisation was significantly reduced following CDK inhibition in the condition with GFP-NSL1 WT (Figure 3.5E-F). Contrastingly, CDK inhibition had no further effect on the loss of KNL1 observed in the GFP-NSL1 Y270A and GFP-NSL1 2TA cells (Figure 3.5E-F). However, a significant reduction in KNL1 localisation was still observed following CDK inhibition in the condition with GFP-NSL1 2TD, which appeared to behave much like the WT condition (Figure 3.5E-F). Overall, mutation of T242 and its preceding residue in NSL1 specifically and significantly affected KNL1's interaction with NSL1 and KNL1's localisation at the kinetochore. However, while the phospho-mimetic mutations were able to rescue the loss of KNL1 observed in the phospho-null condition, they were not sufficient to rescue the loss of KNL1 that occurs following CDK inhibition.

3.4 Investigating the effect of loss of CDK1 regulation of outer-kinetochore assembly on checkpoint signalling and cell cycle regulation

The importance of this level of CDK1 regulation for checkpoint signalling and cell cycle progression was investigated by observing the effect of the NSL1 T242 mutations on mitotic timings and the frequency of mitotic errors. Following NSL1 RNAi rescue and cell synchronisation using thymidine, Flp-In T-REx GFP-NSL1 cells were imaged on an EVOS M7000 imaging system. Based on DNA

morphology, the times from NEBD to anaphase, NEBD to metaphase, and metaphase to anaphase were measured (Figure 3.6A). Given the previous data showing that the Y270A mutation causes widespread outer-kinetochore disassembly, it was unsurprising that this mutation caused a profound delay in mitotic timing. The majority of this delay was between NEBD and metaphase (Figure 3.6A), which corresponds in this mutant with the loss of HEC1 and thus a delay in forming stable microtubule-kinetochore attachments. Interestingly, both the NSL1 2TA and 2TD mutations only caused minor overall delays in mitotic timings (Figure 3.6A), although the delay occurred at different points of mitosis for the two mutants. For GFP-NSL1 2TA, the delay occurred prior to metaphase, with cells appearing to be delayed in forming a stable metaphase plate (Figure 3.6A). In contrast to this, GFP-NSL1 2TD cells were significantly delayed at the metaphase-to-anaphase transition (Figure 3.6A). Cells formed a metaphase plate but were unable to begin chromosome segregation. This observation led to the hypothesis that, while not a complete phospho-mimetic rescue, the GFP-NSL1 2TD cell lines were unable to efficiently remove KNL1 from the kinetochore and thus turn off the SAC. This caused a delay between formation of the metaphase plate and anaphase onset.

In addition to mitotic timings, mitotic outcomes and the frequency of mitotic errors were assessed and quantified (Figure 3.6B). Representative images for each cell line are shown in Figure 3.6C. As expected, a significant increase in mitotic errors was seen in the GFP-NSL1 Y270A cell lines (Figure 3.6B), with cell death before metaphase and DNA bridges being the highest frequency outcomes. The cells that died prior to metaphase appeared to struggle forming stable attachments

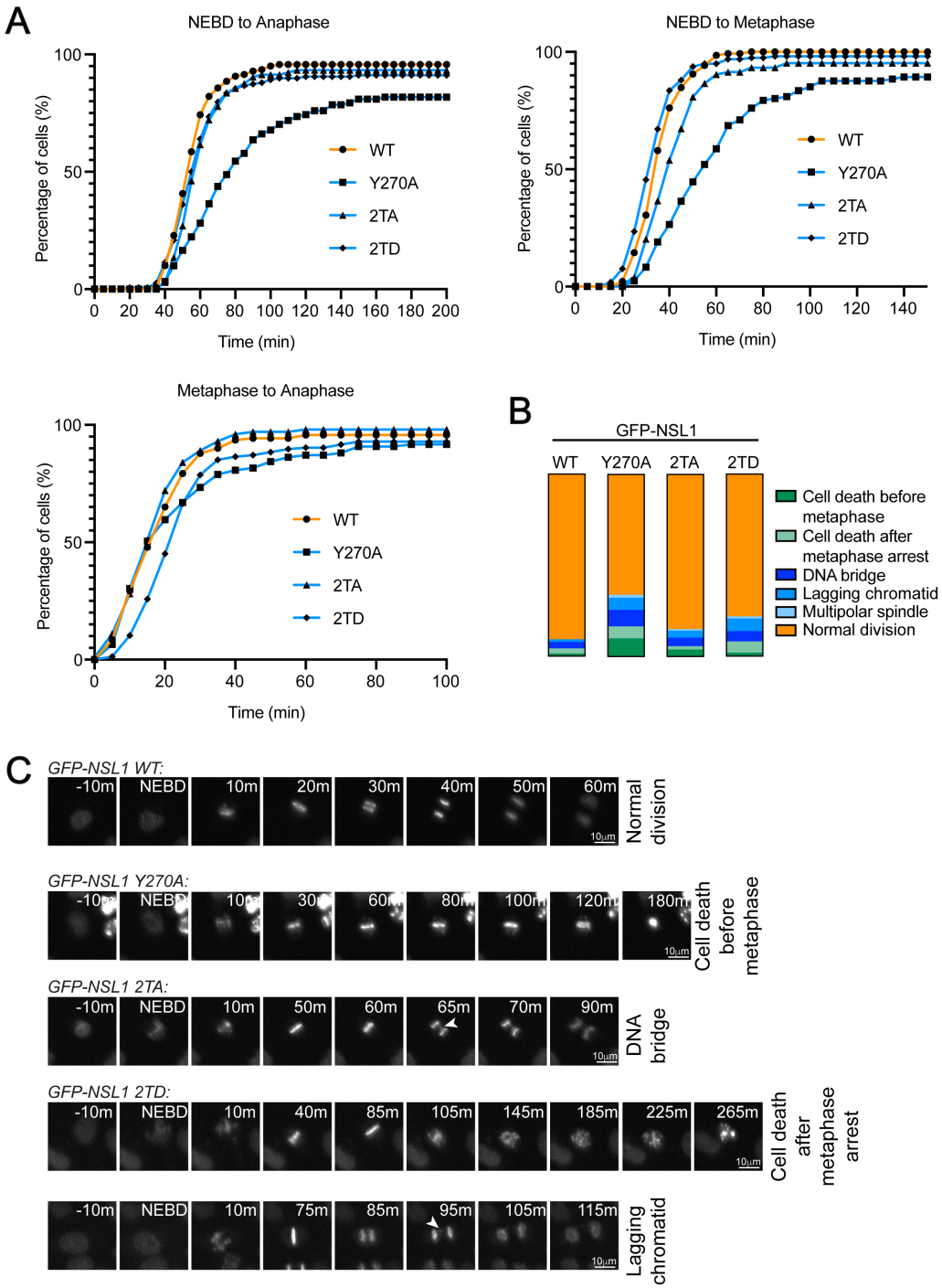


Figure 3.6 CDK1 regulation of outer-kinetochore assembly is critical for SAC signalling and cell cycle regulation

(A) Cumulative frequency graphs show mean time from NEBD to anaphase (min), NEBD to metaphase (min) and metaphase to anaphase (min) for HeLa Flp-In/T-REx GFP-NSL1 cell lines incubated with 100 nM SiR-DNA. Cells were synchronised for 18 h using 2 mM thymidine. Cells were imaged 9 h after thymidine release (≥ 106

cells per condition). (B) HeLa Flp-In/T-REx GFP-NSL1 cell lines were assessed for mitotic outcome status and the proportions of each outcome quantified as a percentage. (C) Representative movie stills of HeLa Flp-In/T-REx GFP-NSL1 WT, Y270A, 2TA and 2TD cell lines incubated with 100 nM SiR-DNA.

and couldn't reach a metaphase plate (Figure 3.6C). A marginal increase in mitotic errors was observed in the GFP-NSL1 2TA cell lines, particularly DNA bridges and lagging chromatids (Figure 3.6B-C). However, there was a significant increase in the number of mitotic errors in the GFP-NSL1 2TD cell lines, including lagging chromatids (Figure 3.6B-C). Of particular note was the increased occurrence of a phenotype termed "cell death following metaphase arrest". As shown in Figure 3.6C, cells reached a metaphase plate, arrested and eventually lost chromosome alignment and returned to a prometaphase-like state before dying. This phenotype strongly supports the hypothesis that cells with the 2TD mutation are unable to efficiently remove KNL1 and thus are not able to overcome the checkpoint arrest and enter anaphase. The exact cause of the above phenotype is not clear and will be discussed below.

3.5 Discussion

At the start of this chapter, the primary hypothesis for the novel role of CDK1 in checkpoint signalling was the involvement of CDK1 in regulating outer-kinetochore assembly. Indeed, previous studies have described the key role of CDK1 phosphorylation of CENP-T in regulating the assembly of the outer-kinetochore in mitosis (Gascoigne et al., 2011; Rago et al., 2015). However, research carried out here revealed further previously unknown levels of CDK1 regulation in outer-kinetochore assembly. Published data would predict that

MIS12 and KNL1 would respond identically to CDK inhibition as they assemble onto the kinetochore as a complex via a single CDK1 phosphorylation on CENP-T (Gascoigne and Cheeseman, 2013; Rago et al., 2015; Huis in 't Veld et al., 2016; Petrovic et al., 2010). In contrast, the novel data here revealed that KNL1 and MIS12 localisations had different sensitivities to the CDKi, suggesting that there is an additional level of CDK1 regulation between the MIS12-C and KNL1. Indeed, within the short CDK inhibition used, no difference was observed in the localisation of MIS12 or HEC1, while KNL1 was significantly reduced. This further suggested that while KNL1 is dynamically regulated during mitosis, HEC1 and MIS12 are much more stably associated with the kinetochore via CENP-T. These results were supported by high-resolution live cell imaging which revealed that that KNL1 is rapidly lost from the kinetochore at mitotic exit, significantly earlier than other outer-kinetochore proteins.

Together, these data provide a compelling hypothesis for the regulation of the SAC response. Through regulating the structure of the KMN network, CDK1 regulates the key scaffold protein for the SAC signal, KNL1 (Yamagishi et al., 2012; London et al., 2012; Shepperd et al., 2012; Primorac et al., 2013). In particular, the rapid loss of KNL1 may provide a mechanism for regulating checkpoint shutdown following chromosome alignment but maintaining microtubule attachments via the NDC80-C until later in anaphase. During anaphase it is critical that kinetochore attachments to microtubules are maintained until chromatid separation has occurred to avoid lagging chromatids and potential aneuploidy. However, it is equally important that the SAC does not reactivate following the initiation of chromosome separation. Previously,

directionality of the metaphase-to-anaphase transition has been attributed to the opposing activities of CDK1 and PP2A-B55 acting on the principal checkpoint kinase MPS1 to define the checkpoint permissive period and prevent checkpoint reactivation after this period has ended (Hayward et al., 2019a). A role of CDK1 and the outer-kinetochore in regulating directionality has not previously been proposed and is therefore an intriguing avenue for further investigation.

In addition to the information gleaned from the mitotic exit kinetics of KMN components, the data also gave an insight into KMN assembly kinetics at mitotic entry. It was observed that MIS12 and KNL1 assemble onto the kinetochore significantly earlier than HEC1, which does not assemble until after NEBD, in agreement with previously published low-resolution assembly kinetics (Gascoigne and Cheeseman, 2013). This difference in assembly timings suggests that the CENP-C pathway of KMN network assembly, where the MIS12-C is assembled before the NDC80-C (Rago et al., 2015), plays a more dominant role in KMN assembly in G2 prior to CDK1 levels reaching their maximum. This is supported by the fact that the NDC80-C is excluded from the nucleus until NEBD so cannot form the platform for KMN assembly initially (Gascoigne and Cheeseman, 2013). Once CDK1 levels have increased and the NDC80-C has gained access to kinetochores, the CENP-T pathway of KMN assembly takes on a more dominant role to build on and amplify the initial outer-kinetochore formed in late G2/early mitosis. This enables the creation of the extensive KMN network required for mitosis. Although this is a satisfying hypothesis, the exact contributions and importance of each pathway of KMN assembly have not yet been explored. Dissecting these two pathways to understand their contributions

will prove helpful in understanding KMN network assembly. Interestingly, assembly kinetics also revealed that although both MIS12 and KNL1 assemble onto the kinetochore prior to NEBD, KNL1 assembles marginally later than MIS12. This provides further evidence of an additional level of regulation between the MIS12-C and KNL1. It could be hypothesised that NSL1 only becomes phosphorylated by CDK1 once at the kinetochore therefore resulting in the slight delay between the MIS12-C assembly and KNL1 assembly.

During this project, significant progress was made in identifying the exact nature of the novel level of CDK1 regulation specifically regulating KNL1 localisation. Previous structural work has extensively characterised the interaction domains of the MIS12-C (Petrovic et al., 2010, 2016; Dimitrova et al., 2016). Interaction with KNL1 occurs through the MIS12-C component NSL1. However, these studies have not investigated any levels of cell cycle regulation in this interaction. Preliminary mass spectrometry data identified T242 as a key candidate CDK1 phosphorylation site on NSL1. Future mass spectrometry experiments will aim to manipulate this phosphorylation site with various kinase inhibitions to observe the effect of these on the phosphorylation status of T242 and the subsequent effect on NSL1 interaction partners, particularly KNL1. This will be particularly important to exclude an indirect role of CDK1 in regulating NSL1 phosphorylation. Due to the requirement for CDK1 for localising both PLK1 (Elia et al., 2003a; b) and Aurora B (Hümmer and Mayer, 2009; Tsukahara et al., 2010) during mitosis, it is possible that one of these kinases is actually phosphorylating NSL1 and that the effects of CDK inhibition observed are indirect. Immunoprecipitation data following kinase inhibitions suggested this is not the case, and that the disruption

of the NSL1:KNL1 interaction is specific to CDK inhibition. However, future phospho-proteomics looking at this phosphorylation site following kinase inhibitions will ensure this is conclusively excluded.

In addition to biochemical and mass spectrometry analysis, it was critical to look at the role of T242 *in vivo*. At the time of writing, a phospho-specific antibody against NSL1 pT242 was being generated. This will allow *in vivo* experiments, such as IF, to specifically look at the phosphorylation status of T242 under different conditions and uncover exactly how this phosphorylation is affecting kinetochore protein dynamics. Mutagenesis studies looking at T242 (and T241) revealed that this residue plays a clear role in the regulation of KNL1 localisation. However, although the phospho-mimetic mutation was able to rescue the loss of KNL1 seen in the phospho-null mutation, it was not able to render KNL1 localisation independent of CDK1. An understandable conclusion would be that, in this scenario, the mutation to aspartate is not functioning as a phospho-mimetic. However, non-functional phospho-mimetics tend to function like phospho-null mutations as they can no longer be phosphorylated. This is not the case here; the phospho-mimetic was able to recruit KNL1 at a higher level than the phospho-null, albeit at a marginally lower level than the WT. It is therefore important that confirm this observation using an alternative phospho-mimetic mutation such as glutamic acid in future experiments. The most compelling explanation for this observation is that further CDK1 phosphorylations on NSL1 are required for the interaction with KNL1. Within the KNL1 interaction region of NSL1 there are three more reported phosphorylation sites, albeit non-consensus CDK1 sites. Several of these are clustered around the T242 consensus site:

T237, T241 and T244 (Petrovic et al., 2010; Hornbeck et al., 2015). Hypothetically, several sites within this region of NSL1 may be phosphorylated by CDK1 to create a phosphorylated patch that is recognised by KNL1. Further mutagenesis studies and *in vitro* binding assays will be required to investigate this. Alternatively, phosphorylation at sites outside of the KNL1 interaction region may contribute to the interaction by, for example, altering the structure of NSL1 to allow KNL1 access to bind. A more detailed structural analysis of the KNL1:NSL1 interaction will hopefully shed light on this hypothesis.

Until now, regulation of the KNL1:NSL1 interaction through the phosphorylation of KNL1 has not been considered. However, it is conceivable that KNL1 must also be phosphorylated by CDK1 for the interaction with NSL1 to occur and, therefore, a phospho-mimetic of only the NSL1 phosphorylation site is not sufficient for the interaction to occur without CDK1. KNL1 is a very large protein that is heavily phosphorylated, particularly by MPS1 (Shepperd et al., 2012; London et al., 2012; Yamagishi et al., 2012). It contains 17 potential CDK1 consensus sites, however none of these are found in the region that interacts with NSL1 (KNL1 2106-2316) (Petrovic et al., 2010). Of course, there may be non-consensus CDK1 sites within this region, but these will be much harder to identify. Alternatively, CDK1 phosphorylation of consensus sites outside the NSL1 interaction may be involved by, for example, relieving internal inhibition in KNL1 that blocks the interaction with NSL1.

A detailed understanding of the KNL1:NSL1 interaction is, of course, important to this story. However, to place this mechanism within the wider understanding

of SAC regulation, it was vital to uncover the effects of its loss on SAC functionality, accurate chromosome segregation, and mitotic progression. A dysfunctional SAC results in severe chromosome segregation defects and aneuploidy (Kops et al., 2005; Weaver and Cleveland, 2006; Dobles et al., 2000). Based on the prediction that this regulatory mechanism results in the loss of KNL1 to silence the SAC, an expected phenotype in a phospho-null mutant may have been complete SAC failure. However, the delay in mitotic timing and increased mitotic errors observed in the phospho-null condition is in agreement with data following a partial KNL1 depletion, where cells can only partially align their chromosomes and are delayed in prometaphase with a SAC arrest (Cheeseman and Desai, 2008; Kline et al., 2006; Pagliuca et al., 2009). Interestingly, a complete KNL1 depletion, which is challenging to achieve, does result in a failure of the checkpoint and rapid mitotic progression (Cheeseman and Desai, 2008; Kline et al., 2006; Pagliuca et al., 2009). The absence of this phenotype in the phospho-null mutant supports the IF data showing only a reduction in KNL1 at the kinetochore, not a complete loss. Therefore, although this mutation results in errors in chromosome segregation and is important for an accurate metaphase-to-anaphase transition, it alone does not cause a SAC failure.

Potentially more revealing are the results from the phospho-mimetic cell lines. Although the data revealed that this mimetic is not able to fully rescue the effects of CDK inhibition, a striking phenotype was still observed in live imaging. In particular, a delay was seen in the metaphase-to-anaphase transition and there was an increase in cell death following a metaphase arrest. This phenotype

strongly supports the hypothesis that cell lines with the phospho-mimetic mutation are unable to efficiently remove KNL1 and thus are not able to overcome a checkpoint arrest and enter anaphase. This vital evidence underlines the importance of this mechanism in ensuring efficient SAC silencing and providing directionality to the metaphase-to-anaphase transition through the rapid and timely removal of KNL1. Subsequent experiments investigating the status of the checkpoint in relation to KNL1 localisation in these metaphase arrests will be crucial to confirm this mechanism. Taken together, the live imaging data highlights the combinatorial nature of SAC signalling as well as its high sensitivity and the importance of individual regulatory mechanisms. Loss of one regulatory mechanism alone does not completely disrupt SAC signalling, but continued or inappropriate action of one regulatory mechanism can result in severe mitotic defects and delays.

An interesting outstanding question surrounds the reason for the loss of alignment prior to cell death in the GFP-NSL1 2TD mutants arrested in mitosis. There are two potential explanations from published work. An intriguing hypothesis is “cohesion fatigue” (Daum et al., 2011; Sapkota et al., 2018). This phenomenon involves the release of sister chromatid cohesion and the asynchronous separation of chromatids while the cell remains in mitosis. The mechanism of cohesion loss is not known, but it does not involve the usual mechanism of separase activation due to its continued inhibition. A simple test for this hypothesis would be to observe the presence/absence of cohesin or sister chromatid pairs in cells that have lost alignment but not yet undergone cell death. Alternatively, the loss of alignment could be due to a loss of microtubule

attachment to one sister chromatid because of error correction action at the prolonged metaphase plate. Indeed, recent evidence suggests that error correction can occur at attachments under tension and that monopolar attachments are selectively stabilised (Chen et al., 2021). This means that error correction can result in the loss of one sister chromatid attachment but not both in a prolonged metaphase plate arrest. Subsequently, this would result in the metaphase plate falling apart as pairs of chromatids are pulled to different poles. This could be confirmed by detecting the presence of attachments in this scenario and the number of attachments to each chromatid pair. Discovering the exact nature of this loss of alignment will be illuminating for both this novel level of SAC regulation but also a wider understanding of error correction and the response of cells to prolonged metaphase arrests. Importantly, however, both scenarios highlight the key phenotype of the phospho-mimetic cells: an inability to progress from metaphase to anaphase.

Chapter 4: Identifying differential phosphatase regulation of outer-kinetochore protein localisation

4.1 Identifying the phosphatases opposing outer-kinetochore assembly in mitosis

This thesis has, so far, only considered the generation of phosphorylations by CDK1. However, a key outstanding question from Chapter 3 is how KNL1 is lost from kinetochores earlier than other outer-kinetochore proteins. The answer to this question will provide key information as to how this process contributes to the regulation of the SAC. Therefore, attention must now turn to the phosphatases that oppose CDK1 at mitotic exit: PP1 and PP2A-B55. Previous work has shown that PP2A-B55 opposes CDK1 regulation of the NDC80-C at the kinetochore and suggests differential phosphatase regulation of outer-kinetochore components (Gascoigne and Cheeseman, 2013). However, data looking at the phosphatases opposing localisation of all KMN components, particularly KNL1, is lacking. It was therefore essential to conclusively identify the phosphatases opposing each outer-kinetochore component, and the timings with which this occurs.

Identification of the phosphatases opposing outer-kinetochore assembly relied on the ability to specifically deplete PP1 and PP2A-B55. RNAi was selected as the technique to deplete the phosphatases. Two 3'UTR oligos against the key mitotic isoforms of PP1, PPP1CA and PPP1CC (Bancroft et al., 2020), and a

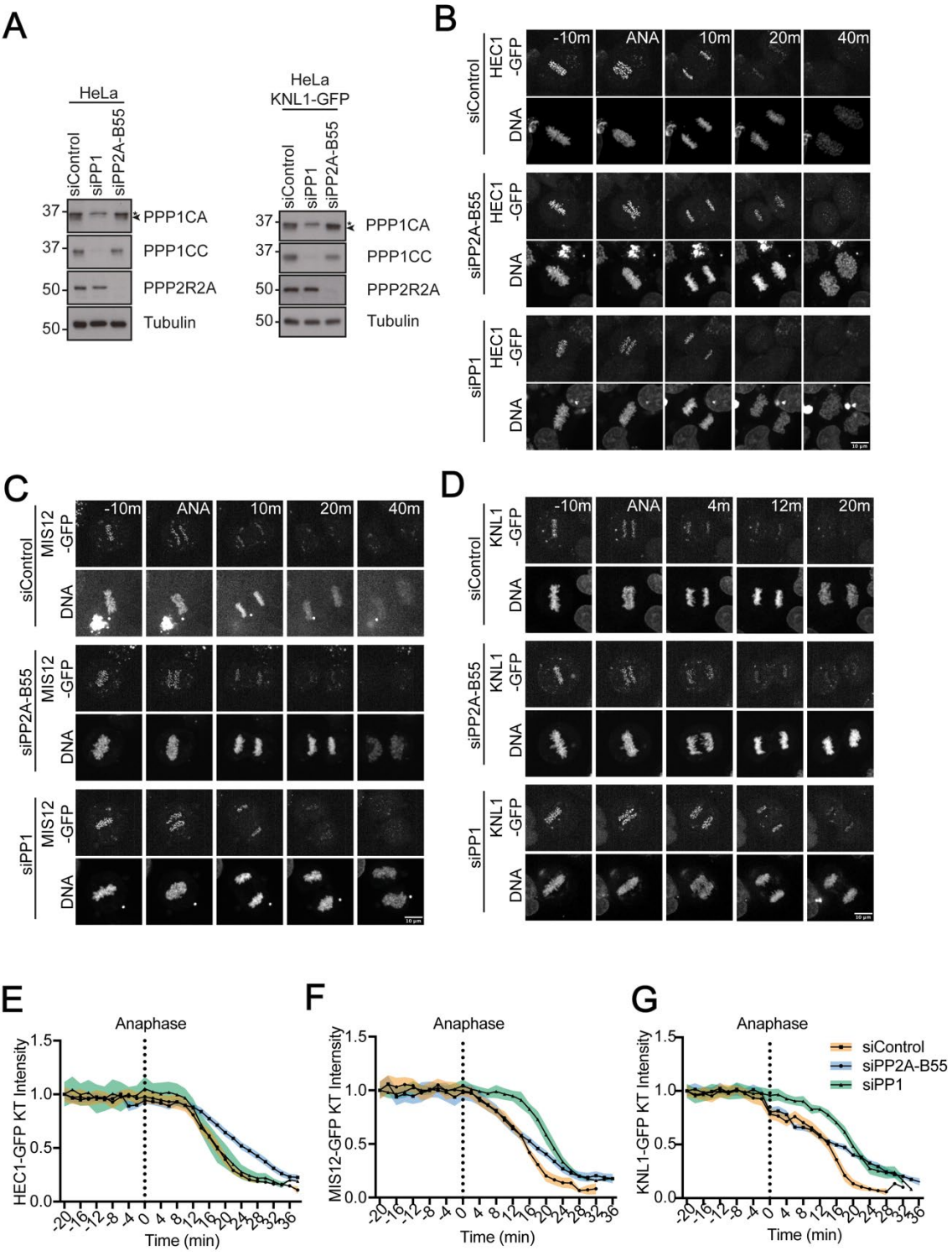


Figure 4.1 Identifying the phosphatases opposing outer-kinetochore assembly in mitosis

(A) Western blot showing depletion of PPP1CA and PPP1CC (siPP1) or PPP2R2A, PPP2R2B, PPP2R2C and PPP2R2D (siPP2A-B55) following a 72 h RNAi in HeLa cells or HeLa cells expressing KNL1-GFP. GL2 was used as a control RNAi. * indicates non-specific bands. Arrow indicates PPP1CA. (B)-(D) Movie stills of HeLa

cells expressing (B) HEC1-GFP, (C) MIS12-GFP or (D) KNL1-GFP and incubated with 100 nM SiR-DNA. Cells were depleted of PP1, PP2A-B55 or a control siRNA as indicated for 72 h then synchronised for 18 h using 2 mM thymidine. Cells were imaged 9 h after thymidine release. (E)-(G) Graphs show mean kinetochore intensities of (E) HEC1-GFP, (F) MIS12-GFP or (G) KNL1-GFP at 2 min intervals as a fraction of the maximum intensity. Shaded regions indicate the SEM (≥ 7 cells per condition from 2 independent experiments).

SmartPool against all PP2A-B55 regulatory subunits (Hayward et al., 2019a) were used. Cells were treated with the siRNA oligos for 72 h and successful depletion in HeLa and HeLa KNL1-GFP cell lines was confirmed by western blotting (Figure 4.1A). It should be noted that due to the length of RNAi required for efficient depletion, off-target effects or effects at other cell cycle stages may occur and this should be taken into consideration when interpreting results.

High-resolution live cell imaging was carried out using endogenously tagged outer-kinetochore protein cell lines where either PP2A-B55 or PP1 (or a control siRNA) was depleted from cells prior to imaging. Cells were imaged as they exited mitosis, and the kinetochore intensity of the tagged outer-kinetochore protein was quantified (Figure 4.1B-G). Depletion of PP2A-B55 resulted in a significant delay in the loss of HEC1-GFP from kinetochores compared to the control depletion. The same delay was not seen following a PP1 depletion (Figure 4.1B, E). This confirmed the previous report that the NDC80-C localisation at the kinetochore is opposed by PP2A-B55 (Gascoigne and Cheeseman, 2013). Contrastingly, live imaging of the MIS12-GFP cell lines revealed a significant delay in the loss of MIS12 at the kinetochore following depletion of PP1 (Figure 4.1C, F). Intriguingly, following depletion of PP2A-B55, MIS12 loss from

kinetochore was not initially affected but a slight delay was observed in late anaphase when compared to the control condition (Figure 4.1C, F). From this, it could be inferred that the main method, or at least initial method, of MIS12 loss is via PP1. However, following activation of PP2A-B55 later in anaphase, both phosphatases provide a concerted effort to disassemble the entire outer-kinetochore. Finally, live imaging of KNL1-GFP cells revealed a delay in the loss of KNL1 from kinetochores following PP1 depletion (Figure 4.1D, G). However, the effect occurred earlier in mitosis than for MIS12, matching the timings of outer-kinetochore loss observed in Chapter 3. As seen with MIS12, following depletion of PP2A-B55, a slight delay in KNL1 loss was observed in late anaphase as compared to the control condition (Figure 4.1D, G). The data indicate that at least a significant pool of KNL1 is rapidly lost from the kinetochore following chromosome alignment by the action of PP1, while the remainder of KNL1 is lost later in anaphase by the concerted action of PP1 and PP2A-B55.

4.2 Restoring checkpoint signalling through specific phosphatase depletion

The live imaging data above does not conclusively show that it is CDK1 phosphorylations that are being opposed by PP1 and PP2A-B55. To understand the implications on checkpoint regulation, it is crucial to confirm that PP1 is opposing CDK1 to result in the loss of KNL1 at the kinetochore, thus connecting this data on the opposing phosphatases to the previous results regarding CDK1 phosphorylation of NSL1. Therefore, the “checkpoint reactivation assay” was carried out on HeLa KNL1-GFP cells where either PP1 or PP2A-B55 was depleted and CDK1 was inhibited. As before, cells were fixed and stained for imaging, and the localisation of KNL1 at the kinetochore was quantified (Figure

4.2A-B). As observed previously, KNL1 localisation at the kinetochore was reduced following CDK inhibition. However, this loss was rescued by depletion of PP1; even when CDK1 was inhibited, KNL1 was correctly localised to the kinetochore if PP1 was depleted (Figure 4.2A-B). Indeed, depletion of PP1 actually appeared to result in an increase in the levels of KNL1 at the kinetochore. Therefore, PP1 is specifically opposing CDK1 regulation of KNL1 localisation. A partial rescue of KNL1 kinetochore levels was observed following a PP2A-B55 depletion, but not to the same extent as a PP1 depletion (Figure 4.2A-B). This confirms the observations seen in Figure 4.1G that PP1 appears to be the main phosphatase opposing KNL1 localisation but PP2A-B55 may contribute to its complete loss at mitotic exit.

As PP1 depletion was able to rescue the loss of KNL1 at the kinetochore following CDK inhibition, the effect of PP1 depletion on the ability of cells to generate a checkpoint signal following CDK inhibition was investigated using the "checkpoint reactivation assay". Flp-In T-REx GFP-MIS12-MPS1 cell lines were specifically depleted of either PP1 or PP2A-B55 and CDK1 was inhibited. As before, cells were fixed and stained for imaging, and the localisation of BUB1 at the kinetochore was quantified (Figure 4.2C-D). As observed previously, BUB1 localisation at the kinetochore was reduced following CDK inhibition, even though MPS1 was correctly localised. However, this loss was rescued by the depletion of PP1 (Figure 4.2C-D). Therefore, even though CDK1 was inhibited, cells were able to recruit BUB1 and generate a checkpoint signal. The same rescue was not observed following a PP2A-B55 depletion (Figure 4.2C-D). Now that a checkpoint signal can be generated in the presence of a CDKi, it can be concluded that the

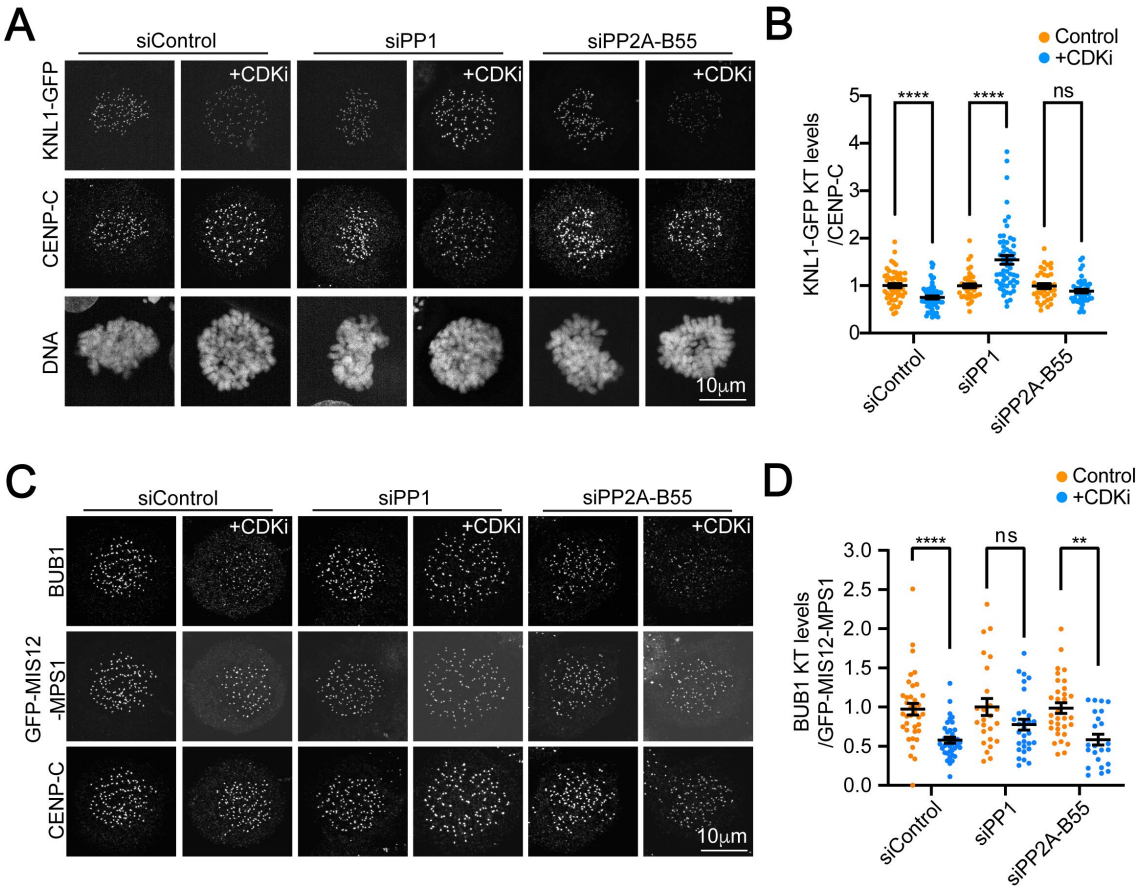


Figure 4.2 Depletion of PP1 restores checkpoint signalling in the absence of CDK1

(A) HeLa cells expressing KNL1-GFP cells were depleted of PP1, PP2A-B55 or a control siRNA as indicated. After 72 h cells were arrested for 2.5 h with 20 μM MG132, then treated with 3 μM nocodazole for the final 5 min, fixed with PTEMF, and immunostained as indicated. If CDK1 was inhibited, 5 μM flavopiridol was added 1 min before nocodazole treatment (+CDKi). (B) Graph shows mean levels of KNL1-GFP at kinetochores relative to CENP-C levels. Bars indicate the SEM (each point represents a single cell average intensity of 20 kinetochores, ≥ 36 cells per condition in 3 independent experiments). (C) HeLa Flp-In/T-REx GFP-MIS12-MPS1 cells were depleted of PP1, PP2A-B55 or a control siRNA as indicated. After 24 h cells were depleted of endogenous MPS1. GFP-MIS12-MPS1 transgene was induced by addition of doxycycline. After a further 48 h, cells were arrested for 2.5 h with 20 μM MG132, then treated with 3 μM nocodazole for the final 5 min, fixed with PTEMF, and immunostained as indicated. If CDK1 was inhibited, 5 μM flavopiridol was added 1 min before nocodazole treatment (+CDKi). (B) Graph shows mean levels of BUB1 at kinetochores relative to GFP-MIS12-MPS1 levels. Bars indicate the SEM (each point

represents a single cell average intensity of 20 kinetochores, ≥ 23 cells per condition in 3 independent experiments).

key upstream CDK1 regulatory elements of checkpoint signalling (up to BUB1 recruitment) have been identified and overcome. Indeed, this highlights the critical role of regulating KNL1 localisation alongside regulating MPS1 localisation for control of SAC signalling initiation and the metaphase-to-anaphase transition.

4.3 Discussion

Critical to mitotic exit is the removal of mitotic phosphorylations by phosphoprotein phosphatases. PP1 and PP2A-B55 specifically are the main phosphatases opposing CDK1 at mitotic exit. Research here confirmed and further uncovered the differential phosphatase regulation of outer-kinetochore components (Gascoigne and Cheeseman, 2013).

Combining this data with that from Chapters 2-3, the following model for a novel mechanism of checkpoint regulation and silencing is proposed (Figure 4.3). Specific phosphatase-mediated disassembly of the outer-kinetochore supports complete checkpoint shutdown through the rapid loss of KNL1 following chromosome alignment, while leaving microtubule-kinetochore attachments intact until later in anaphase through the retention of the NDC80-C. This critically depends on the different timings of CDK1 phosphorylation removal by different phosphatases at the metaphase-to-anaphase transition (Figure 4.3, panels 2-3). This is possible due to the difference in inhibition mechanisms of PP1 and PP2A-B55 by CDK1, resulting in differential activation of the phosphatases. As PP2A-

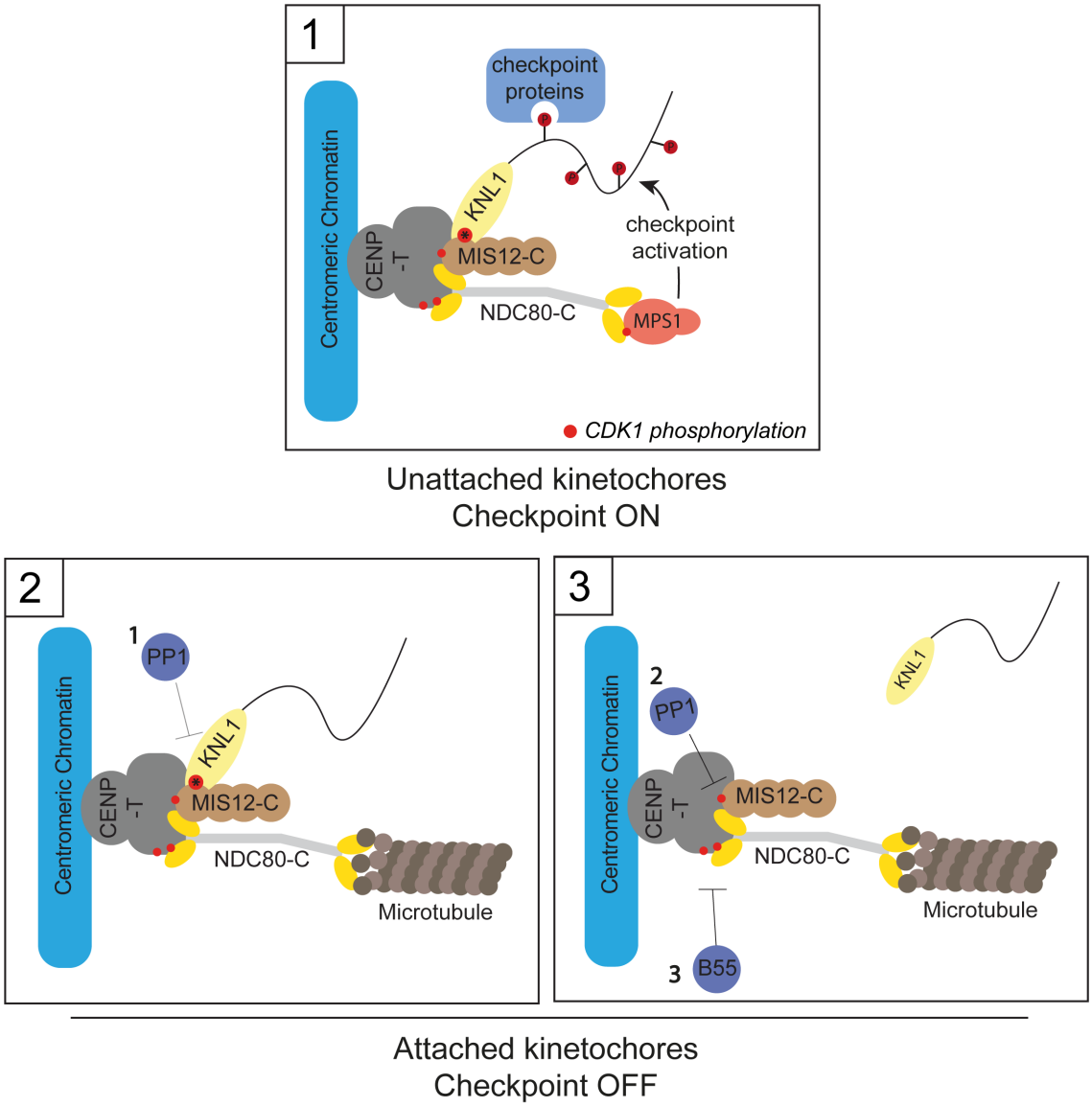


Figure 4.3 A novel mechanism of Spindle Assembly Checkpoint regulation

Schematic of a novel mechanism of Spindle Assembly Checkpoint regulation. Panel 1, unattached kinetochore (prometaphase): KMN network is assembled at the kinetochore through CDK1 phosphorylations on CENP-T and NSL1. MPS1 is recruited to the kinetochore and the SAC is active. Phosphatases opposing CDK1 are inhibited. Panel 2, attached kinetochore (metaphase/early anaphase): following SAC satisfaction, CDK1 levels decrease, chromosome segregation begins and PP1 rapidly becomes active. PP2A-B55 is still inhibited. PP1 removes CDK1 phosphorylation on NSL1 to remove KNL1 from the kinetochore. This prevents SAC reactivation. The rest of the KMN network remains at the kinetochore, maintaining microtubule attachments via the NDC80-C. Panel 3, attached kinetochore (late anaphase): PP1 and PP2A-

B55 are active and remove CDK1 phosphorylations on CENP-T. The whole KMN network disassembles before cytokinesis.

B55 is indirectly inhibited by CDK1 via the Greatwall pathway, there is a delay in its activation following the decrease in CDK1 activity (Blake-Hodek et al., 2012; Gharbi-Ayachi et al., 2010; Mochida et al., 2010; Williams et al., 2014; Castro and Lorca, 2018). Contrastingly, PP1 is directly inhibited by CDK1 (Dohadwala et al., 1994; Yamano et al., 1994). Therefore, at the metaphase-to-anaphase transition, PP1 becomes active before PP2A-B55 does (Figure 4.3, panel 2). This work has identified a hitherto unrecognised level of CDK1 regulation between KNL1 and NSL1 which regulates KNL1 localisation independently to the rest of the outer-kinetochore (Figure 4.3, panel 1). Upon chromosome alignment, this CDK1 phosphorylation is rapidly lost due to the rapid activation of PP1 (Figure 4.3, panel 2). This results in the loss of KNL1 from the kinetochore and so prevents the reactivation of the checkpoint following the initiation of chromosome segregation. In contrast, the NDC80-C and the MIS12-C remain at the kinetochore through CDK1 phosphorylations on CENP-T that are dephosphorylated more slowly (Figure 4.3, panel 2). This ensures cells sufficiently segregate sister chromatids before releasing the kinetochore-microtubule interactions, therefore reducing the risk of chromatids remaining in the region of the midbody where cytokinesis will occur. Eventually, the entire outer-kinetochore is lost late in anaphase following PP2A-B55 activation by the combined effort of PP1 and PP2A-B55 (Figure 4.3, panel 3). This level of regulation ensures faithful chromosome segregation in mitosis and the directionality of the metaphase-to-anaphase transition.

The rapid activation of PP1 following chromosome alignment is a critical element of this new model. Current understanding of PP1 regulation would suggest that, after the decrease in CDK1 activity following chromosome segregation, the kinase/phosphatase balance is tipped to favour PP1 auto-dephosphorylation and therefore activation (Dohadwala et al., 1994; Yamano et al., 1994; Wu et al., 2009). However, KNL1 loss begins very rapidly following chromosome alignment, indeed several minutes before anaphase onset. One explanation for this is through the auto-activation of PP1 (Dohadwala et al., 1994; Wu et al., 2009; Yamano et al., 1994). It is conceivable that the clustering of PP1 at sites such as the kinetochore may allow PP1 to become active through auto-dephosphorylation prior to CDK1 levels decreasing. However, this has not been proven experimentally and presents the question as to what would regulate the clustering of PP1 at the kinetochore to ensure that PP1 only becomes active and removes KNL1 following chromosome alignment. The regulation of the localisation and activity of PP1 is very poorly understood in mammalian cells. Previous research has presented Aurora B as a candidate for regulating PP1 kinetochore localisation via PIP phosphorylation (Liu et al., 2010; Welburn et al., 2010; Nasa et al., 2019). Aurora B phosphorylation of PIPs at the kinetochore in response to attachment and tension status may restrict PP1 recruitment to prior to microtubule attachment. The subsequent chapter of this thesis will begin to tackle some of the unanswered questions around PP1 to shed light on this. In particular, the role of Aurora B in PP1 kinetochore recruitment will be investigated in Chapter 5.2.

An outstanding question of this model is the difference in timing of MIS12 and KNL1 kinetochore loss even though they are both opposed by PP1. Given the early activation of PP1, it would be expected that MIS12 would be lost as rapidly as KNL1. However, this is not the case. The data, instead, point towards PP1 removing the CDK1 phosphorylation on NSL1 before that on CENP-T, and therefore removing KNL1 before MIS12. Two hypotheses stand to explain why this may occur. First, steric hindrance simply prevents PP1 from accessing the site on CENP-T until KNL1 is lost from the kinetochore. In-depth structural data of the outer-kinetochore will be required to understand the exact sterics of the different proteins. Second, phosphatases have been reported to show preferences or biases for particular phosphorylation sites and sequences (Cundell et al., 2016; Bouchoux and Uhlmann, 2011; Holder et al., 2020). In particular this has been demonstrated for PP2A-B55, which shows a preference for threonine residues over serine residues (Cundell et al., 2016; Bouchoux and Uhlmann, 2011). PP1 has also been reported to show a preference for threonine over serine, as well as showing a preference for the exclusion of acidic amino acids immediately downstream of the phosphorylation site (Holder et al., 2020). This absence of acidic amino acids downstream of the phosphorylation is particularly seen in PP1 sites with a short phosphorylation half-life (Holder et al., 2020). Interestingly, the CDK1 site on CENP-T (T195) is followed by a number of glutamic acid residues, whereas the CDK1 site on NSL1 (T242) only contains a single acidic amino acid in the subsequent sequence. Therefore, the threonine on NSL1 may be favoured by PP1 over the threonine on CENP-T and therefore be dephosphorylated earlier.

An unexpected observation was the apparent joint role of the phosphatases in complete outer-kinetochore disassembly during late anaphase. Both KNL1 and MIS12, whose localisations are opposed by PP1, also appear to be opposed by PP2A-B55 during late anaphase. This would indicate that the main method or initial method of MIS12 and KNL1 loss is via PP1. However, once PP2A-B55 becomes active later in anaphase, both phosphatases provide a concerted effort to disassemble the entire outer-kinetochore. Indeed, previous studies have shown that the difference in function between the two phosphatase families is less about specificity to certain phosphorylation sites and more to do with phospho-regulation of activity and localisation (Smith et al., 2019). Therefore, once both phosphatases are active and correctly localised at the kinetochore, they are able to dephosphorylate all remaining CDK1 phosphorylation sites. This ensures complete and efficient outer-kinetochore disassembly before cytokinesis. This places greater importance on the regulation of the activity and localisation of phosphatases, particularly that of PP1, for ensuring the initial, specific loss of only KNL1 from kinetochores.

An alternative explanation for this observation is that different phosphatases act on the different pathways of outer-kinetochore assembly; CENP-T and CENP-C pathways (Rago et al., 2015). Due to the nature of the live imaging experiments, it was not possible to differentiate between the two pathways. Therefore, PP1 may be opposing the CDK1-regulated pathway of outer-kinetochore assembly for MIS12 and KNL1 while PP2A-B55 is opposing the Aurora B-regulated pathway. Further research should therefore focus on replicating these experiments in an

environment where one pathway of outer-kinetochore assembly can be observed in isolation.

Looking beyond these experiments, future research now needs to define the interplay between the two critical upstream regulatory roles of CDK1 in the SAC: regulation of outer-kinetochore assembly and regulation of MPS1 localisation (Hayward et al., 2019a). Based on the data in this thesis, the previous understanding of an MPS1/PP2A-B55-defined checkpoint permissive period is insufficient. Therefore, it is important to understand the relative importance and timings these two mechanisms make to defining the checkpoint permissive period. The localisation of MPS1 at the kinetochore is opposed by the phosphatase PP2A-B55 (Hayward et al., 2019a) and therefore, removal of this phosphorylation would be expected to occur later than the removal of KNL1 from the kinetochore (a PP1 site). MPS1 localisation at the kinetochore and particularly its response to kinetochore attachment status is a topic of much research and debate (Hiruma et al., 2015; Ji et al., 2015; Hayward et al., 2022, 2019a). However, phosphatase timing data would predict that removal of KNL1 precedes the termination of SAC permissive period as defined by the S281 phosphorylation state (Hayward et al., 2019a). Therefore, the initial rapid loss of KNL1 from kinetochores may provide an initial mechanism for preventing checkpoint re-activation following chromosome alignment and shortly after this, the SAC permissive period is formally terminated by the dephosphorylation of MPS1. Understanding the exact timings and contributions these two mechanisms of directionality make to defining the checkpoint signalling period and their relative importance for accurate chromosome segregation will prove challenging

to answer but are critical for understanding the overarching roles of CDK1 in the SAC and how this ensures accurate chromosome segregation.

Chapter 5: Further investigating the key role of PP1 in the metaphase-to-anaphase transition

5.1 Investigating the localisation of endogenous PP1 isoforms

Kinetochore-associated PP1 is a key candidate phosphatase at the metaphase-to-anaphase transition because of its critical role in yeast SAC silencing and progression to anaphase (Pinsky et al., 2009; Meadows et al., 2011; Vanoosthuyse and Hardwick, 2009; Nijenhuis et al., 2014). However, the specifics of PP1 action in mammalian cells are poorly understood. This is due, in part, to a lack of tools to accurately observe and manipulate PP1 in mammalian cells. Therefore, it is essential to develop such reagents to allow investigation into PP1 to progress.

Understanding of PP1 localisation has been limited to its observation in overexpression cell lines, which, although valuable, do not always accurately represent the endogenous protein (Trinkle-Mulcahy et al., 2003, 2006). To observe the endogenous localisation of the key mitotic PP1 isoforms (PPP1CC and PPP1CA), a CRISPR/Cas9 knock-in system was employed to generate cell lines with PPP1CA and PPP1CC tagged with a GFP tag at the C-terminus attached via a 12 amino acid linker (Figure 5.1A). Initial generation of tagged PP1 isoforms was carried out in HeLa cells. PCR screening and western blot analysis confirmed successful generation of homozygous clones of both PP1 isoforms (Figure 5.1B-C). For each cell line, multiple homozygous clones were successfully generated and characterised before selecting one for in-depth

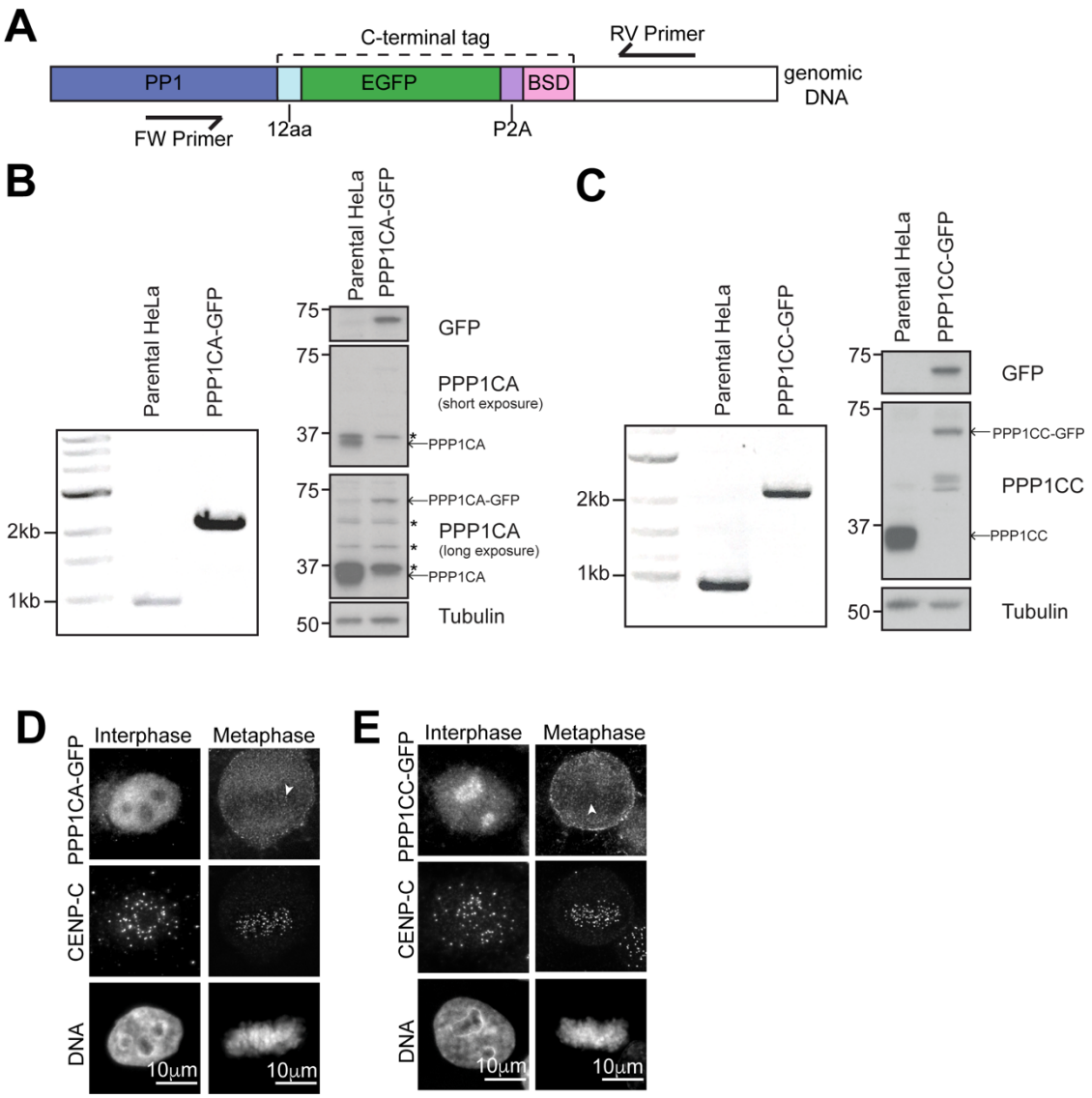


Figure 5.1 Visualising endogenous PP1 in HeLa cells using CRISPR/Cas9 fluorescent tagging

(A) Schematic of tag inserted at the C-terminus of PP1 and primers used for CRISPR/Cas9 PCR screening. Primers flanking the target locus amplified genomic DNA from clones. BSD indicates blasticidin resistance gene. (B)-(C) PCR and western blot screen confirms HeLa homozygous clones of (B) PPP1CA-GFP and (C) PPP1CC-GFP. Note, the anti-PPP1CA antibody does not efficiently detect the C-terminal GFP-fusion. * indicates non-specific bands. (D)-(E) Asynchronous populations of (D) PPP1CA-GFP and (E) PPP1CC-GFP HeLa cells were fixed with PTEMF and immunostained as indicated. Arrows indicate kinetochore-localised PP1-GFP.

analysis. IF revealed the targeting of PP1 isoforms to specific sites throughout

the cell cycle including specific nuclear structures and the cell cortex (Figure 5.1D-E). In confirmation of overexpression data, in interphase, PPP1CC-GFP accumulated within the nucleolus (Figure 5.1E) but PPP1CA-GFP was excluded from the nucleolus (Figure 5.1D). Upon initial observation, metaphase localisation of both isoforms was undefined but increased magnification and image deconvolution confirmed cortical localisation and weak kinetochore localisation of both isoforms (Figure 5.1D-E). Importantly, HeLa cells are aneuploid and have an extra copy of each PP1 isoform. Consequently, excess cytoplasmic PP1-GFP may be masking kinetochore-localised PP1-GFP, preventing successful visualisation. Therefore, CRISPR/Cas9 tagging of PP1 isoforms was repeated in HCT116 cells, a diploid human colorectal carcinoma cell line. As before, PCR screening and western blot analysis confirmed successful generation of homozygous clones of both isoforms (Figure 5.2A-B). Multiple homozygous clones were successfully generated and characterised before selecting one for in-depth analysis. IF revealed that interphase localisations were in agreement with previous cell lines and published data (Figure 5.2C-D). Metaphase localisation similarly showed cortical and kinetochore localisation for both isoforms. However, kinetochore localisation, although brighter than in HeLa cells, was still weak when compared to published overexpression cell lines (Figure 5.2C-D).

The low kinetochore PP1-GFP signal may be indicative of naturally low levels of endogenous PP1 found at the kinetochore. This discrepancy to cells with overexpressed PP1 highlights the importance of using endogenously tagged PP1. Therefore, to effectively visualise endogenous PP1 for further studies,

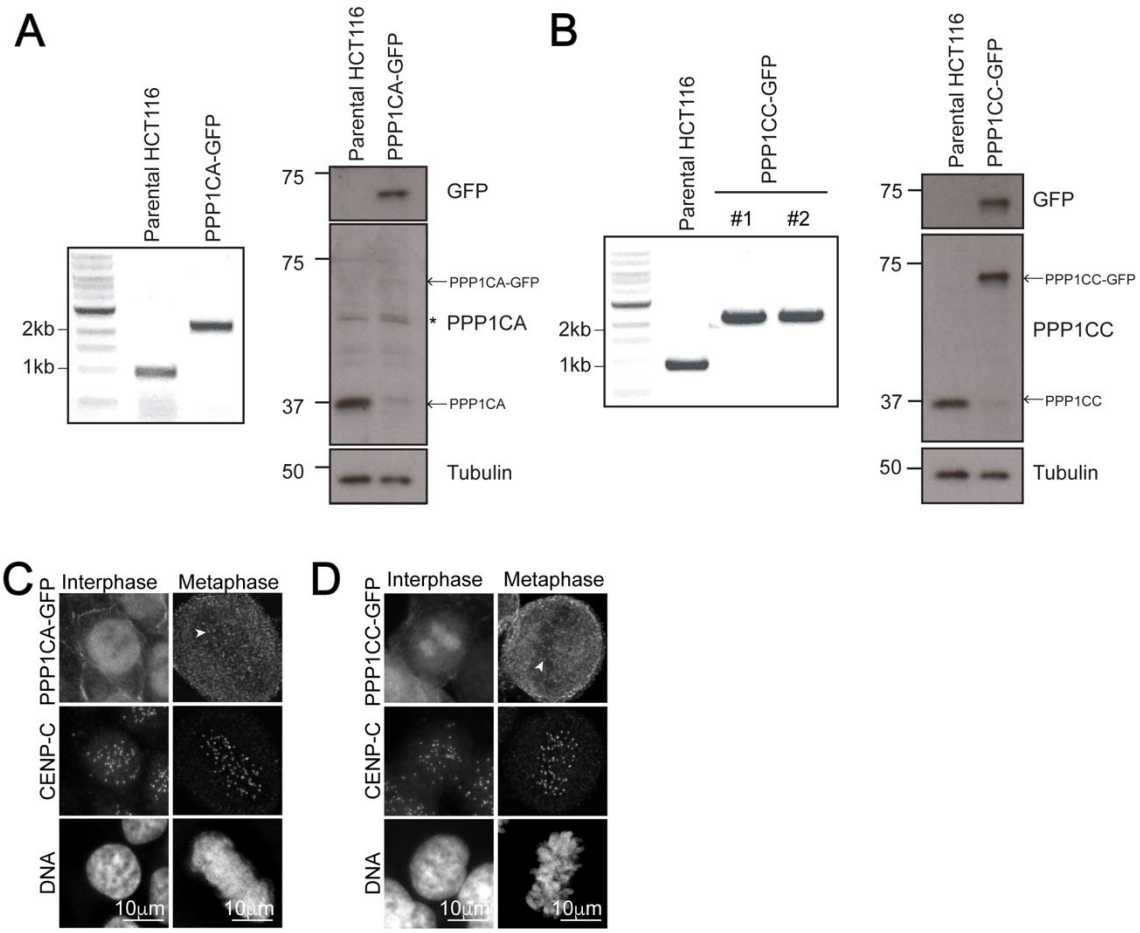


Figure 5.2 Visualising endogenous PP1 in HCT116 cells using CRISPR/Cas9 fluorescent tagging

(A)-(B) PCR and western blot screen confirms HCT116 homozygous clones of (A) PPP1CA-GFP and (B) PPP1CC-GFP. Note, the anti-PPP1CA antibody does not efficiently detect the C-terminal GFP-fusion. * indicates non-specific bands. (C)-(D) Asynchronous populations of (C) PPP1CA-GFP and (D) PPP1CC-GFP HCT116 cells were fixed with PTEMF and immunostained as indicated. Arrows indicate kinetochore-localised PP1-GFP.

optimisation of imaging methods for both HeLa and HCT116 cell lines was carried out. Initially, the super-resolution functionality of a SoRa spinning disc confocal microscope was employed to enhance resolution of fine structures such as kinetochores. In fixed HeLa and HCT116 cells, this resulted in a minor improvement in PPP1CC-GFP kinetochore signal (Figure 5.3A). However, kinetochore resolution was still insufficient for further investigation. During cell

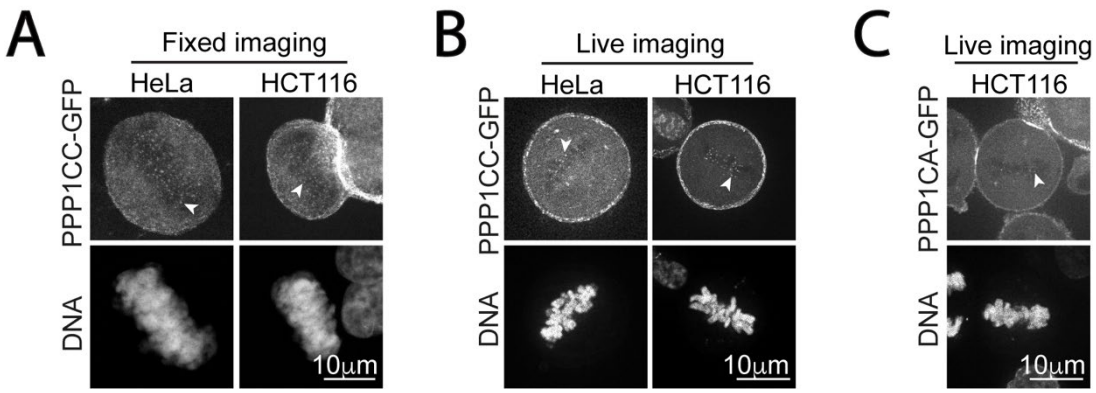


Figure 5.3 Optimising imaging methodology for visualising endogenous PP1-GFP

(A) Asynchronous populations of PPP1CC-GFP HeLa or HCT116 cells were fixed with PTEMF and immunostained as indicated. Arrows indicate kinetochore-localised PPP1CC-GFP. (B) Asynchronous populations of PPP1CC-GFP HeLa or HCT116 cells were imaged without fixation following incubation with 100 nM SiR-DNA. Arrows indicate kinetochore-localised PPP1CC-GFP. (C) Asynchronous population of PPP1CA-GFP HCT116 cells were imaged without fixation following incubation with 100 nM SiR-DNA. Arrow indicates kinetochore-localised PPP1CA-GFP.

fixation and slide mounting, cells are flattened onto coverslips. This may result in an intensification of the cytoplasmic PP1 signal over kinetochore signals, particularly in rounded mitotic cells. To overcome this issue, PPP1CC-GFP in HeLa and HCT116 cells was imaged without fixation on a SoRa spinning disc confocal microscope using the super-resolution functionality (Figure 5.3B). This resulted in a significant improvement in visualisation of specific PP1 localisation. In this live imaging protocol, cortical localisation of PPP1CC-GFP in metaphase was very pronounced and clear kinetochore localisation was observed (Figure 5.3B). In HeLa cells, cytoplasmic PPP1CC-GFP was still relatively high, clearly highlighting the issue of additional copies of PP1 causing excess cytoplasmic PP1-GFP (Figure 5.3B). However, for the HCT116 cell lines, a level of resolution was achieved that could be used for subsequent investigation of kinetochore-

localised PP1. Using this established live imaging protocol, PPP1CA-GFP HCT116 cells were imaged (Figure 5.3C). Comparing the metaphase localisations of the two PP1 isoforms in HCT116 cells, both PPP1CC and PPP1CA localised to the cortex of the cell (Figure 5.3B-C). As previously published (Trinkle-Mulcahy et al., 2003, 2006) and observed at lower resolution, both isoforms localised to the kinetochore during metaphase. However, PPP1CC localised to the kinetochore at a much higher level than PPP1CA (Figure 5.3B-C). This may be indicative of a difference in function at the kinetochore.

Before progressing to functional experiments, live cell imaging was carried out to ensure that the addition of a GFP tag on PP1 had no effect on its function during mitosis. The PP1-GFP HCT116 cell lines were imaged on an EVOS M7000 imaging system and the time from NEBD to anaphase was measured in comparison to HCT116 parental cells (Figure 5.4A). There was no significant difference in mitotic timing and no observable increase in mitotic errors in these cell lines. Overall, it was concluded that the addition of a GFP tag did not affect PP1 functionality.

To progress the current understanding of PP1, it was critical to observe where the different PP1 isoforms are localised throughout the cell cycle and specifically the different stages of mitosis. Therefore, high-resolution live cell imaging was carried out using PPP1CA-GFP and PPP1CC-GFP in the HCT116 background and the localisation of PP1 was observed (Figure 5.4B-C). As super-resolution imaging could not be used for long-term time course imaging, live imaging to observe fine structures such as kinetochores was not possible. However, high-

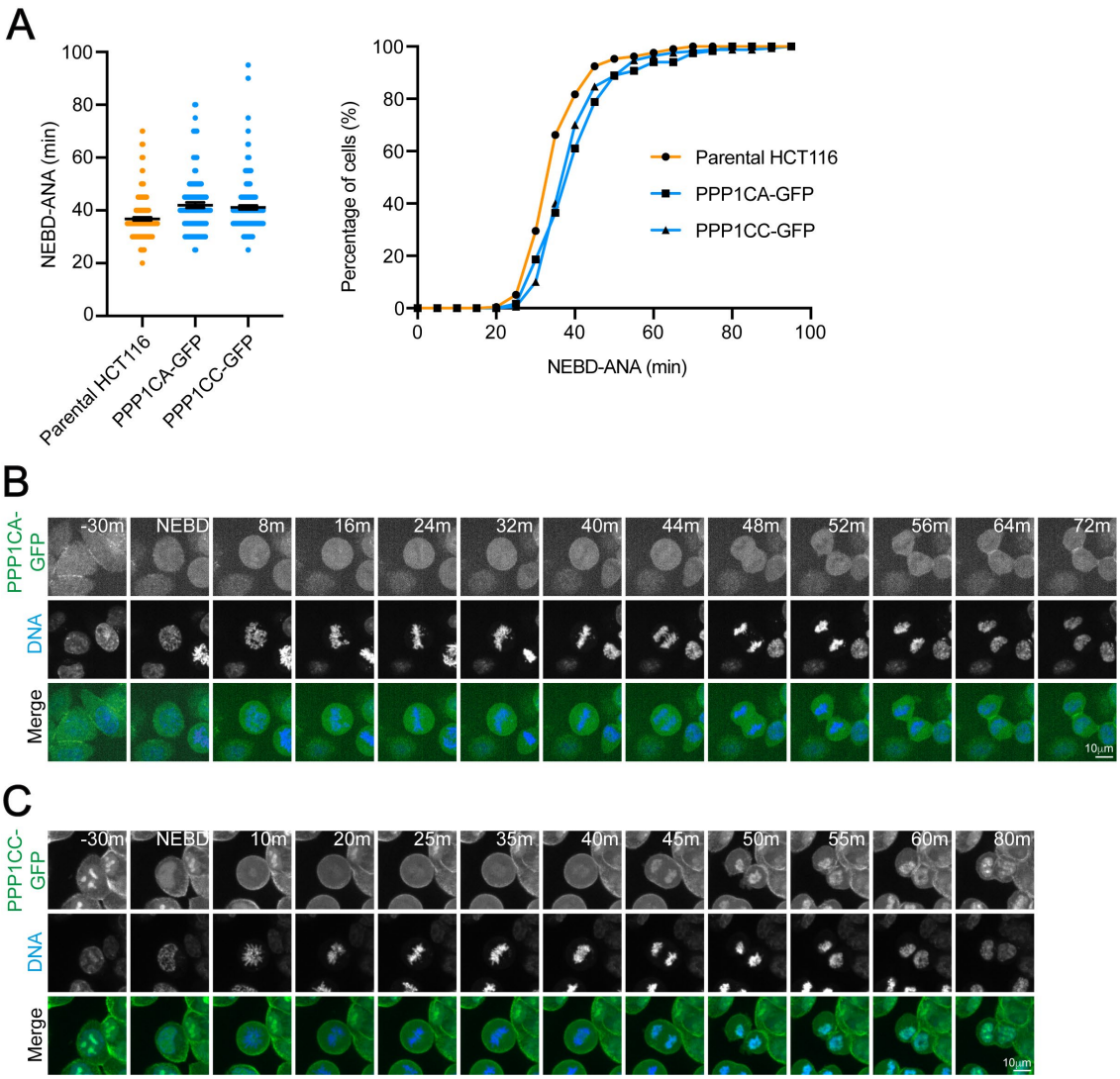


Figure 5.4 PPP1CA and PPP1CC show distinct cellular localisations through mitosis

(A) Bar graph and cumulative frequency graph show mean time from NEBD to anaphase (ANA) (min) in PPP1CA-GFP and PPP1CC-GFP HCT116 cells compared to parental HCT116 cells. Bars indicate SEM (≥ 118 cells per condition, from 3 independent experiments). (B) Movie stills of HCT116 cells expressing PPP1CA-GFP and incubated with 100 nM SiR-DNA. (C) Movie stills of HCT116 cells expressing PPP1CC-GFP and incubated with 100 nM SiR-DNA.

resolution timing data was obtained showing the trend of PP1 isoforms through the cell cycle. As observed in previous imaging, PPP1CA-GFP (Figure 5.4B) was diffuse within the nucleus during interphase, although excluded from the nucleolus. During mitosis, it faintly localised to the cell cortex but kinetochore

localisation could not be seen at this resolution. Upon anaphase onset, PPP1CA-GFP was clearly excluded from the chromatin. Finally, it appeared to return to the cell cortex and to a diffuse nuclear localisation following cytokinesis. For PPP1CC-GFP (Figure 5.4C), during interphase, a strong nucleolus localisation was observed which was dispersed at NEBD. During mitosis, clear cortical localisation was observed as well as a faint kinetochore localisation during prometaphase/metaphase. Upon anaphase onset, PPP1CC-GFP dramatically re-localised to the chromatin where it remained until cytokinesis. Following cytokinesis and nuclear envelope reformation, PPP1CC-GFP returned to its localisation predominantly within the nucleolus. The isoform-specific localisations observed, particularly during interphase and anaphase, provide evidence for distinct roles of PPP1CA and PPP1CC. However, the isoforms localised similarly during early mitosis, raising the question of if and how they carry out distinct functions during the SAC and metaphase-to-anaphase transition.

5.2 Exploring regulation of PP1 localisation

PP1 (and specifically PPP1CC) kinetochore localisation in prometaphase is reportedly opposed by Aurora B phosphorylation of the PP1 binding motif, RVSF, in KNL1 (Welburn et al., 2010; Liu et al., 2010). To investigate this using endogenously tagged cell lines, PPP1CC-GFP HCT116 cells were arrested in a prometaphase state using the microtubule depolymerising drug nocodazole. Under these conditions, the SAC was active and PPP1CC kinetochore localisation was low. The proteasome inhibitor MG132 was added to prevent mitotic exit, before an Aurora B inhibitor was added for 10 min (Figure 5.5A). Cells were imaged using the previously optimised super-resolution live imaging

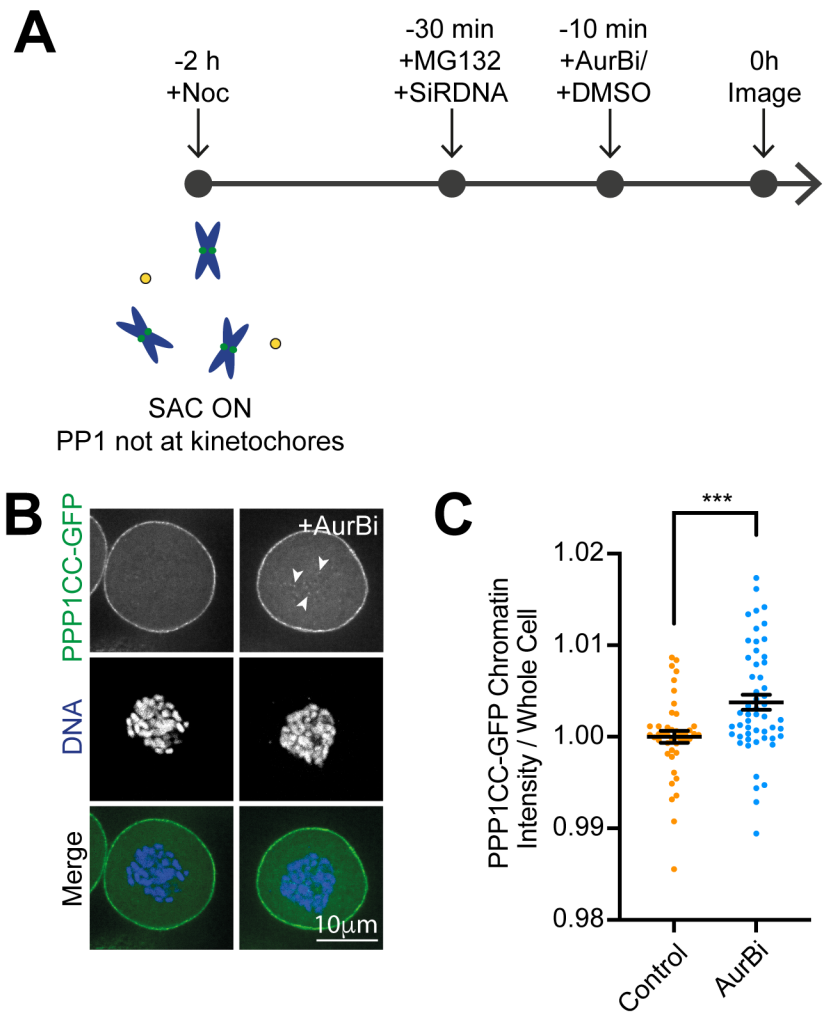


Figure 5.5 Aurora B negatively regulates PPP1CC kinetochore localisation

(A) Schematic of the Aurora B inhibition assay. (B) HCT116 cells expressing PPP1CC-GFP were arrested for 2 h with 0.3 µM nocodazole, and treated with 20 µM MG132 for the final 30 min, incubated with 100 nM SiR-DNA and imaged live. If Aurora B was inhibited, 10 µM ZM44743 was added 10 min before imaging (+AurBi). Arrows indicate kinetochore-localised PPP1CC-GFP. (C) Graph shows mean PPP1CC-GFP intensity at chromatin compared to whole cell GFP levels. Bars indicate the SEM (≥ 41 cells per condition from 2 independent experiments).

protocol (Figure 5.5B). Analysis revealed a small but significant increase in the localisation of PPP1CC to the chromatin region of cells (Figure 5.5C). Kinetochore localisation could not be specifically measured due to the inability to observe a kinetochore marker in live conditions. However visual examination

showed that the increased PPP1CC-GFP signal occurred at regions of expected kinetochore localisation (Figure 5.5B). This preliminary experiment provides endogenous protein confirmation that Aurora B regulates PP1 localisation. Future experiments using these tools can now build on this to understand exactly how Aurora B and the RVxF motif regulate the localisation and function of PP1 isoforms and particularly how this regulates the timings of PP1 localisation in relation to microtubule attachment.

5.3 Observing the effect of PP1 isoform-specific loss

To understand the exact importance and function of each PP1 isoform, a lentivirus CRISPR knock-out (KO) protocol was employed to generate cell lines with individual PP1 isoforms constitutively knocked out (Shalem et al., 2014). In brief, a plasmid containing a chimeric guide RNA and hSpCas9 was inserted into cells using lentivirus infection. This targeted the Cas9 to a location near the start codon of the gene of interest. Cas9 created a cut in the gene of interest and a repair-induced frame shift mutation resulted in non-functional protein production. Constitutive KO was chosen over traditional methods such as RNAi to ensure complete loss of PP1 isoforms. To facilitate the screening, generation of KOs was carried out in HeLa cells with the isoform to be knocked-out tagged with GFP. Observation of the loss of PPP1CA-GFP or PPP1CC-GFP by western blot analysis confirmed successful generation of homozygous KOs of both isoforms, thus all alleles of each isoform have been knocked-out (Figure 5.6A-B). Interestingly, multiple viable KO clones were successfully made for both isoforms, indicating that neither isoform alone is essential for cell survival. The

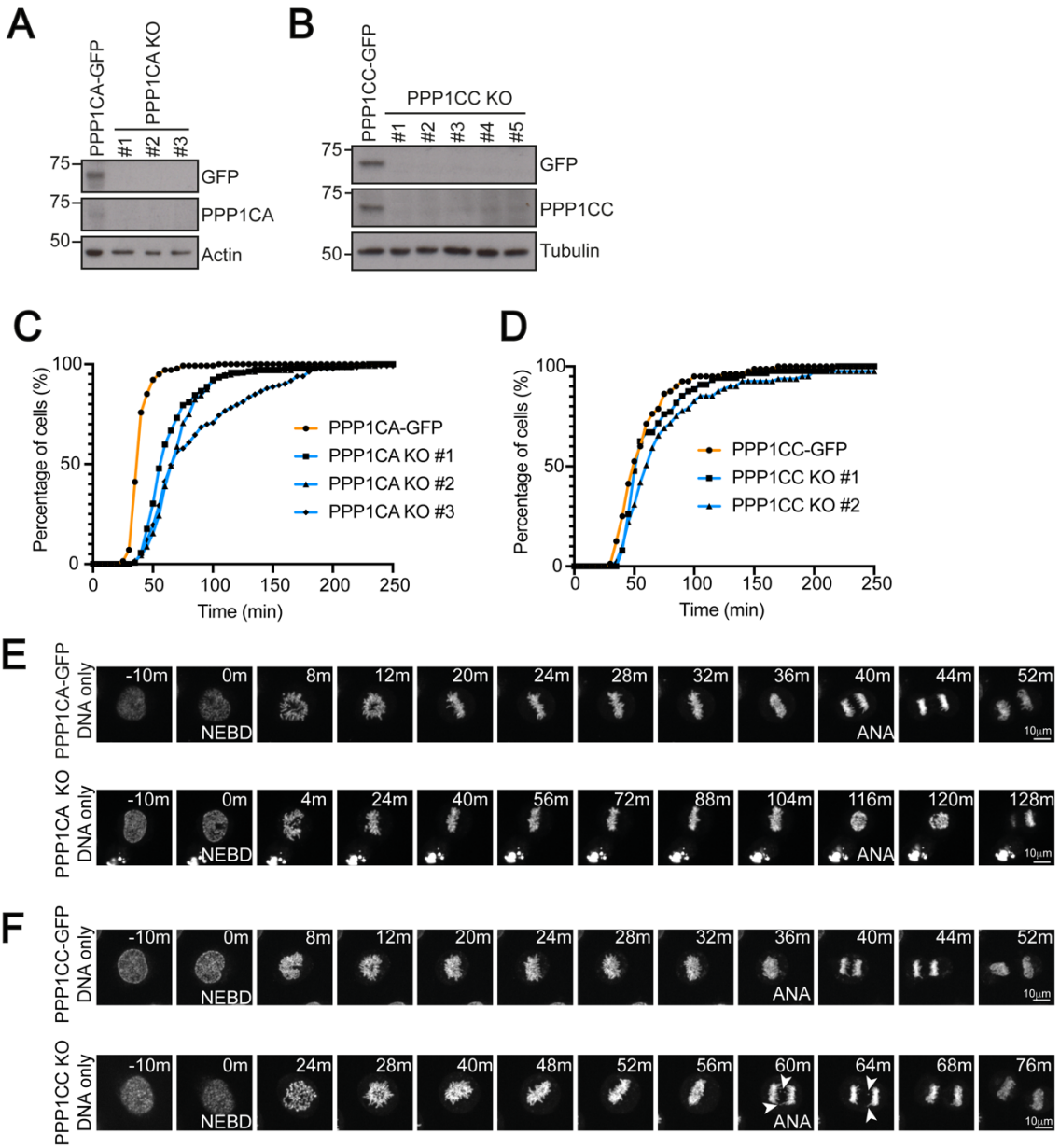


Figure 5.6 Generating and observing the effects of constitutive PP1 isoform knock-outs

(A) Western blot screen confirming homozygous knock-out of PPP1CA from PPP1CA-GFP HeLa parental cells. (B) Western blot screen confirming homozygous knock-out of PPP1CC from PPP1CC-GFP HeLa parental cells. (C) Cumulative frequency graph shows mean time from NEBD to anaphase (min) in PPP1CA KO HeLa cells (≥ 133 cells per condition). Cells were synchronised for 18 h using 2 mM thymidine. Cells were incubated with 100 nM SiR-DNA and imaged 9 h after thymidine release. (D) Cumulative frequency graph shows mean time from NEBD to anaphase (min) in PPP1CC KO HeLa cells (≥ 80 cells per condition). Cells were synchronised for 18 h using 2 mM thymidine. Cells were incubated with 100 nM SiR-DNA and

imaged 9 h after thymidine release. (E) Movie stills of PPP1CA KO HeLa cells incubated with 100 nM SiR-DNA. (F) Movie stills of PPP1CC KO HeLa cells incubated with 100 nM SiR-DNA. White arrows indicate lagging chromatids.

multiple clones of each cell line were characterised before selecting one for in-depth analysis.

To establish if loss of individual PP1 isoforms had an effect on cell cycle progression, PP1 KO cell lines were imaged on a EVOS M7000 imaging system and the time from NEBD to anaphase was measured in comparison to parental cells (Figure 5.6C-D). Unexpectedly, KO of PPP1CA caused a dramatic delay in mitotic timing in all clones (Figure 5.6C) whereas KO of PPP1CC caused only a minor mitotic delay (Figure 5.6D). This suggested that PPP1CA is more critical to early mitotic progression than PPP1CC, a result that is seemingly in contrast with the higher kinetochore localisation of PPP1CC observed in Figure 5.3B-C.

High resolution live cell imaging was subsequently carried out on the PP1 KO cell lines to observe any specific mitotic or chromosome segregation errors that were occurring as a result of loss of a specific PP1 isoform. Representative images of each cell line are displayed in Figure 5.6E-F. In the PPP1CA KO condition (Figure 5.6E), cells entered mitosis normally but were delayed at the metaphase-to-anaphase transition and exhibited a prolonged metaphase plate arrest. In contrast, PPP1CC KOs showed a significant delay at mitotic entry and in chromosome condensation (Figure 5.6F). Furthermore, PPP1CC KOs exited mitosis with a significantly higher rate of DNA bridges and lagging chromatids as indicated in the example (Figure 5.6F). The differences in mitotic outcomes seen

in the PP1 isoform KOs is compelling evidence for isoform-specific functions, with the exact phenotypes providing clues as to the functions of each isoform. The implications of this will be discussed below.

5.4 Discussion

The functions of PP1 in mitosis are very poorly understood in mammalian cells. Investigation of PP1 in mammalian cells has been limited, in part, due to a lack of reagents and tools to observe and manipulate endogenous PP1 in mitosis. Therefore, this chapter has focussed on beginning the work of generating such reagents. In particular, the generation of endogenously tagged PP1 isoforms in human cells has allowed the visualisation of endogenous PP1 for the first time. Initial studies using these cell lines have revealed differences to previous over-expression cell lines (Trinkle-Mulcahy et al., 2003, 2006). In particular, the levels of PP1 observed at the kinetochore were much lower than previously observed. The discrepancy to published data on overexpressed PP1 highlights the need for more studies using endogenously tagged PP1, since overreliance on data from overexpression studies may give misleading information. Therefore, although this chapter alone has not solved the mystery of PP1, it has generated essential tools for further investigation and highlighted some key areas to begin investigation.

It has long been questioned whether the different isoforms of PP1 carry out unique roles. Initial experiments using both the endogenously tagged PP1-GFP cell lines and the constitutive KO cell lines have revealed some intriguing differences between the two critical mitotic isoforms (PPP1CA and PPP1CC). In

agreement with overexpression cell lines (Trinkle-Mulcahy et al., 2003, 2006), differences in the localisations of the two isoforms was observed throughout the cell cycle highlighting potential location- and isoform-specific roles. For example, PPP1CC clearly localises to the chromatin during anaphase whereas PPP1CA is excluded from the chromatin. This supports studies observing the specific interaction of PPP1CC with Repo-Man to recruit PPP1CC to the chromatin in anaphase (Trinkle-Mulcahy et al., 2006). Previous overexpression studies have detailed the localisation of both PPP1CC and PPP1CA to the kinetochore during mitosis, in particular at attached kinetochores in metaphase (Trinkle-Mulcahy et al., 2003, 2006; Conti et al., 2019). However, this work revealed a key difference in the metaphase levels of the different PP1 isoforms at the kinetochore. Endogenously tagged PPP1CC showed a stronger kinetochore localisation than PPP1CA. Although level of kinetochore localisation is not necessarily an indicator of importance, this observation is seemingly at odds with the isoform differences observed following constitutive KO where PPP1CA appeared to be more critical than PPP1CC to a timely mitosis. Subsequent analysis of PP1 isoform localisations relative to other proteins such as checkpoint proteins and PIPs, and to attachment status will hopefully shed further light on isoform-specific function.

Information on the mitotic roles of the specific PP1 isoforms can also be gleaned from the specific mitotic defects observed following loss of each PP1 isoform. KO of PPP1CA resulted in a pronounced delay at the metaphase-to-anaphase transition. This observation presents PPP1CA as the potential key isoform involved in the proposed PP1 roles of SAC silencing and APC/C activation such as CDC20 dephosphorylation (Bancroft et al., 2020; Nijenhuis et al., 2014). The

failure of such events would be expected to prevent the cell progressing into anaphase. In contrast, KO of PPP1CC appeared to result in a significant delay in chromosome condensation. Interestingly, a role of PPP1CC in chromosome condensation has be previously reported in late mitosis through its interaction with Repo-Man (Xin et al., 2020). Whether this mechanism also applies to or may relate to initial chromosome condensation is unknown but this new observation indicates that it is an area worthy of further investigation. Additionally, PPP1CC KO resulted in an increase in the incidence of mitotic errors, suggesting a role of PPP1CC in accurate chromosome segregation such as in attachment formation or the SAC. As the phenotype of PPP1CC KO is different to that of PPP1CA KO, it would be expected that they carry out different roles within this area of accurate chromosome segregation. For example, PPP1CA may be involved in activation of the APC/C as described whereas PPP1CC may play a role in SAC silencing in for example BUB1, MELT motif or MPS1 T loop dephosphorylation (Nijenhuis et al., 2014; Moura et al., 2017; Holder et al., 2020). Observing SAC signalling in both cell lines in future experiments will hopefully shed light on this hypothesis. Some of the defects observed for PPP1CC may also relate to the functions of Repo-Man-PPP1CC complex in anaphase, which has been reported to be the phosphatase for key mitotic histone phosphorylations such as the Aurora B phosphorylation of histone H3-S10 and the haspin phosphorylation on histone H3-T3 (Qian et al., 2011, 2013). Of course, there are likely many more critical functions of PP1 during mitosis that are currently unknown. Further research into these isoform-specific roles using the tools generated here will undoubtedly uncover a more accurate picture of PP1 isoform-specific function.

It is important to discuss the potential negative implications of CRISPR genome editing and in particular the constitutive PP1 KO cell lines. Firstly, CRISPR could result in off-target effects or cuts throughout the genome. This is a potential risk associated with all CRISPR-edited cell lines. An alternative approach to reduce off-target effects is to use Cas9 nickase, a mutant version of Cas9, instead of traditional Cas endonucleases (Mali et al., 2013). The combined use of one or two Cas9 nickases with a pair of gRNAs creates staggered double-strand breaks with overhangs resulting more accurate and targeted genome editing and repair.

Endogenous PP1 KOs result in the complete removal of PP1 and fewer off-target effects than RNAi. However, they do not remove the risk of effects of PP1 loss at stages of the cell cycle beyond mitosis. In particular, PP1 has a known role in S phase and DNA replication, therefore errors observed in mitosis could also be due to erroneous DNA replication (Hiraga et al., 2017). Another potential issue surrounds cells compensating for the detrimental effects of KOs. Cells may obtain further mutations that provide a survival advantage with the loss of a PP1 isoform. This can be very difficult to exclude as a side effect in any experiments, beyond a full genome sequence of the cell line. Therefore, although constitutive KOs have exciting potential, for future observation of mitosis specific effects and roles of PP1, focus should also turn to developing inducible degron cell lines. One potential system is the dTag system (Nabet et al., 2018), a proteasome-dependent degradation system that achieves rapid, targeted protein degradation by utilising a cell permeable drug to link a degron-tagged fusion protein and an E3 ligase. This would allow for the specific degradation of PP1 isoforms during

mitosis and observation of mitosis-specific effects without long term or other cell cycle stage effects.

The scope of future investigation of PP1 is vast now that appropriate tools have been generated. Beyond observing isoform-specific PP1 localisations in mitosis, the endogenously tagged PP1 cell lines offer much potential for subsequent studies. In particular, these cell lines can be used to carry out isoform-specific PP1 immunoprecipitations without the limitations of poor specificity anti-PP1 antibodies. Pairing this with mass spectrometry will uncover information regarding PP1 isoform specificity and functional pools of PP1 within the cell, as well as potentially identifying new PIPs and targets. Future work with the constitutive KO cell lines should be focussed on genome-scale KO screens to identify genes that confer a resistance to the PP1 KO phenotype (Shalem et al., 2014). This exciting and challenging study would hopefully identify genes opposing specific PP1 isoform function and thus highlight new pathways or targets involving the function of specific PP1 isoforms.

Chapter 6: Conclusions

The Spindle Assembly Checkpoint (SAC) is essential for maintaining genomic stability by monitoring attachment of chromosomes to the mitotic spindle and preventing premature chromosome segregation in mitosis (Musacchio and Salmon, 2007; Lara-Gonzalez et al., 2012). Its regulation through the balance of kinase and phosphatase activity is a complex and intriguing area of cell cycle research (Nilsson, 2019).

CDK1 is the major mitotic kinase required for activating the SAC (Olsen et al., 2010; D'Angiolella et al., 2003; Alfonso-Pérez et al., 2019; Hayward et al., 2019a). However, the exact targets of CDK1 in SAC signalling have been poorly defined. Several studies have begun investigations into the downstream roles of CDK1 in the SAC signalling pathway, for example, BUB1 (Qian et al., 2017; Zhang et al., 2017; Ji et al., 2017) and CDC20 phosphorylation (D'Angiolella et al., 2003; Yudkovsky et al., 2000; Hein et al., 2017; Labit et al., 2012). However, the upstream, initiatory roles of CDK1 in the SAC have, to a large extent, remained a mystery. Substantial progress was made in this area by Hayward et al. (2019a), revealing a requirement for CDK1 for defining the checkpoint permissive period through regulation of MPS1 kinetochore recruitment. However, this was not the complete picture.

This thesis uncovered a new dimension to the role of CDK1 in upstream checkpoint signalling through a combinatorial approach of live and fixed imaging and biochemical assays. The data suggest that specific phosphatase-mediated

disassembly of the outer-kinetochore supports the complete shutdown of the checkpoint through the removal of CDK1 phosphorylations regulating KNL1 localisation following chromosome alignment but maintains microtubule-kinetochore attachments through the maintenance of CDK1 phosphorylations regulating the NDC80-C localisation until later in anaphase. This model revealed the intersection of the outer-kinetochore assembly and SAC regulatory pathways for the first time to show that the outer-kinetochore plays a key role in defining the time frame during which SAC signalling can occur. Furthermore, this work emphasised the previously described overarching role of CDK1:cyclin B as the principal regulator of mitosis (Santamaría et al., 2007; Vassilev et al., 2006; Nigg, 1995; Nigg et al., 1996; D'Angiolella et al., 2003; Olsen et al., 2010). Not only is CDK1 required for initiating checkpoint signalling and regulating outer-kinetochore assembly, but it connects these processes together through the regulation of KNL1 kinetochore localisation. Therefore, CDK1 provides efficient synchronisation between the multiple elements required for accurate chromosome segregation and this ensures directionality and timely progression through the metaphase-to-anaphase transition.

As described in Chapter 1.3.5, CDK1 has many proposed roles downstream of MPS1 and KNL1 in the SAC. As depletion of PP1 rescued the observed loss of BUB1 following CDK inhibition, the key upstream regulatory elements (up to BUB1 recruitment) have now been identified. Attention should now turn to the downstream roles of CDK1 and how they act to produce a finely tuned and highly responsive SAC. In particular, the role of CDK1 in the recruitment MAD1 is of much interest (Qian et al., 2017; Ji et al., 2017; Zhang et al., 2017). This CDK1

site on BUB1 is a proposed PP1 site (Holder et al., 2020) and therefore would be rapidly removed following chromosome alignment, thus preventing further MAD1 accumulation. Building a full and complete picture of the overarching role of CDK1 in the SAC and the phosphatases that oppose these roles will provide a much greater understanding of how the SAC signal is regulated.

Looking beyond the work of this thesis, it is important to place this novel model of regulation into the wider context of SAC signalling regulation and timely SAC silencing. In particular, understanding how the interplay between the critical upstream regulatory roles of CDK1 in the SAC (regulation of KNL1 and MPS1 kinetochore localisation) defines the checkpoint permissive period and provides directionality to the metaphase-to-anaphase transition will be fascinating. As discussed in Chapter 4.4, current understanding of the phosphatases opposing these mechanisms offers a prediction of the timings with which these mechanisms act at the metaphase-to-anaphase transition. A compelling hypothesis is that rapid loss of KNL1 from kinetochores may provide an initial mechanism for preventing checkpoint re-activation after chromosome alignment. Shortly after this, the SAC permissive period is formally terminated by the dephosphorylation of MPS1. However, it is essential to uncover the exact timings and the contribution each mechanism makes to SAC control. In particular, it will be key to understand the responsiveness of the checkpoint during the window between KNL1 loss and MPS1 dephosphorylation.

Looking to the wider context of SAC silencing, this model has further highlighted the importance of a combinatorial approach to ensuring timely and efficient SAC

silencing. SAC silencing is driven by a significant number of dephosphorylation events including MELT motif (Espert et al., 2014; Nijenhuis et al., 2014), MPS1 T loop (Hayward et al., 2019c; Moura et al., 2017), BUB1 (Qian et al., 2017; Holder et al., 2020) and CDC20 (Bancroft et al., 2020; Hein et al., 2017) dephosphorylation, in addition to removal of the critical upstream CDK1 phosphorylations. This places high importance on the timely activation and coordination of the PPPs to ensure each phosphorylation is removed at the appropriate time so mitosis progresses correctly. Future research into the exact timings of these dephosphorylation events and how they fit in with other SAC silencing mechanisms such SAC protein stripping and MCC disassembly will aid the building of complete picture of efficient SAC silencing.

This work also highlighted the key role of PP1 as a phosphatase opposing CDK1 at the metaphase-to-anaphase transition in mammalian cells (Bancroft et al., 2020; Barr et al., 2011; Nilsson, 2019; Shi, 2009). In particular, the novel model of checkpoint regulation revealed the importance of PP1 as the first-activated CDK1-opposing phosphatase in the metaphase-to-anaphase transition for ensuring efficient checkpoint shutdown and mitotic directionality. A key outstanding question is regarding the pool of PP1 that targets the outer-kinetochore. Interestingly, KNL1 is a binding partner of PP1 (Nijenhuis et al., 2014; Rosenberg et al., 2011; Shepperd et al., 2012; Liu et al., 2010; Espeut et al., 2012), presenting an hypothetical feedback loop where KNL1 recruits the phosphatase that results in its loss from the kinetochore. However, the specifics of PP1 action in mammalian cells are still poorly understood, particularly regarding the specific pools of PP1 in mitosis. The generation of critical reagents

in this thesis to examine PP1 in mitosis has made the first step in changing this. Indeed, preliminary experiments suggested that the isoform-specific roles of PP1 in mitosis are critical for accurate chromosome segregation and timely mitosis, emphasising the importance of the continuation of this research.

In conclusion, this thesis has uncovered important new information regarding the critical of roles of kinases and phosphatases in the regulation of the SAC. This has provided the foundation for subsequent studies to further explore the overarching role of CDK1 and its opposition by protein phosphatases such as PP1 in ensuring a timely metaphase-to-anaphase transition and accurate chromosome segregation.

Chapter 7: Materials and Methods

7.1 Reagents and Antibodies

General laboratory chemicals and reagents were obtained from Sigma-Aldrich and Thermo Fisher Scientific unless specifically indicated. Inhibitors and drugs used in this study are listed in Table 7.1. Drugs were dissolved in DMSO (Merck) unless otherwise stated.

Table 7. 1 List of drugs and inhibitors

Drug	**Use**	**Source**	**Stock Conc.**	**Working Conc.**
Calyculin A	Protein phosphatase inhibitor	Tocris	1 mM	25 nM
Doxycycline	Tetracycline class antibiotic	Insight	2mM (in water)	2 µM
Flavopiridol	CDK inhibitor (CDKi)	Tocris	5 mM	5 µM
Hoechst 33342	Blue light emitting DNA dye	Thermo	16.2 mM	16.2 µM
MG132	Proteasome inhibitor	Insight	20 mM	20 µM
Nocodazole	Microtubule polymerisation inhibitor	Merck	0.6 mM	0.3 – 3 µM
Okadaic acid	Protein phosphatase inhibitor	Tocris	1mM	100nM

SiR-DNA	Far red light emitting DNA dye	Universal Biologicals	100 µM	100 nM
Thymidine	For S phase arrest	Millipore	100 mM (in water)	2 mM
ZM44743	Aurora B inhibitor (AurBi)	Millipore	10 mM	10 µM

Transfection reagents oligofectamine (Invitrogen) for siRNA oligos, and LT1 (Mirus-Bio) for plasmids were used according to the manufacturer's instructions. Opti-MEM (Gibco) was used to set up transfections.

Primary antibodies used in this study are listed in Table 7.2. All secondary antibodies were used at 1:1000 dilutions based on stock concentrations. Secondary donkey antibodies against mouse, rabbit or sheep and labelled with Alexa Fluor 350, Alexa Fluor 555 were purchased from ThermoFisher Scientific (stock concentration of 2 mg/ml). Secondary donkey antibodies against guinea pig labelled with Alexa Fluor 647 (stock concentration of 1.5 mg/ml) and secondary donkey antibodies against mouse, rabbit or sheep labelled with HRP (stock concentration of 1 mg/ml) were purchased from Jackson ImmunoResearch Laboratories. Protein A and protein G conjugated to HRP were purchased from Merck (stock concentration of 1 mg/ml).

Table 7. 2 Primary antibody details

Target	Species	Supplier	Stock conc.	Working Conc.	
				IF	WB
ß-Actin (conjugated to HRP)	Mo	Santa Cruz (sc-47778)	200 µg/ml	/	0.04 µg/ml (*1:5000*)
Aurora A	Rb	Cell Signalling, 3092S	50 µg/ml	/	0.05 µg/ml (*1:1000*)
BUB1	Rb	Bethyl, A300-373A	1000 µg/ml	0.2 µg/ml (*1:5000*)	/
BUBR1	Rb	Bethyl, A300-386A	1000 µg/ml	0.5 µg/ml (*1:2000*)	/
CENP-C	Gp	MBL, PD030	1000 µg/ml	/	0.5 µg/ml (*1:2000*)
GFP	Sh	Barr lab	2730 µg/ml	/	1.09 µg/ml (*1:2500*)
HEC1	Sh	Homemade	400 µg/ml	0.4 µg/ml (*1:1000*)	/
HEC1	Mo	GeneTex, GTX70268	3440 µg/ml	3.44 µg/ml (*1:1000*)	/
HEC1	Rb	Abcam, ab109496	160 µg/ml	/	0.16 µg/ml (*1:1000*)
KNL1	Sh	Homemade	3000 µg/ml	1.5 µg/ml (*1:2000*)	3 µg/ml (*1:1000*)
MAD1	Rb	GeneTex, GTX10507	1000 µg/ml	0.5 µg/ml (*1:2000*)	/
mCherry	Sh	Barr lab	274 µg/ml	/	0.11 µg/ml (*1:2500*)

MIS12	Sh	Homemade	220 µg/ml	0.22 µg/ml (*1:1000*)	0.22 µg/ml (*1:1000*)
MPS1	Mo	Merck, 05-682	1000 µg/ml	/	0.5 µg/ml (*1:2000*)
NSL1	Rb	Bethyl, [anti-DC8] A300-795A	1000 µg/ml	1 µg/ml (*1:1000*)	1 µg/ml (*1:1000*)
PPP1CA	Rb	Bethyl, A300-904A	1000 µg/ml	/	1 µg/ml (*1:1000*)
PPP1CC	Go	Santa Cruz Biotechnology, sc-6108	200 µg/ml	/	0.2 µg/ml (*1:1000*)
Tubulin	Mo	Sigma, [DM1A] T6199	1000 µg/ml	/	0.1 µg/ml (*1:10000*)
ZW10	Mo	Abcam, ab21582	1000 µg/ml	1 µg/ml (*1:1000*)	/
	Rb = rabbit; Sh = sheep; Mo = mouse; Go = goat; Gp = guinea pig IF = immunofluorescence; WB = western blotting				

7.2 SDS-PAGE and western blotting

Protein concentrations were measured by Bradford assay using Protein Assay Dye Reagent Concentrate (Bio-Rad). For Coomassie gels, proteins were separated by SDS-PAGE and gels stained using InstantBlue Coomassie Stain (Abcam) before photographing. For western blotting, proteins were separated by SDS-PAGE and transferred to nitrocellulose using a Trans-blot Turbo system (Bio-Rad): 2.5A, 25V, 7 min for two gels. For proteins over 150kDa a “high molecular weight” transfer protocol was used: 2.5A, 25V, 10 min for two gels. Membranes were blocked in 5% cow’s milk (wt/vol) in phosphate buffered saline (PBS), 0.1% Tween-20 (PBST). Antibodies were incubated in 5% milk (wt/vol) in

PBST for 0.5-24 h. PBST was used to wash membranes for an hour, between antibody incubations and prior to developing. Western blots were revealed using ECL (GE Healthcare) on films.

For analysis of protein phosphorylation, polyacrylamide separating gels were prepared with the addition of 200 µM $MnCl_2$ and 50 µM Phos-tag reagent (Wako Chemicals, AAL-107S1). Prior to transfer, gels were equilibrated with 3x 5 min washes in transfer buffer (20 mM Tris; 150 mM Glycine, 0.1% [wt/vol] SDS, 20% [vol/vol] MeOH, 20 mM EDTA) and subsequently 3x 5 min washes in transfer buffer without EDTA (20 mM Tris; 150 mM Glycine, 0.1% [wt/vol] SDS, 20% [vol/vol] MeOH). Western blotting then proceeded as above.

7.3 Molecular biology

Human MPS1 and NSL1 were amplified from Human testis cDNA (Marathon cDNA; Takara Bio Inc.) using Pfu polymerase (Promega). Mammalian expression constructs were made using pcDNA5/FRT/TO (Invitrogen) modified to encode EGFP- or FLAG-reading frames. Generation of GFP-MIS12-MPS1 construct has been previously described (Hayward et al., 2019a). Mutagenesis was performed using the QuickChange method (Agilent Technologies) and the primers used are described in Table 7.3. DNA primers were obtained from Invitrogen. Gibson assembly was carried out using NEBuilder HiFi DNA Assembly Master Mix (NEB) according to the manufacturer's instructions for primer design and experimental method.

Table 7. 3 Mutagenesis primers

Primer name	DNA sequence (5'-3')
MPS1_KD(D664A)_FW	ATGCTAAAGCTAATTGCTTTTGGGATTGCAAAC
MPS1_KD(D664A)_RV	GTTTGCAATCCCAAAAGCAATTAGCTTTAGCAT
MPS1_S821A_FW	CTTGTTGGTCTGAATGCTCCTAACTCCATTTTG
MPS1_S821A_RV	CAAAATGGAGTTAGGAGCATTCAGACCAACAA G
MPS1_S821D_FW	CTTGTTGGTCTGAATGAT CCTAACTCCATTTTG
MPS1_S821D_RV	CAAAATGGAGTTAGGATCATTCAGACCAACAA G
MPS1_S821E_FW	CTTGTTGGTCTGAATGAACCTAACTCCATTTTG
MPS1_S821E_FW	CAAAATGGAGTTAGGTTCATTCAGACCAACAA G
MPS1_S281A_FW	GTTAACCTTCTAAATGCCCCAGATTGTGATGTG
MPS1_S281A_RV	CACATCACAATCTGGGGCATTTAGAAGGTTAA C
MPS1_S281E_FW	GTTAACCTTCTAAATGAGCCAGATTGTGATGTC
MPS1_S281E_RV	CACATCACAATCTGGCTCATTTAGAAGGTTAAC
MPS1_S436A_FW	TCAGTTTCAAAACAGGCACCACCAATATCAACA
MPS1_S436A_RV	TGTTGATATTGGTGGTGCCTGTTTTGAAACTGA
MPS1_S436E_FW	TCAGTTTCAAAACAGGAACCACCAATATCAACA
MPS1_S436E_RV	TGTTGATATTGGTGGTTCCTGTTTTGAAACTGA
MPS1_T453A_FW	AAATCTATTTGTAAGGCACCAAGCAGCAATAC C
MPS1_T453A_RV	GGTATTGCTGCTTGGTGCCTTACAAATAGATTT
MPS1_T453E_FW	AAATCTATTTGTAAGGAACCAAGCAGCAATACC
MPS1_T453E_RV	GGTATTGCTGCTTGGTTCCTTACAAATAGATTT
NSL1_ORF_FW	TCAGTTTGATGAAATCATCGTTGACATTGCGAC TAAACGTAAGCAGTAT
NSL1_ORF_RV	ATACTGCTTACGTTTAGTCGCAATGTCAACGAT GATTTCATCAAACTGA
NSL1_Y270A_FW	CAGAGAAAATGGGCTCCATTGCGGCCA

NSL1_Y270A_RV	TGGCCGCAATGGAGCCCATTTTCTCTG
NSL1_2TA_FW	ACAGATAGAAGCCGCACCAACAGAGACTGC
NSL1_2TA_RV	GCAGTCTCTGTTGGTGCGGCTTCTATCTGT
NSL1_2TD_FW	ACAGATAGAAGACGACCCAACAGAGACTGC
NSL1_2TD_RV	GCAGTCTCTGTTGGGTCGTCTTCTATCTGT
PPP1CA_PAM_FW	AACCCCCGCAGCTTACCCTGTGCCCCAGATGA
PPP1CA_PAM_RV	TCATCTGGGGCACAGGGTAATGTGCGGGGGT T
PPP1CC_PAM_FW	GTTTTGACACTGCTTAGTCGGGACTTGTAAC
PPP1CC_PAM_RV	AAGTCCCGACTAAGCAGTGTCAAAACGAC

7.4 Cell Culture

7.4.1 Tissue culture

HeLa and HEK293T cells were cultured in DMEM with 1% (vol/vol) GlutaMAX (Life Technologies) supplemented with 10% (vol/vol) bovine calf serum and 1% (v/v) penicillin-streptomycin (Gibco, 10,000 U/ml) at 37°C and 5% CO_2. T-REx doxycycline-inducible Flp-In HeLa cell lines expressing GFP-MIS12-MPS1 and GFP-NSL1 were cultured in medium supplemented with 200 µg/ml hygromycin B (InvivoGen) and 4 µg/ml blasticidin (InvivoGen). HCT116 cells were cultured in McCoy's 5a media (Life Technologies) supplemented with 10% (vol/vol) bovine calf serum and 1% (vol/vol) penicillin-streptomycin (Gibco, 10,000 U/ml) at 37°C and 5% CO_2.

7.4.2 Production of Flp-In stable cell lines

HeLa cells with inducible single integrated copies of a desired transgene were created using the T-REx doxycycline-inducible Flp-In system (Tighe et al., 2004; Invitrogen, 2012). 100 ng of pcDNA5/FRT/TO/EGFP vectors were co-transfected

into Flp-In TRex doxycycline transactivator HeLa cells with 900 ng of the Flp recombinase encoding plasmid pOG44. Cells were selected in 4 µg/ul blasticidin and 200 µg/ul hygromycin B for 2 weeks. Immunofluorescence and western blotting were used to screen for successful, homogenous clones. Clones were then checked in a doxycycline negative background to confirm there was no leaky expression. Transgene expression was induced by addition of 2 µM doxycycline for a minimum of 24 h.

7.4.3 Production of stable cell lines using CRISPR editing

Homozygous CRISPR/Cas9-edited HeLa and HCT116 cells with inserted GFP tags at the C-termini of PPP1CA or PPP1CC were generated following a published protocol with some modifications (Stewart-Ornstein and Lahav, 2016). Briefly, homology recombination cassettes containing the desired knock-in DNA with flanking regions of homology of approximately 800 bp to the target locus were co-transfected with a version of pSpCAS9(BB) (Addgene, 48139) containing the relevant guide RNA (Table 7.4), modified to removed puromycin resistance. The knock-in sequence contained the EGFP fluorescent protein, preceded by a glycine-serine rich flexible linker. The EGFP was followed by a P2A ribosome-skipping sequence and a blasticidin resistance marker. Antibiotic resistant clones were selected and successful modification confirmed by PCR screening, immunofluorescence and western blotting.

Table 7. 4 CRISPR/Cas9 guide RNAs

Target gene	**Guide RNA (5'-3')**
PPP1CA	CACCGCCATCATCTGGGGCACAGGGTGG
PPP1CC	CTATGTTACAAGTCCCGACT

Heterozygous CRISPR/Cas12a-edited HeLa cells with inserted GFP tags at the C-termini of HEC1, KNL1 or MIS12 were generated following a published PCR tagging method (Fueller et al., 2020). Briefly, a gene-specific PCR cassette was generated using two gene specific tagging oligos (Table 7.5) which provided the homology arms and a generic cassette containing the GFP tag, selection marker and Cas12a specific crRNA gene (Addgene 120016). PCRs were carried out using HiFi polymerase (Takara Bio UK Ltd) according to the manufacturer's instructions. The PCR cassette was transfected into HeLa cells with a helper plasmid containing AsCas12a endonuclease (Addgene 89353). Following cleavage, insertion of the PCR cassette into the DNA by homologous recombination yielded a fusion of the GFP tag and the gene of interest. Antibiotic resistant clones were selected and successful modification confirmed by immunofluorescence and western blotting.

Table 7. 5 CRISPR/Cas12 PCR tagging primers

Target Gene	**Primer Name**	**DNA sequence (5'-3')**
HEC1	M1_HEC1	GAATGCATGTCAGAAGATCTCTCGGAAAATATTAAAGAGATTAGAGATAAGTATGAGAAGAAAGCTACTCTAATTAAGTCTTCTGAAGAATCAGGTGGAGGAGGTAGTG
HEC1	M2_HEC1_AsCpf1_TATV	TACTGAGACAATTTTATTCACTATGGATATATATACATGATCAACATTTTATCTAAAAAAAGTCTTCTGAAGAATGAAGAATCTACAAGAGTAGAAATTAGCTAGCTGCATCGGTACC
KNL1	M1_KNL1	CTATCTAAAGTGCCACTGGAGAACAACTACCTGAAGAATGTAGTCAAGCAAATTTACCAAGATCTGTTT

		CAGGACTGCCATTTCTACCACTCAGGTGGAGGA GGTAGTG
KNL1	M2_KNL1_ AsCpf1_TA TV	CCTGAAATAATATCAAGTACATTCTGCTTGGTTGT TCCAATGGTGGTCCAAGGGTAAAAAAGGTCCAAG GGTCTAGTGGTAATCTACAAGAGTAGAAATTAGC TAGCTGCATCGGTACC
MIS12	M1_MIS12	GAGAGTTTAGTATCCCTGGTTCAGAACTCCAGAA AACTACAGAACATTAGAGACAATGTGGAAAAGGA ATCGAAACGACTGAAAATATCTTCAGGTGGAGGA GGTAGTG
MIS12	M2_MIS12_ AsCas12a_ TATV	AACAGTCCTTATGATTCTACTTTTTGACAGGCTCC TCCTTTTGACTACTGAGCAAAAAAAATTTGACTAC TGAGCAATTAAATCTACAAGAGTAGAAATTAGCTA GCTGCATCGGTACC

HeLa cells with PPP1CA or PPP1CC constitutively knocked-out were generated following a published lentiviral CRISPR/Cas9 protocol (Shalem et al., 2014). Briefly, lentiCRISPR v2-Blast or -Puro constructs (Addgene 52961 and 83480, respectively) containing the guide RNA sequence targeting human PPP1CA and PPP1CC respectively (Table 7.6), pMD2.G and psPAX2 constructs (Addgene 12259 and 12260, respectively) were used for lentiviral-based packaging from HEK293T cells, and the supernatant was used to infect PPP1CA-GFP or PPP1CC-GFP HeLa cells respectively. After infection, antibiotic resistant clones were selected and successful knock-out confirmed by western blotting and immunofluorescence.

Table 7. 6 Lentiviral CRISPR/Cas9 KO guide RNAs

Target gene	KO Guide RNA (5'-3')
PPP1CA	CGGATCTCGTTCTCTGTCAG
PPP1CC	ATTTTTCTCTTGCAGTGAGA

For PCR screening, genomic DNA was extracted from cells using squishing buffer (10 mM Tris-HCl pH 8.0, 1 mM EDTA, 25 mM NaCl, 200 µg/ml Proteinase K) and amplified using primers flanking the target locus and Q5 polymerase (NEB).

For western blot screening, cells were harvested using 1mM EDTA. Cell pellets were lysed in lysis buffer supplemented with phosphatase and protease inhibitors (20 mM Tris-HCl, pH 7.5, 150 mM NaCl, 1% [vol/vol] IGEPAL CA-630, 1 mM PMSF, 1:250 protease inhibitor cocktail (Sigma), 1:100 phosphatase inhibitor cocktail (Sigma)), and run on SDS-PAGE gels.

For immunofluorescence screening, cells were fixed, stained and imaged as described in Chapter 7.6.1.

7.5 Transfection and rescue experiments

7.5.1 Transient transfection for protein expression

Transient protein expression for *in vitro* kinase assays, immunoprecipitation and mass spectrometry was carried out in HEK293T cells. Cells were seeded 24 h prior to transfection. Transfection mixtures were prepared with 24 µl LT1 (Mirus-Bio), 800 µl Opti-MEM (Gibco) and 8 µg plasmids encoding GFP- or FLAG-tagged constructs. 0.3 µM nocodazole (Merck) was added 30 h after transfection

and incubated for 18 h. Cells were harvested by mitotic shake-off and processed depending on subsequent analysis.

7.5.2 RNAi

Cells were seeded 24 h prior to depletion. siRNA mixtures were prepared using oligofectamine (Invitrogen) and Opti-MEM (Gibco) according to the manufacturer's instructions. All RNAi depletions were performed for either 48 h or 72 h. siRNA duplexes or siRNA pools and their optimised usage are listed in Table 7.7. Control RNAi was performed against GL2 (luciferase) (5'-CGUACGCGGAAUACUUCGAUU-3') (Dharmacon (#D-001100-01-20)). Following the optimised depletion period, cells were either imaged, fixed for immunofluorescence or harvested for western blotting.

Table 7. 7 siRNA oligos

siRNA target	**Sense sequence (5'-3')/Smartpool ID**	**Part of transcript targeted**	**RNAi length**	**Source**
GL2 (luciferase)	*CGUACGCGGAAUACUUCGAUU*	*ORF*	*/*	*Dharmacon (#D-001100-01-20)*
MPS1	Combination of 3 oligos (UUGGACUGUUAUACUCUUGAA, GUGGAUAGCAAGUAUAUUCUA, CUUGAAUCCCUGUGGAAAU)	3' UTR	48 h	Invitrogen (Hayward et al., 2019a)
NSL1	CAUAGUAGAUAUAGCCACA	ORF	48 h	Invitrogen

PPP1CA	UGGAUUGAUUGUACAGAAAUU	3' UTR	72 h	Invitrogen (Bancroft et al., 2020)
PPP1CC	GCGGUGAAGUUGAGGCUUAUU	3' UTR	72 h	Invitrogen (Bancroft et al., 2020)
PP2A-B55	Combination of 4 smartpools against each isoform (L-004824-00, L-003022-005, L-019167-00, and L-032298-00)	3' UTR	72 h	Dharmacon (Hayward et al., 2019a)

7.5.3 RNAi rescue assays

RNAi rescues assays with GFP-MIS12-MPS1 or GFP-NSL1 transgenes were all performed using the same protocol. Transgene induction was initiated with the addition of 2 µM doxycycline (InvivoGen) 3 h prior to siRNA addition. Endogenous MPS1 or NSL1 was depleted for 48 h as described in Chapter 7.5.2. A second induction was performed 24 h into siRNA depletion. Successful RNAi rescue was confirmed by western blotting for all cell lines.

7.6 Imaging techniques

7.6.1 Immunofluorescence staining

Samples seeded on #1.5 mm coverslips were fixed with PTEMF (20 mM Pipes-KOH, pH 6.8, 0.2% [vol/vol] Triton X-100, 1 mM $MgCl_2$, 10 mM EGTA, and 4% [wt/vol] formaldehyde) for 12 min. Following fixation, coverslips were washed in PBS and incubated in blocking buffer (3% wt/vol bovine serum albumin in PBS).

Antibody dilutions were performed in blocking buffer. Coverslips were incubated face-down on 80 µl droplets of primary antibody dilutions in a humidified chamber for 1.5 h. Following primary antibody incubation coverslips were washed 3x in PBS. Coverslips were incubated face-down on 80 µl droplets of secondary antibody dilutions in a humidified chamber for 45 min. Coverslips were washed 3x in PBS and 1x in deionised water. Coverslips were left to dry completely before being mounted with 6 µl Mowiol 4-88 (Sigma) according to the manufacturer's instructions.

7.6.2 Immunofluorescence microscopy

Samples were prepared for imaging as in Chapter 7.6.1. Imaging was performed on a DeltaVision Core light microscopy system (GE Healthcare) using a 60x/1.35 NA objective fitted to an Olympus IX-71 microscope stand. Standard filter sets for DAPI, FITC and Cy5, a CoolSnap HQ2 charge-coupled device (CCD) camera (Photometrics) and the software package softWoRx (GE Healthcare) were used. Cells were imaged using a 0.2 µm interval and a total stack of 4 µm, and deconvolved for presentation using softWoRx.

For quantification, imaging was performed using a 60x/1.35 NA oil immersion objective on a BX61 Olympus microscope with filter sets for DAPI, EGFP/Alexa Fluor 488, Alexa Fluor 555, Alexa Fluor 647 (Chroma Technology Corp.) to sequentially excite and collect fluorescence images on a CoolSNAP HQ2 camera (Roper Scientific) using MetaMorph 7.5 imaging software (GE Healthcare). Cells were imaged using a 0.2 µm interval and a total stack of 2.4 µm.

7.6.3 SoRa Confocal Microscopy

For live imaging of PPP1CA-GFP and PPP1CC-GFP, cells seeded on circular glass bottom Fluorodish imaging dishes (World Precision Instruments). Media was replaced with Fluorobrite media (ThermoFisher Scientific) supplemented with 10% (vol/vol) bovine calf serum and 1% (vol/vol) GlutaMAX (Life Technologies), and SiR-DNA (Spirochrome) was added at a concentration of 100 nM 3h prior to imaging. For fixed imaging, samples were prepared as in Chapter 7.6.1. Live or fixed super-resolution imaging was performed on an Olympus SoRa spinning disk confocal microscope using a 60x/1.5-NA objective fitted to an Olympus IX-83 microscope stand with 3.2x optical zoom and a Yokogawa CSU-W1 SoRa super-resolution spinning disk. Solid state lasers emitting 405 nm, 488 nm, 561 nm and 633 nm were used. Images were captured with a Prime BSI sCMOS camera (photometrics) using the Olympus cellSens software package. Images were acquired with a 0.2 µm interval over a total distance of 4 µm. Super-resolution enhancement and constrained iterative deconvolution was performed on cellSens.

7.6.4 Spindle Assembly Checkpoint assays

For the “checkpoint reactivation assay” (Vleugel et al., 2015) cells were treated with 20 µM MG132 for 2.5 h. At 5 min before fixation, 3 µM nocodazole was added. If CDK1 was inhibited, 5 µM flavopiridol was added 1 min or 5 min before nocodazole treatment, with DMSO at the same volume used as a control. For the “checkpoint maintenance assay” cells were treated with 0.3 µM nocodazole for 2 h. At 30 min before fixation, 20 µM MG132 was added to prevent mitotic exit. If CDK1 was inhibited, 5 µM flavopiridol was added 6 min before fixation, with

DMSO at the same volume used as a control. All cells were fixed in PTEMF and immunostained as indicated in figure legends before imaging.

For the Aurora B inhibition assay, PPP1CC-GFP cells were treated with 0.3 µM nocodazole for 2 h. At 30 min before imaging, 20 µM MG132 was added to prevent mitotic exit and SiR-DNA (Spirochrome) was added at a concentration of 100 nM. If Aurora B was inhibited, 10 µM ZM44743 was added for 10 min before imaging, with DMSO at the same volume used as a control. Cells were then imaged in live as described in Chapter 7.6.3.

7.6.5 Live cell imaging assays

For low-resolution timelapse data, cells were seeded on glass bottom 6-well imaging dishes (IBL Baustoff and Labor GmBH). Cells were treated for 18 h with 2 mM thymidine. The thymidine was removed by washing 6x with PBS. After washes, the PBS was replaced with Fluorobrite media (ThermoFisher Scientific) supplemented with 10% (vol/vol) bovine calf serum and 1% (vol/vol) GlutaMAX (Life Technologies). SiR-DNA (Spirochrome) was added at 100 nM. Imaging commenced 9 h after thymidine release on an 20x/0.75 NA air objective on an EVOS M7000 (ThermoFisher) microscope with software version 2.0.2094.0, equipped with an onstage incubator. Cells were imaged at 37^{o}C, 5% CO_2 every 5 min for 12 h. 5 Fields of View (FOV) were selected per well. At each time point and stage position, a stack of 5 z-planes was taken spaced approximately 2 µm apart in the brightfield, FITC and Cy5 channels.

For high-resolution timelapse imaging, cells were seeded on circular glass bottom Fluorodish imaging dishes (World Precision Instruments). Cells were treated for 18 h with 2 mM thymidine. The thymidine was removed by washing 6x with PBS. After washes, the PBS was replaced with Fluorobrite media (ThermoFisher Scientific) supplemented with 10% (vol/vol) bovine calf serum and 1% (vol/vol) GlutaMAX (Life Technologies). SiR-DNA (Spirochrome) was added at a concentration of 100 nM. Imaging commenced 9 h after thymidine release at 37°C, 5% CO_2 on an Olympus SoRa spinning disk confocal microscope using a 60x/1.5-NA objective fitted to an Olympus IX-83 microscope stand with a Yokogawa CSU-W1 SoRa super-resolution spinning disk. Solid state lasers emitting 488 nm and 633 nm were used. Images were captured with a Prime 95B sCMOS camera (photometrics) using the Olympus cellSens software package. Images were acquired with a stack of 12 z-planes spaced approximately 1 µm apart, every 2 min for 5 h.

7.7 Image processing and analysis

Image processing and analysis was performed using the FIJI distribution of ImageJ (Schindelin et al., 2012).

For figures, deconvolved images acquired on either a DeltaVision Core light microscopy system or an Olympus SoRa spinning disk confocal microscopy system were maximum projected and saved as 8-bit TIFF files. TIFF files were imported into Illustrator CS6 (Adobe) for figure production. Quantitation was performed on images of cells from a BX61 Olympus microscopy system which were cropped to 250 x 250 px and sum projected through 7 z-slices. Kinetochore

intensities were determined by placing 8 px-diameter circular ROIs at the maxima of kinetochores and measuring mean pixel intensity of each channel within selections. Where possible, 20 kinetochores were measured per cell. Background measurements were generated by taking an equivalent number of pixels as were in the ROI as close to the ROI without overlapping with kinetochores. Data analysis was performed in Excel (Microsoft). Kinetochore signal intensities were background-adjusted by subtracting the background signal on a channel-by-channel basis. The mean intensity of the channel of interest was then divided by the mean intensity of either the CENP-C or GFP channel as stated on a per-kinetochore basis. Mean kinetochore localisation intensities were then calculated for each cell. Normalisation was performed within repeats by dividing the cell's mean kinetochore localisation intensity by that of the group which was being normalised to.

Quantitation of kinetochore signals in cells without a kinetochore marker (Figure 5.5C) was performed on sum-projected images of cells from an Olympus SoRa spinning disk confocal microscopy system. A ROI was drawn around the chromatin region using the DNA channel and the mean pixel intensity of the GFP channel measured. This measurement was divided by the mean pixel intensity of the GFP channel measured within a ROI around the whole cell (determined by the GFP channel). Normalisation was performed within repeats by dividing the cell's mean chromatin localisation intensity by that of the group which was being normalised to.

For low-resolution timelapse data, maximum-projected live cell imaging data from an EVOS M7000 (ThermoFisher) microscope was used to quantify the times at which NEBD, metaphase, and anaphase occurred, based on DNA morphology. Arbitrary descriptors of mitotic outcome were assigned based on DNA morphology. For figures, individual cells from specific timepoints were cropped and saved as 8-bit TIFF files. TIFF files were imported into Illustrator CS6 (Adobe) for figure production.

For measurement of kinetochore intensity from high-resolution timelapse imaging, maximum-projected images of timelapse imaging data from an Olympus SoRa spinning disk confocal microscopy system microscope were used. 10x 8 px-diameter circular ROIs were placed at the maxima of GFP positive kinetochores and mean pixel intensity at the first timepoint they were visible was measured. The same ROIs were then measured at previous timepoints. 10x 8 px-diameter circular ROIs at the maxima of GFP positive kinetochores were then measured for each subsequent timepoint until they were no longer visible. The same ROIs as the final visible timepoint were then measured at subsequent timepoints. Background measurements were taken from 10 chromatin free cytoplasmic regions. For figures, individual cells from specific timepoints were cropped and saved as 8-bit TIFF files. TIFF files were imported into Illustrator CS6 (Adobe) for figure production.

All statistical analysis and graph production was performed in GraphPad Prism version 9.2.0 (GraphPad Software). Each cell measured was considered as a biological replicate (n), hence the mean cell averages of kinetochores was used

for statistical analysis. At least three independent repeats of each experiment were performed, with statistical analysis performed using a sum of biological replicates from all independent experiments. Data sets were tested for normal distribution via a D'Agostino-Pearson omnibus K2 test. If all groups in an experiment were normally distributed, then the means were compared using an unpaired 2 tailed t-test (with Welch's correction if the groups had unequal standard deviations). If all groups did not exhibit a normal distribution, then medians were compared using a Mann-Whitney test. Unless otherwise stated, graphs display the mean ±SEM. P-values are shown on graphs as follows: $p > 0.05$ = not significant (ns), $p \leq 0.05$ = *, $p \leq 0.01$ = **, $p \leq 0.001$ = ***, $p \leq 0.0001$ = ****.

7.8 Biochemical assays

7.8.1 λ-phosphatase treatment

For mitotic cell population, HeLa cells were arrested in 0.3 μM nocodazole for 18 h and harvested by mitotic shake-off. For asynchronous cell population, HeLa cells were harvested using 1mM EDTA. Cell pellets were lysed and subsequently incubated with λ-protein phosphatase (NEB) for 1 h at 30°C according to the manufacturer's instructions. 1x Laemmli buffer was added and samples denatured at 100°C for 5 min. Samples were run on Phos-tag or SDS-PAGE gels and analysed by western blotting.

7.8.2 Immunoprecipitation

Cells were grown in 15 cm dishes (number of dishes varied depending on the size of immunoprecipitation). For GFP-NSL1 Flp-In cell lines, transgene

expression was induced by addition of 2 µM doxycycline for 24 h. In all experiments, cells were arrested in 0.3 µM nocodazole for 18 h and harvested by mitotic shake-off. Cells were pelleted at 500 xg for 4 min at room temperature, washed with PBS and pelleted again. If kinase inhibitions were carried out, pellets were resuspended in 1 ml Opti-MEM. 10 µM ZM44743 or 5 µM flavopiridol was added for 10 min, with DMSO at the same volume used as a control. Further dephosphorylation was stopped after 10 min by addition of 25 nM Calyculin A and cells were pelleted at 500 xg for 4 min at room temperature.

Pellets were lysed in lysis buffer (20 mM Tris-HCl pH 7.4, 150 mM NaCl, 1% IGEPAL, 0.1% sodium deoxycholate, 100 nM okadaic acid, 40 mM sodium β-glycerophosphate, 10 mM NaF, 0.3 mM sodium vanadate, 1:250 protease inhibitor cocktail (Sigma), 1:100 phosphatase inhibitor cocktail (Sigma)) for 30 min at 4ºC before being clarified at 14,000 rpm for 15 min at 4ºC. Per 1 mg of lysate, 1 µg appropriate antibody was added (homemade sheep anti-GFP or homemade sheep anti-mCherry as a negative IgG control). Anti-GFP immunoprecipitations were performed using Protein-G Dynabeads (Invitrogen), anti-FLAG immunoprecipitations were performed using anti-FLAG M2 magnetic beads (Merck). All beads were washed 3x in lysis buffer prior to use. Immunoprecipitations were performed at 4ºC for 2 h. Beads were washed 6x, 3x in lysis buffer and 3x in wash buffer (20 mM Tris-HCl pH 7.4, 150 mM NaCl, 0.1% IGEPAL, 40 mM sodium β-glycerophosphate, 10 mM NaF, 0.3 mM sodium vanadate). Beads were separated from the flow-through using a magnet. If samples were used for western blot analysis, 1x Laemmli buffer was added and samples denatured at 100ºC for 5 min.

7.8.3 *In vitro* kinase assays

For kinase assays, 1 µg recombinant FLAG-MPS1 WT/KD/S281A/4A purified by immunoprecipitation on anti-FLAG M2 magnetic beads from HEK293T cells was auto-phosphorylated for 10 min at 30°C in 50 mM Tris-HCl pH 7.3, 50 mM KCl, 10 mM $MgCl_2$, 20 mM sodium β-glycerophosphate, 15 mM EGTA, 0.1 mM ATP, 1 mM DTT, and 1 µCi [^{32}P]γ-ATP per reaction. The reaction was terminated by addition of 2x Laemmli buffer and samples run on SDS-PAGE gels. Incorporation of γ^{32}P into FLAG-MPS1 was used as a readout of kinase activity.

7.8.4 Mass spectrometry

GFP-NSL1 was immunoprecipitated from HEK293T cells that had been transiently transfected with GFP-NSL1. Cell harvesting and immunoprecipitation was carried out as described in Chapter 7.8.2, with the only variation of reduced IGEPAL in buffers: 0.5% IGEPAL in lysis buffer, 0% IGEPAL in wash buffer. Following immunoprecipitation, Protein-G Dynabeads (Invitrogen) were washed 3x in PBS at 4°C. The following protocol was provided by and carried out by Oxford Advanced Proteomics Facility. Samples were digested using lysyl endopeptidase (R) and trypsin. Peptides were separated by nano liquid chromatography (Thermo Scientific Easy-nLC 1000) coupled in line to a Q Exactive mass spectrometer equipped with an Easy-Spray source (Thermo Fischer Scientific). Peptides were trapped onto a C18 PepMac100 precolumn (300 µm i.d.x5 mm, 100 Å, ThermoFischer Scientific) using Solvent A (0.1% Formic acid, HPLC grade water). The peptides were further separated onto an Easy-Spray RSLC C18 column (75 µm i.d., 50 cm length, Thermo Fischer

Scientific) using a 30 min linear gradient (15% to 35% solvent B (0.1% formic acid in acetonitrile)) at a flow rate 200 nl/min. The raw data were acquired on the mass spectrometer in a data-dependent acquisition mode (DDA). Full-scan MS spectra were acquired in the Orbitrap (Scan range 350-1500 m/z, resolution 70,000; AGC target, 3e6, maximum injection time, 100 ms). The 10 most intense peaks were selected for higher-energy collision dissociation (HCD) fragmentation at 30% of normalised collision energy. HCD spectra were acquired in the Orbitrap at resolution 17,500, AGC target 5e4, maximum injection time 120 ms with fixed mass at 180 m/z. Charge exclusion was selected for unassigned and 1+ ions. The dynamic exclusion was set to 5 s.

Chapter 8: Bibliography

Abrieu, A., L. Magnaghi-Jaulin, J.A. Kahana, M. Peter, A. Castro, S. Vigneron, T. Lorca, D.W. Cleveland, and J.C. Labbé. 2001. Mps1 is a kinetochore-associated kinase essential for the vertebrate mitotic checkpoint. *Cell*. 106:83–93.

Alexander, J., D. Lim, B.A. Joughin, B. Hegemann, J.R.A. Hutchins, T. Ehrenberger, F. Ivins, F. Sessa, O. Hudecz, E.A. Nigg, A.M. Fry, A. Musacchio, P.T. Stukenberg, K. Mechtler, J.M. Peters, S.J. Smerdon, and M.B. Yaffe. 2011. Spatial exclusivity combined with positive and negative selection of phosphorylation motifs is the basis for context-dependent mitotic signaling. *Sci. Signal.* 4:35–37.

Alfieri, C., L. Chang, and D. Barford. 2018. Mechanism for remodelling of the cell cycle checkpoint protein MAD2 by the ATPase TRIP13. *Nature*. 559:274–278.

Alfieri, C., L. Chang, Z. Zhang, J. Yang, S. Maslen, M. Skehel, and D. Barford. 2016. Molecular basis of APC/C regulation by the spindle assembly checkpoint. *Nature*. 536:431–436.

Alfonso-Pérez, T., D. Hayward, J. Holder, F.A. Barr, and U. Gruneberg. 2019. MAD1-dependent recruitment of CDK1-CCNB1 to kinetochores promotes spindle checkpoint signaling. *J. Cell Biol.* 218:1108–1117.

Allan, L.A., M. Camacho Reis, G. Ciossani, P.J. Huis in 't Veld, S. Wohlgemuth, G.J. Kops, A. Musacchio, and A.T. Saurin. 2020. Cyclin B1 scaffolds MAD 1 at the kinetochore corona to activate the mitotic checkpoint. *EMBO J.* 39:e103180.

Alushin, G.M., V. Musinipally, D. Matson, J. Tooley, P. Todd, E. Nogales, C. Biology, M. Genetics, S. Division, L. Berkeley, and C. Biology. 2012. Multi-modal microtubule binding by the Ndc80 kinetochore complex. 19:1161–1167.

Alushin, G.M., V.H. Ramey, S. Pasqualato, D.A. Ball, N. Grigorieff, A. Musacchio, and E. Nogales. 2010. The Ndc80 kinetochore complex forms oligomeric arrays along microtubules. *Nature*. 467:805–810.

Álvarez-Fernández, M., R. Sánchez-Martínez, B. Sanz-Castillo, P.P. Gan, M. Sanz-Flores, M. Trakala, M. Ruiz-Torres, T. Lorca, A. Castro, and M. Malumbres. 2013. Greatwall is essential to prevent mitotic collapse after nuclear envelope breakdown in mammals. *Proc. Natl. Acad. Sci. U. S. A.* 110:17374–17379.

Amaro, A.C., C.P. Samora, R. Holtackers, E. Wang, I.J. Kingston, M. Alonso, M. Lampson, A.D. McAinsh, and P. Meraldi. 2010. Molecular control of kinetochore-microtubule dynamics and chromosome oscillations. *Nat. Cell Biol.* 12:319–329.

De Antoni, A., C.G. Pearson, D. Cimini, J.C. Canman, V. Sala, L. Nezi, M. Mapelli, L. Sironi, M. Faretta, E.D. Salmon, and A. Musacchio. 2005. The Mad1/Mad2 Complex as a Template for Mad2 Activation in the Spindle Assembly Checkpoint. *Curr. Biol.* 15:214–225.

Aravamudhan, P., A.A. Goldfarb, and A.P. Joglekar. 2015. The kinetochore encodes a mechanical switch to disrupt spindle assembly checkpoint signalling. *Nat. Cell Biol.* 17:868–879.

Bancroft, J., J. Holder, Z. Geraghty, T. Alfonso-Pérez, D. Murphy, F.A. Barr,

and U. Gruneberg. 2020. PP1 promotes cyclin B destruction and the metaphase-anaphase transition by dephosphorylating CDC20. *Mol. Biol. Cell*. 31:2315–2330.
Barr, A.R., and F. Gergely. 2007. Aurora-A: The maker and breaker of spindle poles. *J. Cell Sci.* 120:2987–2996.
Barr, F.A., P.R. Elliot, and U. Gruneberg. 2011. Protein phosphatases in the regulation of mitosis. *J. Cell Biol.* 124:2323–2334.
Barr, F.A., and U. Gruneberg. 2007. Cytokinesis: Placing and Making the Final Cut. *Cell*. 131:847–860.
Basto, R., R. Gomes, and R.E. Karess. 2000. Rough deal and Zw10 are required for the metaphase checkpoint in Drosophila. *Nat. Cell Biol.* 2:939–943.
Bentley, A., G. Normand, J. Hoyt, and R.W. King. 2007. Distinct Sequence Elements of Cyclin B1 Promote Localization to Chromatin, Centrosomes, and Kinetochores during Mitosis. *Mol. Biol. Cell*. 18:4847–4858.
Bhaduri, S., and P.M. Pryciak. 2011. Cyclin-specific docking motifs promote phosphorylation of yeast signaling proteins by G1/S Cdk complexes. *Curr. Biol.* 21:1615–1623.
Blake-Hodek, K.A., B.C. Williams, Y. Zhao, P. V. Castilho, W. Chen, Y. Mao, T.M. Yamamoto, and M.L. Goldberg. 2012. Determinants for Activation of the Atypical AGC Kinase Greatwall during M Phase Entry. *Mol. Cell. Biol.* 32:1337–1353.
Bolanos-Garcia, V.M., and T.L. Blundell. 2011. BUB1 and BUBR1: Multifaceted kinases of the cell cycle. *Trends Biochem. Sci.* 36:141–150.
Bollen, M., W. Peti, M.J. Ragusa, and M. Beullens. 2010. The extended PP1 toolkit: Designed to create specificity. *Trends Biochem. Sci.* 35:450–458.
Bouchoux, C., and F. Uhlmann. 2011. A quantitative model for ordered Cdk substrate dephosphorylation during mitotic exit. *Cell*. 147:803–814.
Brinkley, B.R., and E. Stubblefield. 1966. The fine structure of the kinetochore of a mammalian cell in vitro. *Chromosoma*. 19:28–43.
Buffin, E., C. Lefebvre, J. Huang, M.E. Gagou, and R.E. Karess. 2005. Recruitment of Mad2 to the kinetochore requires the Rod/Zw10 complex. *Curr. Biol.* 15:856–861.
Burgess, A., S. Vigneron, E. Brioudes, J.C. Labbé, T. Lorca, and A. Castro. 2010. Loss of human Greatwall results in G2 arrest and multiple mitotic defects due to deregulation of the cyclin B-Cdc2/PP2A balance. *Proc. Natl. Acad. Sci. U. S. A.* 107:12564–12569.
Caldas, G. V, T. Lynch, R.S. Anderson, S. Afreen, D. Varma, and J. DeLuca. 2015. The RZZ complex localizes to the N-terminus of KNL1 to mediate robust Mad1 kinetochore localization in human cells. *Open Biol.* 5:150160–150168.
Carmena, M., M. Wheelock, H. Funabiki, and W.C. Earnshaw. 2012. The chromosomal passenger complex (CPC): From easy rider to the godfather of mitosis. *Nat. Rev. Mol. Cell Biol.* 13:789–803.
Carroll, C.W., K.J. Milks, and A.F. Straight. 2010. Dual recognition of CENP-A nucleosomes is required for centromere assembly. *J. Cell Biol.* 189:1143–1155.
Carroll, C.W., M.C.C. Silva, K.M. Godek, L.E.T. Jansen, and A.F. Straight. 2009. Centromere assembly requires the direct recognition of CENP-A nucleosomes by CENP-N. *Nat. Cell Biol.* 11:896–902.

Cassimeris, L., C.L. Rieder, G. Rupp, and E.D. Salmon. 1990. Stability of microtubule attachment to metaphase kinetochores in PtK1 cells. *J. Cell Sci.* 96:9–15.
Castilho, P. V., B.C. Williams, S. Mochida, Y. Zhao, and M.L. Goldberg. 2009. The M Phase Kinase Greatwall (Gwl) Promotes Inactivation of PP2A/B55ϛ, a Phosphatase Directed Against CDK Phosphosites. *Mol. Biol. Cell*. 20:4524–4530.
Castro, A., and T. Lorca. 2018. Greatwall kinase at a glance. *J. Cell Sci.* 131:1–6.
Chae, H.B., J. Yun, Y.J. Bang, and D.Y. Shin. 2004. Cdk2-dependent phosphorylation of the NF-Y transcription factor is essential for the expression of the cell cycle-regulatory genes and cell cycle G1/S and G2/M transitions. *Oncogene*. 23:4084–4088.
Cheeseman, I.M. 2014. The Kinetochore. *Cold Spring Harb. Perspect. Biol.* 6:1–18.
Cheeseman, I.M., J.S. Chappie, E.M. Wilson-Kubalek, and A. Desai. 2006. The Conserved KMN Network Constitutes the Core Microtubule-Binding Site of the Kinetochore. *Cell*. 127:983–997.
Cheeseman, I.M., and A. Desai. 2008. Molecular architecture of the kinetochore-microtubule interface. *Nat. Rev. Mol. Cell Biol.* 9:33–46.
Cheeseman, I.M., T. Hori, T. Fukagawa, and A. Desai. 2008. KNL1 and the CENP-H/I/K Complex Coordinately Direct Kinetochore Assembly in Vertebrates. *Mol. Biol. Cell*. 19:587–294.
Chen, G.Y., F. Renda, H. Zhang, A. Gokden, D.Z. Wu, D.M. Chenoweth, A. Khodjakov, and M.A. Lampson. 2021. Tension promotes kinetochore–microtubule release by aurora B kinase. *J. Cell Biol.* 220:e202007030.
Chen, Q., X. Zhang, Q. Jiang, P.R. Clarke, and C. Zhang. 2008. Cyclin B1 is localized to unattached kinetochores and contributes to efficient microtubule attachment and proper chromosome alignment during mitosis. *Cell Res.* 18:268–280.
Ciferri, C., S. Pasqualato, E. Screpanti, G. Varetti, S. Santaguida, G. Dos Reis, A. Maiolica, J. Polka, J.G. De Luca, P. De Wulf, M. Salek, J. Rappsilber, C.A. Moores, E.D. Salmon, and A. Musacchio. 2008. Implications for Kinetochore-Microtubule Attachment from the Structure of an Engineered Ndc80 Complex. *Cell*. 133:427–439.
Cimini, D., and F. Degrassi. 2005. Aneuploidy: A matter of bad connections. *Trends Cell Biol.* 15:442–451.
Cimini, D., D. Fioravanti, E.D. Salmon, and F. Degrassi. 2002. Merotelic kinetochore orientation versus chromosome mono-orientation in the origin of lagging chromosomes in human primary cells. *J. Cell Sci.* 115:507–515.
Cimini, D., B. Howell, P. Maddox, A. Khodjakov, F. Degrassi, and E.D. Salmon. 2001. Merotelic kinetochore orientation is a major mechanism of aneuploidy in mitotic mammalian tissue cells. *J. Cell Biol.* 152:517–527.
Cimini, D., B. Moree, J.C. Canman, and E.D. Salmon. 2003. Merotelic kinetochore orientation occurs frequently during early mitosis in mammalian tissue cells and error correction is achieved by two different mechanisms. *J. Cell Sci.* 116:4213–4225.
Clute, P., and J. Pines. 1999. Temporal and spatial control of cyclin B1 destruction in metaphase. *Nat. Cell Biol.* 1:82–87.
Cohen, P.T.W. 2002. Protein phosphatase 1 - Targeted in many directions. *J.*

Cell Sci. 115:241–256.
Combes, G., I. Alharbi, L.G. Braga, and S. Elowe. 2017. Playing polo during mitosis: PLK1 takes the lead. *Oncogene*. 36:4819–4827.
Combes, G., H. Barysz, C. Garand, L. Gama Braga, I. Alharbi, P. Thebault, L. Murakami, D.P. Bryne, S. Stankovic, P.A. Eyers, V.M. Bolanos-Garcia, W.C. Earnshaw, J. Maciejowski, P. V. Jallepalli, and S. Elowe. 2018. Mps1 Phosphorylates Its N-Terminal Extension to Relieve Autoinhibition and Activate the Spindle Assembly Checkpoint. *Curr. Biol.* 28:872-883.e5.
Conti, D., P. Gul, A. Islam, J.M. Martín-Durán, R.W. Pickersgill, and V.M. Draviam. 2019. Kinetochores attached to microtubule-ends are stabilised by Astrin bound PP1 to ensure proper chromosome segregation. *Elife*. 8:1–28.
Cooke, C.A., M.M.S. Heck, and W.C. Earnshaw. 1987. The inner centromere protein (INCENP) antigens: Movement from inner centromere to midbody during mitosis. *J. Cell Biol.* 105:2053–2067.
Cordeiro, M.H., R.J. Smith, and A.T. Saurin. 2020. Kinetochore phosphatases suppress autonomous Polo-like kinase 1 activity to control the mitotic checkpoint. *J. Cell Biol.* 219:e202002020.
Cundell, M.J., R.N. Bastos, T. Zhang, J. Holder, U. Gruneberg, B. Novak, and F.A. Barr. 2013. The BEG (PP2A-B55/ENSA/Greatwall) Pathway Ensures Cytokinesis follows Chromosome Separation. *Mol. Cell*. 52:393–405.
Cundell, M.J., L.H. Hutter, R.N. Bastos, E. Poser, J. Holder, S. Mohammed, B. Novak, and F.A. Barr. 2016. A PP2A-B55 recognition signal controls substrate dephosphorylation kinetics during mitotic exit. *J. Cell Biol.* 214:539–554.
D'Angiolella, V., C. Mari, D. Nocera, L. Rametti, and D. Grieco. 2003. The spindle checkpoint requires cyclin-dependent kinase activity. *Genes Dev.* 17:2520–2525.
D P Cahill, J.Y. C Lengauer, G J Riggins, J K Willson, S D Markowitz, K W Kinzler, and B Vogelstein. 1998. Mutations of mitotic checkpoint genes in human cancers. *Nature*. 19:3–300.
Daum, J.R., T.A. Potapova, S. Sivakumar, J.J. Daniel, J.N. Flynn, S. Rankin, and G.J. Gorbsky. 2011. Cohesion fatigue induces chromatid separation in cells delayed at metaphase. *Curr. Biol.* 21:1018–1024.
DeAntoni, A., V. Sala, A. Musacchio, M. Herbert, J.K. Heriche, and T. Mitchison. 2005. Explaining the oligomerization properties of the spindle assembly checkpoint protein Mad2. *Philos. Trans. R. Soc. B Biol. Sci.* 360:637–648.
DeLuca, J.G., W.E. Gall, C. Ciferri, D. Cimini, A. Musacchio, and E.D. Salmon. 2006. Kinetochore Microtubule Dynamics and Attachment Stability Are Regulated by Hec1. *Cell*. 127:969–982.
DeLuca, J.G., B. Moree, J.M. Hickey, J. V. Kilmartin, and E.D. Salmon. 2002. hNuf2 inhibition blocks stable kinetochore-microtubule attachment and induces mitotic cell death in HeLa cells. *J. Cell Biol.* 159:549–555.
DeLuca, J.G., and A. Musacchio. 2012. Structural organization of the kinetochore-microtubule interface. *Curr. Opin. Cell Biol.* 24:48–56.
DeLuca, K.F., S.M.A. Lens, and J.G. DeLuca. 2011. Temporal changes in Hec1 phosphorylation control kinetochore - Microtubule attachment stability during mitosis. *J. Cell Sci.* 124:622–634.
Dephoure, N., C. Zhou, J. Villén, S.A. Beausoleil, C.E. Bakalarski, S.J. Elledge,

and S.P. Gygi. 2008. A quantitative atlas of mitotic phosphorylation. *Proc. Natl. Acad. Sci. U. S. A.* 105:10762–10767.
Desai, A., S. Rybina, T. Müller-Reichert, A. Shevchenko, A. Shevchenko, A. Hyman, and K. Oegema. 2003. KNL-1 directs assembly of the microtubule-binding interface of the kinetochore in C. elegans. *Genes Dev.* 17:2421–2435.
Desai, D., H.C. Wessling, R.P. Fisher, and D.O. Morgan. 1995. Effects of phosphorylation by CAK on cyclin binding by CDC2 and CDK2. *Mol. Cell. Biol.* 15:345–350.
Diaz-Martinez, L.A., W. Tian, B. Li, R. Warrington, L. Jia, C.A. Brautigam, X. Luo, and H. Yu. 2015. The Cdc20-binding Phe Box of the Spindle Checkpoint Protein BubR1 Maintains the Mitotic Checkpoint Complex During Mitosis. *J. Biol. Chem.* 290:2431–2443.
Dimitrova, Y.N., S. Jenni, R. Valverde, Y. Khin, and S.C. Harrison. 2016. Structure of the MIND Complex Defines a Regulatory Focus for Yeast Kinetochore Assembly. *Cell*. 167:1014–1027.
Diril, M.K., X. Bisteau, M. Kitagawa, M.J. Caldez, S. Wee, J. Gunaratne, S.H. Lee, and P. Kaldis. 2016. Loss of the Greatwall Kinase Weakens the Spindle Assembly Checkpoint. *PLoS Genet.* 12:1–26.
Dobles, M., V. Liberal, M.L. Scott, R. Benezra, and P.K. Sorger. 2000. Chromosome missegregation and apoptosis in mice lacking the mitotic checkpoint protein Mad2. *Cell*. 101:635–645.
Dodson, C.A., T. Haq, S. Yeoh, A.M. Fry, and R. Bayliss. 2013. The structural mechanisms that underpin mitotic kinase activation. *Biochem. Soc. Trans.* 41:1037–1041.
Dohadwala, M., E.E.F. Da Cruz Silva, F.L. Hall, R.T. Williams, D.A. Carbonaro-Hall, A.C. Nairn, P. Greengard, and N. Berndt. 1994. Phosphorylation and inactivation of protein phosphatase 1 by cyclin- dependent kinases. *Proc. Natl. Acad. Sci. U. S. A.* 91:6408–6412.
Dou, Z., C. von Schubert, R. Körner, A. Santamaria, S. Elowe, and E.A. Nigg. 2011. Quantitative mass spectrometry analysis reveals similar substrate consensus motif for human Mps1 kinase and Plk1. *PLoS One*. 6:e18793.
Draetta, G., L. Brizuela, J. Potashkin, and D. Beach. 1987. Identification of p34 and p13, human homologs of the cell cycle regulators of fission yeast encoded by cdc2+ and suc1+. *Cell*. 50:319–325.
Dunsch, A.K., E. Linnane, F.A. Barr, and U. Gruneberg. 2011. The astrin-kinastrin/SKAP complex localizes to microtubule plus ends and facilitates chromosome alignment. *J. Cell Biol.* 192:959–968.
Dynlacht, B.D., J.A. Lees, and E. Harlow. 1994. Differential regulation of E2F trans-activation by cyclin / cdk2 complexes. *Genes Dev.* 130:1772–1786.
Egloff, M.-P., D.F. Johnson, G. Moorhead, P.T.W. Cohen, P. Cohen, and D. Barford. 1997. Structural basis for the recognition of regulatory subunits by the catalytic subunit of protein phosphatase 1 location, organelle or process (reviewed in Hubbard and. *EMBO J.* 16:1876–1887.
Elia, A.E.H., L.C. Cantley, and M.B. Yaffe. 2003a. Proteomic screen finds pSer/pThr-binding domain localizing Plk1 to mitotic substrates. *Science.* 299:1228–1231.
Elia, A.E.H., P. Rellos, L.F. Haire, J.W. Chao, F.J. Ivins, K. Hoepker, D. Mohammad, L.C. Cantley, S.J. Smerdon, and M.B. Yaffe. 2003b. The molecular basis for phosphodependent substrate targeting and regulation

of Plks by the Polo-box domain. *Cell*. 115:83–95.
Elledge, S.J., and M.R. Spottswood. 1991. A new human p34 protein kinase, CDK2, identified by complementation of a cdc28 mutation in Saccharomyces cerevisiae, is a homolog of Xenopus Eg1. *EMBO J.* 10:2653–2659.
Elowe, S., S. Hümmer, A. Uldschmid, X. Li, and E.A. Nigg. 2007. Tension-sensitive Plk1 phosphorylation on BubR1 regulates the stability of kinetochore-microtubule interactions. *Genes Dev.* 21:2205–2219.
Emanuele, M.J., W. Lan, M. Jwa, S.A. Miller, C.S.M. Chan, and P.T. Stukenberg. 2008. Aurora B kinase and protein phosphatase 1 have opposing roles in modulating kinetochore assembly. *J. Cell Biol.* 181:241–254.
Espert, A., P. Uluocak, R.N. Bastos, D. Mangat, P. Graab, and U. Gruneberg. 2014. PP2A-B56 opposes Mps1 phosphorylation of Knl1 and thereby promotes spindle assembly checkpoint silencing. *J. Cell Biol.* 206:833–842.
Espeut, J., D.K. Cheerambathur, L. Krenning, K. Oegema, and A. Desai. 2012. Microtubule binding by KNL-1 contributes to spindle checkpoint silencing at the kinetochore. *J. Cell Biol.* 196:469–482.
Espeut, J., P. Lara-Gonzalez, M. Sassine, A. Shiau, A. Desai, and A. Abrieu. 2015. Natural loss of Mps1 kinase in nematodes uncovers a role for Polo-like kinase 1 in spindle checkpoint initiation Julien. *Cell Rep.* 12:100–106.
Evans, T., E.T. Rosenthal, J. Youngblom, D. Distel, and T. Hunt. 1983. Cyclin: A protein specified by maternal mRNA in sea urchin eggs that is destroyed at each cleavage division. *Cell*. 33:389–396.
Faesen, A.C., M. Thanasoula, S. Maffini, C. Breit, F. Müller, S. Van Gerwen, T. Bange, and A. Musacchio. 2017. Basis of catalytic assembly of the mitotic checkpoint complex. *Nature*. 542:498–502.
Fang, G. 2002. Checkpoint Protein BubR1 Acts Synergistically with Mad2 to Inhibit Anaphase-promoting Complex. *Mol. Biol. Cell*. 13:2170–2179.
Fang, G., H. Yu, and M.W. Kirschner. 1998. The checkpoint protein MAD2 and the mitotic regulator CDC20 form a ternary complex with the anaphase-promoting complex to control anaphase initiation. *Genes Dev.* 12:1871–1883.
Di Fiore, B., N.E. Davey, A. Hagting, D. Izawa, J. Mansfeld, T.J. Gibson, and J. Pines. 2015. The ABBA motif binds APC/C activators and is shared by APC/C substrates and regulators. *Dev. Cell*. 32:358–372.
Di Fiore, B., C. Wurzenberger, N.E. Davey, and J. Pines. 2016. The Mitotic Checkpoint Complex Requires an Evolutionary Conserved Cassette to Bind and Inhibit Active APC/C. *Mol. Cell*. 64:1144–1153.
Foley, E.A., and T.M. Kapoor. 2013. Microtubule attachment and spindle assembly checkpoint signalling at the kinetochore. *Nat. Rev. Mol. Cell Biol.* 14:25–37.
Foley, E.A., M. Maldonado, and T.M. Kapoor. 2011. Formation of stable attachments between kinetochores and microtubules depends on the B56-PP2A phosphatase. *Nat. Cell Biol.* 13:1265–1271.
Foltz, D.R., L.E.T. Jansen, B.E. Black, A.O. Bailey, J.R. Yates, and D.W. Cleveland. 2006. The human CENP-A centromeric nucleosome-associated complex. *Nat. Cell Biol.* 8:458–469.
Foster, S.A., and D.O. Morgan. 2012. The APC/C Subunit Mnd2/Apc15 Promotes Cdc20 Autoubiquitination and Spindle Assembly Checkpoint

Inactivation. *Mol. Cell*. 47:921–932.
Francisco, L., W. Wang, and C.S. Chan. 1994. Type 1 protein phosphatase acts in opposition to IpL1 protein kinase in regulating yeast chromosome segregation. *Mol. Cell. Biol.* 14:4731–4740.
Fueller, J., K. Herbst, M. Meurer, K. Gubicza, B. Kurtulmus, J.D. Knopf, and D. Kirrmaier. 2020. CRISPR-Cas12a – assisted PCR tagging of mammalian genes. *J. Cell Biol.* 219:e201910210.
Fujimitsu, K., M. Grimaldi, and H. Yamano. 2016. Cyclin-dependent kinase 1 – dependent activation of APC/C ubiquitin ligase. *Cell Cycle*. 352:1121–1124.
Fujimitsu, K., and H. Yamano. 2020. PP2A-B56 binds to Apc1 and promotes Cdc20 association with the APC/C ubiquitin ligase in mitosis. *EMBO Rep.* 21:1–12.
Gabrielli, B.G., J.M. Clark, A.K. McCormack, and K.A.O. Ellem. 1997. Hyperphosphorylation of the N-terminal domain of cdc25 regulates activity toward cyclin B1/cdc2 but not cyclin A/cdk2. *J. Biol. Chem.* 272:28607–28614.
Gascoigne, K.E., and I.M. Cheeseman. 2013. CDK-dependent phosphorylation and nuclear exclusion coordinately control kinetochore assembly state. *J. Cell Biol.* 201:23–32.
Gascoigne, K.E., K. Takeuchi, A. Suzuki, T. Hori, T. Fukagawa, and I.M. Cheeseman. 2011. Induced ectopic kinetochore assembly bypasses the requirement for CENP-A nucleosomes. *Cell*. 145:410–422.
Gassmann, R., A.J. Holland, D. Varma, X. Wan, F. Çivril, D.W. Cleveland, K. Oegema, E.D. Salmon, and A. Desai. 2010. Removal of Spindly from microtubule-attached kinetochores controls spindle checkpoint silencing in human cells. *Genes Dev.* 24:957–971.
Geraghty, Z., C. Barnard, P. Uluocak, and U. Gruneberg. 2021. The association of Plk1 with the astrin-kinastrin complex promotes formation and maintenance of a metaphase plate. *J. Cell Sci.* 134:1–10.
Gharbi-Ayachi, A., J.C. Labbé, A. Burgess, S. Vigneron, J.-M. Strub, E. Brioudes, A. Van-Dorsselaer, A. Castro, and T. Lorca. 2010. The Substrate of Greatwall Kinase, Arpp19, Controls Mitosis by Inhibiting Protein Phosphatase 2A. *Science.* 330:1673–1677.
Gould, K.L., and P. Nurse. 1989. Tyrosine phosphorylation of the fission yeast cdc2+ protein kinase regulates entry into mitosis. *Nature*. 342:39–45.
Grallert, A., E. Boke, A. Hagting, B. Hodgson, Y. Connolly, J.R. Griffiths, D.L. Smith, J. Pines, and I.M. Hagan. 2015. A PP1-PP2A phosphatase relay controls mitotic progression. *Nature*. 517:94–98.
Gruneberg, U., R. Neef, R. Honda, E.A. Nigg, and F.A. Barr. 2004. Relocation of Aurora B from centromeres to the central spindle at the metaphase to anaphase transition requires MKlp2. *J. Cell Biol.* 166:167–172.
Guse, A., C.W. Carroll, B. Moree, C.J. Fuller, and A.F. Straight. 2011. In vitro centromere and kinetochore assembly on defined chromatin templates. *Nature*. 477:354–358.
Habu, T., S.H. Kim, J. Weinstein, and T. Matsumoto. 2002. Identification of a MAD2-binding protein, CMT2, and its role in mitosis. *EMBO J.* 21:6419–6428.
Häfner, J., M.I. Mayr, M.M. Möckel, and T.U. Mayer. 2014. Pre-anaphase chromosome oscillations are regulated by the antagonistic activities of

Cdk1 and PP1 on Kif18A. *Nat. Commun.* 5:1–14.
Hanahan, D., and R.A. Weinberg. 2011. Hallmarks of cancer: The next generation. *Cell*. 144:646–674.
Hanks, S.K. 1987. Homology probing: Identification of cDNA clones encoding members of the protein-serine kinase family. *Proc. Natl. Acad. Sci. U. S. A.* 84:388–392.
Hartwell, L.H., and T.A. Weinert. 1989. Checkpoints: Controls that ensure the order of cell cycle events. *Science.* 246:629–634.
Harvey, S.L., A. Charlet, W. Haas, S.P. Gygi, and D.R. Kellogg. 2005. Cdk1-dependent regulation of the mitotic inhibitor Wee1. *Cell*. 122:407–420.
Hayward, D., T. Alfonso-Pérez, M.J. Cundell, M. Hopkins, J. Holder, J. Bancroft, L.H. Hutter, B. Novak, F.A. Barr, and U. Gruneberg. 2019a. CDK1-CCNB1 creates a spindle checkpoint-permissive state by enabling MPS1 kinetochore localization. *J. Cell Biol.* 218:1182–1199.
Hayward, D., T. Alfonso-Pérez, and U. Gruneberg. 2019b. Orchestration of the spindle assembly checkpoint by CDK 1-cyclin B1. *FEBS Lett.* 593:1–19.
Hayward, D., J. Bancroft, D. Mangat, T. Alfonso-Pérez, S. Dugdale, J. McCarthy, F.A. Barr, and U. Gruneberg. 2019c. Checkpoint signaling and error correction require regulation of the MPS1 T-loop by PP2A-B56. *J. Cell Biol.* 218:3188–3199.
Hayward, D., E. Roberts, and U. Gruneberg. 2022. MPS1 localizes to microtubule-attached kinetochores and actively promotes microtubule release. *Curr. Biol.* 32:5200–5208.
Heim, A., A. Konietzny, and T.U. Mayer. 2015. Protein phosphatase 1 is essential for Greatwall inactivation at mitotic exit. *EMBO Rep.* 16:1501–1510.
Hein, J.B., E.P.T. Hertz, D.H. Garvanska, T. Kruse, and J. Nilsson. 2017. Distinct kinetics of serine and threonine dephosphorylation are essential for mitosis. *Nat. Cell Biol.* 19:1433–1440.
Hellwig, D., C. Hoischen, T. Ulbricht, and S. Diekmann. 2009. Acceptor-photobleaching FRET analysis of core kinetochore and NAC proteins in living human cells. *Eur. Biophys. J.* 38:781–791.
Hendrickx, A., M. Beullens, H. Ceulemans, T. Den Abt, A. Van Eynde, E. Nicolaescu, B. Lesage, and M. Bollen. 2009. Docking Motif-Guided Mapping of the Interactome of Protein Phosphatase-1. *Chem. Biol.* 16:365–371.
Hertz, E.P.T., T. Kruse, N.E. Davey, B. López-Méndez, J.O. Sigurðsson, G. Montoya, J. V. Olsen, and J. Nilsson. 2016. A Conserved Motif Provides Binding Specificity to the PP2A-B56 Phosphatase. *Mol. Cell*. 63:686–695.
Heun, P., S. Erhardt, M.D. Blower, S. Weiss, A.D. Skora, and G.H. Karpen. 2006. Mislocalization of the drosophila centromere-specific histone CID promotes formation of functional ectopic kinetochores. *Dev. Cell*. 10:303–315.
Hewitt, L., A. Tighe, S. Santaguida, A.M. White, C.D. Jones, A. Musacchio, S. Green, and S.S. Taylor. 2010. Sustained Mps1 activity is required in mitosis to recruit O-Mad2 to the Mad1-C-Mad2 core complex. *J. Cell Biol.* 190:25–34.
Higashi, H., I. Suzuki-Takahashi, Y. Taya, K. Segawa, S. Nishimura, and M. Kitagawa. 1995. Differences in substrate specificity between Cdk2-cyclin A and Cdk2-cyclin E in vitro. *Biochem. Biophys. Res. Commun.* 216:520–

525.
Hinshaw, S.M., and S.C. Harrison. 2019. The structure of the ctf19c/ccan from budding yeast. *Elife*. 8:1–20.
Hiraga, S., T. Ly, J. Garzón, Z. Hořejší, Y. Ohkubo, A. Endo, C. Obuse, S.J. Boulton, A.I. Lamond, and A.D. Donaldson. 2017. Human RIF 1 and protein phosphatase 1 stimulate DNA replication origin licensing but suppress origin activation . *EMBO Rep.* 18:403–419.
Hiruma, Y., C. Sacristan, S.T. Pachis, A. Adamopoulous, T. Kuijt, M. Ubbink, E. Von Castelmur, A. Perrakis, and G.J.P.L. Kops. 2015. Competition between microtubules and MPS1 kinase for kinetochore binding directly regulates spindle checkpoint signaling. *Science.* 348:1264–1267.
Hoffmann, I., P.R. Clarke, M.J. Marcote, E. Karsenti, and G. Draetta. 1993. Phosphorylation and activation of human cdc25-C by cdc2-cyclin B and its involvement in the self-amplification of MPF at mitosis. *EMBO J.* 12:53–63.
Holder, J., S. Mohammed, and F.A. Barr. 2020. Ordered dephosphorylation initiated by the selective proteolysis of cyclin B drives mitotic exit. *Elife*. 9:1–33.
Van Hooser, A.A., I.I. Ouspenski, H.C. Gregson, D.A. Starr, T.J. Yen, M.L. Goldberg, K. Yokomori, W.C. Earnshaw, K.F. Sullivan, and B.R. Brinkley. 2001. Specification of kinetochore-forming chromatin by the histone H3 variant CENP-A. *J. Cell Sci.* 114:3529–3542.
Hori, T., M. Amano, A. Suzuki, C.B. Backer, J.P. Welburn, Y. Dong, B.F. McEwen, W.H. Shang, E. Suzuki, K. Okawa, I.M. Cheeseman, and T. Fukagawa. 2008. CCAN Makes Multiple Contacts with Centromeric DNA to Provide Distinct Pathways to the Outer Kinetochore. *Cell*. 135:1039–1052.
Hori, T., W.H. Shang, K. Takeuchi, and T. Fukagawa. 2013. The CCAN recruits CENP-A to the centromere and forms the structural core for kinetochore assembly. *J. Cell Biol.* 200:45–60.
Hornbeck, P. V., B. Zhang, B. Murray, J.M. Kornhauser, V. Latham, and E. Skrzypek. 2015. PhosphoSitePlus, 2014: Mutations, PTMs and recalibrations. *Nucleic Acids Res.* 43:D512–D520.
Hornig, N.C.D., P.P. Knowles, N.Q. McDonald, and F. Uhlmann. 2002. The dual mechanism of separase regulation by securin. *Curr. Biol.* 12:973–982.
Howell, B.J., B.F. McEwen, J.C. Canman, D.B. Hoffman, E.M. Farrar, C.L. Rieder, and E.D. Salmon. 2001. Cytoplasmic dynein/dynactin drives kinetochore protein transport to the spindle poles and has a role in mitotic spindle checkpoint inactivation. *J. Cell Biol.* 155:1159–1172.
Hoyt, M.A., L. Totis, and B.T. Roberts. 1991. S. cerevisiae genes required for cell cycle arrest in response to loss of microtubule function. *Cell*. 66:507–517.
Huis in ’t Veld, P.J., S. Jeganathan, A. Petrovic, P. Singh, J. John, V. Krenn, F. Weissmann, T. Bange, and A. Musacchio. 2016. Molecular basis of outer kinetochore assembly on CENP-T. *Elife*. 5:1–24.
Hümmer, S., and T.U. Mayer. 2009. Cdk1 Negatively Regulates Midzone Localization of the Mitotic Kinesin Mklp2 and the Chromosomal Passenger Complex. *Curr. Biol.* 19:607–612.
Hunt, T. 1989. Maturation promoting factor, cyclin and the control of M-phase. *Curr. Opin. Cell Biol.* 1:268–274.
Hwang, S., P. Cavaliere, R. Li, L.J. Zhu, N. Dephoure, and E.M. Torres. 2021. Consequences of aneuploidy in human fibroblasts with trisomy 21. *Proc.*

Natl. Acad. Sci. U. S. A. 118:e2014723118.
Ikeda, M., and K. Tanaka. 2017. Plk1 bound to Bub1 contributes to spindle assembly checkpoint activity during mitosis. *Sci. Rep.* 7:1–15.
Invitrogen. 2012. For Generating Stable , Inducible Mammalian Expression Cell Lines by Flp Recombinase-Mediated Integration.
Izawa, D., and J. Pines. 2015. The mitotic checkpoint complex binds a second CDC20 to inhibit active APC/C. *Nature*. 517:631–634.
Izuta, H., M. Ikeno, N. Suzuki, T. Tomonaga, N. Nozaki, C. Obuse, Y. Kisu, N. Goshima, F. Nomura, N. Nomura, and K. Yoda. 2006. Comprehensive analysis of the ICEN (Interphase Centromere Complex) components enriched in the CENP-A chromatin of human cells. *Genes to Cells*. 11:673–684.
Jackman, M., C. Marcozzi, M. Barbiero, M. Pardo, L. Yu, A.L. Tyson, J.S. Choudhary, and J. Pines. 2020. Cyclin B1-Cdk1 facilitates MAD1 release from the nuclear pore to ensure a robust spindle checkpoint. *J. Cell Biol.* 219.
Jacobs, C.W., A.E. Adams, P.J. Szaniszlo, and J.R. Pringle. 1988. Functions of microtubules in the Saccharomyces cerevisiae cell cycle. *J. Cell Biol.* 107:1409–1426.
Jansen, L.E.T., B.E. Black, D.R. Foltz, and D.W. Cleveland. 2007. Propagation of centromeric chromatin requires exit from mitosis. *J. Cell Biol.* 176:795–805.
Janssens, V., and J. Goris. 2001. Protein phosphatase 2A: A highly regulated family of serine/threonine phosphatases implicated in cell growth and signalling. *Biochem. J.* 353:417–439.
Jelluma, N., A.B. Brenkman, N.J.F. van den Broek, C.W.A. Cruijsen, M.H.J. van Osch, S.M.A. Lens, R.H. Medema, and G.J.P.L. Kops. 2008a. Mps1 Phosphorylates Borealin to Control Aurora B Activity and Chromosome Alignment. *Cell*. 132:233–246.
Jelluma, N., A.B. Brenkman, I. McLeod, J.R. Yates, D.W. Cleveland, R.H. Medema, and G.J.P.L. Kops. 2008b. Chromosomal instability by inefficient Mps1 auto-activation due to a weakened mitotic checkpoint and lagging chromosomes. *PLoS One*. 3:1–8.
Jelluma, N., T.B. Dansen, T. Sliedrecht, N.P. Kwiatkowski, and G.J.P.L. Kops. 2010. Release of Mps1 from kinetochores is crucial for timely anaphase onset. *J. Cell Biol.* 191:281–290.
Ji, Z., H. Gao, L. Jia, B. Li, and H. Yu. 2017. A sequential multi-target Mps1 phosphorylation cascade promotes spindle checkpoint signaling. *Elife*. 6:1–23.
Ji, Z., H. Gao, and H. Yu. 2015. Kinetochore attachment sensed by competitive Mps1 and microtubule binding to Ndc80C. *Science.* 348:1260–1264.
Jokelainen, P.T. 1967. The ultrastructure and spatial organization of the metaphase kinetochore in mitotic rat cells. *J. Ultrasructure Res.* 19:19–44.
Kalitsis, P., E. Earle, K.J. Fowler, and K.H.A. Choo. 2000. Bub3 gene disruption in mice reveals essential mitotic spindle checkpoint function during early embryogenesis. *Genes Dev.* 14:2277–2282.
Kang, J., Y. Chen, Y. Zhao, and H. Yu. 2007. Autophosphorylation-dependent activation of human Mps1 is required for the spindle checkpoint. *Proc. Natl. Acad. Sci. U. S. A.* 104:20232–20237.
Kato, H., J. Jiang, B.R. Zhou, M. Rozendaal, H. Feng, R. Ghirlando, T.S. Xiao,

A.F. Straight, and Y. Bai. 2013. A conserved mechanism for centromeric nucleosome recognition by centromere protein CENP-C. *Science.* 340:1110–1113.
Kellogg, D.R. 2003. Wee1-dependent mechanisms required for coordination of cell growth and cell division. *J. Cell Sci.* 116:4883–4890.
Kim, S., and H. Yu. 2015. Multiple assembly mechanisms anchor the KMN spindle checkpoint platform at human mitotic kinetochores. *J. Cell Biol.* 208:181–196.
Kim, T., P. Lara-Gonzalez, B. Prevo, F. Meitinger, D.K. Cheerambathur, K. Oegema, and A. Desai. 2017. Kinetochores accelerate or delay APC/C activation by directing Cdc20 to opposing fates. *Genes Dev.* 31:1089–1094.
Kim, Y., A.J. Holland, W. Lan, and D.W. Cleveland. 2010. Aurora kinases and protein phosphatase 1 mediate chromosome congression through regulation of CENP-E. *Cell*. 142:444–455.
King, R.W., J.M. Peters, S. Tugendreich, M. Rolfe, P. Hieter, and M.W. Kirschner. 1995. A 20s complex containing CDC27 and CDC16 catalyzes the mitosis-specific conjugation of ubiquitin to cyclin B. *Cell*. 81:279–288.
Kiss, A., F. Erdődi, and B. Lontay. 2019. Myosin phosphatase: Unexpected functions of a long-known enzyme. *Biochim. Biophys. Acta - Mol. Cell Res.* 1866:2–15.
Kitagawa, M., S.Y.S. Fung, U.F.S. Hameed, H. Goto, M. Inagaki, and S.H. Lee. 2014. Cdk1 coordinates timely activation of MKlp2 kinesin with relocation of the chromosome passenger complex for cytokinesis. *Cell Rep.* 7:166–179.
Klare, K., J.R. Weir, F. Basilico, T. Zimniak, L. Massimiliano, N. Ludwigs, F. Herzog, and A. Musacchio. 2015. CENP-C is a blueprint for constitutive centromere-associated network assembly within human kinetochores. *J. Cell Biol.* 210:11–22.
Kline, S.L., I.M. Cheeseman, T. Hori, T. Fukagawa, and A. Desai. 2006. The human Mis12 complex is required for kinetochore assembly and proper chromosome segregation. *J. Cell Biol.* 173:9–17.
Kops, G.J.P.L., and R. Gassmann. 2020. Crowning the Kinetochore: The Fibrous Corona in Chromosome Segregation. *Trends Cell Biol.* 30:653–667.
Kops, G.J.P.L., B.A.A. Weaver, and D.W. Cleveland. 2005. On the road to cancer: Aneuploidy and the mitotic checkpoint. *Nat. Rev. Cancer*. 5:773–785.
Krenn, V., A. Wehenkel, X. Li, S. Santaguida, and A. Musacchio. 2012. Structural analysis reveals features of the spindle checkpoint kinase Bub1-kinetochore subunit Knl1 interaction. *J. Cell Biol.* 196:451–467.
Kruse, T., G. Zhang, M.S.Y. Larsen, T. Lischetti, W. Streicher, T.K. Nielsen, S.P. Bjørn, and J. Nilsson. 2013. Direct binding between BubR1 and B56-PP2A phosphatase complexes regulate mitotic progression. *J. Cell Sci.* 126:1086–1092.
Kulukian, A., J.S. Han, and D.W. Cleveland. 2009. Unattached Kinetochores Catalyze Production of an Anaphase Inhibitor that Requires a Mad2 Template to Prime Cdc20 for BubR1 Binding. *Dev. Cell*. 16:105–117.
Labit, H., K. Fujimitsu, N.S. Bayin, T. Takaki, J. Gannon, and H. Yamano. 2012. Dephosphorylation of Cdc20 is required for its C-box-dependent activation

of the APC/C. *EMBO J.* 31:3351–3362.
Lammer, C., S. Wagerer, R. Saffrich, D. Mertens, W. Ansorge, and I. Hoffmann. 1998. The cdc25B phosphatase is essential for the G2/M phase transition in human cells. *J. Cell Sci.* 111:2445–2453.
Lampson, M.A., K. Renduchitala, A. Khodjakov, and T.M. Kapoor. 2004. Correcting improper chromosomes-spindle attachments during cell division. *Nat. Cell Biol.* 6:232–237.
Laoukili, J., M. Alvarez, L.A.T. Meijer, M. Stahl, S. Mohammed, L. Kleij, A.J.R. Heck, and R.H. Medema. 2008. Activation of FoxM1 during G 2 Requires Cyclin A/Cdk-Dependent Relief of Autorepression by the FoxM1 N-Terminal Domain . *Mol. Cell. Biol.* 28:3076–3087.
Lara-Gonzalez, P., F.G. Westhorpe, and S.S. Taylor. 2012. The spindle assembly checkpoint. *Curr. Biol.* 22:R966–R980.
Lee, M.G., and P. Nurse. 1987. Complementation used to clone a human homologue of the fission yeast cell cycle control gene cdc2. *Nature*. 327:31–35.
Lehner, C.F., and P.H. O'Farrell. 1990. The Roles of Drosophila Cyclins A and B in Mitotic Control. *Cell*. 61:553–54.
Levine, M.S., and A.J. Holland. 2018. The impact of mitotic errors on cell proliferation and tumorigenesis. *Genes Dev.* 32:620–638.
Li, R., and A.W. Murray. 1991. Feedback Control of Mitosis in Budding Yeast. *Cell*. 66:519–531.
Li, X., and R.B. Nicklas. 1995. Mitotic forces control a cell-cycle checkpoint. *Nature*. 373:630–632.
Liu, D., and M.A. Lampson. 2009. Regulation of kinetochore-microtubule attachments by Aurora B kinase. *Biochem. Soc. Trans.* 37:976–980.
Liu, D., G. Vader, M.J.M. Vromans, M.A. Lampson, and S.M.A. Lens. 2009. Sensing Chromosome Bi-Orientation by Spatial Separation of Aurora B Kinase from Kinetochore Substrates. *Science.* 323:1350–1354.
Liu, D., M. Vleugel, C.B. Backer, T. Hori, T. Fukagawa, I.M. Cheeseman, and M.A. Lampson. 2010. Regulated targeting of protein phosphatase 1 to the outer kinetochore by KNL1 opposes Aurora B kinase. *J. Cell Biol.* 188:809–820.
Liu, S.T., J.B. Rattner, S.A. Jablonski, and T.J. Yen. 2006. Mapping the assembly pathways that specify formation of the trilaminar kinetochore plates in human cells. *J. Cell Biol.* 175:41–53.
Liu, X., and M. Winey. 2012. The MPS1 family of protein kinases. *Annu. Rev. Biochem.* 81:561–585.
London, N., S. Ceto, J.A. Ranish, and S. Biggins. 2012. Phosphoregulation of Spc105 by Mps1 and PP1 Regulates Bub1 Localization to Kinetochores. *Curr. Biol.* 22:900–906.
Loog, M., and D.O. Morgan. 2005. Cyclin specificity in the phosphorylation of cyclin-dependent kinase substrates. *Nature*. 434:104–108.
Losiewicz, M.D., B.A. Carlson, G. Kaur, E.A. Sausville, and P.J. Worland. 1994. Potent Inhibition of Cdc2 Kinase Activity by the Flavonoid L86-8275. *Biochem. Biophys. Res. Commun.* 201:589–595.
Lucocq, J., G. Warren, and J. Pryde. 1991. Okadaic acid induces Golgi apparatus fragmentation and arrest of intracellular transport. *J. Cell Sci.* 100:753–759.
Luo, X., Z. Tang, G. Xia, K. Wassmann, T. Matsumoto, J. Rizo, and H. Yu.

2004. The Mad2 spindle checkpoint protein has two distinct natively folded states. *Nat. Struct. Mol. Biol.* 11:338–345.
Luo, X., and H. Yu. 2008. Protein Metamorphosis: The Two-State Behavior of Mad2. *Structure*. 16:1616–1625.
Ma, S., S. Vigneron, P. Robert, J.M. Strub, S. Cianferani, A. Castro, and T. Lorca. 2016. Greatwall dephosphorylation and inactivation upon mitotic exit is triggered by PP1. *J. Cell Sci.* 129:1329–1339.
Maciejowski, J., H. Drechsler, K. Grundner-Culemann, E.R. Ballister, J.A. Rodriguez-Rodriguez, V. Rodriguez-Bravo, M.J.K. Jones, E. Foley, M.A. Lampson, H. Daub, A.D. McAinsh, and P. V. Jallepalli. 2017. Mps1 Regulates Kinetochore-Microtubule Attachment Stability via the Ska Complex to Ensure Error-Free Chromosome Segregation. *Dev. Cell*. 41:143–156.
Maiato, H., J. DeLuca, E.D. Salmon, and W.C. Earnshaw. 2004. The dynamic kinetochore-microtubule interface. *J. Cell Sci.* 117:5461–5477.
Major, M.L., R. Lepe, and R.H. Costa. 2004. Forkhead Box M1B Transcriptional Activity Requires Binding of Cdk-Cyclin Complexes for Phosphorylation-Dependent Recruitment of p300/CBP Coactivators. *Mol. Cell. Biol.* 24:2649–2661.
Mali, P., J. Aach, B.P. Stranges, K.M. Esvelt, M. Moosburner, S. Kosuri, L. Yang, and G.M. Church. 2013. CAS9 transcriptional activators for target specificity screening and paired nickases for cooperative genome engineering. *Nat. Biotechnol.* 31:833–838.
Mansfeld, J., P. Collin, M.O. Collins, J.S. Choudhary, and J. Pines. 2011. APC15 drives the turnover of MCC-CDC20 to make the spindle assembly checkpoint responsive to kinetochore attachment. *Nat. Cell Biol.* 13:1234–1243.
Mapelli, M., F. V. Filipp, G. Rancati, L. Massimiliano, L. Nezi, G. Stier, R.S. Hagan, S. Confalonieri, S. Piatti, M. Sattler, and A. Musacchio. 2006. Determinants of conformational dimerization of Mad2 and its inhibition by p31comet. *EMBO J.* 25:1273–1284.
Maresca, T.J., and E.D. Salmon. 2009. Intrakinetochore stretch is associated with changes in kinetochore phosphorylation and spindle assembly checkpoint activity. *J. Cell Biol.* 184:373–381.
Masui, Y., and C.L. Markert. 1971. Cytoplasmic control of nuclear behavior during meiotic maturation of frog oocytes. *J. Exp. Zool.* 90:461–466.
Mattison, C.P., W.M. Old, E. Steiner, B.J. Huneycutt, K.A. Resing, N.G. Ahn, and M. Winey. 2007. Mps1 activation loop autophosphorylation enhances kinase activity. *J. Biol. Chem.* 282:30553–30561.
Maure, J.F., E. Kitamura, and T.U. Tanaka. 2007. Mps1 Kinase Promotes Sister-Kinetochore Bi-orientation by a Tension-Dependent Mechanism. *Curr. Biol.* 17:2175–2182.
May, K.M., and K.G. Hardwick. 2006. The spindle checkpoint. *J. Cell Sci.* 119:4139–4142.
McCleland, M.L., M.J. Kallio, G.A. Barrett-Wilt, C.A. Kestner, J. Shabanowitz, D.F. Hunt, G.J. Gorbsky, and P.T. Stukenberg. 2004. The Vertebrate Ndc80 Complex Contains Spc24 and Spc25 Homologs, which Are Required to Establish and Maintain Kinetochore-Microtubule Attachment. *Curr. Biol.* 14:131–137.
Meadows, J.C., L.A. Shepperd, V. Vanoosthuyse, T.C. Lancaster, A.M. Sochaj,

G.J. Buttrick, K.G. Hardwick, and J.B.A. Millar. 2011. Spindle checkpoint silencing requires association of PP1 to both Spc7 and kinesin-8 motors. *Dev. Cell*. 20:739–750.
Meraldi, P., V.M. Draviam, and P.K. Sorger. 2004. Timing and checkpoints in the regulation of mitotic progression. *Dev. Cell*. 7:45–60.
Minshull, J., R. Golsteyn, C.S. Hill, and T. Hunt. 1990. The A- and B-type cyclin associated cdc2 kinases in Xenopus turn on and off at different times in the cell cycle. *EMBO J.* 9:2865–2875.
Mochida, S., S.L. Maslen, M. Skehel, and T. Hunt. 2010. Greatwall Phosphorylates an Inhibitor of Protein Phosphatase 2A That Is Essential for Mitosis. *Science.* 330:1670–1673.
Mochida, S., S. Rata, H. Hino, T. Nagai, and B. Novák. 2016. Two Bistable Switches Govern M Phase Entry. *Curr. Biol.* 26:3361–3367.
Morin, V., S. Prieto, S. Melines, S. Hem, M. Rossignol, T. Lorca, J. Espeut, N. Morin, and A. Abrieu. 2012. CDK-dependent potentiation of MPS1 kinase activity is essential to the mitotic checkpoint. *Curr. Biol.* 22:289–295.
Morla, A.O., G. Draetta, D. Beach, and J.Y.J. Wang. 1989. Reversible tyrosine phosphorylation of cdc2: Dephosphorylation accompanies activation during entry into mitosis. *Cell*. 58:193–203.
Moura, M., M. Osswald, N. Leça, J. Barbosa, A.J. Pereira, H. Maiato, C.E. Sunkel, and C. Conde. 2017. Protein Phosphatase 1 inactivates Mps1 to ensure efficient Spindle Assembly Checkpoint silencing. *Elife*. 6:1–29.
Murray, A.W., M.J. Solomon, and M.W. Kirschner. 1989. The role of cyclin synthesis and degradation in the control of maturation promoting factor activity. *Natur*. 339:280–286.
Musacchio, A. 2015. The Molecular Biology of Spindle Assembly Checkpoint Signaling Dynamics. *Curr. Biol.* 25:R1002–R1018.
Musacchio, A., and A. Desai. 2017. A molecular view of kinetochore assembly and function. *Biology (Basel).* 6:5–52.
Musacchio, A., and E.D. Salmon. 2007. The spindle-assembly checkpoint in space and time. *Nat. Rev. Mol. Cell Biol.* 8:379–393.
Nabet, B., J.M. Roberts, D.L. Buckley, J. Paulk, S. Dastjerdi, A. Yang, A.L. Leggett, M.A. Erb, M.A. Lawlor, A. Souza, T.G. Scott, S. Vittori, J.A. Perry, J. Qi, G.E. Winter, K.K. Wong, N.S. Gray, and J.E. Bradner. 2018. The dTAG system for immediate and target-specific protein degradation. *Nat. Chem. Biol.* 14:431–441.
Nasa, I., S.F. Rusin, A.N. Kettenbach, and G.B.G. Moorhead. 2019. Aurora B opposes PP1 function in mitosis through phosphorylation of the conserved RVxF binding motif in PP1 regulatory proteins. *Sci Signal.* 11:1–12.
Nigg, E.A. 1995. Cyclin-dependent protein kinases: key regulators of the eukaryotic cell cycle. *BioEssays*. 6:471–480.
Nigg, E.A. 2001. Mitotic kinases ad reguators of cell division and its checkpoints. *Nat. Rev. Mol. Cell Biol.* 2:21–32.
Nigg, E.A., A. Blangy, and H.A. Lane. 1996. Dynamic changes in nuclear architecture during mitosis: On the role of protein phosphorylation in spindle assembly and chromosome segregation. *Exp. Cell Res.* 229:174–180.
Nijenhuis, W., E. Von Castelmur, D. Littler, V. De Marco, E. Tromer, M. Vleugel, M.H.J. Van Osch, B. Snel, A. Perrakis, and G.J.P.L. Kops. 2013. A TPR domain-containing N-terminal module of MPS1 is required for its

kinetochore localization by Aurora B. *J. Cell Biol.* 201:217–231.
Nijenhuis, W., G. Vallardi, A. Teixeira, G.J.P.L. Kops, and A.T. Saurin. 2014. Negative feedback at kinetochores underlies a responsive spindle checkpoint signal. *Nat. Cell Biol.* 16:1257–1264.
Nilsson, J. 2019. Protein phosphatases in the regulation of mitosis. *J. Cell Biol.* 218:395–409.
Nilsson, J., M. Yekezare, J. Minshull, and J. Pines. 2008. The APC/C maintains the spindle assembly checkpoint by targeting Cdc20 for destruction. *Nat. Cell Biol.* 10:1411–1420.
Nishino, T., F. Rago, T. Hori, K. Tomii, I.M. Cheeseman, and T. Fukagawa. 2013. CENP-T provides a structural platform for outer kinetochore assembly. *EMBO J.* 32:424–436.
Nishino, T., K. Takeuchi, K.E. Gascoigne, A. Suzuki, T. Hori, T. Oyama, K. Morikawa, I.M. Cheeseman, and T. Fukagawa. 2012. CENP-T-W-S-X forms a unique centromeric chromatin structure with a histone-like fold. *Cell*. 148:487–501.
Novak, B., and J.J. Tyson. 1993. Numerical analysis of a comprehensive model of M-phase control in Xenopus oocyte extracts and intact embryos. *J. Cell Sci.* 106:1153–1168.
Novak, B., J.J. Tyson, B. Gyorffy, and A. Csikasz-nagy. 2007. Irreversible cell-cycle transitions are due to systems- level feedback. *Nat. Cell Biol.* 9:724–728.
Nurse, P. 1990. Universal control mechanism regulating cell cycle timing of M-phase. *Nature*. 344:503–508.
Okada, M., I.M. Cheeseman, T. Hori, K. Okawa, I.X. McLeod, J.R. Yates, A. Desai, and T. Fukagawa. 2006. The cenp-H–I complex is required for the efficient incorporation of newly synthesized CENP-A into centromeres. *Nat. Cell Biol.* 8:446–457.
Okada, M., K. Okawa, T. Isobe, and T. Fukagawa. 2009. CENP-H–containing Complex Facilitates Centromere Deposition of CENP-A in Cooperation with FACT and CHD1. *Mol. Biol. Cell*. 20:3986–3995.
Olsen, J. V., M. Vermeulen, A. Santamaria, C. Kumar, M.L. Miller, L.J. Jensen, F. Gnad, J. Cox, T.S. Jensen, E.A. Nigg, S. Brunak, and M. Mann. 2010. Quantitative phosphoproteomics reveals widespread full phosphorylation site occupancy during mitosis. *Sci. Signal.* 3:1–15.
Örd, M., K. Möll, A. Agerova, R. Kivi, I. Faustova, R. Venta, E. Valk, and M. Loog. 2019a. Multisite phosphorylation code of CDK. *Nat. Struct. Mol. Biol.* 26.
Örd, M., R. Venta, K. Möll, E. Valk, and M. Loog. 2019b. Cyclin-Specific Docking Mechanisms Reveal the Complexity of M-CDK Function in the Cell Cycle. *Mol. Cell*. 75:76–89.
Overlack, K., I. Primorac, M. Vleugel, V. Krenn, S. Maffini, I. Hoffmann, G.J.P.L. Kops, and A. Musacchio. 2015. A molecular basis for the differential roles of Bubl and BubR1 in the spindle assembly checkpoint. *Elife*. 2015:1–24.
Pachis, S.T., and G.J.P.L. Kops. 2018. Leader of the SAC: Molecular mechanisms of Mps1/TTK regulation in mitosis. *Open Biol.* 8:180109–180119.
Pagliuca, C., V.M. Draviam, E. Marco, P.K. Sorger, and P. De Wulf. 2009. Roles for the conserved Spc105p/Kre28p complex in kinetochore-microtubule binding and the spindle assembly checkpoint. *PLoS One*.

4:e7640.
Pagliuca, F.W., M.O. Collins, A. Lichawska, P. Zegerman, J.S. Choudhary, and J. Pines. 2011. Quantitative Proteomics Reveals the Basis for the Biochemical Specificity of the Cell Cycle Machinery Felicia. *Mol. Cell*. 43:406–417.
Palmer, D.K., K. O'Day, H.L.E. Trong, H. Charbonneau, and R.L. Margolis. 1991. Purification of the centromere-specific protein CENP-A and demonstration that it is a distinctive histone. *Proc. Natl. Acad. Sci. U. S. A.* 88:3734–3738.
Palmer, D.K., K. O'Day, M.H. Wener, B.S. Andrews, and R.L. Margolis. 1987. A 17-kD centromere protein (CENP-A) copurifies with nucleosome core particles and with histones. *J. Cell Biol.* 104:805–815.
Pardee, A.B. 1987. Molecules Involved in Proliferation of Normal and Cancer Cells: Presidential Address. *Cancer Res.* 47:1488–1491.
Pardee, A.B. 1989. G1 events and regulation of cell proliferation. *Science.* 246:603–608.
Paris, J., R. Le Guellec, A. Couturier, K. Le Guellec, F. Omilli, J. Camonis, S. MacNeill, and M. Philippe. 1991. Cloning by differential screening of a Xenopus cDNA coding for a protein highly homologous to cdc2. *Proc. Natl. Acad. Sci. U. S. A.* 88:1039–1043.
Perera, D., V. Tilston, J.A. Hopwood, M. Barchi, R.P. Boot-Handford, and S.S.S. Taylor. 2007. Bub1 Maintains Centromeric Cohesion by Activation of the Spindle Checkpoint. *Dev. Cell*. 13:566–579.
Perpelescu, M., and T. Fukagawa. 2011. The ABCs of CENPs. *Chromosoma*. 120:425–446.
Pesenti, M.E., D. Prumbaum, P. Auckland, C.M. Smith, A.C. Faesen, A. Petrovic, M. Erent, S. Maffini, S. Pentakota, J.R. Weir, Y.C. Lin, S. Raunser, A.D. McAinsh, and A. Musacchio. 2018. Reconstitution of a 26-Subunit Human Kinetochore Reveals Cooperative Microtubule Binding by CENP-OPQUR and NDC80. *Mol. Cell*. 71:923–939.
Pesenti, M.E., T. Raisch, D. Conti, K. Walstein, I. Hoffmann, D. Vogt, D. Prumbaum, I.R. Vetter, S. Raunser, and A. Musacchio. 2022. Structure of the human inner kinetochore CCAN complex and its significance for human centromere organization. *Mol. Cell*. 82:2113–2131.
Peters, J.-M. 2004. The Anaphase-Promoting Complex. *Mol. Cell*. 9:931–943.
Petrovic, A., J. Keller, Y. Liu, K. Overlack, J. John, Y.N. Dimitrova, S. Jenni, S. van Gerwen, P. Stege, S. Wohlgemuth, P. Rombaut, F. Herzog, S.C. Harrison, I.R. Vetter, and A. Musacchio. 2016. Structure of the MIS12 Complex and Molecular Basis of Its Interaction with CENP-C at Human Kinetochores. *Cell*. 167:1028-1040.e15.
Petrovic, A., S. Mosalaganti, J. Keller, M. Mattiuzzo, K. Overlack, V. Krenn, A. DeAntoni, S. Wohlgemuth, V. Cecatiello, S. Pasqualato, S. Raunser, and A. Musacchio. 2014. Modular Assembly of RWD Domains on the Mis12 Complex Underlies Outer Kinetochore Organization. *Mol. Cell*. 53:591–605.
Petrovic, A., S. Pasqualato, P. Dube, V. Krenn, S. Santaguida, D. Cittaro, S. Monzani, L. Massimiliano, J. Keller, A. Tarricone, A. Maiolica, H. Stark, and A. Musacchio. 2010. The MIS12 complex is a protein interaction hub for outer kinetochore assembly. *J. Cell Biol.* 190:835–852.
Pines, J., and T. Hunt. 1987. Molecular cloning and characterization of the

mRNA for cyclin from sea urchin eggs. *EMBO J.* 6:2987–2995.
Pines, J., and T. Hunter. 1989. Isolation of a human cyclin cDNA: Evidence for cyclin mRNA and protein regulation in the cell cycle and for interaction with p34cdc2. *Cell*. 58:833–846.
Pinna, L.A., A. Donella, G. Clari, and V. Moret. 1976. Preferential dephosphorylation of protein bound phosphorylthreonine and phosphorylserine residues by cytosol and mitochondrial “casein phosphatases.” *Biochem. Biophys. Res. Commun.* 70:1308–1315.
Pinsky, B.A., C.R. Nelson, and S. Biggins. 2009. Protein Phosphatase I Regulates Exit from the Spindle Checkpoint in Budding Yeast. *Curr. Biol.* 19:1182–1187.
Pomerening, J.R., E.D. Sontag, and J.E. Ferrell. 2003. Building a cell cycle oscillator: Hysteresis and bistability in the activation of Cdc2. *Nat. Cell Biol.* 5:346–351.
Primorac, I., J.R. Weir, E. Chiroli, F. Gross, I. Hoffmann, S. van Gerwen, A. Ciliberto, and A. Musacchio. 2013. Bub3 reads phosphorylated MELT repeats to promote spindle assembly checkpoint signaling. *Elife*. 2013:1–20.
Qian, J., M. Beullens, B. Lesage, and M. Bollen. 2013. Aurora B defines its own chromosomal targeting by opposing the recruitment of the phosphatase scaffold Repo-Man. *Curr. Biol.* 23:1136–1143.
Qian, J., M.A. García-Gimeno, M. Beullens, M.G. Manzione, G. Van der Hoeven, J.C. Igual, M. Heredia, P. Sanz, L. Gelens, and M. Bollen. 2017. An Attachment-Independent Biochemical Timer of the Spindle Assembly Checkpoint. *Mol. Cell*. 68:715–730.
Qian, J., B. Lesage, M. Beullens, A. Van Eynde, and M. Bollen. 2011. PP1/repo-man dephosphorylates mitotic histone H3 at T3 and regulates chromosomal aurora B targeting. *Curr. Biol.* 21:766–773.
Qiao, R., F. Weissmann, M. Yamaguchi, N.G. Brown, R. VanderLinden, R. Imre, M.A. Jarvis, M.R. Brunner, I.F. Davidson, G. Litos, D. Haselbach, K. Mechtler, H. Stark, B.A. Schulman, and J.M. Peters. 2016. Mechanism of APC/CCDC20 activation by mitotic phosphorylation. *Proc. Natl. Acad. Sci. U. S. A.* 113:E2570–E2578.
Rago, F., K.E. Gascoigne, and I.M. Cheeseman. 2015. Distinct organization and regulation of the outer kinetochore KMN network downstream of CENP-C and CENP-T. *Curr. Biol.* 25:671–677.
Rattani, A., P.K. Vinod, J. Godwin, K. Tachibana-Konwalski, M. Wolna, M. Malumbres, B. Novák, and K. Nasmyth. 2014. Dependency of the spindle assembly checkpoint on Cdk1 renders the anaphase transition irreversible. *Curr. Biol.* 24:630–637.
Reddy, S.K., M. Rape, W.A. Margansky, and M.W. Kirschner. 2007. Ubiquitination by the anaphase-promoting complex drives spindle checkpoint inactivation. *Nature*. 446:921–925.
Reyes-Lamothe, R., X. Wang, and D. Sherratt. 2008. Escherichia coli and its chromosome. *Trends Microbiol.* 16:238–245.
Rieder, C.L., R.W. Cole, A. Khodjakov, and G. Sluder. 1995. The checkpoint delaying anaphase in response to chromosome monoorientation is mediated by an inhibitory signal produced by unattached kinetochores. *J. Cell Biol.* 130:941–948.
Rodriguez-Rodriguez, J.A., C. Lewis, K.L. Mckinley, V. Sikirzhytski, J. Corona,

J. Maciejowski, A. Khodjakov, I.M. Cheeseman, and P. V. Jallepalli. 2018. Distinct roles of RZZ and Bub1-KNL1 in mitotic checkpoint signaling and kinetochore expansion. *Curr. Biol.* 28:3422–3429.
Roos, U.P. 1976. Light and electron microscopy of rat kangaroo cells in mitosis - III. Patterns of chromosome behavior during prometaphase. *Chromosoma*. 54:363–385.
De Rop, V., A. Padeganeh, and P.S. Maddox. 2012. CENP-A: The key player behind centromere identity, propagation, and kinetochore assembly. *Chromosoma*. 121:527–538.
Rosenberg, J.S., F.R. Cross, and H. Funabiki. 2011. KNL1/Spc105 Recruits PP1 to Silence the Spindle Assembly Checkpoint. *Curr. Biol.* 21:942–946.
Ruchaud, S., M. Carmena, and W.C. Earnshaw. 2007. Chromosomal passengers: Conducting cell division. *Nat. Rev. Mol. Cell Biol.* 8:798–812.
Russell, P., and P. Nurse. 1986. Schizosaccharomyces pombe and saccharomyces cerevisiae: A look at yeasts divided. *Cell*. 45:781–782.
Russo, A.A., P.D. Jeffrey, and N.P. Pavletich. 1996. Structural basis of cyclin-dependent kinase activation by phosphorylation. *Nat. Struct. Biol.* 3:696–700.
Santaguida, S., and A. Musacchio. 2009. The life and miracles of kinetochores. *EMBO J.* 28:2511–2531.
Santaguida, S., A. Tighe, A.M. D'Alise, S.S. Taylor, and A. Musacchio. 2010. Dissecting the role of MPS1 in chromosome biorientation and the spindle checkpoint through the small molecule inhibitor reversine. *J. Cell Biol.* 190:73–87.
Santaguida, S., C. Vernieri, F. Villa, A. Ciliberto, and A. Musacchio. 2011. Evidence that Aurora B is implicated in spindle checkpoint signalling independently of error correction. *EMBO J.* 30:1508–1519.
Santamaría, D., C. Barrière, A. Cerqueira, S. Hunt, C. Tardy, K. Newton, J.F. Cáceres, P. Dubus, M. Malumbres, and M. Barbacid. 2007. Cdk1 is sufficient to drive the mammalian cell cycle. *Nature*. 448:811–815.
Sapkota, H., E. Wasiak, J.R. Daum, and G.J. Gorbsky. 2018. Multiple determinants and consequences of cohesion fatigue in mammalian cells. *Mol. Biol. Cell*. 29:1811–1824.
Sarangapani, K.K., L.B. Koch, C.R. Nelson, C.L. Asbury, and S. Biggins. 2021. Kinetochore-bound Mps1 regulates kinetochore–microtubule attachments via Ndc80 phosphorylation. *J. Cell Biol.* 220:e202106130.
Saurin, A.T., M.S. Van Der Waal, R.H. Medema, S.M.A. Lens, and G.J.P.L. Kops. 2011. Aurora B potentiates Mps1 activation to ensure rapid checkpoint establishment at the onset of mitosis. *Nat. Commun.* 2.
Saville, M.K., and R.J. Watson. 1998. The cell-cycle regulated transcription factor B-Myb is phosphorylated by Cyclin A/Cdk2 at sites that enhance its transactivation properties. *Oncogene*. 17:2679–2689.
Schindelin, J., I. Arganda-Carreras, E. Frise, V. Kaynig, M. Longair, T. Pietzsch, S. Preibisch, C. Rueden, S. Saalfeld, B. Schmid, J.-Y. Tinevez, D.J. White, V. Hartenstein, K. Eliceiri, P. Tomancak, and A. Cardona. 2012. Fiji: an open-source platform for biological-image analysis. *Nat. Methods*. 9:676–82.
von Schubert, C., F. Cubizolles, J.M. Bracher, T. Sliedrecht, G.J.P.L. Kops, and E.A. Nigg. 2015. Plk1 and Mps1 Cooperatively Regulate the Spindle Assembly Checkpoint in Human Cells. *Cell Rep.* 12:66–78.

Serena, M., R.N. Bastos, P.R. Elliott, and F.A. Barr. 2020. Molecular basis of MKLP2-dependent Aurora B transport from chromatin to the anaphase central spindle. *J. Cell Biol.* 219:e201910059.
Shalem, O., N.E. Sanjana, E. Hartenian, X. Shi, D.A. Scott, T.S. Mikkelsen, D. Heckl, B.L. Ebert, D.E. Root, J.G. Doench, and F. Zhang. 2014. Genome-Scale CRISPR-Cas9 Knockout Screening in Human Cells. *Science.* 343:84–88.
Shannon, K.B., and E.D. Salmon. 2002. Chromosome dynamics: New light on Aurora B kinase function. *Curr. Biol.* 12:458–460.
Shepperd, L.A., J.C. Meadows, A.M. Sochaj, T.C. Lancaster, J. Zou, G.J. Buttrick, J. Rappsilber, K.G. Hardwick, and J.B.A. Millar. 2012. Phosphodependent recruitment of Bub1 and Bub3 to Spc7/KNL1 by Mph1 kinase maintains the spindle checkpoint. *Curr. Biol.* 22:891–899.
Shi, Y. 2009. Serine/Threonine Phosphatases: Mechanism through Structure. *Cell*. 139:468–484.
Silió, V., A.D. McAinsh, and J.B. Millar. 2015. KNL1-Bubs and RZZ Provide Two Separable Pathways for Checkpoint Activation at Human Kinetochores. *Dev. Cell*. 35:600–613.
Sironi, L., M. Mapelli, S. Knapp, A. De Antoni, K.T. Jeang, and A. Musacchio. 2002. Crystal structure of the tetrameric Mad1-Mad2 core complex: Implications of a “safety belt” binding mechanism for the spindle checkpoint. *EMBO J.* 21:2496–2506.
Sivakumar, S., and G.J. Gorbsky. 2015. Spatiotemporal regulation of the anaphase-promoting complex in mitosis. *Nat. Rev. Mol. Cell Biol.* 16:82–94.
Smith, L.D., and R.E. Ecker. 1971. The interaction of steroids with Rana pipiens oocytes in the induction of maturation. *Dev. Biol.* 25:232–247.
Smith, R.J., M.H. Cordeiro, N.E. Davey, G. Vallardi, A. Ciliberto, F. Gross, and A.T. Saurin. 2019. PP1 and PP2A Use Opposite Phospho-dependencies to Control Distinct Processes at the Kinetochore. *Cell Rep.* 28:2206–2219.
Stegmeier, F., and A. Amon. 2004. Closing mitosis: The functions of the Cdc14 phosphatase and its regulation. *Annu. Rev. Genet.* 38:203–232.
Stewart-Ornstein, J., and G. Lahav. 2016. Dynamics of CDKN1A in single cells defined by an endogenous fluorescent tagging toolkit. *Cell Rep.* 14:1800–1811.
Stucke, V.M., H.H.W. Silljé, L. Arnaud, and E.A. Nigg. 2002. Human Mps1 kinase is required for the spindle assembly checkpoint but not for centrosome duplication. *EMBO J.* 21:1723–1732.
Sudakin, V., G. Chan, and T. Yen. 2001. Checkpoint inhibition of the APC/C in HeLa cells is mediated by a complex of BUBR1, BUB3, CDC20, and MAD2. *J. Cell Biol.* 154:925–936.
Sudakin, V., D. Ganoth, A. Dahan, H. Heller, J. Hershko, F.C. Luca, J. V. Ruderman, and A. Hershko. 1995. The cyclosome, a large complex containing cyclin-selective ubiquitin ligase activity, targets cyclins for destruction at the end of mitosis. *Mol. Biol. Cell*. 6:185–198.
Suijkerbuijk, S.J.E., M. Vleugel, A. Teixeira, and G.J.P.L. Kops. 2012. Integration of Kinase and Phosphatase Activities by BUBR1 Ensures Formation of Stable Kinetochore-Microtubule Attachments. *Dev. Cell*. 23:745–755.
Takaki, T., M. Montagner, M.P. Serres, M. Le Berre, M. Russell, L. Collinson, K.

Szuhai, M. Howell, S.J. Boulton, E. Sahai, and M. Petronczki. 2017. Actomyosin drives cancer cell nuclear dysmorphia and threatens genome stability. *Nat. Commun.* 8:16013.
Tanaka, T.U., N. Rachidi, C. Janke, G. Pereira, M. Galova, E. Schiebel, M.J.R. Stark, and K. Nasmyth. 2002. Evidence that the Ipl1-Sli15 (Aurora Kinase-INCENP) complex promotes chromosome bi-orientation by altering kinetochore-spindle pole connections. *Cell*. 108:317–329.
Taylor, S.S., E. Ha, and F. McKeon. 1998. The human homologue of Bub3 is required for kinetochore localization of Bub1 and a Mad3/Bub1-related protein kinase. *J. Cell Biol.* 142:1–11.
Teichner, A., E. Eytan, D. Sitry-Shevah, S. Miniowitz-Shemtov, E. Dumin, J. Gromis, and A. Hershko. 2011. p31comet promotes disassembly of the mitotic checkpoint complex in an ATP-dependent process. *Proc. Natl. Acad. Sci. U. S. A.* 108:3187–3192.
Terrak, M., F. Kerff, K. Langseimo, T. Tao, and R. Dominguez. 2004. Structural basis of protein phosphatase 1 regulation. *Nature*. 429:780–784.
Thebault, P., D.Y. Chirgadze, Z. Dou, T.L. Blundell, S. Elowe, and V.M. Bolanos-Garcia. 2012. Structural and functional insights into the role of the N-terminal Mps1 TPR domain in the SAC (spindle assembly checkpoint). *Biochem. J.* 448:321–328.
Tighe, A., V.L. Johnson, and S.S. Taylor. 2004. Truncating APC mutations have dominant effects on proliferation, spindle checkpoint control, survival and chromosome stability. *J. Cell Sci.* 117:6339–6353.
Trinkle-Mulcahy, L., J. Andersen, W.L. Yun, G. Moorhead, M. Mann, and A.I. Lamond. 2006. Repo-Man recruits PP1γ to chromatin and is essential for cell viability. *J. Cell Biol.* 172:679–692.
Trinkle-Mulcahy, L., P.D. Andrews, S. Wickramasinghe, J. Sleeman, A. Prescott, Y. Wah Lam, C. Lyon, J.R. Swedlow, and A.I. Lamond. 2003. Time-lapse Imaging Reveals Dynamic Relocalization of PP1gamma throughout the Mammalian Cell Cycle. *Mol. Biol. Cell*. 14:107–117.
Tsukahara, T., Y. Tanno, and Y. Watanabe. 2010. Phosphorylation of the CPC by Cdk1 promotes chromosome bi-orientation. *Nature*. 467:719–723.
Uzunova, K., B.T. Dye, H. Schutz, R. Ladurner, G. Petzold, Y. Toyoda, M.A. Jarvis, N.G. Brown, I. Poser, M. Novatchkova, K. Mechtler, A.A. Hyman, H. Stark, B.A. Schulman, and J.M. Peters. 2012. APC15 mediates CDC20 autoubiquitylation by APC/C MCC and disassembly of the mitotic checkpoint complex. *Nat. Struct. Mol. Biol.* 19:1116–1123.
Vanoosthuyse, V., and K.G. Hardwick. 2009. A Novel Protein Phosphatase 1-Dependent Spindle Checkpoint Silencing Mechanism. *Curr. Biol.* 19:1176–1181.
Varma, D., and E.D. Salmon. 2012. The KMN protein network - Chief conductors of the kinetochore orchestra. *J. Cell Sci.* 125:5927–5936.
Vassilev, L.T., C. Tovar, S. Chen, D. Knezevic, H. Sun, D.C. Heimbrook, L. Chen, S. Chent, and X. Zhao. 2006. Selective mitotic inhibitor functions of human reveals critical mitotic functions of human CDK1. *PNAS*. 103:10660–10665.
Vázquez-Novelle, M.D., L. Sansregret, A.E. Dick, C.A. Smith, A.D. Mcainsh, D.W. Gerlich, and M. Petronczki. 2014. Cdk1 inactivation terminates mitotic checkpoint surveillance and stabilizes kinetochore attachments in anaphase. *Curr. Biol.* 24:638–645.

Vigneron, S., E. Brioudes, A. Burgess, J.C. Labbé, T. Lorca, and A. Castro. 2009. Greatwall maintains mitosis through regulation of PP2A. *EMBO J.* 28:2786–2793.
Vigneron, S., A. Gharbi-Ayachi, A.-A. Raymond, A. Burgess, J.-C. Labbé, G. Labesse, B. Monsarrat, T. Lorca, and A. Castro. 2011. Characterization of the Mechanisms Controlling Greatwall Activity. *Mol. Cell. Biol.* 31:2262–2275.
Vink, M., M. Simonetta, P. Transidico, K. Ferrari, M. Mapelli, A. De Antoni, L. Massimiliano, A. Ciliberto, M. Faretta, E.D. Salmon, and A. Musacchio. 2006. In Vitro FRAP Identifies the Minimal Requirements for Mad2 Kinetochore Dynamics. *Curr. Biol.* 16:755–766.
Visconti, R., L. Palazzo, R. Della Monica, and D. Grieco. 2012. Fcp1-dependent dephosphorylation is required for M-phase-promoting factor inactivation at mitosis exit. *Nat. Commun.* 3:894.
Visintin, R., S. Prinz, and A. Amon. 1997. CDC20 and CDH1: A family of substrate-specific activators of APC- dependent proteolysis. *Science.* 278:460–463.
Vleugel, M., T.A. Hoek, E. Tromer, T. Sliedrecht, V. Groenewold, M. Omerzu, and G.J.P.L. Kops. 2015. Dissecting the roles of human BUB1 in the spindle assembly checkpoint. *J. Cell Sci.* 128:2975–2982.
Vleugel, M., E. Tromer, M. Omerzu, V. Groenewold, W. Nijenhuis, B. Snel, and G.J.P.L. Kops. 2013. Arrayed BUB recruitment modules in the kinetochore scaffold KNL1 promote accurate chromosome segregation. *J. Cell Biol.* 203:943–955.
Waizenegger, I.C., S. Hauf, A. Meinke, and J.M. Peters. 2000. Two distinct pathways remove mammalian cohesin from chromosome arms in prophase and from centromeres in anaphase. *Cell*. 103:399–410.
Wan, X., R.P. O'Quinn, H.L. Pierce, A.P. Joglekar, W.E. Gall, J.G. DeLuca, C.W. Carroll, S.T. Liu, T.J. Yen, B.F. McEwen, P.T. Stukenberg, A. Desai, and E.D. Salmon. 2009. Protein Architecture of the Human Kinetochore Microtubule Attachment Site. *Cell*. 137:672–684.
Wang, H., X. Zhang, L. Teng, and R.J. Legerski. 2015. DNA damage checkpoint recovery and cancer development. *Exp. Cell Res.* 334:350–358.
Wang, K., B. Sturt-Gillespie, J.C. Hittle, D. Macdonald, G.K. Chan, T.J. Yen, and S.T. Liu. 2014a. Thyroid hormone receptor interacting protein 13 (TRIP13) AAA-ATPase is a novel mitotic checkpoint-silencing protein. *J. Biol. Chem.* 289:23928–23937.
Wang, W., Y. Yang, Y. Gao, Q. Xu, F. Wang, S. Zhu, W. Old, K. Resing, N. Ahn, M. Lei, and X. Liu. 2009. Structural and mechanistic insights into Mps1 kinase activation. *J. Cell. Mol. Med.* 13:1679–1694.
Wang, X., H. Yu, L. Xu, T. Zhu, F. Zheng, C. Fu, Z. Wang, and Z. Dou. 2014b. Dynamic autophosphorylation of mps1 kinase is required for faithful mitotic progression. *PLoS One*. 9:1–10.
Wassmann, K., and R. Benezra. 1998. Mad2 transiently associates with an APC/p55Cdc complex during mitosis. *Proc. Natl. Acad. Sci. U. S. A.* 95:11193–11198.
Weaver, B.A., and D.W. Cleveland. 2006. Does aneuploidy cause cancer? *Curr. Opin. Cell Biol.* 18:658–667.
Weaver, B.A.A., A.D. Silk, C. Montagna, P. Verdier-Pinard, and D.W.

Cleveland. 2007. Aneuploidy Acts Both Oncogenically and as a Tumor Suppressor. *Cancer Cell*. 11:25–36.
Wei, R.R., J. Al-Bassam, and S.C. Harrison. 2007. The Ndc80/HEC1 complex is a contact point for kinetochore-microtubule attachment. *Nat. Struct. Mol. Biol.* 14:54–59.
Weinert, T.A., and L.H. Hartwell. 1988. The RAD9 gene controls the cell cycle response to DNA damage in saccharomyces cerevisiae. *Science.* 241:317–322.
Weir, J.R., A.C. Faesen, K. Klare, A. Petrovic, F. Basilico, J. Fischböck, S. Pentakota, J. Keller, M.E. Pesenti, D. Pan, D. Vogt, S. Wohlgemuth, F. Herzog, and A. Musacchio. 2016. Insights from biochemical reconstitution into the architecture of human kinetochores. *Nature*. 537:249–253.
Weiss, E., and M. Winey. 1996. The Saccharomyces cerevisiae spindle pole body duplication gene MPS1 is part of a mitotic checkpoint. *J. Cell Biol.* 132:111–123.
Welburn, J.P.I., M. Vleugel, D. Liu, J.R. Yates, M.A. Lampson, T. Fukagawa, and I.M. Cheeseman. 2010. Aurora B phosphorylates spatially distinct targets to differentially regulate the kinetochore-microtubule interface. *Mol. Cell*. 38:383–392.
Westhorpe, F.G., A. Tighe, P. Lara-Gonzalez, and S.S. Taylor. 2011. p31 comet-mediated extraction of Mad2 from the MCC promotes efficient mitotic exit. *J. Cell Sci.* 124:3905–3916.
De Wever, V., I. Nasa, D. Chamousset, D. Lloyd, M. Nimick, H. Xu, L. Trinkle-Mulcahy, and G.B.G. Moorhead. 2014. The human mitotic kinesin KIF18A binds protein phosphatase 1 (PP1) through a highly conserved docking motif. *Biochem. Biophys. Res. Commun.* 453:432–437.
Wigge, P.A., O.N. Jensen, S. Holmes, S. Souès, M. Mann, J. V Kilmartin, D.J. Riley, P. Chen, and W.L.M. Cell. 1998. Analysis of the Saccharomyces Spindle Pole by Matrix-assisted Laser Desorption/Ionization (MALDI) Mass Spectrometry. *J. Cell Biol.* 141:967–977.
Wigge, P.A., and J. V. Kilmartin. 2001. The Ndc80p complex from Saccharomyces cerevisiae contains conserved centromere components and has a function in chromosome segregation. *J. Cell Biol.* 152:349–360.
Williams, B.C., J.J. Filter, K.A. Blake-Hodek, B.E. Wadzinski, N.J. Fuda, D. Shalloway, and M.L. Goldberg. 2014. Greatwall-phosphorylated Endosulfine is both an inhibitor and a substrate of PP2A-B55 heterotrimers. *Elife*. 2014:1–34.
Wojcik, E., R. Basto, M. Serr, F. Scaírou, R. Karess, and T. Hays. 2001. Kinetochore dynein: Its dynamics and role in the transport of the Rough deal checkpoint protein. *Nat. Cell Biol.* 3:1001–1007.
Wu, J.Q., J.Y. Guo, W. Tang, C. Yang, D. Freel, C. Chen, A.C. Nairn, and S. Kornbluth. 2009. PP1-mediated dephosphorylation of phosphoproteins at mitotic exit is controlled by inhibitor-1 and PP1 phosphorylation. *Nat. Cell Biol.* 11:644–651.
Xia, G., X. Luo, T. Habu, J. Rizo, T. Matsumoto, and H. Yu. 2004. Conformation-specific binding of p31comet antagonizes the function of Mad2 in the spindle checkpoint. *EMBO J.* 23:3133–3143.
Xin, G., J. Fu, J. Luo, Z. Deng, Q. Jiang, and C. Zhang. 2020. Aurora B regulates PP1g-Repo-Man interactions to maintain the chromosome condensation state. *J. Biol. Chem.* 295:14780–14788.

Xing, Y., Y. Xu, Y. Chen, P.D. Jeffrey, Y. Chao, Z. Lin, Z. Li, S. Strack, J.B. Stock, and Y. Shi. 2006. Structure of Protein Phosphatase 2A Core Enzyme Bound to Tumor-Inducing Toxins. *Cell*. 127:341–353.
Xu, P., E.A. Raetz, M. Kitagawa, D.M. Virshup, and S.H. Lee. 2013. BUBR1 recruits PP2A via the B56 family of targeting subunits to promote chromosome congression. *Biol. Open*. 2:479–486.
Xu, Y., Y. Xing, Y. Chen, Y. Chao, Z. Lin, E. Fan, J.W. Yu, S. Strack, P.D. Jeffrey, and Y. Shi. 2006. Structure of the Protein Phosphatase 2A Holoenzyme. *Cell*. 127:1239–1251.
Yamagishi, Y., C.H. Yang, Y. Tanno, and Y. Watanabe. 2012. MPS1/Mph1 phosphorylates the kinetochore protein KNL1/Spc7 to recruit SAC components. *Nat. Cell Biol.* 14:746–752.
Yamaguchi, M., R. VanderLinden, F. Weissmann, R. Qiao, P. Dube, N.G. Brown, D. Haselbach, W. Zhang, S.S. Sidhu, J.M. Peters, H. Stark, and B.A. Schulman. 2016. Cryo-EM of Mitotic Checkpoint Complex-Bound APC/C Reveals Reciprocal and Conformational Regulation of Ubiquitin Ligation. *Mol. Cell*. 63:593–607.
Yamano, H., K. Ishii, and M. Yanagida. 1994. Phosphorylation of dis2 protein phosphatase at the C-terminal cdc2 consensus and its potential role in cell cycle regulation. *EMBO J.* 13:5310–5318.
Yamashiro, S., Y. Yamakita, G. Totsukawa, H. Goto, K. Kaibuchi, M. Ito, D. Hartshorne, and F. Matsumura. 2008. Myosin phosphatase targeting subunit 1 regulates mitosis by antagonizing Polo-like kinase 1. *Dev. Cell*. 14:787–797.
Yamashita, K., H. Yasuda, J. Pines, K. Yasumoto, H. Nishitani, M. Ohtsubo, T. Hunter, T. Sugimura, and T. Nishimoto. 1990. Okadaic acid, a potent inhibitor of type 1 and type 2A protein phosphatases, activates cdc2/H1 kinase and transiently induces a premature mitosis-like state in BHK21 cells. *EMBO J.* 9:4331–4338.
Yang, Y., F. Wu, T. Ward, F. Yan, Q. Wu, Z. Wang, T. McGlothen, W. Peng, T. You, M. Sun, T. Cui, R. Hu, Z. Dou, J. Zhu, W. Xie, Z. Rao, X. Ding, and X. Yao. 2008. Phosphorylation of HsMis13 by Aurora B kinase is essential for assembly of functional kinetochore. *J. Biol. Chem.* 283:26726–26736.
Yatskevich, S., K.W. Muir, D. Bellini, Z. Zhang, J. Yang, T. Tischer, M. Predin, T. Dendooven, S.H. McLaughlin, and D. Barford. 2022. Structure of the human inner kinetochore bound to a centromeric CENP-A nucleosome. *Science.* 376:844–852.
Ye, A.A., T.J. Maresca, A.A. Ye, and T.J. Maresca. 2017. It's all relative : Centromere- versus pole-based error correction. 4101:78–80.
Ye, Q., S.C. Rosenberg, A. Moeller, J.A. Speir, T.Y. Su, and K.D. Corbett. 2015. TRIP13 is a protein-remodeling AAA+ ATPase that catalyzes MAD2 conformation switching. *Elife*. 2015:1–44.
Yoo, H.Y., A. Kumagai, A. Shevchenko, A. Shevchenko, and W.G. Dunphy. 2004. Adaptation of a DNA replication checkpoint response depends upon inactivation of Claspin by the Polo-like kinase. *Cell*. 117:575–588.
Yu, J., S.L. Fleming, B. Williams, E. V. Williams, Z.X. Li, P. Somma, C.L. Rieder, and M.L. Goldberg. 2004. Greatwall kinase: A nuclear protein required for proper chromosome condensation and mitotic progression in Drosophila. *J. Cell Biol.* 164:487–492.
Yudkovsky, Y., M. Shteinberg, T. Listovsky, M. Brandeis, and A. Hershko.

2000. Phosphorylation of Cdc20/Fizzy negatively regulates the mammalian cyclosome/APC in the mitotic checkpoint. *Biochem. Biophys. Res. Commun.* 271:299–304.

Zhang, G., T. Kruse, C. Guasch Boldú, D.H. Garvanska, F. Coscia, M. Mann, M. Barisic, and J. Nilsson. 2019. Efficient mitotic checkpoint signaling depends on integrated activities of Bub1 and the RZZ complex . *EMBO J.* 38:1–18.

Zhang, G., T. Kruse, B. López-Méndez, K.B. Sylvestersen, D.H. Garvanska, S. Schopper, M.L. Nielsen, and J. Nilsson. 2017. Bub1 positions Mad1 close to KNL1 MELT repeats to promote checkpoint signalling. *Nat. Commun.* 8:1–12.

Zhang, S., L. Chang, C. Alfieri, Z. Zhang, J. Yang, S. Maslen, M. Skehel, and D. Barford. 2016. Molecular mechanism of APC/C activation by mitotic phosphorylation. *Nature*. 533:260–264.

Zhu, T., Z. Dou, B. Qin, C. Jin, X. Wang, L. Xu, Z. Wang, L. Zhu, F. Liu, X. Gao, Y. Ke, Z. Wang, F. Aikhionbare, C. Fu, X. Ding, and X. Yao. 2013. Phosphorylation of microtubule-binding protein hec1 by mitotic kinase aurora b specifies spindle checkpoint kinase mps1 signaling at the kinetochore. *J. Biol. Chem.* 288:36149–36159.

Zirkle, R.E. 1970. Ultraviolet-Microbeam Irradiation of Newt-Cell Cytoplasm: Spindle Destruction, False Anaphase, and Delay of True Anaphase. *Radiat. Res.* 41:516–537.